Are the Northland rivers of New Zealand in synchrony with global Holocene climate change?

A thesis presented in partial fulfilment of the requirements for the degree of

Doctor of Philosophy in Geography

at Massey University, Palmerston North, New Zealand

MASSEY UNIVERSITY

Jane Richardson

2013

Abstract

Climate during the Holocene has not been stable, and with predictions of human induced climate change it has become increasingly important to understand the underlying 'natural' dynamics of the global climate system. Fluvial systems are sensitive respondents to and recorders of environmental change (including climate).

This research integrates meta-data analysis of a New Zealand fluvial radiocarbon (^{14}C) database with targeted research in catchments across the Northland region to determine the influence of Holocene climate change on river behaviour in New Zealand, and to assess whether or not Northland rivers are in synchrony with global climate change. The research incorporates ^{14}C dating and meta-analysis techniques, sedimentology, geophysics, ground survey (RTK-dGPS) and Geographic Information Systems analysis to investigate the response of New Zealand and Northland rivers to Holocene climate and anthropogenic change.

The emerging pattern of Holocene river behaviour in New Zealand is one of increased river activity in southern regions (South Island) in response to enhanced westerly atmospheric circulation (promoted by negative Southern Annular Mode [SAM]-like circulation), while in northern regions (North Island) river activity is enhanced by meridional atmospheric circulation (promoted by La Niña-like and positive SAM-like circulation). In Northland, Holocene floodplain development reflects the interplay between valley configuration and accommodation space, sediment supply, fluctuation in climate and anthropogenic factors in the last several hundred years. Evidence from Northland rivers suggests that a globally extensive abrupt climate change signal can promote a synchronous fluvial response, overprinting complex regional patterns of Holocene river behaviour.

The research demonstrates that at the centennial-scale, regional atmospheric circulation change is a key driver of river behaviour, with anthropogenic catchment disturbance responsible for enhanced river activity and floodplain aggradation in the last ~ 500 years. It is therefore likely that any future climate change involving a shift in the atmospheric

circulation regime will have an impact on river behaviour in New Zealand. However, at the catchment- or reach-scale, river response will be largely determined by local controls such as sediment supply and accommodation space, with these factors largely moderated by the post-settlement fluvial history.

Acknowledgements

I would like to express my appreciation to my supervisors, Dr Ian Fuller (Massey University), Dr Kat Holt (Massey University), Dr Nicola Litchfield (GNS Science) and Professor Mark Macklin (Aberystwyth University) for their support and guidance during this PhD research. I am also particularly grateful for the technical support provided by David Feek (Massey University) during the fieldwork phase of this project.

I wish to thank the following organisations for their financial support over the last three years: the Tertiary Education Commission (Top Achiever Doctoral Scholarship), New Zealand Federation of Graduate Women (Susan Byrne Memorial Award), Zonta Manawatu (Women in Science and Technology Scholarship sponsored by Graduate Women Manawatu), Massey University School of People, Environment and Planning (Graduate Research Fund) and Massey University Institute of Agriculture and Environment.

Several people have contributed their time and expertise, and I would like to acknowledge their contribution: Dr Henry Lamb (Aberystwyth University) for undertaking the XRF core scanning, Michael Hayes for supplying information on the settlement of Kaeo, Dr Bob Stewart (Massey University) and Professor Vince Neall (Massey University) for advice on sedimentology, Dr Mark Bebbington (Massey University) for assistance with statistical analysis, Dr Anja Moebis (Massey University) for help with grain size analysis and Hamish Mckoy (formerly Victoria University of Wellington) for training in the use of the percussion coring equipment. LiDAR data was kindly supplied by the Northland Regional Council (Bob Cathcart, Joseph Camuso, Jonathan Santos and Colin Anderson). I would also like to thank the landowners for permitting access to the Northland study sites.

Special thanks also to my fellow students for their contributions and support, especially Rob Dykes and Dr Alastair Clement for their technical advice. Finally, I would like to thank my family and friends. Thank you to Glen, Georgia, Sophie, Jack and Isabel for all their tolerance, love and support, and to Monica and Dennis who instilled in me the desire for knowledge.

Thesis structure and authorship

This thesis consists of four manuscripts written for publication in appropriate journals (currently still under review) and six supporting chapters.

Jane Richardson carried out all the fieldwork in Northland between November 2009 and October 2011, and was assisted at different times by Dr Ian Fuller, Dr Katherine Holt, Dr Nicola Litchfield and David Feek. Jane Richardson also undertook all laboratory work included in this thesis with the assistance of Dr Henry Lamb (Aberystwyth University), Dr Anja Moebis (Massey University) and Dr Bob Stewart (Massey University).

Jane Richardson wrote all the text in this thesis and was the principal author in the preparation of manuscripts included in this thesis. Manuscripts are co-authored by others to acknowledge their input (see Appendix F for statements of contribution). Dr Ian Fuller and Prof. Mark Macklin developed the initial project, and all supervisors provided general advice and edited manuscripts. Dr Mark Bebbington performed the statistical analysis in Chapter 4. Dr Anna Jones advised on the analysis of the New Zealand fluvial radiocarbon database and contributed to the final editing of the manuscript presented in Chapter 4. Use of the New Zealand fluvial radiocarbon database is referenced as Macklin et al. (2012a).

Signed by Principal Supervisor:

Dr Ian Fuller

Contents

List of Figures

List of Tables

Chapter 1

Introduction

1.1 Background and research motivation

Global climate during the Holocene, defined as the last 11,700 calendar years before 2000 AD (Walker et al., 2009), has not been stable, undergoing periods of rapid change as a result of solar forcing and the internal dynamics of the interconnected ocean-atmosphere-cryosphere system (Mayewski et al., 2004; Wanner et al., 2011). Although not of the same magnitude as glacial-interglacial climate transitions, Holocene climate variability has impacted on human societies and ecosystems (e.g., Mayewski et al., 2004; Walker et al. 2012). In recent decades Holocene palaeoclimate research has been invigorated by the need to develop a greater understanding of the natural patterns and processes of the climate system, in order to better inform models looking to forecast the impacts of anthropogenic climate change (e.g., Pearson and Dawson, 2003; Collins et al., 2006; Vera et al., 2006; Kundzewicz et al., 2008).

Central to an improved knowledge of Holocene climate dynamics is understanding the relationship between climate in the Northern and Southern Hemispheres, and a key question in palaeoclimate research is whether climate change is synchronous, or out of phase between these two regions (Turney et al., 2003; Mayewski et al., 2004; Alloway et al., 2007; Denton and Broecker, 2008; Macklin et al., 2012a). An asynchronous Holocene insolation pattern between the Northern and Southern Hemispheres suggests that a synchronous climate response is not to be expected based on solar forcing alone (Hodell et al., 2001b), and a number of authors have presented evidence for this out-of-phase relationship (Charles et al., 1996; Schaefer et al., 2009; Macklin et al., 2012a). However, the complex array of

interactions, feedbacks and teleconnections within the climate system does not preclude a globally synchronous response to climatic change (Mayewski et al., 2004; Wanner et al., 2011). In order to fully explore global climate dynamics, more well-dated high resolution palaeoclimate proxy records are required, especially from Southern Hemisphere regions (Denton and Broecker, 2008; Wanner et al., 2011).

The climate record of New Zealand, located in the mid-latitudes of the Southern Hemisphere, is considered to be of global importance due to New Zealand's small size, oceanic climate and the absence of extensive ice sheet cover during the Last Glacial Maximum (McGlone et al., 1993; Alloway et al., 2007; Schaefer et al., 2009). The long narrow New Zealand landmass, spanning 13 degrees of latitude (34°S to 47°S), is subject to both subtropical and Antarctic climatic influences, and lies adjacent to major oceanic and atmospheric circulation boundaries. Interactions between the prevailing westerly circulation and axial ranges in both islands ensure strong regional hydro-climatic contrasts. New Zealand river systems reflect this combination of a climatically sensitive location and responsive landscape, their sediments and landforms preserving a record of past hydrological conditions (e.g., Clement and Fuller, 2007).

Fluvial systems respond to climate and other environmental changes, preserving a sedimentary record of river response and creating an archive that can be used to explore the relationship between river system behaviour and external environmental influences (e.g., Starkel, 1983; Passmore et al., 1992; Ely et al., 1993; Knox, 1993; Tipping, 1994; Rumsby and Macklin, 1996; Knox, 2000). A major recent advance in fluvial research has been the development and application of radiocarbon (^{14}C) databases and meta-analysis of large fluvial ^{14}C datasets for reconstructing centennial-scale hydro-climate change (Macklin and Lewin, 2003; Johnstone et al., 2006; Hoffmann et al., 2008; Macklin et al., 2010). This methodology uses ^{14}C-dated sedimentary fluvial archives to produce probability-based reconstructions of Holocene river behaviour, which can in turn be correlated with independent palaeoclimate proxy data and other environmental records (Harden et al., 2010; Macklin et al., 2010; Turner et al., 2010). Meta-analysis of ^{14}C-dated fluvial units in the Northern Hemisphere has demonstrated that the Holocene fluvial record comprises clusters of flood events, associated with large-scale atmospheric circulation changes (Macklin et al., 2006; Harden et al., 2010; Macklin et al., 2010; Zielhofer et al., 2010). Inter-regional comparisons between the UK and New Zealand probability-based flood series also suggests large-scale atmospheric changes are involved in driving major episodes of flooding, which are predominantly out of phase between the two regions (Macklin et al., 2012a).

In New Zealand, as in the Northern Hemisphere, there has also been a strong emphasis on climate as the dominant control on fluvial erosion and sedimentation (e.g., Grant, 1985; Vella et al., 1988; Marden and Neall, 1990; Berryman et al., 2000). Alluvial terrace sequences in the North Island indicate that the predominant response to climate amelioration during the Holocene was degradational (Clement and Fuller, 2007), with major phases of erosion and alluviation in New Zealand during the late Holocene linked to atmospheric circulation changes (Grant, 1985). However, New Zealand's active tectonic setting on the convergent boundary of the Australian and Pacific plates, means that tectonics (e.g., Pillans, 1986; Berryman et al., 2000; Litchfield and Berryman, 2006) and volcanic activity (e.g., Hume et al., 1975; Manville, 2002) are also major controls influencing river dynamics (Clement and Fuller, 2007). Anthropogenic impacts on catchment stability have also been significant (e.g., Wilmshurst et al., 1999), but are confined to the last ~ 800 years (Prickett, 2002). To date, fluvial research in New Zealand has been dominated by catchment- or reach-scale enquiry, and several regions remain unexamined in terms of their fluvial history. There has been no comprehensive reconstruction of New Zealand Holocene river behaviour in response to environmental (including climate) change at the regional scale. This research addresses this knowledge gap, applying meta-analysis techniques to a database of ^{14}C-dated Holocene fluvial units in New Zealand to produce a centennial-scale probability-based reconstruction of river behaviour.

The river systems of Northland, the most northern region of New Zealand, are among the least researched catchments, and very little is known about their behaviour during the Holocene. Northland's distance from the main zone of plate convergence between the Australian and Pacific plates, and the Taupo Volcanic Zone, means that tectonic- and volcanic-controls on Holocene river behaviour are not a factor. Erosion and sedimentation in Northland catchments particularly prior to human settlement (~ 800 years ago) will therefore be primarily influenced by climate. The reconstruction of Northland fluvial histories therefore represents an ideal opportunity to examine river behaviour and floodplain evolution at a regional scale, to elucidate the role that climate and late Holocene anthropogenic impacts have had on rivers and to produce a centennial-scale record of hydro-climatic change. This research incorporates geochronology (^{14}C dating), sedimentology, geophysics (ground penetrating radar), high precision ground survey (RTK-dGPS) and Geographic Information Systems (GIS) analysis to investigate the response of Northland rivers to Holocene climate and anthropogenic change. Meta-data analysis of new ^{14}C-ages, obtained from organic material incorporated within alluvium preserved in Northland catchments, is used to produce a high-resolution record of Holocene flooding in the region which is compared with independent regional and global palaeoclimate data.

This research is the first in the Southern Hemisphere to integrate fluvial ^{14}C meta-data analysis with targeted field research, thereby making an original contribution to global research in palaeohydrology. In addition, this research contributes to an understanding of the impact of human settlement on landscape stability associated with Māori and European colonisation. The analysis of Northland Holocene fluvial histories and New Zealand river behaviour also assesses, for the first time, the impacts and significance of global and regional climate change on Holocene river behaviour. Results are used to answer the question: are the Northland rivers of New Zealand in synchrony with global Holocene climate change?

1.2 Thesis aims

The aim of this thesis is to:

1. Determine the influence of Holocene climate change on river behaviour in New Zealand.

2. Establish a detailed chronology of river activity in selected Northland catchments during the Holocene.

3. Reconstruct the fluvial history of key localities in Northland rivers and catchments.

4. Apply meta-data analysis on new radiocarbon ages from Northland catchments.

5. Assess the degree of synchronicity between global climate changes and river behaviour in Northland during the Holocene.

6. Identify human impacts on catchment stability following Māori and European settlement in Northland.

1.3 Thesis organisation

This thesis integrates fluvial meta-data analysis of the New Zealand fluvial ^{14}C database with targeted field research in catchments across the Northland region to reconstruct Holocene river response to climate and anthropogenic change at the regional and national scale.

The first two chapters review Holocene climate variability and river response to climate and other environmental change. Chapter 2 discusses Holocene climate, including: the mechanisms responsible for climate change, interhemispheric dynamics and New Zealand climate and its drivers. A review of the palaeoclimate of New Zealand and Northland provides the background for further discussion in subsequent chapters. Chapter 3 examines fluvial response to Holocene environmental change. The key mechanisms involved in driving Holocene river behaviour and the nature of river response to environmental change are outlined. This chapter also examines how New Zealand rivers have responded to environmental change signals during the Holocene.

Chapter 4 is contained within the manuscript: J.M. Richardson, I.C. Fuller, M.G. Macklin, A.F Jones, K.A. Holt, N.J. Litchfield, M. Bebbington, Holocene river behaviour in New Zealand: response to regional centennial-scale climate forcing, which is published in the journal *Quaternary Science Reviews*. The chapter presents meta-analyses of ^{14}C-dated Holocene fluvial units and probability-based records of Holocene river behaviour in New Zealand using an existing database (Macklin et al., 2012a) that does not include any Northland ^{14}C dates. River activity records are compared with independent Southern Hemisphere hydro-climate proxy records and a model of river response to climate and anthropogenic forcing is proposed.

Chapter 5 provides background information for the Northland region and presents a model for Holocene floodplain development based on data from eight sites in six Northland catchments and comprises the manuscript: J.M. Richardson, I.C. Fuller, K.A. Holt, N.J. Litchfield, M.G. Macklin: The role of valley floor confinement as a control on Holocene floodplain development: an example from Northland, New Zealand, which is in review in the journal *Geomorphology.* In this chapter new ^{14}C-dated evidence is presented and the controls on river behaviour in Northland are discussed.

Chapter 6 presents a revised meta-analysis of 422 ^{14}C-dated Holocene fluvial units in New Zealand obtained from combining the New Zealand fluvial ^{14}C database (Chapter 4) and dates from targeted field research in Northland (Chapter 5). Episodes of river activity in the North and South Islands, and the coherent precipitation regions, including northern New Zealand, are identified and compared with independent regional palaeoclimate records. The implications of adding the northern New Zealand ^{14}C dates to the model presented in Chapter 4 are discussed.

Chapter 7 comprises the manuscript: J.M. Richardson, I.C. Fuller, K.A. Holt, N.J. Litchfield, M.G. Macklin: Fluvial records of Holocene climate variability and evidence of a 3500–2800 cal. yr BP cold event from northern New Zealand, which is in review in the journal *The Holocene*. In this chapter meta-analysis techniques are applied to ^{14}C-dated Holocene fluvial deposits in Northland to produce a probability-based record of Holocene fluvial behaviour for this region. The Northland river activity record for the Holocene is compared with independent palaeoclimate proxy records from Northland, elsewhere in New Zealand and globally, to determine the underlying controls on river behaviour in Northland. The chapter focuses on a phase of river activity at 3500–2800 cal. yr BP that occurred in response to a globally extensive Holocene cold event.

Floodplain sedimentation and river response to post-settlement catchment disturbance is examined in Chapter 8 using data from the flood prone Kaeo catchment in eastern Northland and ^{14}C data from eight other Northland floodplain sites. The chapter is contained within the manuscript: J.M. Richardson, I.C. Fuller, K.A. Holt, N.J. Litchfield, M.G. Macklin: Post-settlement fluvial response in Northland, New Zealand, which is in review in the journal *Catena*. Reconstruction of the floodplain morphology and Holocene floodplain sedimentation history contributes to a better understanding of the river dynamics associated with anthropogenically-driven catchment disturbance.

The final chapters, Chapters 9 and 10, provide further discussion in support of preceding chapters and a synthesis which draws together the major research findings. The conclusion section of Chapter 10 addresses the specific research aims detailed in Chapter 1. Finally, the research implications and potential direction of future research are outlined.

1.4 Summary

More palaeoclimate proxy records from Southern Hemisphere regions are required to fully explore global climate dynamics. Meta-data analysis of large ^{14}C datasets in Northern Hemisphere river systems has demonstrated the utility of fluvial sedimentary archives for reconstructing centennial-scale hydro-climate change. This research focuses on the Northland region, a region remote (in New Zealand terms) from volcanic and tectonic disturbance, and an area where little is known of its Holocene river histories. The research is the first of its kind in the Southern Hemisphere to integrate targeted field research with fluvial ^{14}C meta-data analysis to produce centennial-scale resolution ^{14}C-dated records of river activity in New Zealand and Northland. Providing an assessment of the importance of global and regional climate in controlling river behaviour in New Zealand, and addressing

the question of whether Northland rivers are in synchrony with global climate change. The following Chapter 2 examines the patterns and processes involved in Holocene climate variability, globally and within the New Zealand region.

Chapter 2

Holocene climate change

2.1 Introduction

In order to address the question of whether Northland rivers are in synchrony with global climate, an understanding of Holocene climate dynamics at the global and regional scale is required. This chapter examines global Holocene climate change, the mechanisms responsible for this variability, and the state of knowledge as to the extent of the phase relationship between climatic change in the Northern and Southern Hemispheres. A review of New Zealand climate, the major oscillatory climate modes responsible for the climate patterns in the Southern Hemisphere and the impact these systems have on New Zealand climate is also presented. A brief overview of the Holocene palaeoclimate of New Zealand is outlined and provides a basis for more in-depth discussion in subsequent chapters. Finally, a more comprehensive review of the palaeoclimate of Northland provides some context for Chapters 5 to 8.

2.2 Holocene climate change

Evidence from globally distributed palaeoclimate data has shown that climate during the Holocene, defined as the last 11,700 calendar years before 2000 AD (Walker et al., 2009), has not been stable (O'Brien et al., 1995; Masson et al., 2000; Bond et al., 2001; Mayewski et al., 2004; Alloway et al., 2007; Donders et al., 2008; Charman, 2010; Wanner et al., 2011). Although Holocene climate dynamics have not exhibited the dramatic fluctuations observed during the Last Glacial period, climate variability has been of a sufficient magnitude to impact human societies and ecosystems (e.g., Buckland et al., 1995; deMenocal et al., 2000; Hodell et al., 2001a; Mayewski et al., 2004; Walker et al., 2012). Early influential research

based on glacier activity (Denton and Karlén, 1973), ice core (O'Brien et al., 1995) and ice rafted debris records (Bond et al., 1997) from the northern North Atlantic region, has suggested that the timing of Holocene climatic events has exhibited millennial-scale cyclicity. Research based on marine sediment records of ice rafted debris identified the existence of a ~ 1500 year cycle (termed 'Bond cycle') in the Holocene climate of the North Atlantic (Bond et al., 1997). Nine Bond cycles have been recognised within the Holocene, representing cool climate events involving a shift in ocean hydrography and the advection of cold ice-bearing surface water southward and eastward from the Nordic and Labrador seas (Bond et al., 1997). However, the existence and origin of these quasi-periodic cycles still remains the subject of debate, and many records show no consistent cyclicity at millennial or centennial timescales (e.g., Risebrobakken et al., 2003; Schulz et al., 2004; Moros et al., 2006).

Despite the high level of complexity involved in the climate system, compilation of global palaeoclimate records has provided some insights into the temporal and spatial patterns of climate variability (e.g., Mayewski et al., 2004; Wanner et al., 2011). A review by Mayewski et al. (2004) of ~ 50 palaeo-precipitation/humidity and palaeo-temperature proxy data, including information from pollen, speleothems, ice cores, glacier landforms and sediments, identified six periods (at 9000–8000, 6000–5000, 4200–3800, 3500–2500, 1200–1000, and 600–150 cal. yr BP) of globally extensive rapid climate change (Fig. 2.1). The main features of all but the most recent multi-centennial length climatic event, which was characterised by cool poles and wet tropics, involved lower temperatures in the polar regions and reduced precipitation in the low-latitudes (Mayewski et al., 2004). In an even more comprehensive review of global climate proxy data, Wanner et al. (2011) also identified six cold relapses at 8200, 6300, 4700, 2700, 1550 and 550 cal. yr BP (Fig. 2.1). The majority of the non-cyclic cold relapses were characterised by cooler temperatures, dry anomalies and glacier advance. The climate events identified by Wanner et. al. (2011) are broadly consistent with the periods of rapid climate change identified by Mayewski et al. (2004) and show the closest correlation with Bond cycles 5b, 2, 1 and 0 (Fig. 2.1).

2.2.1 Causes of Holocene climate variability

Global climate is a dynamic expression of the complex and interconnected ocean-atmosphere-cryosphere systems. Climatic variation is forced by alterations in these coupled systems, with the extent of change either amplified or dampened through the operation of system feedbacks. A number of different forcing factors, feedbacks and teleconnections, operating across a range of spatial and temporal scales, have been implicated in Holocene

climate change, including: solar variability (e.g., Bond et al., 2001; Wang et al., 2005), variations in oceanic circulation (e.g., Jones, 1994; Debret et al., 2007), variations in atmospheric circulation (e.g., Sijp and England, 2009), volcanic activity (Douglass and Knox, 2005), surface albedo effects (e.g., Foley et al., 1994) and greenhouse gas flux (e.g., Crutzen and Stoermer, 2000).

2.2.1.1 Solar variability

A large body of evidence suggests that solar variability is the key driver of millennial to centennial-scale Holocene climate change (e.g., Karlén and Kuylenstierna, 1996; Bond et al., 2001; Nielsen et al., 2004; Wang et al., 2005; Fleitmanna et al., 2007). During the Holocene the amount of summer insolation has varied due to orbital precessional changes (Fig. 2.1). Summer insolation in the Northern Hemisphere has decreased from an early Holocene maximum, when the boreal summer solstice coincided with perihelion (the point in Earth's orbit when it is closest to the sun), while insolation in the Southern Hemisphere has been increasing over the last ~ 11,700 years (Berger and Loutre, 1991) (Fig. 2.1). Superimposed on this pattern are shorter term variations in solar activity, which can be measured in the environment as variations in the production rate of cosmogenic isotopes such as ^{14}C and ^{10}Be (Stuiver and Braziunas, 1989). Evidence for a solar influence on North Atlantic climate has been provided by close correlation between cosmogenic nuclides and proxies of drift ice measured in marine sediment cores (Bond et al., 2001). However, to fully explain how gradual insolation change and relatively small variations in solar output can induce large, widespread, abrupt and non-linear climate responses, additional mechanisms are required.

2.2.1.2 Ocean circulation

Many authors have discussed the role that changes in ocean circulation has played in Holocene climate fluctuations (Street-Perrott and Perrott, 1990; Stuiver et al., 1995; Bond et al., 1997; Duplessy et al., 2001; Risebrobakken et al., 2003; Rohling and Palike, 2005; Debret et al., 2007; Bentley et al., 2009; Varma et al., 2010). It has been postulated that the North Atlantic thermohaline circulation system is sensitive to changes in salinity caused by freshwater pulses from ice-sheet melting (Tornqvist and Hijma, 2012). Such changes affect heat transport between the low and high latitudes and are reported to be responsible for causing widespread climate impacts (Street-Perrott and Perrott, 1990; Klitgaard-Kristensen et al., 1998; Barber et al., 1999; Bianchi and McCave, 1999; deMenocal et al., 2000). Perturbation in the North Atlantic thermohaline circulation has been linked to climatic oscillations and major climate events in the Northern Hemisphere high-latitudes (Alley et al., 1997; Klitgaard-Kristensen et al., 1998; Bianchi and McCave, 1999; Duplessy et al., 2001),

low-latitudes (Arz et al., 2001; Lachniet et al., 2004), Southern Hemisphere mid-latitudes (Sallun et al., 2012) and Southern Ocean (Hodell et al., 2001b). In the Southern Hemisphere, circulation changes in the Southern Ocean and southeast Pacific Ocean have also been implicated in Southern Hemisphere Holocene climate variability (Bentley et al., 2009).

2.2.1.3 Atmospheric circulation

Atmospheric circulation is inherently coupled to ocean circulation (e.g., Speich et al., 2007) and is often cited as a key factor involved in Holocene climate dynamics (Nicholson and Flohn, 1980; Bond et al., 2001; Dean et al., 2002; Sijp and England, 2009; Varma et al., 2010). For example, the Southern Hemisphere subpolar Westerly Winds are a major component of the mid-latitude circulation system, and variations in the strength of these winds have had significant regional climate impacts during the Holocene (Shulmeister et al., 2004; Moreno et al., 2009). The Southern Hemisphere westerly winds are also strongly linked to the Antarctic Circumpolar Current, both of which have been implicated in the control of global ocean thermohaline circulation and climate forcing (Sijp and England, 2009). Atmospheric circulation changes associated with the major tropical monsoon systems have also played a key role in Holocene climate variability, with orbitally forced increased land-ocean temperature contrasts leading to strengthened monsoons (e.g., Kutzbach et al., 1996; Maher and Hu, 2006).

2.2.1.4 Volcanic activity

Volcanic activity also has the potential to perturb the atmosphere and force climate change at the hemispheric or global scale (Angell and Korshover, 1985; Bradley, 1988; Zielinski, 2000; Salzer and Hughes, 2007). The influence of volcanic eruptions on climate is predominantly due to the reflection of incoming solar radiation and absorbance of solar and terrestrial radiation in the stratosphere by ejected debris and volcanic aerosols, causing decadal-scale cooling at the Earth's surface and a warmer stratosphere (Sigurdsson, 1990; Robock, 2000). It is also possible that extremely large eruptions, or periods of more frequent eruptive activity, combined with solar forcing and positive feedback processes, such as ocean heat uptake and sea-ice effects, have impacted climate over longer timescales (Stenchikov et al., 2009). There is evidence that increased volcanic activity (inferred from ice core sulphate peaks) in combination with solar forcing played a role in the Little Ice Age (onset ~ 1275 AD) climatic deterioration (Crowley et al., 2008; Jungclaus et al., 2010), involving cold summers that were sustained for centuries by ocean/sea-ice feedbacks (Miller et al., 2012). Alternatively, some authors have hypothesised that increased volcanism has occurred during periods of rapid climate change as a result of changing stresses associated with crustal

loading (unloading) during the growth (decay) of ice sheets and sea-level changes (Gow and Williamson, 1971; McGuire et al., 1997; Zielinski, 2000; Huybers and Langmuir, 2009).

2.2.1.5 Surface albedo

Other important feedbacks in the climate system include the affects of variation in earth surface albedo through changes in vegetation (e.g., Foley et al., 1994; Kutzbach et al., 1996) or snow and ice cover (e.g., Hodell et al., 2001b). Studies have shown the expansion of boreal forests, initially promoted by high-latitude warming forced by insolation changes, provided a positive feedback mechanism, with a reduced surface albedo resulting in additional warming (Foley et al., 1994; Pielke and Vidale, 1995). In northern Africa, land-surface feedbacks, alongside intensification of the monsoonal system, are also considered important factors when explaining the orbitally forced mid Holocene 'greening' of the Sahara (Claussen and Gayler, 1997; de Noblet-Ducoudré et al., 2000). In polar regions it has been suggested that the expansion of sea-ice has provided a positive feedback mechanism and amplified gradual solar forcing leading to greater cooling (e.g., Clark et al., 1999; Hodell et al., 2001b).

2.2.1.6 Greenhouse gas flux

Atmospheric greenhouse gas flux is also implicated in the dynamics of Holocene climate. Greenhouse gases (including carbon dioxide and methane) play an important role in absorbing and reflecting the infrared thermal radiation emitted from the earth's surface, maintaining a warmer surface and lower atmosphere than would otherwise occur (Kasting et al., 1988). Long-term variations of CO_2 and CH_4 in the atmosphere are believed to be primarily driven by orbital changes (Brook et al., 1996; Petit et al., 1999). However, is has been suggested that anthropogenic emissions in the last ~ 200 years have been responsible for increased concentration of atmospheric greenhouse gases (e.g., Crutzen and Stoermer, 2000), causing climate change (IPCC, 2007). It has also been hypothesised that humans have been influencing greenhouse gas concentrations for thousands of years due to land-use change, which has contributed to significant warming in recent millennia (Ruddiman, 2003).

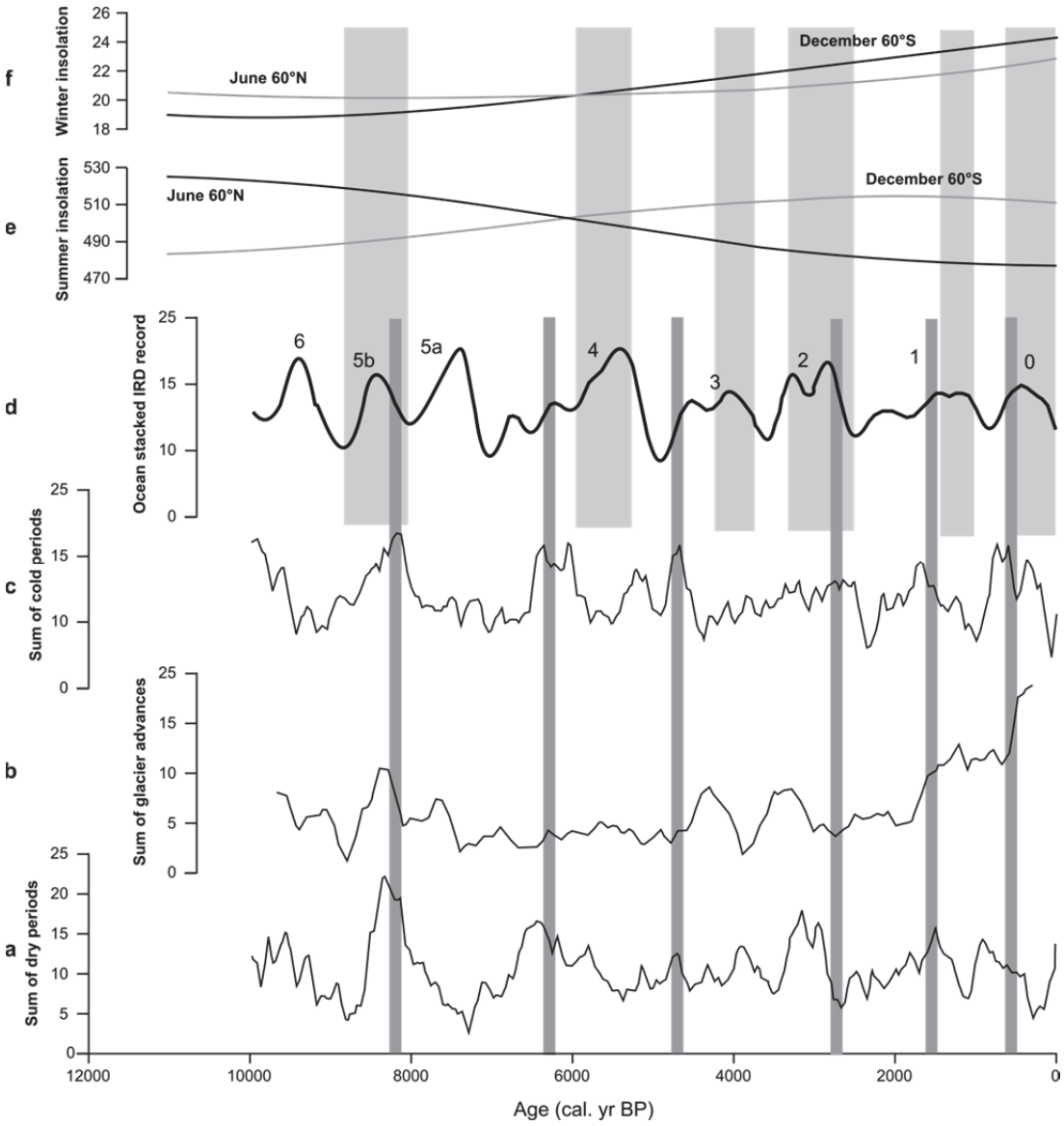

Fig. 2.1. Weighted and smoothed sum of (a) dry periods based on 35 humidity/precipitation proxy records (Wanner et al., 2011), (b) glacier advances (Wanner et al., 2011), (c) cold periods based on 46 temperature proxy records (Wanner et al., 2011). (d) Standardised ocean stacked ice rafted debris (IRD) record labelled with Bond Events 0–6 (Bond et al., 2001). Dark grey vertical bars represent the timing of cold events identified by Wanner et al. (2011), based on analysis of selected 10,000-year-long time series of temperature, humidity/precipitation and glacier advances. (e) Summer insolation values (W m^{-2}) at 60°N (black line) and 60°S latitude (grey line) (Berger and Loutre, 1991). (f) Winter insolation values (W m^{-2}) at 60°N (black line) and 60°S latitude (grey line) (Berger and Loutre, 1991). Light grey vertical bars represent the timing of rapid climate change as identified by Mayewski et al., (2004) from globally distributed palaeoclimate records.

2.2.2 Interhemispheric climate dynamics

Considering the controls involved, and the complexity of Holocene climate variability, it is not surprising that one of the major debates in Holocene climate research is whether or not climate change is synchronous between the Northern and Southern Hemispheres (e.g., Mayewski et al., 2004; Alloway et al., 2007; Denton and Broecker, 2008; Winkler and Matthews, 2010; Newnham et al., 2012). Hodell et al. (2001b) suggest that a globally synchronised climatic response to precessional insolation forcing alone during the Holocene is not expected, as the interhemispheric insolation patterns are out of phase for the same season (Fig. 2.1). However, the myriad of forcing mechanisms and interactions, feedbacks and teleconnections in the climate system do not preclude globally extensive responses to climatic perturbation.

Several authors have demonstrated out-of-phase climate change between the Northern and Southern Hemispheres for a number of temporal periods (e.g., Charles et al., 1996; Turney et al., 2003; Alloway et al., 2007; Schaefer et al., 2009; Macklin et al., 2012a). Turney et al. (2003) identified asynchronous behaviour between Greenland and Antarctica during the last deglaciation (18,000–10,000 cal. yr BP) possibly due to thermohaline circulation dynamics. Denton and Broecker (2008) also discussed the potential role that changes in the strength of Atlantic conveyor circulation could play in driving asynchronous climate changes in the northern and southern polar regions during the Holocene.

Correlations of Holocene glacier behaviour in the Southern Alps of New Zealand and glaciers in the Northern Hemisphere found some evidence of out-of-phase activity, with several glacier advances in New Zealand coinciding with Northern Hemisphere warm periods (Schaefer et al., 2009). However, the lack of a straightforward pattern in the timing of climatically-driven glacier fluctuations suggested that regional climate drivers and amplifying mechanisms have had a strong influence. Winkler and Matthews (2010) also emphasised the difficulties in using Holocene glacier chronologies to make interhemispheric correlations due to local and regional patterns in climatic forcing of glacier dynamics.

Recent research using meta-analysis of radiocarbon dated flood deposits from New Zealand and the UK has shown that the occurrence of centennial- to multicentennial-length episodes of flooding expressed a predominantly asynchronous pattern, prior to human influence from ~ 1000 cal. yr BP (Macklin et al., 2012a). This work demonstrated that short-term climate variability, associated with changes in the atmospheric-oceanic circulation of the mid-latitudes of both Hemispheres, has been out of phase for the majority of the Holocene. These findings support Denton and Broecker's (2008) suggestion of bi-polarity in deep-water

production and ocean conveyor circulation during the Holocene. Short periods of overlap, where flooding was occurring at the same time in both the New Zealand and the UK records, coincide with phases of glacier advance and climatic deterioration detected in both hemispheres, possibly highlighting a global climatic signature (Macklin et al., 2012a).

Despite the research outlined above, a lack of well-dated high resolution palaeoclimate records from the Southern Hemisphere is hampering efforts to better understand the controls and timing of interhemispheric climate change (Denton and Broecker, 2008; Wanner et al., 2011) and interhemispheric comparisons are limited.

2.3 New Zealand climate

New Zealand, located in the Southern Hemisphere mid-latitudes between 34° S and 47° S, lies on the convergent plate boundary of the Pacific and Australian plates. The landmass is subject to both subtropical and Antarctic climatic influences, and is in close proximity to a number of major oceanic and atmospheric circulation boundaries (Fig. 2.2): the Antarctic Circumpolar Current (ACC), Subantarctic Front (SAF), Subtropical Front (STF), Westerly wind belt (W), Southeast Trade Winds (STW) and South Pacific Convergence Zone (SPCZ). Warm subtropical surface waters (STW) flow from Australia, via the Tasman front, around the Northland Peninsula and along the eastern side of the North Island before being deflected eastwards near the Chatham rise. STW water also flows around the bottom of the South Island and northwards along the eastern side of the South Island before also being diverted along the Chatham Rise (Carter, 2001). Along the Chatham Rise these eastward-flowing waters form part of the STF boundary between the STW and the cold, nutrient rich, subantarctic surface water (SAW) (Carter, 2001). To the south of New Zealand is the ACC, a major eastward flowing current that completely encircles the globe, linking the world's oceans (Dijkstra, 2008).

New Zealand's oceanographic setting means that most regions, except the Central Otago region of inland South Island, experience a maritime climate (Lisle and Brown, 1968). Weather is largely dominated by westerly circulation and the progression of troughs, fronts and anticyclones moving across central and southern parts of the country between ~ 30°S and 50°S (Alloway et al., 2007). Strong east-west regional precipitation and temperature contrasts are created by the interaction between these eastward moving weather systems and the main axial ranges in both islands (Salinger, 1980a, 1980b). Based largely on this interaction between the westerly flow and orography, six coherent climate regions (Fig. 2.3) have been identified in New Zealand (Mullan, 1998). Three circulation regimes, trough,

blocking and zonal, comprising 12 different synoptic types, have been recognised for New Zealand (Kidson, 2000). The occurrence of these synoptic regimes creates distinctive temperature and precipitation patterns across the different climate regions. Changes in atmospheric circulation caused by fluctuation in the operation of climate modes, such as the Southern Annular Mode (SAM) and El Niño Southern Oscillation (ENSO), influence the synoptic regime, and can lead to anomalous precipitation or temperature patterns (Kidson, 2000; Ummenhofer et al., 2009).

2.3.1 Major Southern Hemisphere climate modes

Atmospheric processes modulated by orography and land/sea distribution generate perturbations in the atmospheric flow and create planetary-scale waves which circulate air around the globe (Stenseth et al., 2003). Oscillations in the planetary-scale waves cause fluctuations in climate over a range of timescales which demonstrate teleconnections between different geographic areas (Trenberth et al., 1998). A number of such 'teleconnected' climate patterns in both hemispheres have been defined and described using indices based on meteorological data and various statistical methodologies. These climate modes include: the Antarctic and Arctic Oscillations, North Atlantic Oscillation, Northern Annular Mode, Interdecadal Pacific Oscillation and Southern Oscillation. This review focuses on indices devised to describe climate patterns in the Southern Hemisphere.

2.3.1.1 Southern Annular Mode

The Southern Annular Mode (SAM) or Antarctic Oscillation has been described as the leading mode of interannual variability in extratropical circulation in the Southern Hemisphere (Thompson and Wallace, 2000; Marshall, 2007). The SAM essentially describes the large-scale zonally-symmetric transfer of atmospheric mass, resulting in synchronous pressure anomalies of opposite signs between the mid- and high-latitudes (Gong and Wang, 1999; Thompson and Wallace, 2000). Gong and Wang (1999) devised a numerical expression of the Antarctic Oscillation, the Antarctic Oscillation Index (AOI), after recognising that zonally averaged sea-level pressure at 40°S and 65°S were the key components of the extratropical Southern Hemispheric surface pressure system. The AOI is therefore defined as the difference between zonally averaged mean sea-level pressure at 40°S and 65°S. The AOI is described as high during the positive phases of the SAM when sea-level pressures above Antarctica are below average. During positive phases of the SAM zonal wind tends to be stronger between ~ 15–30ºS and ~ 45–60°S, while at the latitudes between ~ 30 and 45°S zonal wind is more likely to be weaker (Meneghini et al., 2007). Alternately, when the AOI is low, as occurs during the negative phase of the SAM, sea-level

pressure above Antarctica are above average. During negative phases of the SAM zonal wind tends to be weaker between ~ 15–30ºS and ~ 45–60°S, while at the latitudes between ~ 30 and 45°S zonal wind are more likely to be stronger (Meneghini et al., 2007).

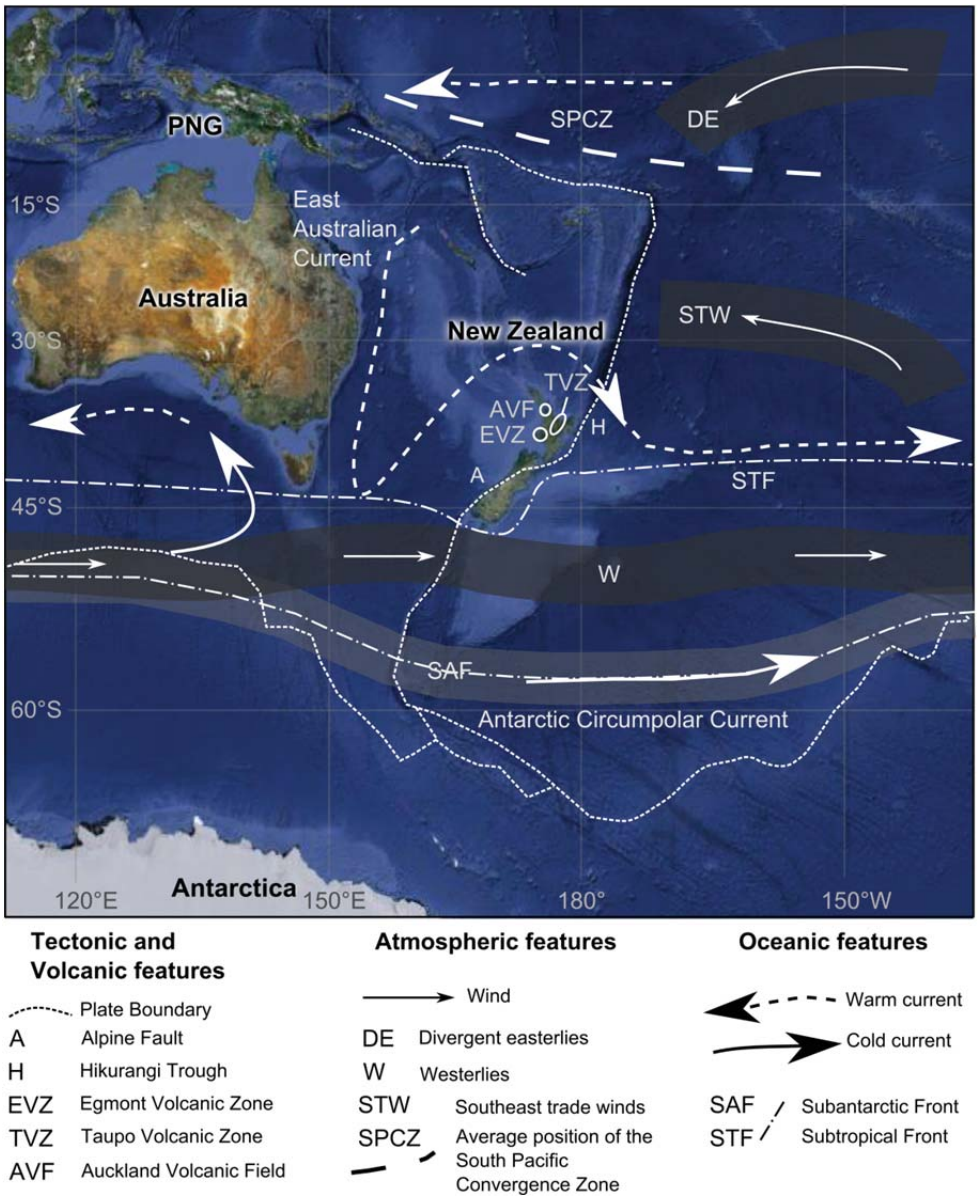

Fig. 2.2. Oceanographic setting of New Zealand in the mid-latitudes of the Southern Hemisphere. Showing major oceanic, atmospheric, tectonic features and volcanic zones (after Lorrey et al., 2012). Base image sourced from GoogleEarth™ (September 2012).

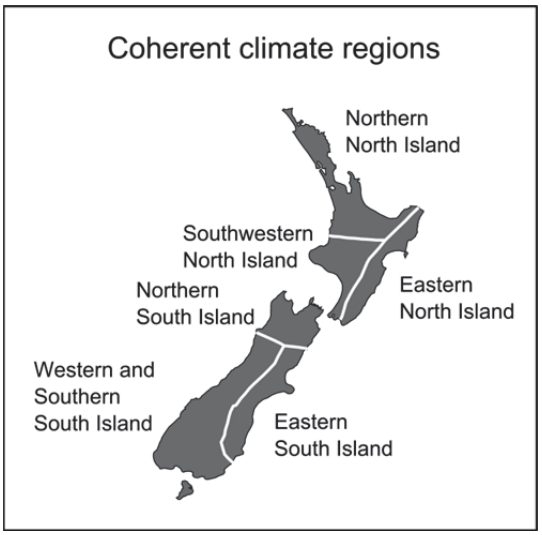

Fig. 2.3. Coherent climate regions of New Zealand (after Kidson, 2000).

Antarctic temperature data indicate that positive phases of the SAM can be correlated with warmer surface temperatures in the Antarctic Peninsula region and cooler near-surface temperatures in East Antarctica (Marshall, 2007). The most recent decades have shown an increasing trend towards positive polarity of the SAM, reflected by high values of AOI, with strengthened circumpolar westerlies, intensified polar vortex (Thompson and Wallace, 2000; Marshall, 2003) and ozone depletion (Kwok and Comiso, 2002). Kwok and Comiso (2002) suggest that increases in the positive polarity of SAM coupled with the increased frequency of negative phases of the Southern Oscillation Index has produced warming over the Antarctic Peninsula and cooling in the East Antarctic.

The climatic influences of the SAM are extensive and are not only confined to the Antarctic region. Research has highlighted the impacts of the SAM on precipitation in southeastern South America (Silvestri and Vera, 2003), winter rainfall over western South Africa (Reason and Rouault, 2005), summer precipitation in central-north China (Wang and Fan, 2005), East Asian precipitation (Fan, 2007) and dust weather frequency in China (Fan and Wang, 2004). As part of an analysis of the SAM-East Asian precipitation relationship, Fan (2007) identified significant zonal asymmetry in the Antarctic Oscillation and concluded that the Southern Oscillation was responsible for part of the Antarctic Oscillation asymmetry. The El Niño Southern Oscillation has also been implicated in the Antarctic Dipole Pattern, which is characterised by zonal fluctuations of sea ice, air temperatures and sea-level pressure between the Eastern Pacific and Atlantic regions of Antarctica (Yuan and Martinson, 2001).

2.3.1.2 Southern Oscillation

The Southern Oscillation (SO) atmospheric phenomenon was first described and named by Sir Gilbert Walker who identified a pattern of irregular out-of-phase sea-level pressure fluctuations between the tropical eastern Pacific and the Indian Ocean, extending from Africa to northern Australia (Julian and Chervin, 1978; Rasmusson and Wallace, 1983). The exchange of air mass between the regions and the operation of the Walker circulation fluctuates at interannual timescales and has a near global influence on climate (Julian and Chervin, 1978).

Several different indices have been devised to quantify the behaviour of the SO, using meteorological data from various locations. The most commonly used Southern Oscillation Index (SOI) is based on the standardized sea-level pressure (SLP) difference between Tahiti (17º33′ S; 149º37′ W) and Darwin (12º28′ S; 130º51′ E). Negative phases of the SOI (anomalously high SLP at Darwin and lower SLP at Tahiti) occur during El Niño events, whereas positive SOI phases define the occurrence of La Niña. Air pressure difference, as defined by the SOI, is a major driver of wind and the Hadley-Walker circulation, and is an important feature of the global atmospheric circulation system (Power and Smith, 2007). The system involves east to west flowing trade winds, descending air in the eastern Pacific Ocean, ascending air in the western Pacific and circulation counter to the trade winds at higher levels (Power and Smith, 2007). Evidence suggests that the Walker circulation is weaker during El Niño years and stronger during La Niña events (Power and Smith, 2007).

The term ‘El Niño’ was originally used to describe the unusual warming of coastal waters off Peru and Ecuador but is now frequently used to describe the Pacific basin-wide sea surface temperature anomalies that influence global climate patterns (Trenberth, 1997). The collective term for describing the atmosphere-ocean interactions in the equatorial Pacific region associated with El Niño events is El Niño-Southern Oscillation (ENSO). The warm phase of ENSO is associated with El Niño events, while periods of anomalously cooler tropical Pacific sea surface temperatures are classified as La Niña events corresponding to the cold phase of ENSO (Trenberth, 1997).

A plethora of research has documented the impacts that ENSO has had on the equatorial Pacific region and teleconnected regions across the globe. These include the influence of ENSO variability on: precipitation in North America (e.g., Ropelewski and Halpert, 1986; McCabe and Dettinger, 1999), precipitation and the incidence of tropical cyclones in the Caribbean and central America (e.g., Landsea, 2000), European climate anomalies (e.g., Fraedrich, 1994; Brönnimann et al., 2007), precipitation patterns in China (e.g., Ronghui and

Yifang, 1989; Zhang et al., 2007), African precipitation (e.g., Nicholson and Entekhabi, 1986; Mason and Lindesay, 1993), Asian/Australian monsoons (e.g., Nicholls, 1983; Huijun, 2002; Hendy et al., 2003), cyclone activity in Australia (e.g., Evans and Allan, 1992), precipitation in New Zealand (e.g., Ummenhofer and England, 2007) and South America (e.g., Pezzi and Cavalcanti, 2001; Coelho et al., 2002).

2.3.1.3 Interdecadal Pacific Oscillation

The Interdecadal Pacific Oscillation (IPO) describes the variability in sea surface temperature patterns at decadal timescales across the Pacific region and has been quantified using various indices, including Empirical Orthogonal Function analysis of seasonal sea-surface temperatures and night-time marine air temperatures (Power et al., 1999). Positive phases of the IPO are characterised by warmer-than-normal sea surface temperatures in the tropical Pacific and negative temperature anomalies in the northern Pacific and southern Pacific near New Zealand. The spatial pattern of sea surface temperature anomalies associated with the IPO have been described as 'ENSO- like' (Zhang et al., 1997). However, there are some differences in sea surface temperature pattern, with the IPO exhibiting less variance in the eastern Pacific region and greater variance in the extratropical regions and western Pacific (Power et al., 1999; Salinger et al., 2001). There is some evidence that the IPO has a modulating effect on interannual ENSO climate variability (Power et al., 1999; Salinger et al., 2001), resulting in temperature and precipitation anomalies at multi-decadal timescales. Data from the most recent IPO phases (after 1946) indicate that for the New Zealand region, positive phases of the IPO tend to strengthen ENSO climate teleconnections (Salinger et al., 2001).

2.3.1.4 The operation of ENSO and the SAM during the Holocene

Analysis of palaeoclimate records from the southern Pacific region suggest that the operation of ENSO and SAM has fluctuated at millennial scales throughout the Holocene in response to precessional forcing (Gomez et al., 2011). So although ENSO and SAM operate at interannual timescales, changes in the frequency or magnitude of the different oscillatory climate phases at the centennial- or millennial-scale could potentially influence centennial- to millennial-scale climate variability. There is evidence that during the early to mid Holocene (12,000 to 5000 cal. yr BP) ENSO was weak or non-operational (Sandweiss et al., 2001; Moy et al., 2002), or operating with reduced precipitation teleconnections (Shulmeister et al., 2006). Palaeoclimate records covering the period 6800 to 4900 cal. yr BP indicate that there was no correlation between ENSO and the SAM during this time, signalling reduced connectivity between the high- and mid-latitudes (Gomez et al., 2011).

Between 5000 and 2000 cal. yr BP there is evidence that ENSO was more variable, occurred more frequently and with stronger teleconnections (Sandweiss et al., 2001; Shulmeister et al., 2006; Donders et al., 2008). ENSO proxy records from Ecuador also point to an increase in ENSO frequency over the last ~ 3000 years (Moy et al., 2002). Temperature records from east Antarctica also show that the behaviour of the SAM varied during the Holocene, with the early Holocene characterised by a predominance of negative SAM conditions, switching to positive polarity for the period ~ 9000–6000 cal. yr BP (Jouzel, 2004). There is also evidence to suggest that the phase relationship of the SAM and ENSO has an impact on the strength of ENSO extratropical teleconnections (e.g., Gomez et al., 2011).

2.3.2 The influence of the SAM, ENSO and IPO on New Zealand climate

El Niño-Southern Oscillation (ENSO) and the SAM both have a strong influence on the interannual climate of New Zealand. Analysis of precipitation anomalies suggests that northern New Zealand is predominantly affected by atmospheric circulation in the tropical Pacific and the operation of ENSO, while the South Island is most affected by circulation changes associated with the subpolar westerlies and the oscillation of the SAM (Ummenhofer and England, 2007). The latitudinal gradation in the relative influence of ENSO and SAM combined with orographic effects produce a high level of spatial variability in precipitation across the country, with strong north-south and east-west contrasts (Ummenhofer and England, 2007).

Precipitation patterns in New Zealand are influenced by the oscillation of ENSO through its influence on the position of the South Pacific Convergence Zone (Folland et al., 2002), the strength of the subtropical and polar front jet streams and migration of the mid-latitude storm tracks (Yuan, 2004). During the El Niño phase of ENSO, precipitation is more likely to be anomalously low across the entire North Island, in eastern South Island and in northern South Island (Ummenhofer and England, 2007) (Fig. 2.4). In contrast, southern and southwestern regions of the South Island experience higher than normal precipitation (Ummenhofer and England, 2007). Westerly and southwesterly flow over New Zealand is enhanced during El Niño, and is characterised by more frequent and stronger zonal synoptic conditions (Kidson, 2000; Renwick, 2011) (Fig. 2.4). Under El Niño conditions, monthly average temperatures in northern and eastern regions tend to be above-average, while southern and western regions of New Zealand experience cooler temperatures (Fig. 2.4). During La Niña phases of ENSO, trough and blocking synoptic regimes dominate (Renwick, 2011). The blocking regime enhances meridional northerly and easterly flow, bringing

above-average monthly precipitation to northern and eastern regions and warmer temperatures across the entire country (Kidson, 2000) (Fig. 2.4). Trough conditions are also more common under La Niña and result in positive precipitation anomalies and negative temperature anomalies for all regions (Renwick, 2011).

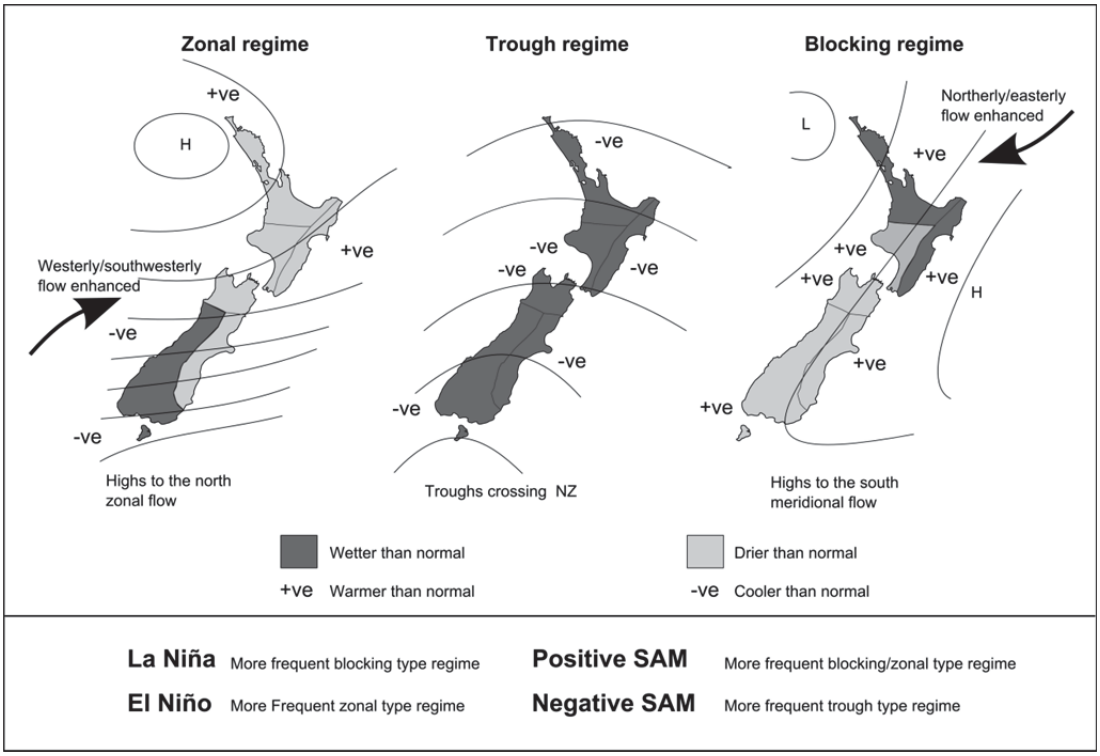

Fig. 2.4. New Zealand's three weather regimes displayed with an example of an associated synoptic pattern (Kidson, 2000). Annotated with average regional temperature anomalies and shaded with average regional precipitation anomalies, based on monthly averages (after Lorrey et al., 2012). The figure also shows the influence of the ENSO cycle and the polarity of the SAM on the relative frequency of occurrence of the synoptic types and associated regimes.

Synoptic-climatological analysis has found that the positive mode of the SAM has been linked to increased frequency of blocking and zonal types, and more trough types during negative SAM (Renwick, 2011). During the negative phase of the SAM westerly flow across New Zealand is enhanced and southern New Zealand experiences increased precipitation (Fig. 2.4). In contrast, during the positive phase of the SAM, westerly flows are weakened, and precipitation to southern New Zealand reduces (Ummenhofer and England, 2007). While in the North Island an enhanced northeasterly flow regime leads to increased moisture transport onto northern New Zealand (Ummenhofer and England, 2007).

The impact of the IPO on New Zealand climate is not well documented. Changes in flood and flow regimes associated with a shift from the negative phase to a positive phase of the IPO in the late 1970's showed that not all regions responded in the same manner (McKercher and Henderson, 2003). For most South Island rivers, flood and low-flow magnitude increased, while for rivers in the North Island and northern South Island there was no consistent response to the interdecadal regime shift (McKercher and Henderson, 2003). Analysis of south Pacific climate by Salinger et al. (2001) showed that not only does the IPO modulate decadal precipitation and temperatures but that it also modulates the response of temperature and precipitation to ENSO at interannual timescales. However, there was no clear relationship between IPO phase and ENSO, with teleconnections enhanced in some regions and weakened in others (Salinger et al., 2001). In the New Zealand region evidence was found for enhanced teleconnections with the SOI during the IPO positive phase (Salinger et al., 2001).

The operation of the Southern Hemisphere climate modes, their interaction and teleconnections, along with New Zealand's latitudinal span, maritime location and orography combine to create a highly regionalised and complex climatic situation. This level of complexity makes it difficult to isolate one singular dominant driver of climate in New Zealand, and leads to strong regional patterns in climate forcing. These patterns can be detected in the palaeoclimate record of New Zealand and can be used to reconstruct past climate regimes, providing information that can be used to inform models and future climate change scenarios (e.g., Lorrey et al., 2012).

2.3.3 The Holocene palaeoclimate of New Zealand

The palaeoclimate record of New Zealand, and a Southern Hemisphere perspective, is considered to be of global importance in terms of developing an understanding of global climate dynamics. New Zealand's small landmass and oceanic climate means that terrestrial records of past climate will directly reflect changes in the ocean-atmosphere system, providing important linkages to data obtained from ice and marine sediment cores. The NZ-INTIMATE (Integration of Ice Core, Marine and Terrestrial archives) project was established in 2003 to improve understanding around the nature and timing of climatic events in the New Zealand region since the end of the Last Glaciation (Alloway et al., 2007). A number of palaeoclimate archives including speleothem records, ice core records, lake and marine sediments, and discontinuous records from glacial and fluvial deposits, were used to outline a climate event stratigraphy for New Zealand over the last 30,000 cal. yr BP (Alloway et al., 2007). The main climatic events recognised for the Holocene were

interglacial conditions after a Lateglacial Climate Reversal at ~ 13,500–11,600 cal. yr BP, with two phases of greatest warmth between 11,600 and 10,800 cal. yr BP, and from 6800 to 6500 cal. yr BP (Alloway et al., 2007). After 6500 cal. yr BP the climate exhibited greater variability, with a number of cooler or wetter excursions identified in palaeoclimate proxy records during this time (Alloway et al., 2007). These palaeoclimate events and regional variability are explored in more detail in the following chapters. The following section examines the palaeoclimate of Northland in order to provide the background for further discussion in Chapters 5 to 8.

2.3.4 The Holocene palaeoclimate and palaeovegetation of Northland

The palaeovegetation record of the Northland region has been reconstructed from pollen and sediment profiles obtained from a range of sites (Fig. 2.5), including valley fill wetlands (e.g., D'Costa et al., 2009), raised bogs (e.g., Elliot, 1998), perched dune lakes (e.g., Elliot et al., 1995), maar lakes (e.g., Augustinus et al., 2012; Stephens et al., 2012) and lakes formed when drainage has been impeded by volcanic activity (e.g., Elliot et al., 1997; Elliot et al., 1998; Newnham et al., 2004). These studies show that the vegetation of Northland has varied over the late Quaternary in response to changes in climate and human impact. Palynological records have shown that during the last glacial cycle there was no widespread loss of forest in far northern New Zealand, with the vegetation comprised of mixed beech-conifer-hardwood communities (Dodson et al., 1988; Kershaw and Strickland, 1988; Elliot, 1998). This is in contrast to more southern areas of New Zealand where forest taxa were restricted and vegetation was dominated by shrub-grassland communities (McGlone et al., 1993; Newnham et al., in press), leading researchers to suggest that during glacial stages the Northland region acted as a refuge for warm-temperate plants (Wardle, 1963). Overall, the pollen evidence indicates that the temperature reductions experienced in Northland during the Last Glacial Coldest Period (LGCP), ~ 28,000–18,000 cal. yr BP (Alloway et al., 2007), were less severe than for areas at higher latitudes, and that the climate was most likely drier (Newnham, 1992; Newnham et al., 2004).

The transition from a cooler drier climate associated with the LGCP is recorded in the pollen record as a decline in *Nothafagus* (beech) pollen and other cooler elements, and an increase in the abundance of warmth-loving species such as *Agathis australis* (kauri). Although the timing and pace of this transition varied between sites, in most cases the beech-podocarp-hardwood forest that dominated during the LGCP had given way to podocarp-beech-hardwood dominated communities by the beginning of the Holocene (Newnham, 1992; Striewski et al., 1996; Elliot, 1998). Palynological evidence from Northland sites show that

the presence and abundance of different forest taxa continued to fluctuate throughout the Holocene (Kershaw and Strickland, 1988; Newnham, 1992; Striewski et al., 1996; Elliot et al., 2005). These variations in forest community composition were facilitated by changes in climate throughout the Holocene, and by anthropogenic impacts associated with Polynesian and European settlement in the late Holocene. A review of the pollen records obtained from sites in the Northland area suggests that the Holocene can be broadly divided into four climatic periods. The Holocene subdivision time-frames below are informal zones that have been formulated to discuss the Northland palaeoclimate record presented here. The zones straddle the Early-Middle Holocene boundary at 8.2 ka BP and Middle-Late Holocene boundary at 4.2 ka BP (both linked to a Global Stratotype Section and Point) proposed by Walker et al. (2012). Figure 2.5 shows the location of the study sites discussed in the following sections.

2.3.4.1 Zone 1: Early Holocene (~ 12,000–10,000 cal. yr BP)

The majority of pollen records from the early Holocene suggest that the Northland climate during this time was slightly colder than present day with cooler taxa still well represented in the pollen record (Newnham, 1992; Striewski et al., 1996; Elliot, 1998). Pollen analysis of sediment taken from Kaitaia Bog showed that during the early Holocene the regional vegetation comprised a mixed podocarp-beech-hardwood forest (Elliot, 1998). Pollen evidence from the Johnsons Swamp suggests that up until 10,150 cal. yr BP catchment vegetation was dominated by beech forest and that the area was devoid of kauri (Striewski et al., 1996). At nearby lake Kai Iwi the pollen record also shows that a cooler climate persisted until 9700 cal. yr BP, with beech and hardy podocarps still abundant in the vegetation (Striewski et al., 1996). Pollen and sediment records from sites located farther north on the Aupouri Peninsular also indicate a cooler early Holocene (Dodson et al., 1988; Striewski et al., 1996). Charcoal evidence from lake sites on the west coast of the Peninsula shows that although natural fires did occur during the early Holocene, the frequency of fires could be considered low (Striewski et al., 1996).

2.3.4.2 Zone 2: Early to mid Holocene (~ 10,000–5000 cal. yr BP)

Dodson et al. (1988) described the early to mid Holocene as having the warmest and most mesic environment in the last 17,000 years, based on vegetation records from the Te Paki wetlands (Paranoa and Te Werahi swamps), far northern New Zealand. Palynological evidence from Paranoa swamp identified the period 10,000–6800 cal. yr BP as a period with the highest complexity of forest development (Dodson et al., 1988). Pollen abundance of species with a preference for warmer moister conditions increased, while cooler elements

declined (Dodson et al., 1988). The charcoal record also suggested a moister environment prevailed during the early to mid Holocene, with low levels of charcoal indicating a low natural fire frequency (Dodson et al., 1988).

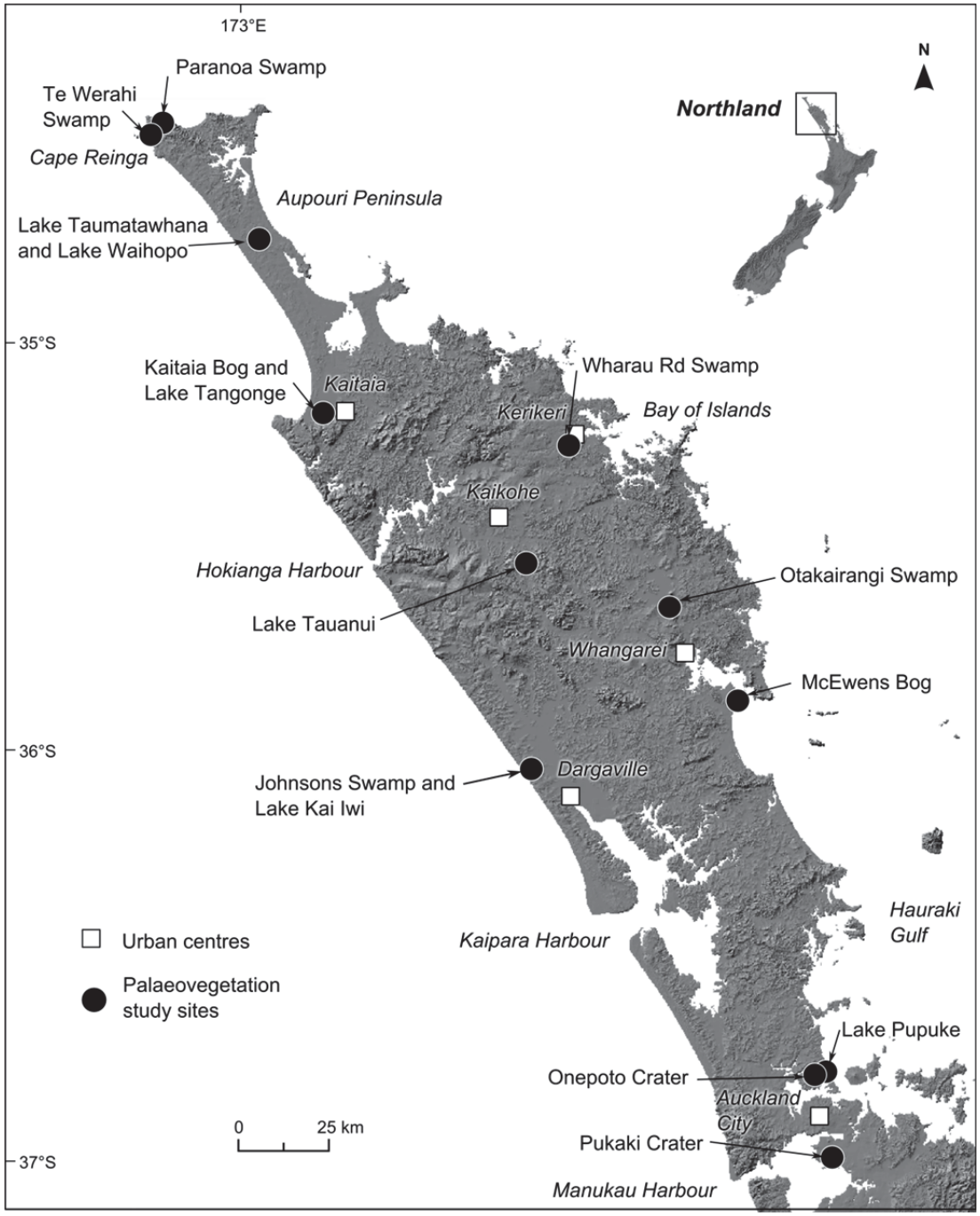

Fig. 2.5. Map of Northland showing the location of the palaeovegetation study sites, Auckland maar craters and the main urban centres.

The majority of the Northland pollen data from other sites tends to support the notion of a warm moist environment during the early to mid Holocene. At Kaitaia Bog there was a rapid post glacial decline in beech from ~ 9500 cal. yr BP and a coincident expansion of kauri, such that beech represented only a minor component of the vegetation by ~ 8000 cal. yr BP (Elliot, 1998). The pollen record from this site also identifies an abundance of *Dacrydium cupressinum* (rimu) and *Metrosideros* sp. during the period ~ 10,500–5000 cal. yr BP (Elliot, 1998). Elliot (1998) also found increases in the abundance of *Dacrycarpus* (kahikatea), an emergent conifer with a preference for moist fertile soils (Wardle, 1991). This abundance of warm loving taxa in the early to mid Holocene, along with low charcoal quantities suggests a warm moist climate prevailed in northern Northland (Elliot, 1998). Charcoal records from Otaikairangi Swamp in central Northland show that natural fires ceased around 8000 years ago, and along with evidence of increasing abundance of kauri, also suggests that the climate at the time was warm and moist (Newnham, 1992).

Pollen records from Lake Waihopo on the Aupouri Peninsula also indicate warmer temperatures, with a forest dominated by podocarps, rimu and kauri, and beech completely eliminated from the record by ~ 7600 cal. yr BP (Striewski et al., 1996). A similar pattern is detected on the west coast of Northland, with vegetation records obtained from Johnsons Swamp indicating that rapid changes in forest composition occurred after ~ 10,150 cal. yr BP, with a transition to a kauri dominated catchment (Striewski et al., 1996). However, the record of kauri dominance at Johnsons Swamp was interrupted around 7000 cal. yr BP with the vegetation showing signs of disturbance, with a temporary disappearance of kauri and emergence of small tree and shrub taxa (Striewski et al., 1996). This sudden decline in kauri pollen may have been the result of the sudden destruction of an over-mature kauri cohort during a storm event (Striewski et al., 1996). At nearby Lake Kai Iwi, the dramatic change from a beech forest to kauri dominance was also detected in the lake sediment palynology, supporting the conclusion of an extended period of postglacial climate amelioration and kauri expansion between ~ 9700 and ~ 2500 cal. yr BP (Striewski et al., 1996).

Pollen evidence from two sites near Kaitaia identify increases in the pollen of the warm-loving species *Ascarina lucida* during the early to mid Holocene warm moist period. At Kaitaia Bog the abundance of *Ascarina* reached a maximum during a warm period between 10,500 and 7600 cal. yr BP (Elliot, 1998). Pollen profiles recovered from Lake Tangonge, located in the same area as Kaitaia Bog, showed a similar trend of maximum *Ascarina* abundance, thought to signify a climate 1–2 °C warmer than present between 10,000 and 7600 cal. yr BP (Elliot et al., 2005).

2.3.4.3 Zone 3: Mid to late Holocene (~ 5000–2000 cal. yr BP)

Evidence from pollen collected from a number of Northland sites and representing the mid to late Holocene suggests that this period was subject to more frequent disturbance and a deterioration in climate. At McEwens Bog on the east coast of central Northland the pollen record indicates that prior to 4000 cal. yr BP the climate was wetter and warmer than today, with rimu the dominant pollen type (Kershaw and Strickland, 1988). After 4000 cal. yr BP increases in beech and podocarps, and declines in some warm-preference taxa after 4500 cal. yr BP, signify a cooler drier climate (Kershaw and Strickland, 1988). This climate trend is also detected in the pollen records of Paranoa Swamp near Cape Reinga (Dodson et al., 1988). At Paranoa Swamp a decline in *Metrosideros* sp. pollen accompanied by slight increases in beech and other cooler preference taxa such as tree ferns, indicates a return to a cooler forest composition between ~ 6800 to 2750 cal. yr BP (Dodson et al., 1988).

At Lake Taumatawhana on the Aupouri Peninsula, palynological evidence also suggests a cooler harsher environment between 5000 and 3400 cal. yr BP, with increases in hardy podocarp pollen type identified (Elliot et al., 1995). At the same site, pollen and charcoal records give some indication that between 3400 and 2600 cal. yr BP the climate conditions were windier and there was increased fire frequency (Elliot et al., 1995). Pollen and sedimentological records from Lake Tauanui also suggest a cooling and drying climate, and a major fire event which damaged the forest and enhanced catchment erosion at ~ 4000 cal. yr BP (Elliot et al., 1998). Pollen evidence of fluctuating abundance of species such as *Ascarina*, kauri and rimu preserved in Lake Tauanui sediments, indicate that the catchment suffered repeated disturbance in the mid to late Holocene (Elliot et al., 1998). Fluctuations in other species such as *Knightia excelsa* (rewarewa) in the Lake Tauanui catchment indicated seral trends associated with forest disturbance, possibly as a result of cyclonic winds and drought from ~ 3500 cal. yr BP (Elliot et al., 1998). Seral trends, with increases in pioneering species such as *Coprosma*, were detected after 4000 cal. yr BP at Wharau Road Swamp on the east coast of central Northland, and were also interpreted as evidence of increased cyclonic activity (Elliot et al., 1997).

Dramatic changes were also identified in the pollen record of Lake Waihopo, when around 3900 cal. yr BP the previous dominance of Podocarpaceae was replaced by increases in sub-canopy species including *Nestegis*, *Griselinia* and grasses (*Poaceae*). Increases in sub-canopy taxa were accompanied by evidence of increased rates of erosion in the catchment (Striewski et al., 1996). Striewski (1996) suggested that apparent increases in canopy openings at Lake Waihopo could be due to storms or natural fires. Results from a 4300 year

palynological record from Wharau Road Swamp, located on the east coast of central Northland, reinforce the notion of a disturbed mid to late Holocene (Elliot et al., 1997). Pollen profiles indicate a cooling and drying climate after 4000 cal. yr BP, characterised by increases in shrub and tree taxa (Elliot et al., 1997). Additional evidence of disturbance in the mid Holocene was detected in the pollen and charcoal records of Te Werahi Swamp, with records showing an increase in fire frequency and changes in forest composition at ~ 4200 cal. yr BP (Striewski et al., 1996).

Pollen records from two sites near Kaitaia, Kaitaia Bog and Lake Tangonge, provide evidence for a more disturbed mid to late Holocene (Elliot, 1998; Elliot et al., 2005). The pollen record of Lake Tangonge for the period between 5000 and 2000 cal. yr BP, shows increases in *Manoao colensoi*, *Podocarpus* and *Prumnopitys taxifolia,* and declines in the warm-preference species *Ascarina* (Elliot et al., 2005). These changes in the catchment forest composition indicate climatic deterioration and a shift to a more seasonal climatic regime, with possible increases in cyclonic events, during the mid to late Holocene (Elliot et al., 2005). At nearby Kaitaia Bog during a similar period, there was an expansion in hardy podocarps and a reduction in the pollen of warmer elements, possibly signalling cooling or drying and an increase in the incidence of summer drought (Elliot, 1998). Evidence from sites located on the west coast of Northland show a similar pattern to those of other Northland studies in terms of describing a more disturbed mid to late Holocene. At Lake Kai Iwi, pollen assemblages changed after 2500 cal. yr BP, with an increased abundance of *Gleichenia* (tangle fern) and *Cyathea* (tree fern) (Striewski et al., 1996). Charcoal peaked at Lake Kai Iwi after 2500 cal. yr BP, and fires also became more common at nearby Johnsons Swamp after 4850 cal. yr BP (Striewski et al., 1996).

2.3.4.4 Zone 4: Late Holocene (~ 2000 cal. yr BP to present)

The late Holocene vegetation record is dominated by anthropogenic impacts associated with Māori and European colonisation, although the earliest date of colonisation continues to be contentious (Sutton et al., 2008). Some Northland sites that have adequate preservation of sediments from the late Holocene show a milder wetter climate in the late Holocene before anthropogenic impacts began to influence the vegetation. At Wharau Road Swamp the pollen record revealed a peak in kauri pollen at ~ 1800 cal. yr BP and increases in rimu, *Ascarina* and tree fern from ~ 2000 cal. yr BP, consistent with a warmer moister climate (Elliot et al., 1997). Peaks in the abundance of kauri were also identified at Lake Taumatawhana and, along with the expansion of *Ascarina* and rimu between 2600 and 900 cal. yr BP, suggest an amelioration in climate in the late Holocene (Elliot et al., 1995). Changes in the forest taxa of Lake Tauanui catchment during the same period were more

indicative of disturbance resulting from increased cyclonic activity rather than significant changes in climate (Elliot et al., 1998). From 1850 cal. yr BP increases in the abundance of pollen from understorey trees and shrubs suggested increasing frequency of disturbance events, with the lack of charcoal lending support to the argument that cyclonic activity was responsible (Elliot et al., 1998). Elliot et al. (1998) ruled out the possibility that humans were impacting the vegetation at this time because of the absence of *Pteridium* and microscopic charcoal in the record.

Late Holocene pollen records from Lake Tauanui identify a date of ~ 1000 cal. yr BP for anthropogenic disturbance, as characterised by declines in all shrub and tree taxa, increases in charcoal and the abundance of *Pteridium* spores (Elliot et al., 1998). At Wharau Road Swamp the date for major anthropogenic forest disturbance was ~ 600 cal. yr BP, marked by a reduction in tree and shrub elements, coinciding with an influx of charcoal and a rise in *Pteridium* spores (Elliot et al., 1997). Pollen records from Lake Taumatawhana suggests that Polynesian deforestation began after ~ 900 cal. yr BP (Elliot et al., 1995). Pollen records show that there was a further major decline in all taxa and increases in the abundance of herbs after the arrival of Europeans to the area (Elliot et al. 1998). The arrival of introduced taxa such as *Cupressus* and *Pinus* in the pollen record marks the beginning of European influence, and at Lake Taumatawhana this occurred for the first time after 250 cal. yr BP (Elliot et al., 1995).

2.3.4.5 Auckland maar lake records

Another source of palaeoenvironmental information for the Northland region are the sedimentary archives obtained from a group of maar craters (Onepoto Crater, Pukaki Crater and Lake Pupuke) within the Auckland Volcanic Field of the northern North Island. These analyses have provided evidence for climate variability during the Holocene (e.g., Sandiford et al., 2003; Horrocks et al., 2005; Augustinus et al., 2008; Augustinus et al., 2012; Stephens et al., 2012). Auckland maar lake sediments comprise organic-rich finely laminated sequences and well-dated tephra horizons, thereby providing a high-resolution millennial- to centennial-scale record of changing climate and catchment hydrology for this region (Sandiford et al., 2003; Horrocks et al., 2005; Augustinus et al., 2008; Augustinus et al., 2012; Stephens et al., 2012). However, most of the Auckland maar lakes experienced marine-breaching associated with postglacial sea-level rise in the early Holocene (Sandiford et al., 2003; Augustinus et al., 2012), and a continuous Holocene record is limited to Lake Pupuke (Horrocks et al., 2005; Augustinus et al., 2008; Stephens et al., 2012). Pollen records from Pukaki Crater prior to breaching indicate an ameliorating climate between 11,500 and 7800 cal. yr BP, with vegetation signalling fewer frosts (Sandiford et al., 2003). The

palaeovegetation record from Onepoto maar also suggest a moist and mild early Holocene climate, characterised by podocarp conifer forest (Augustinus et al., 2011) and stable high lake levels between ~ 12,500 and 10,500 cal. yr BP (Augustinus et al., 2012). At nearby Lake Pupuke, increased organic sedimentation from 10,200 cal. yr BP marks the onset of an early Holocene warm period and limited seasonality between 10,200–7600 cal. yr BP (Stephens et al., 2012), which broadly correlates with the timing of a warm moist climate detected in the other palaeovegetation records from Northland. Evidence of thermal stratification in the geochemical record at Lake Pupuke from 5700 cal. yr BP marks the onset of seasonal thermal stratification and eutrophication, thought to be a consequence of increased seasonality (Stephens et al., 2012). Further intensification in seasonality after 3200 cal. yr BP was also linked to changes in the lake biomass (Stephens et al., 2012). This mid to late Holocene shift to a more seasonal climate regime was also detected in palaeovegetation records located farther north.

2.3.4.6 Kauri dendroclimatology

Tree-ring chronologies developed from subfossil kauri extracted from bog sites in northern New Zealand offer significant potential as a palaeoclimate proxy (Boswijk et al., 2006; Palmer et al., 2006; Fowler et al., 2008b; Turney et al., 2010) and have been used to reconstruct the past climate of the Northland region (e.g., D'Costa et al., 2009; Fowler et al., 2012). New Zealand kauri (*Agathis australis*) is a climatically sensitive large long-lived canopy-emergent tree found between the latitudes of 34–38°S in northern New Zealand (Poole and Adams, 1986). Of particular potential is the kauri tree-ring growth record as a proxy for the ENSO phenomenon (Fowler et al., 2008a). Studies have shown that kauri growth is sensitive to regional atmospheric circulation forcing associated with the operation of ENSO (Fowler et al., 2005, 2008a). During El Niño events the growth of kauri is enhanced, producing wide growth rings, while narrow kauri growth rings are correlated with La Niña phases of the Southern Oscillation (Fowler et al., 2012). An ENSO proxy record for the last 700 years, constructed from a kauri master chronology, highlighted ENSO variance in the New Zealand region, possibly due to centennial-scale fluctuation in ENSO activity or changes in the ENSO teleconnection (Fowler et al., 2012).

2.3.5 Intercomparison of palaeoclimate proxy records

In recent decades there has been a focus by palaeoclimate scientists on improving knowledge of the temporal and spatial patterns of climatic and environmental changes through compilation, intercomparison and synthesis of climate proxy records, and development of regional climate event stratigraphies. Scientific groups have been formed to

review past climate change at different regional and temporal scales including: INTIMATE (INtegration of Ice core, Marine, and Terrestrial records) projects in New Zealand (Alloway et al., 2007), Australia (Turney et al., 2006), Australasia (Reeves et al., 2013) and North Atlantic (Björck et al., 1998); and the PAst Global Changes 2k Consortium (PAGES, 2013). The NZ-INTIMATE group identified key offshore and onshore well-dated proxy records for New Zealand, both continuous high resolution records (i.e., cores) and fragmentary records (i.e., fluvial and glacial deposits), that could be tephrochronologically linked. The result of this compilation was a climate event stratigraphy for New Zealand for the last 30,000 years (Fig. 2.6) that can be used to identify regional widespread climatic events and provide a reference by which other proxy records can be compared (Alloway et al., 2007; Barrell et al., 2013). Such records are vital for developing a better understanding of the patterns, processes, and drivers of natural climate variability.

There are a number of issues and challenges associated with the correlation and comparison of palaeoclimate proxy records, including; inherent limitations of each proxy type, lack of robust chronology, complexity in interpreting individual proxy records and regional complexity. For example, stable isotope records from speleothems are a widely used proxy for temperature and precipitation. However, non-climatic effects such as soil moisture residence times, non-linear growth rates, hiatuses, shifts in the source moisture, CO_2 degassing and local cave processes, can make interpretation of results in relationship to climatic variables problematic. Palynological investigations have their own suite of problems centred around the preservation and production of pollen, and what fluctuation in the abundance of different pollen types actually means climatically or environmentally. In Northland, the palaeoclimatic significance of kauri pollen abundance was called into question by D'Costa et al. (2009) who found that the amount of kauri pollen was mostly influenced by the wetness of the substrate rather than the proximity to the source. In the case of glacial sequences, there remains debate as to what climatic variables, whether it be atmospheric temperature or precipitation, are driving glacier behaviour (Rother and Shulmeister, 2006).

In addition to the complexity created by the limitations associated with individual proxy records and their palaeoclimate interpretation, is the high level of regional variation in climate created by New Zealand's latitudinal span and orography. Palaeoclimate proxy records reflect not only the strong regional contrasts in climate at the level of the coherent precipitation region, but local scale disturbance and the effect of microclimates will also be involved. Approaching palaeoclimate reconstructions using coherent precipitation regions (Kidson, 2000) is one way of accounting for regional variability, although strong regional

difference in climate will be challenging when attempting to make inter-regional comparisons. Also adding to the difficulty of correlating palaeoclimate records from different regions and sources is that the climatic changes being inferred from Holocene proxy records are small compared to the relatively large magnitude climate changes associated with the Last Glacial-Interglacial transition and major climate events such as the Antarctic Cold Reversal and Late glacial cool episode (formerly referred to as the Late Glacial climate reversal), the timing of which have only recently been revised (Barrell et al., 2013; Lowe et al., 2013). The palaeoclimate record of Northland is limited to palynological studies and palaeoclimate inferences are being made based on only subtle vegetation changes, which means that intersite comparisons can be difficult.

The lack of precise and accurate dating control in palaeoclimate records can be an obstacle for robust interrogation of palaeoclimate datasets and comparisons. New Zealand is fortunate to have 24 widespread well-dated tephra marker beds covering the last 30,000 years. Thirteen of these prominent tephras are from eruptions that occurred during the Holocene, and a number of these coincide with significant environmental or climatic events (Table 2.1). These tephra provide a means of chronostratigraphically linking and dating palaeoenvironmental records.

Given the limitations outlined above, a straightforward relationship between different proxies when making comparisons should not be expected. The complexity created by a strongly regionalised climate in New Zealand, along with only relatively subdued Holocene climatic variability (when compared with the Last Glacial-Interglacial transition), means that the most that be expected from intercomparison between records at both a local and regional scale is the detection of broad scale patterns and regionally extensive perturbation. Vegetation records from Northland will reflect environmental change signals that range from the local scale (i.e., catchment) to potentially global scale climate events.

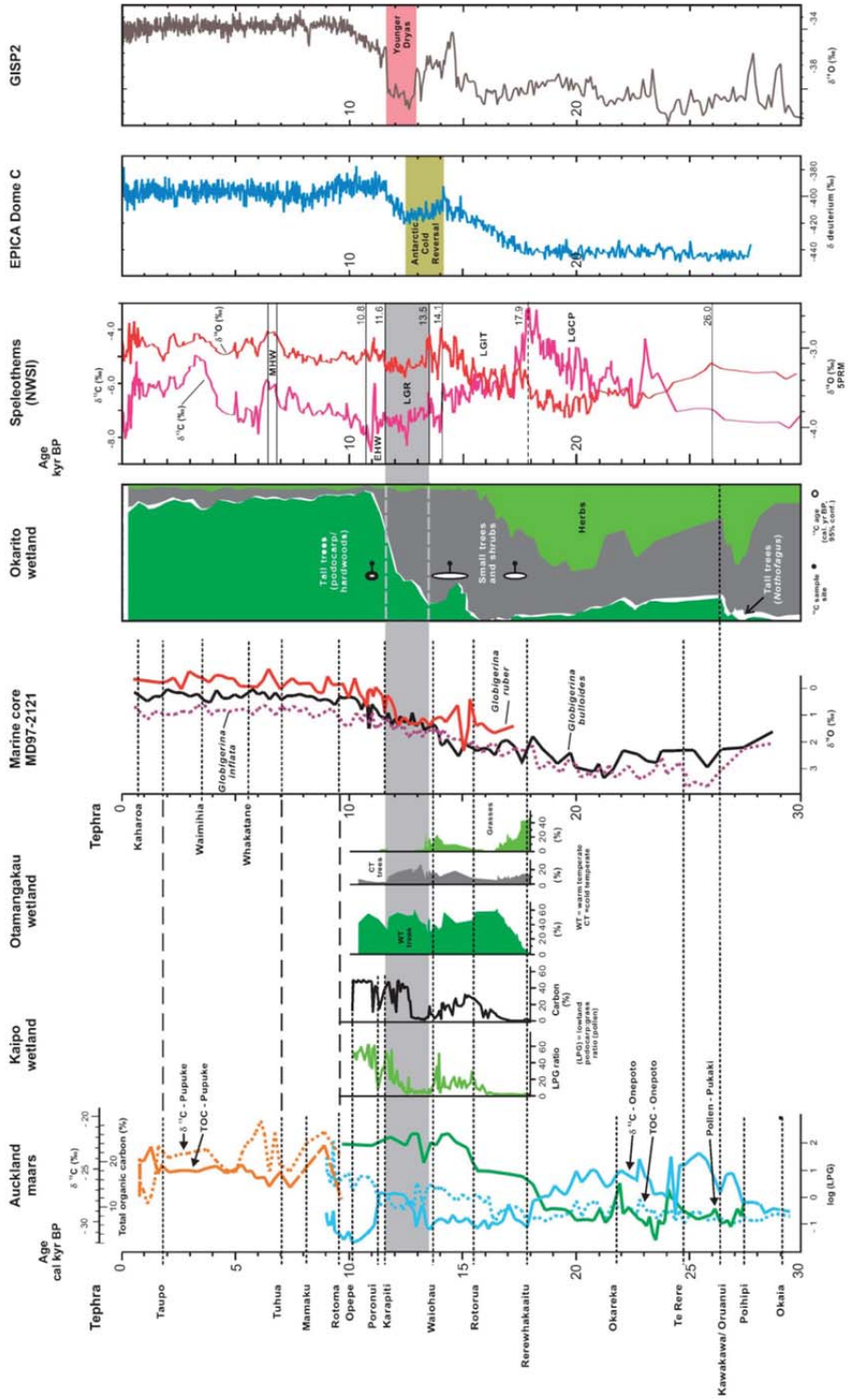

Fig. 2.6. Compilation of palaeoenvironmental records and a climate event stratigraphy linked by key tephra for the last 30,000 cal. yr BP from Alloway et al. (2007). Records displayed include: Antarctic (Dome C) and Greenland (GISP2) ice core records; northwestern South Island speleothem stable isotope records; pollen and total organic carbon records from Auckland maars, Okarito, Otamangakau and Kaipo wetlands; and foraminifera records from marine core MD97-2121. Major climate events are: the Last Glacial Coldest

Period (LGCP) beginning at ca. 28,000 cal. yr BP and ending at Termination I ca. 18,000 cal. yr BP; Last Glacial Interglacial Transition (LGIT) between ca. 18 000 and 11 600 cal. yr BP, including a Lateglacial reversal (LGR) between ca. 13,500 and 11,600 cal. yr BP; and Holocene interglacial condition, with an early Holocene warm episode (EHW) between ca. 11,600 and 10,800 cal. yr BP (EHW) and a mid Holocene warm episode (MHW) from ca. 6800 to 6500 cal. yr BP; and more variability in temperature and precipitation expressed after ca. 6500 cal. yr BP.

Table 2.1

Age models for key tephras in New Zealand erupted during the Holocene and coincidence with important environmental or climatic changes.

Tephra	Source[a]	Calibrated age range (cal. yr BP 2 σ confidence)	Basis of age determination	Source	Coincident significant environmental change
Kaharoa	OK	624–648	Wiggle-match on log	Lowe et al. (2013)	late Holocene warm event (ca. 900 to 500 cal. yr BP) and earliest polynesian settlement datum[b]
Taupo	TP	1708–1728	Wiggle-match on log	Lowe et al. (2013)	Pre-human datum (Hogg et al., 2012)
Waimihia	TP	3293–3516	Wiggle-match on peat	Lowe et al. (2013)	
Unik (K)	TP	4901–5321	Wiggle-match on peat	Lowe et al. (2013)	
Whakatane	OK	5381–5671	Wiggle-match on peat	Lowe et al. (2013)	
Tuhua	TU	6030–7124	Wiggle-match on peat	Lowe et al. (2013)	Mid-Holocene cooling and variability (after ca. 6500 cal. yr BP)[b]
Mamaku	OK	7683–8197	Wiggle-match on peat	Lowe et al. (2013)	North Atlantic cold event ca. 8.2 cal. yr BP (Alley et al., 2007) and Early Holocene-Middle Holocene boundary proposed by Walker et al. (2012)
Rotoma	OK	9303–9543	Wiggle-match on peat	Lowe et al. (2013)	
Opepe (E)	TP	9831–10,151	Wiggle-match on peat	Lowe et al. (2013)	
Poronui (C)	TP	11,055–11,285	Wiggle-match on peat	Lowe et al. (2013)	
Karapiti (B)	TP	11,288–11,632	Wiggle-match on peat	Lowe et al. (2013)	
Okupata	TG	11,575–11,959	Wiggle-match on peat	Lowe et al. (2013)	Early to mid Holocene warming (ca. 11,600–6500 cal. yr BP)
Konini (bed b)	EG	11,697–12,063	Wiggle-match on peat	Lowe et al. (2013)	Pleistocene-Holocene boundary (Walker et al., 2009)

[a]OK, Okataina Volcanic Centre; TP, Taupo Volcanic Centre; TU, Tuhua Volcanic Centre; TG, Tongariro Volcanic Centre; EG, Egmont Volcano.

[b]New Zealand climate event stratigraphy (Alloway et al., 2007).

2.3.6 Comparison between Northland and New Zealand Holocene palaeoenvironment records

To date, the most comprehensive review of New Zealand palaeoenvironmental proxy records which has covered the Holocene period has been by Alloway et al. (2007). The climate event stratigraphy derived from a range of terrestrial, marine and ice core records has recently been updated using subfossil pollen records from western South Island, Pukaki Crater in northern North Island and Kaipo Bog in eastern North Island (Barrell et al., 2013). A regional composite stratotype has been proposed for the last 30,000, but the youngest limit is 12,000 cal. yr BP, and no attempt has been made to define a type section for the Holocene Interglacial (defined as climate event NZce-1; Barrell et al., 2013) due to a lack of a suitable published record. A definitive climate event stratigraphy for the Holocene is still a work in progress. Although the climate variability of the Holocene has yet to be determined, Alloway et al. (2007) and Barrell et al. (2013) have identified some significant periods: Early to mid Holocene warming between ca. 11,600 and 6500 cal. yr BP (Alloway et al., 2007), two episodes of greatest warmth at ca. 11,500–10,800 cal. yr BP and ca. 6900–6500 cal. yr BP (Williams et al. 2010), increased climate variability (temperature and precipitation fluctuations) after ca. 6500 cal yr BP (Alloway et al., 2007; Barrell et al., 2013), and a Late Holocene warm event at ca. 900–500 cal. yr BP (Alloway et al. 2007; Barrell et al., 2013).

The review of palaeoenvironment records from Northland in section 2.3.3 identified four broad climate zones during the Holocene. In Northland, the early to mid Holocene warming identified for New Zealand appears to have commenced slightly later (around ca. 10,000 cal. yr BP) and there is no indication of a prominent warm episode in the early Holocene. The pattern of a cooler early Holocene climate is consistent with glacier records from the Southern Alps that show cooler summer temperatures in the early Holocene, with the largest Holocene glacier extent at 10,690–9870 years ago (Putnam et al., 2012). After ca. 10,000 cal. yr BP the majority of the Northland palynological records suggest a warm moist climate prevailed, agreeing with wider New Zealand records of Holocene warming, although there is no evidence of a prominent mid Holocene warm episode (ca. 6900–6500 cal. yr BP; Williams et al., 2010). Between 5000 and 2000 cal. yr BP the paleovegetation record of Northland indicates more disturbance and/or cooling, which is concordant with a pattern of increased climatic variability in New Zealand since the mid Holocene (ca. 6500 ca. yr BP; Alloway et al. 2007 and reference therein). The late Holocene warm event (ca. 900–500 cal. yr BP) described by Alloway et al. (2007) and Barrell et al. (2013) is not detected in the Northland palaeoclimate records, although it does occur within a timeframe (2000 cal. yr BP

to present) where there was evidence that climate was warmer and wetter prior to the first anthropogenic impacts being recorded (Elliot et al., 1995; 1997).

As in other parts of New Zealand, the deposition of the Kaharoa tephra in Northland immediately precedes the earliest evidence for anthropogenic deforestation (increases in *Pteridium* spores and charcoal) at a number of sites (e.g., Alloway et al., 2007; Elliot et al., 1997; Newnham et al., 2004). At Lake Omapere in central Northland the Kaharoa tephra dates the formation of the lake due to damming and accelerated soil erosion exacerbated by Polynesian deforestation in the catchment. Father south at Lake Pupuke in Auckland, the Rangitoto tephra pre-dates Polynesian settlement (ca. 610 cal yr BP) by 60 years (Striewski et al. 2009). Three other key tephra marker horizons are also present at the Lake Pupuke site, Rotama, Tuhua and Taupo, but none are not associated with any other stratigraphic changes that would signal significant environmental change.

Regional complexity and the inherent issues associated with individual paleoenvironmental proxies makes it difficult to compare records and build up a coherent picture of Holocene climate variability in New Zealand. There has been a concerted effort by dedicated working groups such as NZ-INTIMATE (Alloway et al. 2007) to document a general sequence of climatic events for New Zealand over the last 30,000 years, but to-date the picture for the Holocene remains largely unresolved, with only broad climate episodes or trends differentiated at this stage. Palaeoenvironmental proxy records for Northland are largely limited to pollen-based studies, reflecting environmental changes across a range of spatial and temporal scales. The pattern of climate variability identified in Northland are generally concordant with studies from other New Zealand regions, that is an ameliorating early to mid Holocene, more variability in the mid to late Holocene, and late Holocene anthropogenically-driven environmental change. Of the thirteen Holocene aged key maker tephras used to link regional palaenvironment records in New Zealand (Table 2.1) only the Kaharoa Tephra has been widely identified and referred to in Northland palaeoenvironmental studies.

2.4 Summary

Palaeoclimate research has highlighted the natural variability of climate during the Holocene, forced by a number of different factors, feedbacks and teleconnections, involving rapid changes in the interconnected climate system across a range of spatial and temporal scales. Evidence from globally distributed palaeoclimate data has shown that climate during the Holocene has been variable. New Zealand, located in close proximity to a number of major

oceanic and atmospheric circulation boundaries, and influenced by both tropical and polar oscillatory climate modes (ENSO and SAM), is well positioned to explore Holocene climate dynamics. Palaeoclimate records from New Zealand and the Northland region show that Holocene climate has varied, with records from northern New Zealand indicating that the Holocene can be broadly divided into four climatic periods. The existence of global climate signals and the extent to which climate changes are globally synchronous still remains a major area for investigation, and more high resolution terrestrial Holocene palaeoclimate records from New Zealand are required.

River systems have been shown to be responsive to environmental perturbation and climate change (e.g., Macklin et al., 2012a), with fluvial sediments preserving a record of river behaviour. The following chapter examines fluvial response to Holocene environmental change (that includes climate change) globally, and in New Zealand, and the potential of the fluvial archive for exploring environmental change and climate dynamics.

Chapter 3

Fluvial response to Holocene environmental change

3.1 Introduction

Chapter 2 highlighted the natural variability of climate during the Holocene, Hemispherically and in the New Zealand region, as influenced by a number of different factors, feedbacks and teleconnections operating within the interconnected climate system. Fluvial systems respond to environmental change (including climate), and fluvial sediments preserve a record of how a river has responded to environmental change over time, creating an archive that can be used to explore the relationship between river system behaviour and external environmental influences (e.g., Starkel, 1983; Passmore et al., 1992; Ely et al., 1993; Knox, 1993; Tipping, 1994; Rumsby and Macklin, 1996; Knox, 2000). Like many natural systems, fluvial environments exhibit a high degree of complexity and dynamism, with sediments transported and deposited within the catchment, continually creating and eroding landforms over a range of spatial and temporal scales. This chapter outlines the key mechanisms involved in driving Holocene river response, the nature of river response to environmental perturbation and the way in which fluvial systems record environmental changes. The chapter also reviews the state of knowledge as to how New Zealand rivers have responded to environmental change signals during the Holocene.

3.2 Factors affecting change in the fluvial environment

River morphology is conditioned by the interaction between the sediment and flow regime operating within the constraints imposed by the boundary conditions (Newson, 2002). Fig.

3.1 illustrates the relationship between the sediment-flow regime and the aggradational-degradational balance of river systems. The nature of river response, whether it is aggradation or degradation, is influenced by the size and volume of sediment, and the sediment transport capacity. For any given reach, under conditions of steep slopes and increased discharge the balance will tilt towards degradation (Fig. 3.1). Alternatively, river behaviour will tend towards aggradation when the reach is transport-limited and subject to increased sediment load (Fig. 3.1). The sediment transport regime of a river can be influenced by both external (allogenic) and internal (autogenic) controls, thereby forcing a fluvial response. Allogenic controls involved in driving adjustment in the fluvial system include anthropogenic land-use change, climate change, base-level change, and tectonic and volcanic activity. Autogenic processes also operate within the fluvial system, driving changes in the erosion and deposition of sediment, independently of external control.

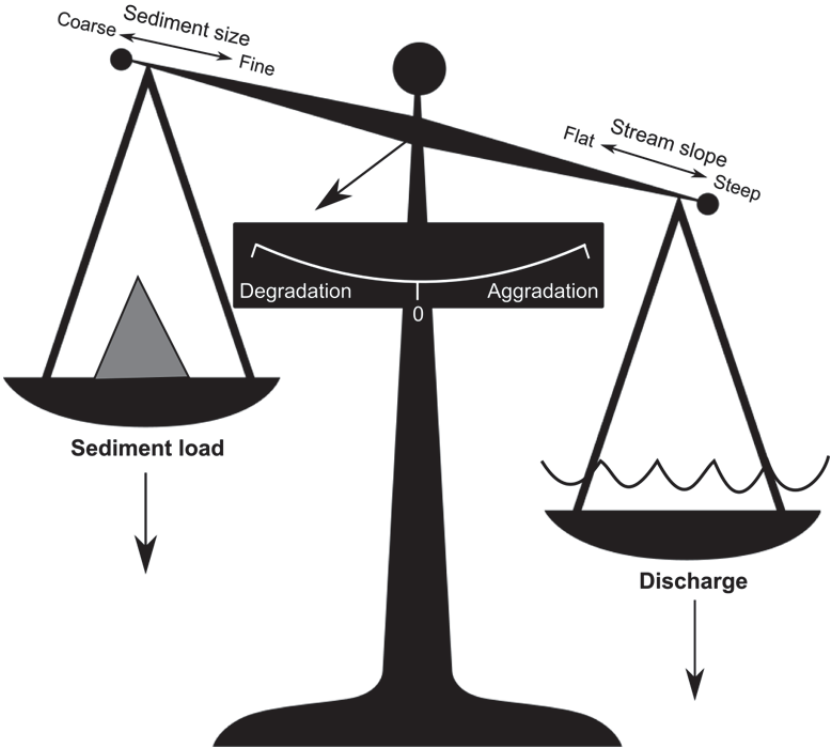

Fig. 3.1. The flow-sediment balance of rivers. Adapted from Brierley and Fryirs (2005). Originally E.W. Lane cited in Chorley et al. (1984).

3.2.1 Allogenic controls

A number of external environmental changes have the potential to influence the hydrological and sediment regime of a river system, including: climate change, anthropogenic activities and land-use change, sea-/base-level change, and volcanic and tectonic activity.

3.2.1.1 Land-use change

In fluvial geomorphology there has been a strong focus on the role that climate and human activity have played in driving river behaviour during the Holocene (Starkel, 1983; Knox, 1993; Macklin and Lewin, 1993; Rumsby and Macklin, 1996; Fuller et al., 1998; Hoffmann et al., 2008). Many authors have documented a close relationship between human-induced increases in sediment yield and runoff, which has led to valley floor alluviation (e.g., Harvey et al., 1981; Macklin and Lewin, 1986; Passmore and Macklin, 1994; Tipping, 1994). Studies from sites in the UK and Ireland, which has a long history of human occupation, suggest that Holocene land-use change has contributed to: slope instabilty and valley floor alluviation in upland and lowland catchments, increased runoff and alteration in the water table in lowland catchments (Foulds and Macklin, 2006 and references therein), and phases of accelerated river incision (Macklin et al., 1992b; Macklin et al., 2012b). Holocene alluvial terrace sequences and debris fan sedimentation have also been linked to human settlement and changes in agricultural practices (e.g., Macklin and Lewin, 1986; Robertson-Rintoul, 1986; Brazier et al., 1988; Macklin et al., 1991). For example, in the Howgill Fells of upland Britain, it was suggested that a phase of soil erosion, debris cone development and gully incision occurred as a result of the establishment of sheep farming around 1000 years ago (Harvey et al., 1981). Studies of sites in upland Britain also show distinct phases of valley floor alluviation associated with Bronze Age deforestation and coal mining (Macklin et al., 1991). In regions where intensive human settlement has been restricted to the last few hundred years, the geomorphic response to anthropogenic impacts can also be marked (e.g., Brooks and Brierley, 1997; Knox, 2006; Damm and Hagedorn, 2010). The behaviour of the upper Mississippi River following Euro-American deforestation typifies the fluvial response to land-use change, with a tenfold acceleration in floodplain sedimentation identified (Knox, 2006).

3.2.1.2 Climate change

Climate change, as a driver of erosion and sedimentation in the fluvial environment, has also been a major strand of enquiry in fluvial research over the last two decades. The idea that rivers respond to climate through changes in flood frequency and magnitude replaced early

paradigms that viewed long-term Holocene river dynamics as predominantly anthropogenically forced. A large body of research has recognised the impacts that millennial- and centennial-scale climate change has had on Holocene river behaviour (e.g., Knox, 1993; Macklin and Lewin, 1993; Rumsby and Macklin, 1994; Anderson et al., 2004; Macklin et al., 2005). Research of this type linked episodes of increased floodplain sedimentation with climatic deterioration detected in independent palaeoclimate proxy records, such as mire surface wetness and fossil pollen (e.g., Macklin and Lewin, 1993; Anderson et al., 2004). In these scenarios the fluvial record was thought to reflect the interplay between climate and cultural controls, with land use playing a key role in altering the sensitivity of river catchments to climatic perturbation (Macklin and Lewin, 2003).

In the last ten years there has been an increased emphasis on the role of climate in river dynamics, reinvigorated by a need to improve our understanding of global Holocene climate dynamics, and the requirement for better models of how river systems will respond to predicted anthropogenically-forced climate change. Central to this more global approach to elucidating the timing and controls of river behaviour during the Holocene, has been the increase in radiocarbon (^{14}C)-dated fluvial deposits and the development of the meta-analysis methodology (Macklin et al., 2012b). Fluvial ^{14}C databases have been compiled and analysed in a growing number of regions to elucidate the role of climate change and human impact on Holocene fluvial environments (e.g., Starkel et al., 2006; Thorndycraft and Benito, 2006b; Hoffmann et al., 2008; Zielhofer and Faust, 2008; Harden et al., 2010; Macklin et al., 2010; Turner et al., 2010; Macklin et al., 2012a).

The most recently reconstructed UK fluvial record was compared with proxy climate data from Britain and Europe, including the North Atlantic drift-ice index, peatland palaeoclimate records in northern England and European glacier advance chronologies. Correlations between the UK flood record and North Atlantic drift ice index indicated that phases of instability and increased flooding during the Holocene can be linked to a cooler climate in the North Atlantic (Macklin and Lewin, 2003; Macklin et al., 2005; Macklin et al., 2006; Macklin et al., 2010). Fluvial records from Ireland also detect underlying climate forcing of river behaviour, with major Holocene flooding coincident with cool and wet climatic conditions in the North Atlantic and UK (Turner et al., 2010).

Analysis of fluvial deposits in Poland identified multiple phases of increased fluvial activity from between 200 and 1000 years duration, during the last 14,000 years (Starkel et al., 2006). These results correlated well with other hydro-climate proxy records, including: lake water levels, vegetation changes, ground water level fluctuations and phases of landsliding and

debris flows (Starkel et al., 2006). The clusters of flood events in the Polish fluvial record correspond to periods when a cooler and wetter climate prevailed over central Europe, associated with phases of lower solar activity (Starkel et al., 2006). The highest peaks in river activity, as identified by overbank floodplain deposition, were thought to be mainly associated with agricultural expansion (Starkel et al., 2006).

In Spain ^{14}C dates obtained from slackwater flood deposits, overbank facies and in-channel units, identified two major phases of alluviation and three periods of increased flood frequency (Thorndycraft and Benito, 2006b). The timing of the earliest periods of flooding and alluviation in the Spanish record corresponds with cooling in the North Atlantic, thought to be the result of reduced solar activity (Thorndycraft and Benito, 2006b). The most recent alluviation phase was most likely driven by land-use changes in the catchment (Thorndycraft and Benito, 2006b). The German fluvial archive also shows that episodes of enhanced river activity occur during periods characterised by a cooler and/or wetter climate (Hoffmann et al., 2008). However, in recent millennia increasing population and agricultural expansion has meant that phases of increased fluvial activity cannot be wholly attributed to climate, with human impact in the last ~ 1000 years considered to be the most dominant forcing mechanism driving river response (Hoffmann et al., 2008).

In contrast to the European model, which indicates an enhanced river response to cooler and wetter climate, compilation and analysis of over 700 ^{14}C dates from alluvial and bedrock river systems in southwestern USA show a relationship between increased flood probability and cooler and drier climatic conditions (Harden et al., 2010). The authors suggest that meteorological factors, such as southward displacement of the jet stream with associated cooler conditions and more winter storms, may play a role in generating increased flooding (Harden et al., 2010). In addition, interactions between reduced precipitation, vegetation changes and potential for increased runoff and sediment flux, may also be involved in driving regional river dynamics (Harden et al., 2010).

The meta-analysis approach not only provides a methodology by which river behaviour can be compared to other long-term records of factors that may control that behaviour, but also provides a means of inter-regional comparisons. This has recently been achieved with a probability-based hydroclimate series constructed from New Zealand and UK fluvial sedimentary archives, (Macklin et al., 2012a). In this work cross-correlation analysis was performed on probability time series representing the flood record in order to assess the statistical significance of the relationship between the timing of flooding in the UK and New Zealand. This work makes a significant contribution to understanding a key question in

palaeoclimate research as to the nature of the inter-hemispheric phase relationship of short-term Holocene climate change (cf. Chapter 2). Results from this analysis suggest that major episodes of flooding, thought to be controlled by changes in the frequency of extreme precipitation events due to large-scale atmospheric changes, are predominantly out of phase between the UK and New Zealand (Macklin et al., 2012a).

3.2.1.3 Volcanic activity

Explosive volcanic eruptions and decay of volcanic cones can have major hydrological, sedimentological and geomorphological impacts on the landscape and its river systems (e.g., Meyer and Martinson, 1989; Lucchitta et al., 2000; Manville, 2002). Explosive eruptions damage and destroy hillslope vegetation, leading to increased runoff which amplifies peak flow discharges (Major, 2003). The deposition of large quantities of easily erodible tephra on hill slopes, in valleys and in channels, disrupts drainage patterns and modifies channel size and shape (Collins and Dunne, 1986; Manville, 2002), facilitating dramatic post-eruptive changes in sediment transport that can last for decades (Major et al., 2000; Manville et al., 2005). Rivers that drain volcanically disturbed landscapes can have extremely high sediment yields due to unlimited sediment supply (Hayes et al., 2002). Channel response to eruptions can involve a complex sequence of post-eruptive adjustments including channel initiation, channel widening, aggradation and incision (Meyer and Martinson, 1989; Manville et al., 2005). Climate also plays a role in controlling the rate, efficiency and type (i.e., debris flow or fluvial transport) of sediment transport within post-eruptive catchments (Hayes et al., 2002; Major, 2003).

3.2.1.4 Base-level change and tectonic activity

River system base-level can be defined as the lower limit to which a river can transport sediment and erode a surface. In most cases base level is also sea level, however, local base level can also be influenced by artificial structures (i.e., dams), lakes and geological controls (e.g., changes in lithology, active faults). Base-level change can be caused by tectonic subsidence or uplift as well as vertical eustatic sea-level movement. Changes in base level alter the balance of erosion and deposition processes operating within the fluvial environment, thereby promoting a response. At its simplest, fluvial response to base-level change involves either aggradation or incision as the river adjusts to a new equilibrium profile (Lane, 1955). However, as Schumm (1993) concluded, there are many factors that contribute to the complexity of river response to changes in base level, including: the direction, duration, magnitude and rate of base-level change, geologic controls (e.g., lithology), valley morphology and potential for adjustment, and alluvium characteristics.

The interaction of these controls ensure varied responses to base-level change across different river systems that range from: knickpoint migration (Crosby and Whipple, 2006) and rapid incision of bedrock channels in tectonically uplifted catchments (Reinhardt et al., 2007), incision and terrace development in alluvial systems in response to lake level lowering (Adams, 2012), fluvial aggradation and avulsion controlled by sea-level rise (Törnqvist, 1994) and changes in channel pattern, shape or channel roughness as a result of minor changes in the base-level (Schumm, 1993).

In addition to the effects that tectonic uplift has on river base-level, tectonic activity also impacts on river dynamics through the enhancement of sediment supply. Tectonic uplift increases basin relief and slope instability, influencing catchment sediment flux (e.g., Quigley et al., 2007). Earthquakes can trigger landslides which mobilise large quantities of sediment that can be transported to the channel during subsequent rainfall events (e.g., Dadson et al., 2004).

3.2.1.5 Nonlinearity and differential response

In the fluvial system there is often not a straightforward cause-and-effect relationship between environmental perturbation and river response. Fluvial systems, like many geomorphic systems, can exhibit nonlinear behaviour in response to external forcing (Coulthard and Van De Wiel, 2007). Nonlinear dynamics, whereby system outputs are disproportionate to system inputs (Phillips, 2003), have been identified in a number of different fluvial processes, including: bed load transport (Gomez and Phillips, 1999), avulsion frequency (Ashworth et al., 2004) and meander behaviour (Hooke, 2003).

The causes of nonlinearity in fluvial systems include factors such as thresholds, self-limiting processes, hysteresis, storage effects, saturation and depletion effects (Phillips, 2003). Geomorphic thresholds can be external or internal, and have been defined as the condition at which point there is abrupt geomorphic change in response to progressive change in external controls, such as climate, base level or land use (Schumm, 1979). Vandenberghe (1995) found that at the centennial scale nonlinear river response to climate change was attributable to thresholds (including climatic, landform and sedimentary thresholds). The operation of thresholds in river systems means that not all environmental perturbations will promote a geomorphic response, with the potential of a river to respond to a disturbance event dependent on river sensitivity and the proximity to threshold conditions (Brierley and Fryirs, 2005). Cyclic floodplain evolution, as described by Nanson (1986), provides an example of nonlinear river response, involving thresholds and self-limiting processes. In this case, progressive floodplain aggradation has occurred, to a point where the floodplain is no longer

regularly inundated, followed by a threshold breach and catastrophic floodplain stripping. Nonlinear behaviour in fluvial systems can also be attributed to hysteresis, storage, saturation and exhaustion effects. An example of these effects is annual hysteresis in a gravel bed river where for a given flow rate, more bedload is transported prior to a threshold flow than following it, due to threshold driven sediment exhaustion (Moog and Whiting, 1998).

The consequence of nonlinear fluvial response, and the influence of factors such as thresholds, fluvial system history, self-limiting and storage affects, is that not all rivers will respond in the same way (spatially or temporally) to environmental change. River response can be lagged as older deposits are reprocessed (e.g., Macklin and Lewin, 2003). For example, the temporal response to external perturbation can vary considerably due to autogenic processing, as sediment inherited from Pleistocene glaciation and climate change is reworked over many millennia (Woodward et al., 2008). In addition to temporal variability in fluvial response, individual reach sensitivity can exhibit a high degree of spatial variability. This can result in differential response to the same environmental perturbation caused by processes such as the passage of sediment waves, local variability in sediment storage and thresholds (Coulthard et al., 2005).

3.2.2 Autogenic controls

Intrinsic fluvial processes erode and deposit sediments within the fluvial system, independent of external controls. Fluvial processes such as lateral migration (e.g., Hickin and Nanson, 1975; Stølum, 1996; Erskine, 2011), bar and bedform development (e.g., Hooke and Yorke, 2011), avulsion (e.g., Makaske et al., 2009) and channel cutoff (e.g., Hooke, 2004) can all occur in the absence of external environmental forcing. For example, an assessment of historical planform changes on the lower Pages River, Australia, found that autogenic processes were responsible for sinuosity variations due to lateral migration and discharge-slope-grainsize threshold breaching (Erskine, 2011). However, the same work by Erskine (2011) also identified numerous allogenic planform changes, involving land-use change, river engineering and changes in the flood regime. It could be argued that autogenic change is of a smaller scale and process-based, while the aggradation-degradation response in rivers primarily reflects allogenic factors through their influence on sediment load and discharge (Fig. 3.1). Differentiating externally driven river response from intrinsic fluvial processes at the centennial scale can be difficult, and in order to make accurate correlations between river behaviour and environmental change, a robust geochronology and local palaeoenvironmental records are required (Macklin et al., 2012b).

3.2.3 River Response to floods

Increasingly the role of flooding is attracting more attention under predictions of anthropogenically-forced climate change. The geomorphic response to floods is variable, ranging from minor morphological changes (e.g., Costa, 1974; Magilligan et al., 1998) to catastrophic adjustment (e.g., Nanson, 1986). The geomorphic effectiveness of floods has been a major strand of enquiry within fluvial research, stimulated by the early research of Wolman and Miller (1960) who suggested that river channels were adjusted to high-frequency flows. However, the role of extreme flood events in conditioning channel form has also been highlighted in more recent work (Erskine, 1994; Reid and Frostick, 1994; Miller, 1995). The nature and magnitude of channel response to flooding has been found to be influenced by a number of factors including: land-use change (e.g., Brooks and Brierley, 1997), flood power (e.g., Kale, 2008), shifts in the climate regime (e.g., Eskine and Warner, 1998) and flood history (e.g., Erskine, 2011). The geomorphic effectiveness of floods is also determined by valley floor and channel configuration. For example, in an assessment of the geomorphic impacts of a 1 in a 100-year flood in Kiwitea Stream (a tributary of the Manawatu River, New Zealand), Fuller (2008) found that diverse channel behaviour in response to a large flood event reflected differences in catchment and reach sensitivity. In particular, catastrophic channel transformation occurred where floodwaters were confined at channel bends, while in less confined reaches dissipation of flood flow significantly reduced erosion (Fuller, 2008).

3.3 New Zealand river response to Holocene environmental change

3.3.1 Climate change

In New Zealand, as in other parts of the world, climate change has been identified as exerting a major control on river dynamics (e.g., McGlone et al., 1978; Grant, 1985; Bull, 1991; Berryman et al., 2000; Litchfield and Berryman, 2005). However, New Zealand's active tectonic setting means that tectonic activity (e.g., Campbell et al., 2003; Litchfield and Berryman, 2005), sea-/base-level change (e.g., Litchfield and Berryman, 2005) and volcanic activity (e.g., Manville and Wilson, 2004) have also been recognised as important external controls on river response.

A review of river behaviour inferred from river terrace sequences preserved in 44 North Island catchments found that the sensitivity of fluvial systems to changes in climate has not

been constant over the past ~ 30,000 years (Clement and Fuller, 2007). An aggradational response to the Last Glacial period dominates the record, with incision only promoted in response to tectonic uplift. For example, four aggradational terraces in the lower Waipaoa River have been correlated with cold climate episodes during the last ~ 140,000 years (Berryman et al., 2000). In the northeastern South Island, flights of aggradation and degradation terraces of the Charwell River have formed in response to climatically forced changes in sediment yield, stream power and resisting power over the last ~ 31,000 years (Bull, 1991). In the piedmont reaches of the Charwell River maximum aggradation occurred during glacial periods, and the aggradational mode persisted until sediment yields decreased and stream power increased with the transition to a warmer and wetter climate by ~ 14 ka (Bull, 1991). After ~ 14 ka degradation dominated, resulting in 65 to 75 m of intermittent incision primarily driven by decreased sediment yield. Although the overall trend was degradational during the Holocene, incision rates varied, with rates decreasing in the late Holocene, while during the mid Holocene warm period more than 30 m of streambed lowering occurred between ~ 7 and 6 ka (Bull, 1991). It was suggested that this phase of enhanced incision at ~ 7–6 ka was associated with increased runoff associated with tropical moisture sources (Bull, 1991).

In an assessment of the controls responsible for fluvial terrace development in eight non-glacial catchments of the eastern North Island, Litchfield and Berryman (2005) also identified climate as a control of Last Glacial Maximum aggradation in response to enhanced sediment supply under reduced vegetation. Post-glacial incision was inferred to have occurred in response to catchment re-vegetation and a reduced sediment supply (Litchfield and Berryman, 2005). Grant (1985) suggested that very high sediment supply during cold climate phases dampened the sensitivity of fluvial systems in New Zealand to relatively smaller-scale climate perturbations. Evidence preserved in alluvial terrace sequences suggests that the predominant response to climate amelioration during the Holocene was degradational (Vella et al., 1988; Marden and Neall, 1990; Litchfield and Berryman, 2005), with more sensitivity exhibited in response to more subtle climate shifts (Clement and Fuller, 2007).

Early work by Grant (1985) highlights the role of relatively small-scale climate change in influencing river dynamics during the late Holocene in New Zealand. He identified eight major periods of erosion and sedimentation over the past ~ 1800 years (Table 3.1). Of the eight periods, seven episodes were attributed to increased northerly airflow due to strengthened circulation in the upper atmosphere (Grant, 1985). During these intervals there was increased erosion of slopes and enhanced sediment transport, valleys were infilled,

floodplains aggraded, out-wash sediment fans were formed, and channels widened, straightened and steepened (Grant, 1985). In contrast to periods of erosion and alluvial sedimentation, tranquil soil forming intervals were thought to be dominated by zonal circulation (westerly), with cooler air temperatures and fewer storms (Grant, 1985). As a result, erosion and sediment transport rates decreased, vegetation became established on fresh surfaces, new soil formed, and in some catchments rivers narrowed and incised (Grant, 1985). Grant (1985) also noted a degree of synchrony between periods of alluviation in other regions of the globe with one or more of the last seven periods recognised in New Zealand (Table 3.1). However, the evidence for synchrony between phases of alluviation in New Zealand was based on very limited correlations, with the majority of records showing coincidence with only one phase of alluviation. In addition, the evidence for similar climatic fluctuations to New Zealand was dominated by comparisons with records from the USA, and the record was limited to the late Holocene.

Overall, research that has focused on the role that climate has played in driving river behaviour in New Zealand during the Holocene, has been both spatially and temporally limited. Studies of terrace sequences have shown that large-scale climate changes during glacial periods have resulted in aggradation while post-glacial climate amelioration has promoted a degradational fluvial response. More subtle climate changes associated with atmospheric circulation changes (and storm driven sedimentation) appear to have driven late Holocene phases of alluviation or incision. However to date, the role of climate in driving New Zealand river behaviour during the Holocene has not been fully examined, and remains an area requiring further research.

3.3.2 Volcanic activity

The earliest episode of alluviation recognised by Grant (1985) was sediment deposition associated with the 1.8 ka Taupo eruption from the Taupo Volcanic Centre. This large magnitude eruption from a rhyolitic caldera volcano in the central North Island destroyed river systems over an area of 20,000 km^2 and filled valleys with up to 70 m of pyroclastic material (Manville, 2002). River response in the vicinity of the eruption included the development of the fluvial system from small ephemeral streams with high sediment loads to permanent braided rivers (Manville, 2002). In many North Island catchments aggradational terraces were formed as a result of enhanced post-Taupo eruption sediment flux and subsequent incision following stabilisation by vegetation (Grant, 1985; Segschneider et al., 2002; Litchfield and Berryman, 2005; Clement and Fuller, 2007). In the Rangitaiki River (east of Lake Taupo) terrace flights underlain by pumice extend up to 17 m above the

modern channel, and have formed in association with meander migration under conditions of continual downcutting since the Taupo eruption (Woolfe and Purdon, 1996).

3.3.3 Base-level change

New Zealand's active tectonic setting, at the convergent plate boundary between the Pacific and Australian plates, has also influenced river behaviour during the Holocene. Base-level changes associated with tectonic uplift have predominantly resulted in degradation terrace development in uplifting regions during the Holocene (Bull, 1990; Nicol and Campbell, 2001; Litchfield and Berryman, 2005). Aggradational terraces, formed as a result of reduction in sediment transport competence associated with rapid sea level rise during the final stages of the post-glacial marine transgression, have also been identified in the lower sections of eastern North Island rivers (Litchfield and Berryman, 2005). River behaviour at the fluvial-estuarine interface is vulnerable to tectonically driven base-level change. Wilson et al. (2007) identified transitions from estuarine to fluvial sedimentary environments in an infilling estuarine setting, despite progressive Holocene eustatic sea-level rise, due to coseismic uplift at the coast.

3.3.4 Land-use change

Anthropogenic impacts on the New Zealand environment are limited to the last few hundred years, with human settlement not thought to have occurred until ~ 700 cal. yr BP (Prickett, 2002; Sutton et al., 2008; Wilmshurst et al., 2008). Colonisation of New Zealand occurred in two phases, first by Polynesians and then by Europeans within the last 200 years. The impact of anthropogenically-enhanced sediment supply on fluvial systems following settlement has, in some New Zealand catchments, been dramatic. The Waipaoa sedimentary system provides a good example of the impacts of human-induced deforestation on catchment dynamics. Although tectonics and geology predispose the Waipaoa system to naturally high rates of sediment delivery, catchment instability has been exacerbated by the removal of forest cover, which has led to a four to five-fold increases in pre-European settlement sediment yields on the continental shelf (Foster and Carter, 1997) and high rates of floodplain vertical accretion (Gomez et al., 1999). Although European settlement appears to have the greatest geomorphic impact on river systems, there is some evidence for fluvial response to Polynesian vegetation clearance by burning. This is exemplified by the formation of a low aggradation terrace following burning in Auckland (Grant-Taylor and Rafter, 1971), and localised increases in floodplain sedimentation in other New Zealand catchments (Grant, 1985).

Table 3.1

Evidence provided by Grant (1985) for coincidence of major periods of alluviation in New Zealand (bold text) with fluvial records in USA, central Europe, Southwest Pacific, Australia and Africa.

Reference	Evidence	Location	Timing							
			Taupo ca. 1764 yr BP	**Post-Taupo 1600–1500 yr BP**	**Pre-Kaharoa 1300–900 yr BP**	**Waihirere 680–600 yr BP**	**Matawhero 450–330 yr BP**	**Wakarara 180–150 yr BP**	**Tamaki 80–50 yr BP**	**Waipawa 1950–1984+ AD**
Grant (1985)	Periods of sedimentation	New Zealand								
Leopold and Miller (1954)	Periods of alluvial deposition	Wyoming, USA				750–550 yr BP				
Brakenridge (1980)	Alluvial chronologies	Missouri, USA		1600–1500 yr BP			500–400 yr BP			
	Alluvial chronologies	Western USA		1600–1500 yr BP	1200 BP (erosion)		500–400 yr BP			
	Floodplain deposition	Central European rivers		1600–1500 yr BP			500–400 yr BP			
Kochel et al. (1982)	Flood sediments (no. of radiocarbon dates)	Texas, USA			3	3	6			
Hurst (1944)	High flood frequency	Nile River							19 floods	
Tyson (1980)	Rainfall	Africa							High rainfall	
Leopold (1976)	Frequent heavy rain	Southwest USA							Heavy rain	
Grant (1981)	Tropical cyclones frequency	Southwest Pacific and Australia								Increase in cyclones
Pittock (1983)	Mean surface temperatures	Eastern Australia								Change in atmospheric circulation
Changnon (1983)	Climate	Illinois, USA								Increased flood frequency
Deutsch and Ruggles (1974)	Flood height	St Louis, USA						Flood		Flood

3.4 The fluvial sedimentary archive

Sediments preserved in the fluvial domain provide an archive of river response to environmental change, without the inherent lags associated with some other palaeoenvironmental proxies (i.e., speleothems and glacier behaviour). Central to the concept of using fluvial sedimentary architecture to investigate the response of alluvial systems to environmental change is the need for precise and accurate chronology. Various methods of dating control have been used to examine river behaviour in the late Quaternary including: dendrochronology (e.g., Becker and Schirmer, 1977), cartography (e.g., Passmore et al., 1992), archaeology (e.g., Tipping, 1994), luminescence dating techniques (e.g., Fuller et al., 1998), soil chronosequences and pedogenic weathering (e.g., Harvey et al., 1995), Electron Spin Resonance (e.g., Woodward et al., 1995), U-series (e.g., Nanson et al., 1991) and tephrochronology (e.g., Eden et al., 2001; Berryman et al., 2010). However, in most cases radiocarbon (^{14}C) dating is the preferred technique for dating Holocene fluvial deposits (Lewin et al., 2005).

The ^{14}C dating technique uses an assessment of the present day measurement of the unstable ^{14}C isotope of carbon and the rate of radioactive decay to calculate the time since death of an organism (Fairbanks et al., 2005). Conventional ^{14}C ages must be corrected for the fluctuation of atmospheric ^{14}C and heterogeneity of ^{14}C within the different carbon reservoirs using tools such as calibration curves (Fig. 3.2a), constructed from organic material of known age, stable isotope ratios and reservoir offsets. Due to variations in the radiocarbon calibration curve the Gaussian probability distribution for the conventional date is converted to a calendar probability distribution (Fig. 3.2a). Large undulations in parts of the calibration curve can mean that a conventional date is converted to a complex probability distribution with more than one range of calibrated ages with differing probabilities (Fig. 3.2a). The Meta-analysis approach (e.g., Lewin et al., 2005; Macklin et al., 2005; Johnstone et al., 2006; Macklin et al., 2010) uses cumulative probability function (CPF) plots (Fig. 3.2b) produced from summing individual probability distributions associated with calibrated fluvial ^{14}C-dated sedimentary fluvial units to produce probability-based reconstructions of river behaviour.

Fluvial units can be preserved in a number of sub-environments within a river valley setting, including both channel and overbank deposits. In the overbank domain, fluvial units can be preserved as floodplain sediments, palaeochannel fills, flood basin sediments and colluvial debris flows/fans (Lewin et al., 2005) (Fig. 3.3). In the channel domain, sedimentation units include lateral accretion deposits, bars and bed aggradation (Lewin et al., 2005). In contrast

to other sedimentary environments such as the ocean, sedimentation in an alluvial setting is intermittent. Accretionary units deposited within channel and overbank environments will also vary in both thickness and spatial extent within the catchment, and may relate to one or more depositional events (Lewin et al., 2005). Also, there is a tendency for the fluvial sedimentary record to be biased toward younger deposits as older deposits are often susceptible to reworking through subsequent fluvial activity (Lewin et al., 2005).

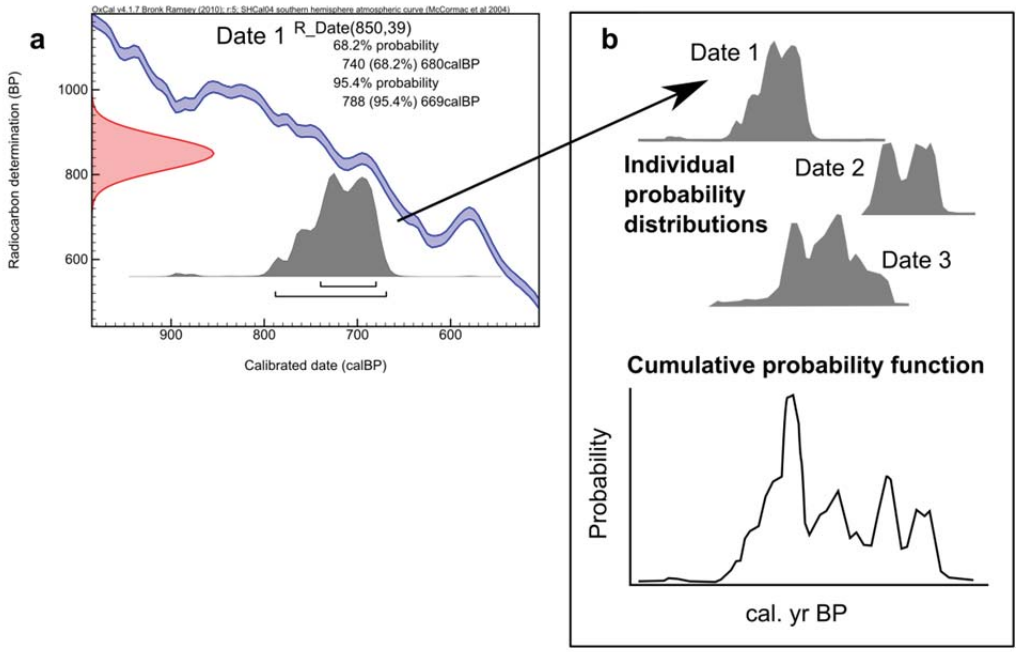

Fig. 3.2. Radiocarbon date calibration and summing individual probability distributions to produce cumulative probability function plots. a) The Gaussian probability distribution for the conventional date (Date 1) is converted to a calendar probability distribution. The conventional date is converted to a complex probability distribution with more than one range of calibrated ages with differing probabilities due to undulations in the calibration curve (blue line). b) A cumulative probability function is produced by summing individual probability distributions associated with calibrated dates (Date 1, 2 and 3).

Radiocarbon dating of organic material incorporated within fluvial units deposited in the different sedimentary settings (Fig. 3.3) provides the geochronology for changes in the depositional or flooding regime. Depending on where the dated material is sampled from within the fluvial unit, the ^{14}C age will provide the chronology for either: i) the onset of deposition (maximum age) from ^{14}C samples at the base of the fluvial unit or in the top of

the unit below, ii) cessation of deposition (minimum age) from ^{14}C samples at the top of the unit or at the base of unit above, or iii) sedimentation where the date 'floats' within the fluvial unit (Fig. 3.3b). Radiocarbon dates that mark a change in the depositional style or rate can be further classified as representing either 'change-before, where the sample is stratigraphically above the change or 'change-after, where the sample is stratigraphically below the change. Change-after dates are considered the most significant for constraining the timing of changes in the flooding regime (Macklin et al., 2010; Macklin et al., 2012a), as they provide the earliest time for the observed sedimentological change. Radiocarbon dates associated with peat and palaeosol units are considered to represent periods of river stability. In the fluvial archive, phases of river activity are characterised by fluvial units such as interbedded silts and sands, fluvial gravels, flood silts and overbank fining sequences.

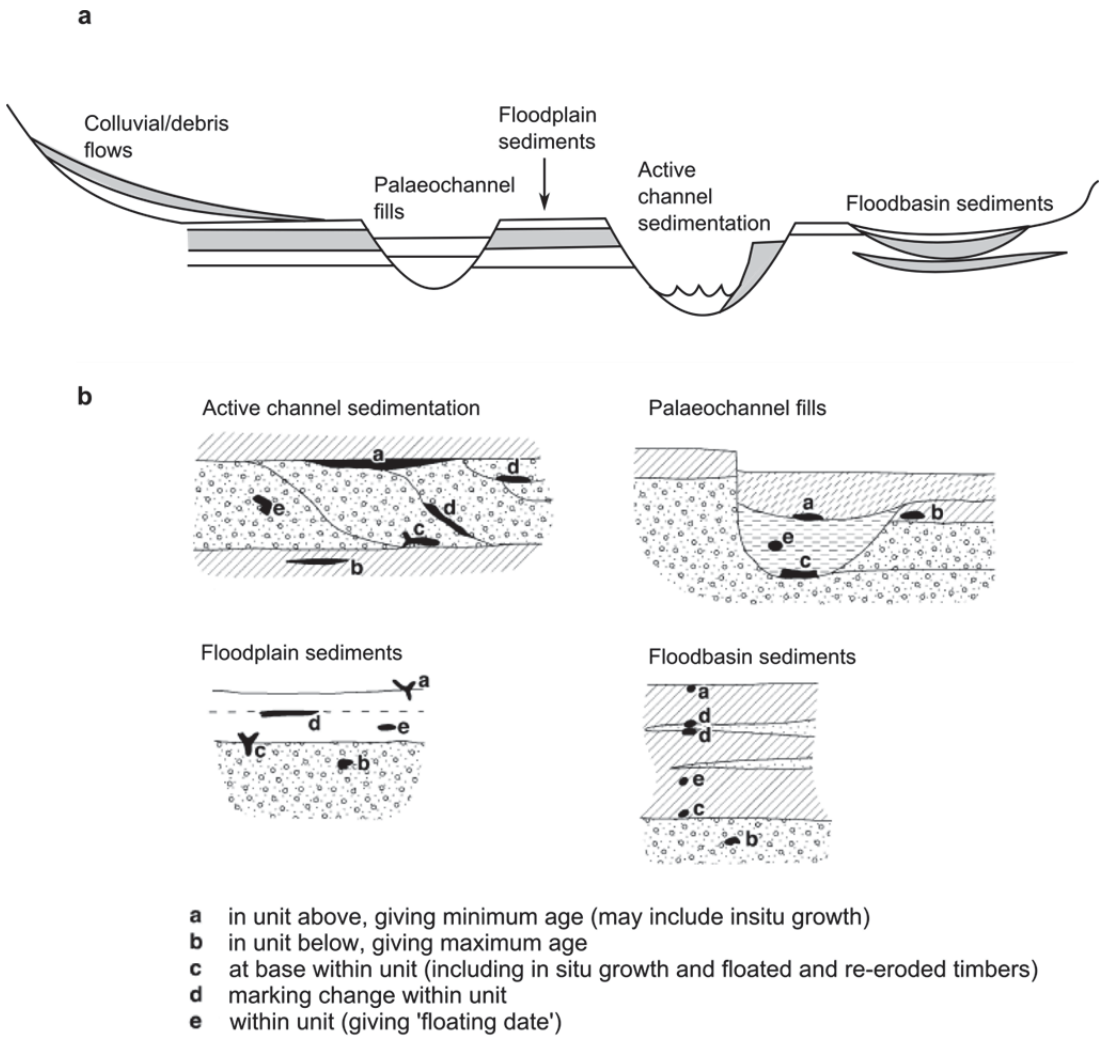

Fig. 3.3. Schematic diagram showing a) five types of alluvial sedimentation units. b) The sedimentary context for dated material in alluvial units. Adapted from Lewin et al. (2005).

3.5 Summary

Fluvial systems record and respond to environmental change through interactions between the sediment and flow regime. This chapter has shown how river response can be driven by both internal processes and external factors that include: climate change, base-level change, anthropogenic land-use change, and tectonic and volcanic impacts. There is often not a straightforward linear relationship between environmental signals and river response due to the complexity of the fluvial system. Not all environmental changes will promote a geomorphic response due to the operation of thresholds, self limiting processes, hysteresis and storage effects, and the nature of the response will vary both temporally and spatially.

However, despite the complexity of the fluvial domain, river sediments are a valuable source of palaeoenvironmental information.

This review has also discussed how New Zealand rivers, like river systems globally, are known to have responded to environmental changes during the Holocene. Holocene climate change associated with atmospheric circulation variability has been shown to influence erosion and sedimentation in New Zealand river systems, with Holocene fluvial behaviour predominantly characterised by degradation and sensitivity to subtle climate shifts. New Zealand's active tectonic setting means that tectonic and volcanic drivers also play a role in New Zealand river dynamics. A widespread phase of alluviation was detected in many North Island catchments following the eruption from the 1.8 ka Taupo eruption and aggradational terraces associated with rapid sea-level rise during the final stages of the post-glacial marine transgression have also been identified in river valleys near the coast. Anthropogenic impacts on sediment flux have been confined to the last several hundred years, and have included high rates of floodplain vertical accretion and low terrace aggradation following deforestation.

Fluvial sediments preserved in the channel and overbank domain preserve a record of river response to environmental change and organic material incorporated within these sediments can be used to constrain the timing of river response to environmental change, whether it be flooding, river activity or stability. Compilation of fluvial ^{14}C databases and the meta-analysis approach provides a methodology by which data from individual fluvial studies can be aggregated and analysed to provide regional assessments of Holocene river behaviour.

The following chapter applies meta-analysis techniques to 401 fluvial ^{14}C-dated fluvial units in New Zealand to produce a probability-based reconstruction of Holocene river behaviour in response to environmental change (including climate) for this region.

Chapter 4

Holocene river behaviour in New Zealand: response to regional centennial-scale climate forcing

4.1 General introduction

Chapter 3 examined the mechanisms involved in driving river behaviour, the nature of river response to environmental perturbation and the way in which fluvial systems record environmental changes. The chapter also reviewed the current knowledge of how New Zealand fluvial systems have responded to Holocene environmental change, including: climate change, tectonics, base-level change, volcanic activity and anthropogenic land-use change. A need for more research in order to develop a better understanding as to the controls of river behaviour in New Zealand was identified, in particular the role of climate change. Thus, the focus of the following Chapter 4 is to examine river Holocene river behaviour at a national and regional scale, and to elucidate the role that regional climate forcing has had on Holocene river activity in New Zealand. This chapter is contained within the manuscript: J.M. Richardson, I.C. Fuller, M.G. Macklin, A.F Jones, K.A. Holt, N.J. Litchfield, M. Bebbington, Holocene river behaviour in New Zealand: response to regional centennial-scale climate forcing, which is published in the journal *Quaternary Science Reviews*.

The chapter applies meta-analysis techniques to 401 fluvial ^{14}C-dated fluvial units in New Zealand to produce a probability-based reconstruction of Holocene river behaviour in

response to environmental change (including climate) for New Zealand. The New Zealand fluvial ^{14}C database and meta-analysis data are contained in Appendix A. In Section 4.5 probability-based records of Holocene river flooding, activity and stability are presented along with a regional assessment of Holocene river activity at the level of the coherent precipitation region. Records of river activity in northern (North Island) and southern (South Island) New Zealand are also produced (Section 4.5) and compared with independent hydro-climate proxy records that reflect regional, tropical and polar influences on Southern Hemisphere climate (Section 4.6). A model is proposed that links the spatial and temporal patterns of Holocene river activity identified in northern and southern New Zealand with large-scale atmospheric changes in the region (Section 4.6.2). Finally, Holocene floodplain sedimentation rates and controls are also examined and discussed in Section 4.6.3.

4.2 Abstract

This paper applies meta-analysis techniques to a database of 401 ^{14}C-dated Holocene fluvial units in New Zealand. We use the database to produce a probability-based reconstruction of Holocene river behaviour at a national and regional scale. Records of river activity in northern (North Island) and southern (South Island) New Zealand are compared with independent hydro-climate proxy records that reflect regional, tropical and polar influences on Southern Hemisphere climate. During the Holocene, 12 multi-centennial length episodes of river activity and flooding were identified in the North Island, and in the South Island record 11 periods exceed the mean relative probability of activity. These records show that episodes of river activity have exhibited a predominantly out-of-phase relationship, suggesting the relationship between ENSO and SAM, and the relative dominance of the two modes, may be influencing Holocene river activity in New Zealand. The emerging pattern in the South Island Holocene fluvial record is one of increased river activity in response to enhanced westerly atmospheric circulation associated with a predominance of trough regime synoptic type (negative SAM-like circulation). In the North Island, episodes of river activity are driven by increased meridional atmospheric circulation associated with blocking regime synoptic conditions (La Niña-like and positive SAM-like circulation). Analysis of floodplain sedimentation rates shows a rapid increase after ~ 500 cal. yr BP, following the arrival of humans and the beginning of widespread deforestation. Regional climate complexity in New Zealand presents opportunities for palaeoclimate reconstruction, with the New Zealand fluvial ^{14}C-database ideally placed to fill geographical gaps in the long-term hydrological record.

4.3 Introduction

Global palaeoclimate data have highlighted the variability of climate throughout the Holocene, involving periods of rapid climate change on a global and hemispheric scale, overprinted with strong regional signals (e.g., Mayewski et al., 2004). Periods of rapid climate change are characterised by lower polar temperatures, with intensified atmospheric circulation and increased low latitude aridity (Mayewski et al., 2004). New Zealand, located in the mid-latitudes of the Southern Hemisphere, is influenced by both polar and subtropical oceanic and atmospheric influences, including the Southern Annular Mode (SAM) (Hall and Visbeck, 2002; Gillett et al., 2006; Renwick and Thompson, 2006; Marshall, 2007), El Niño Southern Oscillation (ENSO) (Trenberth, 1997; Garreaud and Battisti, 1999) and Interdecadal Pacific Oscillation (IPO) (Salinger et al., 2001; Mantua and Hare, 2002). New Zealand's climatically sensitive location, combined with an environmentally responsive landscape comprising short, steep, and well-connected catchments (cf. Fryirs et al., 2007; Macklin et al., 2010), is ideally placed for detecting changes in hydrological and geomorphic systems due to oscillation and interaction of these major climate drivers (e.g., Page et al., 2010).

Research on alluvial sedimentary systems has demonstrated that New Zealand rivers have responded to environmental changes during the late Quaternary (e.g., McGlone et al., 1978; Grant, 1985; Clement and Fuller, 2007). Climate change (e.g., McGlone et al., 1978; Grant, 1985; Berryman et al., 2000; Marden et al., 2008) and land use (e.g., Gomez et al., 2007) have been identified as the major factors driving New Zealand fluvial dynamics, although tectonics (e.g., Campbell et al., 2003; Litchfield and Berryman, 2006), sea-level change (e.g., Litchfield and Berryman, 2005) and volcanic activity (e.g., Grant, 1985; Woolfe and Purdon, 1996; Manville, 2002; Segschneider et al., 2002; Manville and Wilson, 2004; Manville et al., 2005) have also been recognised as locally important external controls of Holocene river development.

Evidence preserved in alluvial terrace sequences in New Zealand indicates that the dominant response to climate amelioration during the early Holocene was degradational (Clement and Fuller, 2007; Marden et al., 2008; Berryman et al., 2010). Early pioneering work by Grant (1985) highlighted the role of relatively small-scale climate change (discrete storm events, or episodes of storminess) in influencing river dynamics during the late Holocene in New Zealand, identifying eight regional periods of erosion and sedimentation over the past ~ 1800 years. Of these eight episodes, seven were attributed to climate fluctuations caused by increased northerly airflow connected with strengthened circulation in the upper atmosphere

(Grant, 1985). Despite recent work that has tried to extend our understanding of New Zealand fluvial response to environmental changes at a regional scale (e.g., Litchfield and Rieser, 2005; Litchfield and Berryman, 2005; Clement and Fuller, 2007), our present knowledge of Holocene river dynamics is somewhat data-poor and catchment-specific (e.g., Pullar and Penhale, 1970; Berryman et al., 2000; Nicol and Campbell, 2001).

With predictions of increased climatic variability and extreme rainfall events in the future (IPCC, 2007), there is a growing need for a more comprehensive understanding of Holocene river behaviour and flooding in New Zealand. The best sources of information on fluvial system response to environmental perturbation are the sedimentary sequences preserved in the alluvial domain. Fluvial archives have been widely and increasingly used to explore the relationship between river system behaviour and environmental change over a range of spatial and temporal scales (e.g., Schumm and Parker, 1973; Starkel, 1983; Passmore et al., 1992; Ely et al., 1993; Knox, 1993; Fuller et al., 1998; Macklin et al., 2002; Macklin et al., 2006; Starkel et al., 2006; Thorndycraft and Benito, 2006b; Harden et al., 2010; Macklin et al., 2010; Macklin et al., 2012a).

A major recent advance for investigating the dynamics of Holocene river system activity and flooding histories has been the development and application of radiocarbon (^{14}C) databases and meta-analysis of ^{14}C fluvial ages (Macklin and Lewin, 2003; Johnstone et al., 2006; Hoffmann et al., 2008; Macklin et al., 2010). This methodology uses ^{14}C-dated sedimentary fluvial archives to produce probability-based reconstructions of Holocene river activity which can be correlated with independent climate proxy and other environmental records (Harden et al., 2010; Macklin et al., 2010; Turner et al., 2010). The technique also enables comparison with other environmental data sets at regional and global scales to determine the degree of synchrony between river systems (Macklin et al., 2012a) and to explore the linkages between human impact, climate change and fluvial response (e.g., Macklin et al., 2010; Turner et al., 2010; Zielhofer et al., 2010). Meta-analysis of ^{14}C-dated fluvial units in the Northern Hemisphere has demonstrated that the Holocene fluvial record comprises clusters of flood events, which are associated with large scale atmospheric circulation changes (Macklin et al., 2006; Harden et al., 2010; Macklin et al., 2010; Zielhofer et al., 2010). New Zealand's short history of human colonisation, with a preferred date of arrival at ca. 800 years cal. yr BP (Prickett, 2002), means that climate and land-use impacts on river development need not be disentangled for most of the Holocene.

This paper presents meta-analyses of ^{14}C-dated Holocene fluvial units in New Zealand obtained from published papers, unpublished reports and data from GNS Science. It

provides a probability-based reconstruction of Holocene river behaviour, revealing the sensitivity of New Zealand river systems to short-term and rapid Holocene climate variations. Episodes of increased river activity are identified and compared with independent Southern Hemisphere hydro-climate proxy records. We also examine the evidence and the effects of climate change and anthropogenic impacts on Holocene river development and fluvial sedimentation in New Zealand, and propose a model of river behaviour related to these external forcing factors.

4.4 Methodology

A database containing 401 fluvial ^{14}C ages was compiled from published papers, unpublished reports and unpublished data from the GNS Science Fossil Records Database and New Zealand Rock Catalogue and geoanalytical database (PETLAB) (Table 4.1 and Fig. 4.1). Figure 4.1 shows the geographical distribution of ^{14}C-dated fluvial sites in New Zealand and the boundaries of the six coherent precipitation variability regions defined by Mullan (1998) using rotated empirical orthogonal function (EOF) analysis of precipitation data. The South Island has the largest number of reported ^{14}C ages (218), with central western and eastern areas of the South Island having the greatest coverage. The majority of the 183 North Island ^{14}C ages included in the analysis are concentrated in the southern half of the island, and there is a significant absence of data from catchments in northern North Island. Other gaps in the geographic coverage occur for river systems in the south and south east of the South Island (Mataura, Oreti and Waitaki catchments), and northern West Coast and Nelson regions (Mokihinui, Buller and Takaka catchments). Almost half of ^{14}C ages in the database are from studies that reported five or fewer dates from the same catchment. The remaining data were obtained from 11 catchments (Waimakariri, Wairau, Waipaoa, Cropp, Waikato, Muaupoko, Okuru, Hilldersden stream, Wharekahika, Twizel and McKays Crossing trench). The largest clusters of dates were from the Waimakariri catchment (n=52), eastern South Island, and Wairau River (n=32), northeastern South Island. In the North Island the largest cluster of dates was obtained from the Waipaoa catchment (n=20), eastern North Island.

Following Johnstone et al. (2006), each database entry contained information on the nature of the dated material, calibrated ^{14}C dates and conventional ^{14}C ages, laboratory codes, location of ^{14}C-dated samples and their sedimentary context. Table 4.2 summarises the range of organic material dated, the total number of ^{14}C dates in each class and the proportion of those which have been designated 'activity' ^{14}C ages. We acknowledge that ^{14}C dating has a number of well documented limitations including: potential bias due to contamination with

old or modern carbon, old wood effects, errors associated with redeposition of organic material (including charcoal) and errors associated with ^{14}C measurement. These limitations have been analysed and discussed for similar datasets (Hoffman et al. 2008; Macklin et al. 2010). During compilation of the database, information associated with ^{14}C ages was scrutinised to reduce the chances of inclusion of erroneous fluvial ^{14}C dates.

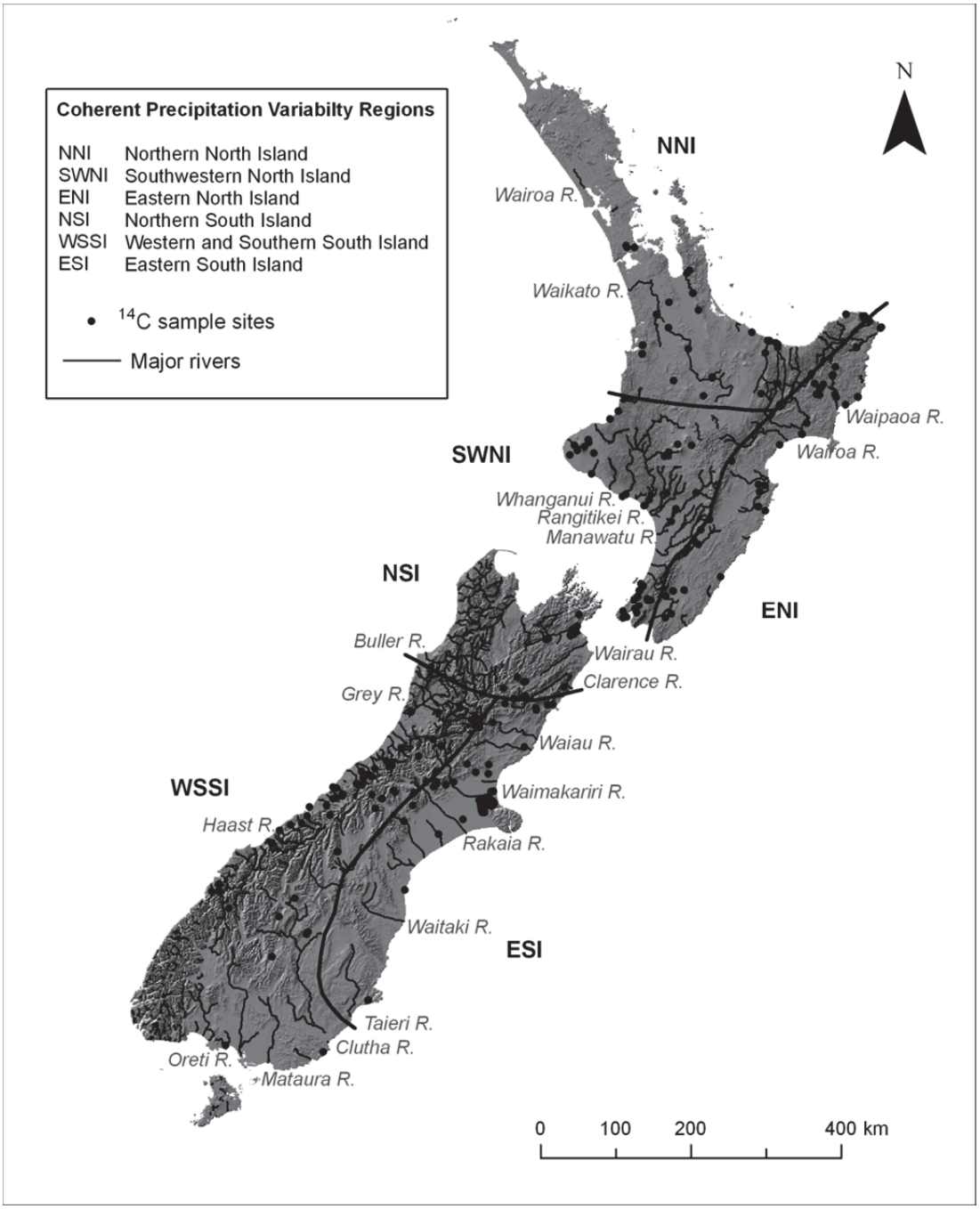

Fig. 4.1. Map showing the six coherent precipitation variability regions in New Zealand (Mullan, 1998), major rivers, and the location of sample sites included in the ^{14}C-dated Holocene fluvial unit database.

Table 4.1

Holocene fluvial ^{14}C dates from New Zealand river catchments. Regional groupings follow Mullan (1998).

Catchment North Island	No. of dates	References	Catchment South Island	No. of dates	References
Northern North Island			*Northern South Island*		
Awakino River	1	Grant (1985)	Acheron River	1	McGlone and Basher (1995)
Awaroa River	3	Grant (1985)	Big Bush Stream	1	McGlone and Basher (1995)
Hobson Bay	1	Grant-Taylor and Rafter (1971)	Clarence River	1	Van Dissen et al. (2006)
Kauaeranga River	3	Grant (1985) GNS[a]	Dillon River	3	McGlone and Basher (1995)
Makara	5	Grant (1985)	Doctors Creek	1	Basher et al. (1995)
Mangatea stream	1	GNS[a]	Hillersden Stream	7	Zachariasen et al. (2006)
Ohinemuri	3	Grant (1985), GNS[a]	Island Gully	1	McGlone and Basher (1995)
Oparau	3	Grant (1985), GNS[a]	Saxon River	1	McGlone and Basher (1995)
Rangtaiki River	4	Pullar and Patel (1972), GNS[a]	Severn River	1	McGlone and Basher (1995)
Te Atatu	1	Grant-Taylor and Rafter (1971)	Waikawa Stream	2	Basher et al. (unpub.)
Upper Waipa	1	Grant (1985)	Wairau River	32	Grant (1985), Basher et al. (1995), GNS[a]
Waikato River	9	Grant-Taylor and Rafter (1963), GNS[a]	Yarra River	1	McGlone and Basher (1995)
Wairakau River	1	Grant (1985)	Total	52	
Waitahanui	2	Grant (1985), GNS[a]	*Western & Southern South Island*		
Whakatane River	4	Grant-Taylor and Rafter (1971), GNS[a]	Aparima River	1(1)	GNS[a]
Whangaparaoa River	1	Ota et al. (1992)	Boyle River	1	GNS[a]
Wharekahika River	6	Ota et al. (1988; 1992)	Branch Creek	1	GNS[a]
Whau Estuary	1	Grant-Taylor and Rafter (1971)	Bullock Creek	1	GNS[a]
Whirinaki River	1	Grant (1985) GNS[a]	Buster Creek	1	GNS[a]
Total	51		Cameron River	2	Grant-Taylor and Rafter (1971), GNS[a]
Southwestern North Island			Cass River	1	Basher et al. (unpub.)
Akatarawa	1	Grant (1985)	Catlins river	1	Grant-Taylor and Rafter (1963)
Blind Gully Stream	1	GNS[a]	Clearwater River	1	GNS[a]
Horokiri Valley	5	Van Dissen and Berryman (1996)	Clyde River	2	GNS[a]
Hutt River	4	Van Dissen and Berryman (1996), Grant-Taylor and Rafter (1963)	Crooked Mary Creek	1	Grant-Taylor and Rafter (1971)
Kahao Creek	1	Grant (1985), Brodie (1957)	Cropp River	13	GNS[a]
Kahao Stream	1	Van Dissen and Berryman (1996)	Geologist Creek	1	GNS[a]
Kaitoke	1	Van Dissen and Berryman (1996)	Grandview Creek	1	Grant (1985)
Karori Wellington	1	Van Dissen et al.	Granite Creek	1	Grant-Taylor and

Coast		(1992)			Rafter (1963)
Mangahao River	3	Langridge et al. (2005)	Havelock River	1	GNS[a]
Manganuiateao	3	Lecointre et al. (1998)	Hokuri Stream	2	GNS[a]
Manor Park	1	Van Dissen and Berryman (1996)	Hope River	4	Basher et al. (unpub.), GNS[a]
McKays Crossing trench	6	Litchfield et al. (2006)	Kaipo River	2	GNS[a]
Muaupoko Stream	9	Litchfield et al. (2004)	Kaka Creek	2	Rattenbury et al. (1988)
Oaonui-Oaoiti Stream	1	GNS[a]	Karangarua River	1	GNS[a]
Ohariu	1	Grant (1985)	Lewis River	2	GNS[a]
Porewa	2	Grant (1985), GNS[a]	Macauley River	1	Grant-Taylor and Rafter (1971)
Rangitawa Stream	1	Grant-Taylor and Rafter (1963)	Mahitahi River	1	GNS[a]
Stony River	1	Grant (1985)	Manuherikia River	2	Basher et al. (unpub.)
Stratford	1	Grant-Taylor and Rafter (1971)	Noisy Creek	2	GNS[a]
Taranaki	1	Grant-Taylor and Rafter (1971)	Okuru River	9	GNS[a]
Tongaporutu River	1	Grant (1985)	Poerua River	1	GNS[a]
Waihohonu	1	Grant-Taylor and Rafter (1963)	Rees River	1	GNS[a]
Wai-iti Stream	1	GNS[a]	River Nevis	1	GNS[a]
Waikanae	1	Van Dissen and Berryman (1996)	Ryton River	1	Basher et al. (unpub.)
Waingongoro River	1	GNS[a]	Stillwater Creek	1	Grant-Taylor and Rafter (1971)
Wainuiomata River	1	Grant-Taylor and Rafter, (1963)	Taramakau River	1	GNS[a]
Waiohine	2	Grant (1985)	Twizel River	6	Basher et al. (unpub.)
Waiongana Stream	1	GNS[a]	Upper Poulter River	3	GNS[a]
Waitotara River	4	Grant (1985), GNS[a]	Waiho River	3	Grant-Taylor and Rafter (1963), Grant (1985), GNS[a]
Waiwakaiho River	3	Grant-Taylor and Rafter, (1963), GNS[a]	Waikukupa River	1	GNS[a]
Wanganui River	4	Grant (1985), Brodie, (1957), Grant-Taylor and Rafter (1963)	Waimakariri River	2	GNS[a]
Wellington City	1	Grant-Taylor and Rafter (1963)	Waita River	1	GNS[a]
Whakapapa	1	Lecointre et al. (1998)	Waitaha River	1	GNS[a]
Whangaehu River	2	Grant (1985)	Wanganui River	3	Grant-Taylor and Rafter (1963), GNS[a]
Total	69		Whataroa River	2	GNS[a]
Eastern North Island			Total	86	
Clive River	1	Grant-Taylor and Rafter (1963)	*Eastern South Island*		
East Cape	2	Ota et al. (1992)	Acheron River	1	GNS[a]
Glenfalloch	1	Grant (1985)	Ashburton River	2	GNS[a]
Hopuruahine	3	Grant (1985)	Ashley River	1	GNS[a]
Huangarua	2	Grant (1985)	Avon River	1	Suggate (1958)
Karakatuwhero River	1	Ota et al. (1992)	Bellbird Creek	1	GNS[a]
Makara River	1	GNS[a]	Bullock Creek	1	GNS[a]

Manawatu River	1	GNS[a]	Charwell River	2	Basher et al. (unpub.)
Mangakuri River	1	GNS[a]	Copland River	1	Grant (1985)
Mangatainoka	1	Grant (1985)	Dunedin	1	Grant-Taylor and Rafter (1963)
Mata	1	Grant (1985)	Eyre River	1	GNS[a]
Motu	1	Grant (1985)	Hurunui River	2	Basher et al. (unpub.)
Ngaruroro	1	Grant (1985)	Lake Lyndon	2	Basher et al. (unpub.)
Pakarae River	4(4)	Wilson et al. (2007)	Middle Creek	2	Grant (1985)
Raparapawai	1	Grant (1985)	Otaio River	1	Basher et al. (unpub.)
Ruamahanga	1	Grant (1985)	Paringa River	1	GNS[a]
Tamaki River	1	GNS[a]	Rakaia River	1	Basher et al. (unpub.)
Te Waikaha	1	Grant (1985)	Rangitata River	1	GNS[a]
Te Waikaha Stream	3	GNS[a]	Rubicon River	3	GNS[a]
Tea Creek Road	3	Van Dissen and Berryman (1996)	Saddle Creek	1	Basher et al. (unpub.)
Waihora	1	Grant (1985)	Taieri River	1	Basher et al. (unpub.)
Waikari River	1(1)	Litchfield (2008)	Waimakariri River	52	Grant-Taylor Rafter (1963), Grant (1985), Basher et al. (1988), GNS[a]
Waikarokaro	1	Grant (1985)	Waipara River	1	Nicol and Campbell (2001)
Waipaoa	20	Brown (1995), GNS[a]	Total	80	
Wairoa River	5	Grant (1985), Ota et al. (1988), GNS[a]			
West Tamaki	1	Grant (1985)			
Whangawehi Stream	1	GNS[a]			
Wharekopae River	2	GNS[a]	(1) No. of dates potentially influenced by sea level		
Total	63		[a] Unpublished data from GNS Science Database		

Table 4.2

The total number of fluvial ^{14}C dates, number of 'activity' dates and proportion of 'activity' dates classified by the organic material used for dating.

Organic material used for ^{14}C dating	Total no. of ^{14}C dates	No. of 'activity' ^{14}C dates	Proportion of 'activity' ^{14}C dates
Bark	2	1	50%
Carbonised wood	3	2	66%
Charcoal	60	41	68%
Charred wood	9	4	44%
Gum	1	1	100%
Leaves and twigs	21	19	90%
Peat	33	3	9%
Roots	5	3	60%
Shell	3	2	66%
Soil	5	1	20%
Wood	251	182	72%
Unclassified	8	5	62%

Four types of depositional environment were differentiated: channel bed sediments, palaeochannel fills, floodplain sediments and debris flow deposits. This differentiation, and an assessment of whether the deposit represented river activity or stability, was based on assessment of sedimentary logs associated with each fluvial ^{14}C age. Radiocarbon ages obtained from fluvial units representing phases of channel or floodplain sedimentation were designated 'activity' dates, while ^{14}C ages associated with peat or palaeosol units, marking periods of river stability and restricted clastic input, were termed 'stability' dates (cf. Hoffmann et al., 2008; Macklin et al., 2010). Sedimentological information was also used to classify dates as 'change dates', when they were located at unit boundaries representing a change in depositional style and/or rate (Macklin and Lewin, 2003). These were further classified as representing either 'change-before' ^{14}C dates, where the sample provides a minimum age for the sedimentological change (sample stratigraphically above the change) or 'change-after' ^{14}C dates, which give a maximum age for the associated sedimentological change (that is, the sample was recovered from stratigraphically beneath the change) (Macklin et al., 2010). In the New Zealand record typical examples of the type of stratigraphy inferring river activity include fluvial gravel units, interbedded sand and gravel layers, flood debris, overbank fining sequences and flood silts, often overlying or underlain by palaeosols, peat units or in situ vegetation.

Using the analytical approach developed by Macklin et al. (2010), all ^{14}C dates were calibrated using SHCAL04 (McCormac et al., 2004) and the individual probabilities summed using the radiocarbon calibration programme OxCal version 4.1 (Bronk Ramsey, 1995, 2001, 2009) to produce cumulative probability function (CPF) plots at a 5-year resolution. This can produce peaks in the CPFs (Figs. 4.2, 4.3 and 4.4), which are an artefact of the calibration curve, or because of preservation or sampling bias of younger fluvial units (Macklin et al., 2010). In archaeology, taphonomic bias in temporal frequency distributions has been corrected using ^{14}C-dated volcanic deposits (Surovell et al., 2009). To eliminate the effects of preservation bias towards younger fluvial units in the New Zealand fluvial record the methodology developed and discussed by Hoffmann et al. (2008) has been used. CPF probabilities associated with subsets of the database, ^{14}C ages representing 'change-after', 'activity' and 'stability', were divided by the probability calculated for the CPF of the entire dataset to produce relative probability plots (Fig. 4.5). This assumes that the preservation bias toward younger ages applies to the entire dataset (and the CPF in Fig. 4.2 for the entire dataset supports this assumption). Therefore, any probability peaks apparent in the most recent past will be of high probability *relative* to the entire database. To normalise the scale of the probability curves for the different groups, each value in the relative probability curve was divided by the highest probability in the dataset.

A cross-correlation analysis was performed on the North and South Island river activity raw data CPF time-series to assess the statistical significance of out-of-phase behaviour. The untransformed CPF data were used as the relative CPF procedure weights the data and changes the correlation structure (cf. Macklin et al., 2012a). The two time-series were prewhitened (Chatfield, 2004) by differencing and fitting an autoregressive model to the North Island difference data. The South Island dataset was fitted to the same autoregressive model, and the lagged correlations between the residual processes were calculated.

The use of CPFs in the analysis of radiocarbon databases to better constrain the timing of Holocene flooding episodes, and their correlation with other proxy records of environmental change, has recently been the subject of debate (Chiverrell et al., 2011b, 2011a; Macklin et al., 2011). Chiverell et al. (2011a) focused on issues associated with ^{14}C calibration and the incorporation of non-contemporaneous organic material in fluvial deposits as reasons in all instances to avoid using the CPF plots. We are fully aware (see Macklin et al., 2006; Macklin et al., 2010; Macklin et al., 2011) of these limitations, which apply to users of ^{14}C dating, and have recently developed new data (Macklin et al., 2010) and statistical analytical methods (Macklin et al., 2012a) to evaluate these potential problems. Most importantly, our approach is not intended to identify *individual* flood events, as recently misconstrued by Chiverrell et al. (2011a), but to provide a probabilistic assessment of centennial length and longer flooding *episodes* (Macklin et al., 2011). Probability values that exceed the mean relative probability of the dataset were used to identify centennial and multi-centennial long episodes of flooding, river activity or stability. We believe that meta-analysis of large databases of ^{14}C-dated fluvial units, such as that compiled for New Zealand, presents an opportunity to explore temporal and spatial patterns in Holocene river behaviour that would not emerge from studies of single sites or catchments.

To avoid over-interpretation of the New Zealand data, the start and end dates for phases of flooding, and river activity and stability are rounded to the nearest 100 years. In addition, in order to assess the hydrological significance of peaks in the relative CPF plots produced for the 'change-after', 'activity' and 'stability' data sets, these were compared with the frequency of dates, using the mean of the 2σ calibrated age range, in 100 year intervals. Peaks in the relative CPF plots above the mean, and corresponding to a minimum of three dates within a 200 year period, were used to identify phases of increased flooding, river activity or stability in the New Zealand fluvial record (cf. Macklin et al., 2010).

4.5 Results

Figure 4.2 displays the CPF plot for the entire New Zealand Holocene fluvial ^{14}C database and the North and South Island subsets. The plots illustrate the effect of preservation bias on the distribution of fluvial ^{14}C ages, with a progressive increase in the number of ages after ~ 2000 cal. yr BP. A reduction in probabilities in the last 200 years or so is the result of radiocarbon dating limitations over this time period. Figure 4.2 also shows prominent peaks in probabilities at ~ 1500 cal. yr BP followed by relatively few dates centred on ~ 1300 cal. yr BP. Such a pattern is not evident in Northern Hemisphere datasets (e.g., Harden et al., 2010; Macklin et al., 2010), suggesting that the effect is not an artefact of calibration. As Macklin and Lewin (1993) pointed out, ^{14}C database analysis identifies only episodes of deposition within the alluvial record. CPF plots for the different sedimentary environments included in the analysis (Fig. 4.3), and 'activity', 'change' and 'stability' subsets (Fig. 4.4) also show similar trends in the distribution of dates. With the exception of debris flow sediments, CPF distributions from all other depositional environments (Fig. 4.3) show an increase in probabilities after ~ 1700 cal. yr BP, including a peak at ~ 1500 cal. yr BP and interrupted by a sharp decline at ~ 1300 cal. yr BP. The lack of deposits dated to around 1300 cal. yr BP from all sedimentary environments in the New Zealand fluvial record suggest a phase of widespread erosion at this time.

Figure 4.3 also shows that most dates are from material recovered from floodplain sediments (82%). A smaller proportion of dates have been obtained from palaeochannel fills (9%) and channel bed sediments (7%), but very few fluvial units preserved in debris flow settings (2%) have yielded ^{14}C dates. It is interesting to note that the distribution of Holocene fluvial dates across the different sedimentary environments in New Zealand differs from that in the UK (Macklin et al., 2010), where palaeochannel fills account for 42% of ^{14}C dates and floodplain deposits make up close to a third of all dates (32%). This most probably reflects contrasts in catchment physiography and environmental conditions that have differently affected Holocene river dynamics in these areas.

For the cross-correlation function covering the period 12,000–5000 cal. yr BP there is a significant negative correlation between the North and South Island activity series at a lag of –5 years and a positive correlation at 15 years (Fig. 4.6). The significance level was checked using the Ljung-Box portmanteau test (Ljung and Box, 1978). For the probability data covering the period 12,000–5000 cal. yr BP the *p*-value, against a null hypothesis of no correlation, is 0.0005, rejecting the null hypothesis. The cross-correlation function for the North Island and South Island data for the period 5000–2000 cal. yr BP shows no significant

correlation between the two time-series with a significance level of $p = 0.065$ (Fig. 4.6). The time period 2000–0 cal. yr BP was also analysed for the North and South Island river activity time series and the results are also shown in Fig. 4.6. The cross-correlation function shows that the North and South Island are out of phase between 2000–0 cal. yr BP, with a significant negative correlation for the two series at lags of 0 and 15 years, and a positive correlation at 5 years. The *p*-value for this data, against a null hypothesis of no correlation, is 4×10^{-14}, rejecting the null hypothesis. Therefore, the differences in the timing of river activity between northern and southern New Zealand are statistically significant between 12000–5000 and 2000–0 cal. yr BP.

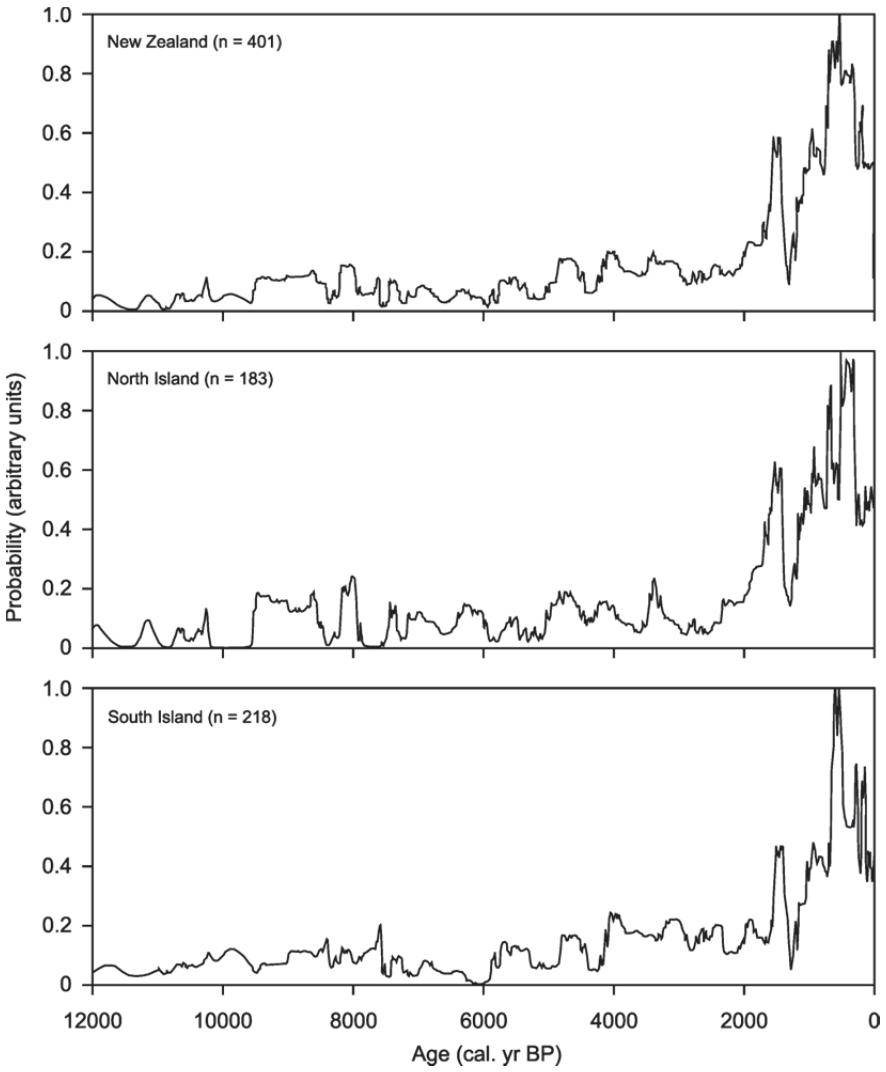

Fig. 4.2. Cumulative probability function (CPF) plots of ^{14}C-dated fluvial units in New Zealand.

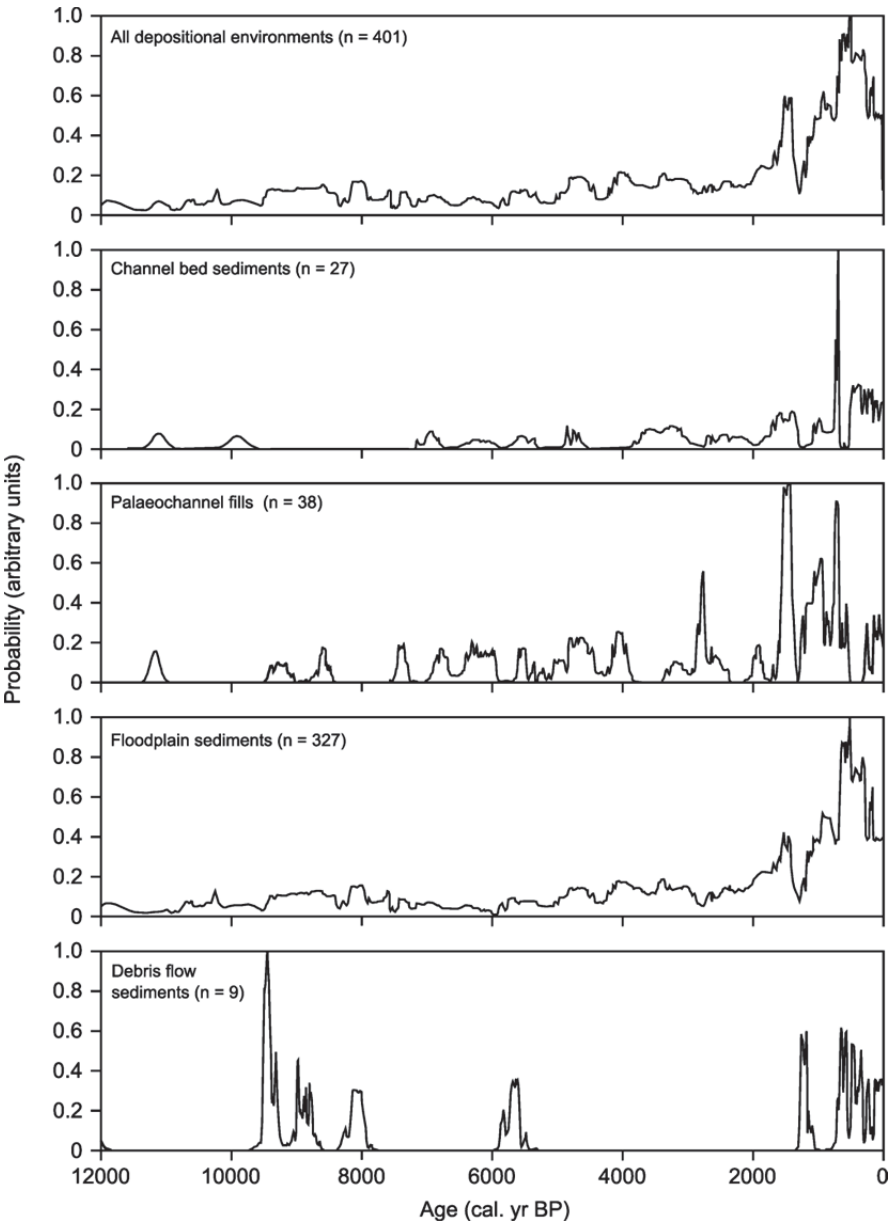

Fig. 4.3. Cumulative probability function (CPF) plots of ^{14}C-dated fluvial units from the five types of fluvial depositional environment.

The relative CPF plots of 'activity', 'stability' and 'change-after' ^{14}C dates for New Zealand are shown in Fig. 4.5. Table 4.3 summarises the results of the relative CPF analysis, identifying 13 major phases of river activity, 9 episodes of river stability and 7 significant episodes of flooding. By including only those probability peaks produced by at least three ^{14}C dates, this approach records the most significant phases of river activity, stability and centennial-scale flooding in New Zealand during the Holocene. These curves should not be read as identifying discrete flood events, but rather 'wet centuries'.

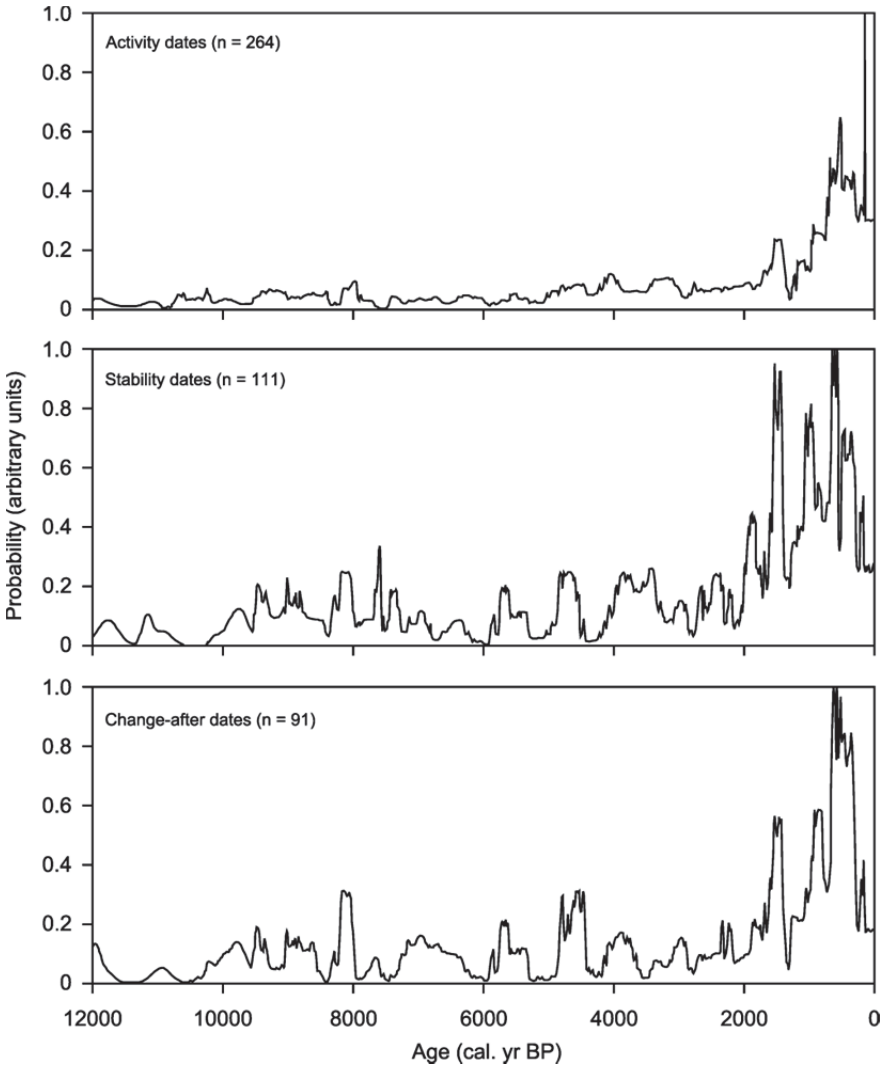

Fig. 4.4. Cumulative probability function (CPF) plots of 'activity', 'stability' and 'change-after' ^{14}C dates from New Zealand Holocene fluvial records.

The regional climate of New Zealand is strongly influenced by interactions between orography and the dominant westerly flow, and has been broadly divided into six homogenous regions (Fig. 4.1) based on historical precipitation and temperature data (Mullan, 1998). A regional analysis of river activity and stability, is presented for the northern (North Island) and southern (South Island) precipitation regions (Figs. 4.7 and 4.8). The North Island record is characterised by 12 periods of increased river activity and four episodes of stability, three of which are recorded in the last 2000 years (Table 4.4). South Island rivers experienced 10 phases of increased fluvial activity and four stable periods during the Holocene. What is striking about the North and South Island records, when

compared, is that the timing of the major phases of Holocene fluvial activity is out of phase (Fig. 4.9). Indeed, there are only three very brief periods (300–100 cal. yr BP, 3300–3200 cal. yr BP and 4100–4000 cal. yr BP) in the entire record where both islands experienced increased activity simultaneously (Table 4.4).

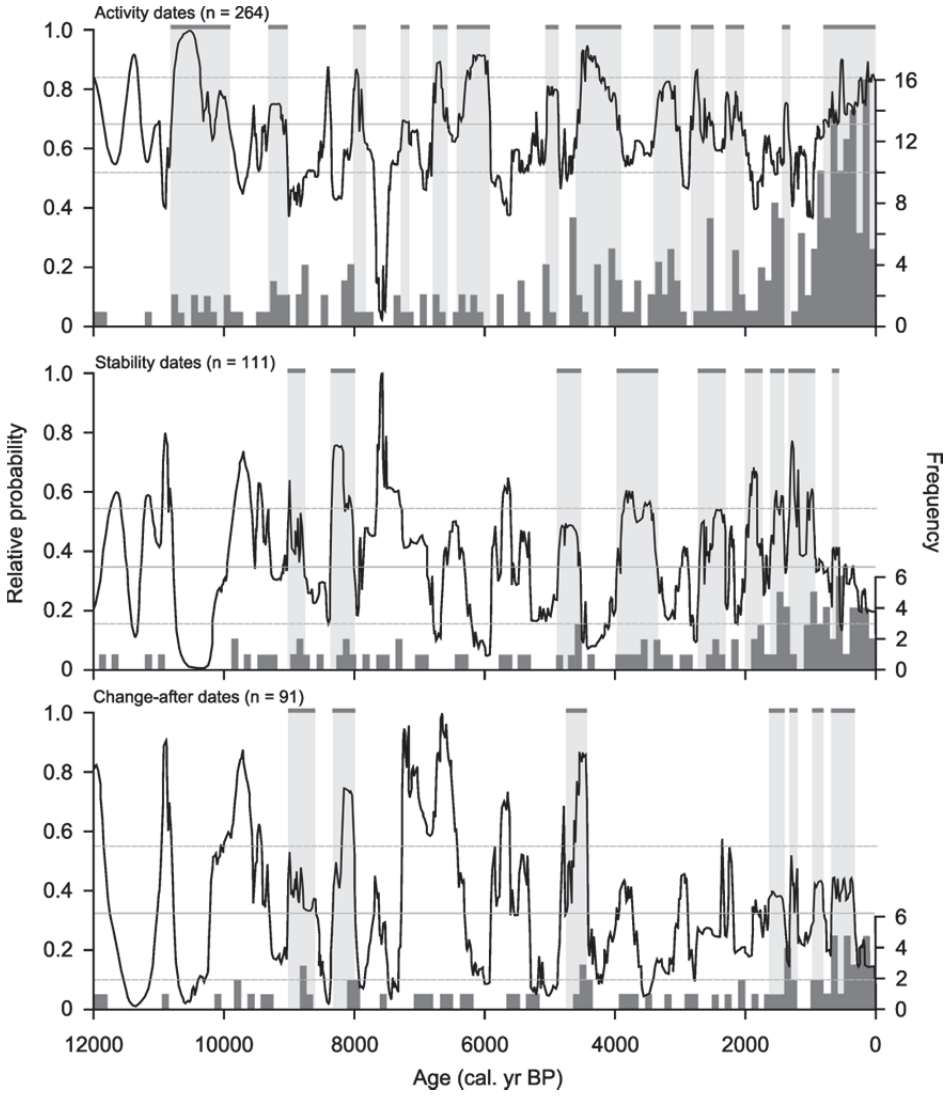

Fig. 4.5. Relative CPF plots of 'activity' (top), 'stability' (middle) and 'change-after'(bottom) ^{14}C dates plotted with frequency of dates per 100 years from New Zealand fluvial units. Horizontal lines indicate the mean (solid line) and one standard deviation above and below the mean (dashed lines). Horizontal grey bars at the top of each plot indicate major episodes of flooding, river activity or stability.

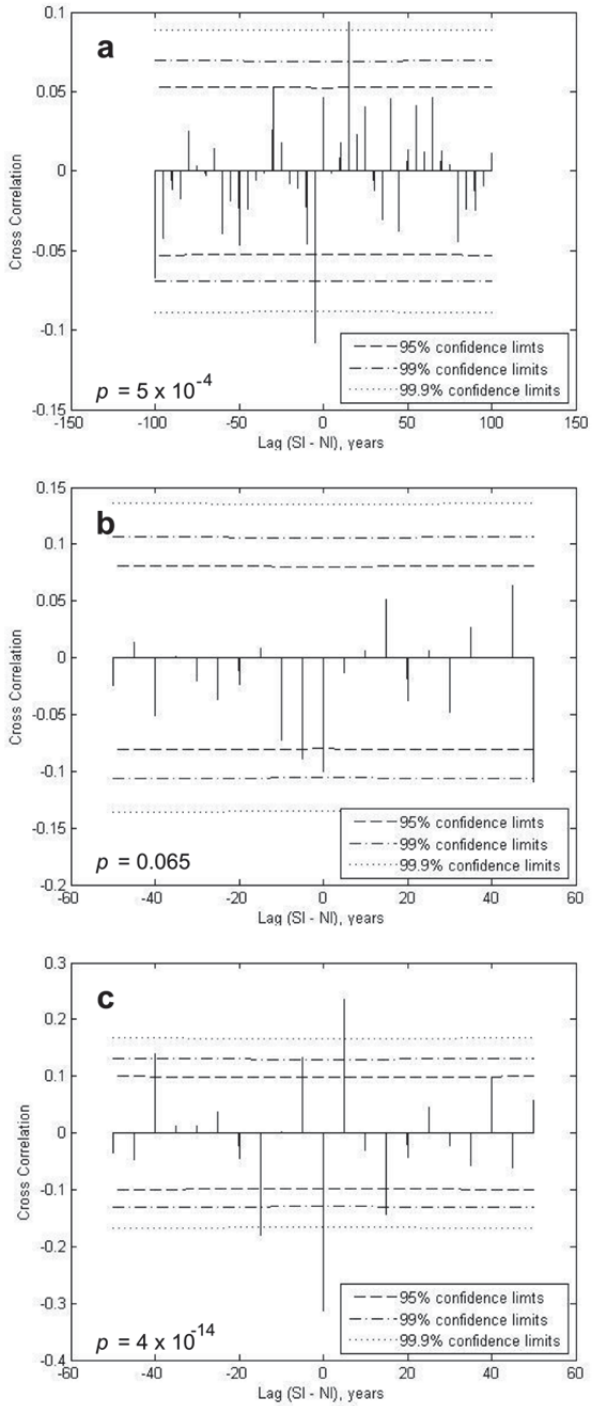

Fig. 4.6. Cross-correlation functions for North and South Island river activity time-series for the periods (a) 12000–5000 cal. yr BP, (b) 5000–2000 cal. yr BP and (c) 2000–0 cal. yr BP.

Table 4.3

Episodes of Holocene river flooding, activity and stability in New Zealand based on analysis of ^{14}C-dated fluvial units.

Change-after dates - NZ (ages in cal. yr BP)	Activity dates - NZ (ages in cal. yr BP)	Stability dates - NZ (ages in cal. yr BP)
	10,800–9900	
	9300–9000	
9000–8600		9000–8800
8300–8000		8400–8000
	8000–7800	
	7300–7200	
	6800–6600	
	6400–5900	
	5100–4900	
4800–4400		4900–4500
	4600–3900	
		4000–3300
	3400–3000	
		2700–2300
	2800–2500	
	2300–2100	
		2000–1700
1600–1400		1600–1400
	1400–1300	
1300–1200		1300–900
1000–800		
700–300		700–600
	800–0	

In a second regional analysis, river activity in the coherent precipitation regions shows that all regions have recorded phases of increased fluvial activity (Fig. 4.10 and Table 4.5), with the majority occurring in the late Holocene. Inevitably, regional analysis thins the data available for interpretation, even for the largest group of dates ('activity'), which means that several prominent peaks are not counted as significant because they are not underlain by the minimum three dates required.

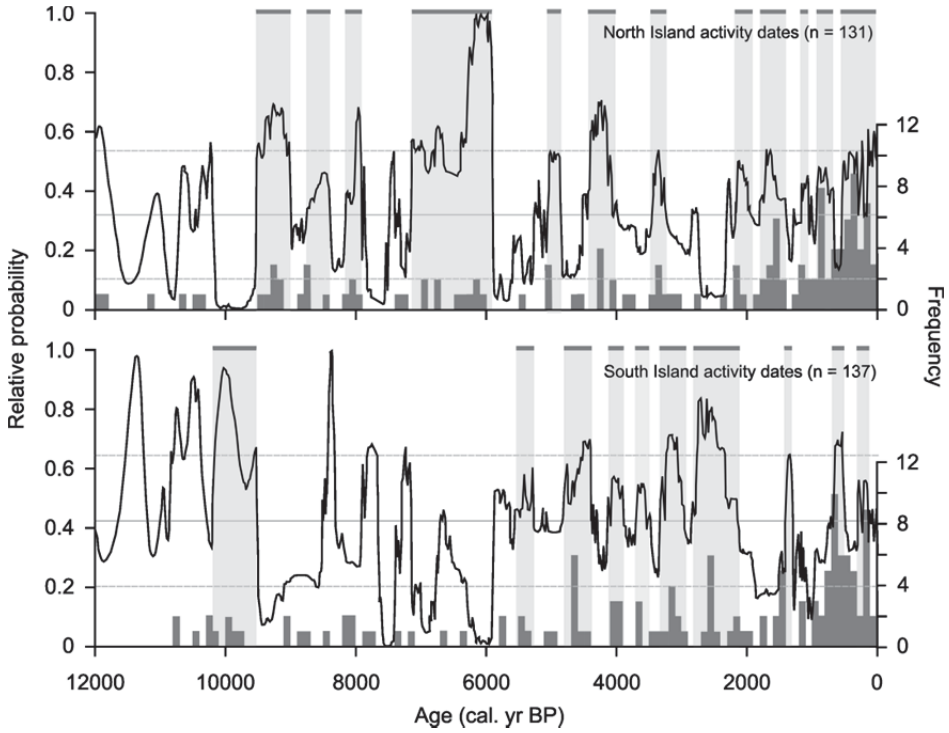

Fig. 4.7. Relative CPF plots of Holocene river 'activity' ^{14}C dates plotted with frequency of dates per 100 years for the North and South Islands, New Zealand. Horizontal lines indicate the mean (solid line) and one standard deviation above and below the mean (dashed lines). Horizontal grey bars at the top of each plot indicate major episodes of river activity.

4.5.1 Holocene floodplain sedimentation rates

Holocene floodplain sedimentation rates for New Zealand have been calculated using the midpoint of the 2 σ age range of ^{14}C ages plotted against sample depths when reported. A total of 207 ^{14}C dates from floodplain depositional environments were used to construct Fig. 4.11. Floodplain sedimentation rates calculated for New Zealand glaciated/unglaciated catchments, New Zealand catchments potentially unaffected/affected by volcanic influences, North and South Island catchments, North Island catchments potentially unaffected/affected by volcanic influences and South Island glaciated/unglaciated catchments show that, for most of the Holocene, sedimentation rates remained below 5 mm yr^{-1}, with a rapid increase occurring after ~ 500 cal. yr BP.

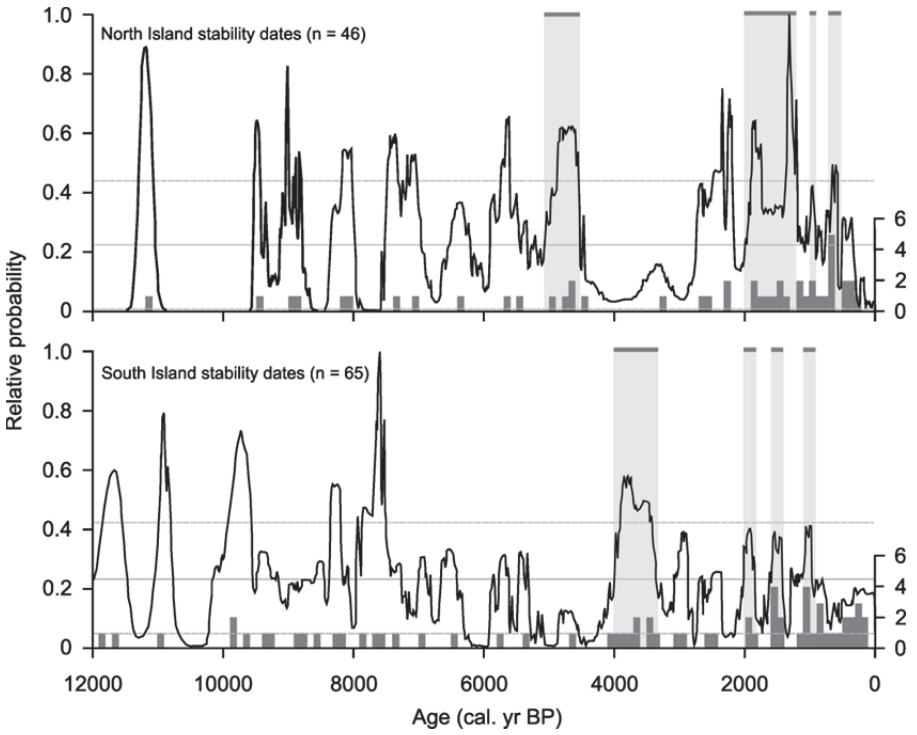

Fig. 4.8. Relative CPF plots of Holocene river 'stability' ^{14}C dates plotted with frequency of dates per 100 years for the North and South Islands, New Zealand. Horizontal lines indicate the mean (solid line) and one standard deviation above and below the mean (dashed lines). Horizontal grey bars at the top of each plot indicate major episodes of river stability.

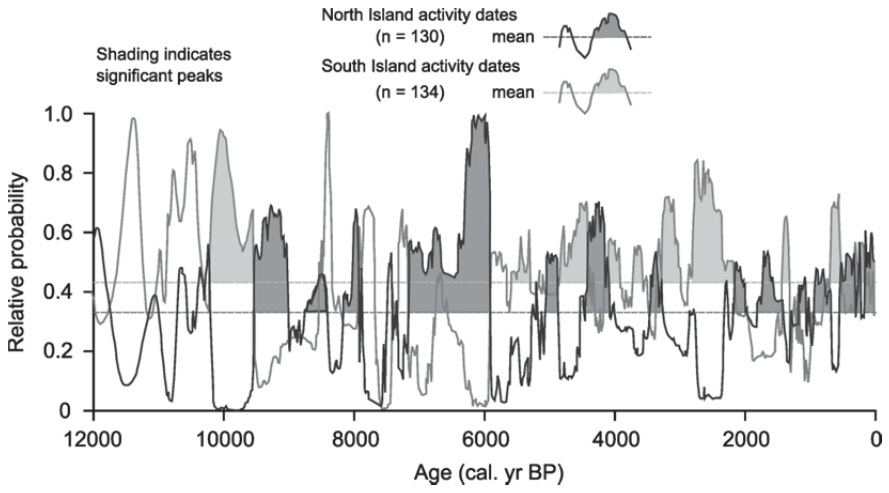

Fig. 4.9. Comparison of relative CPF plots of 'activity' ^{14}C dates from North and South Island fluvial units. Horizontal lines indicate the mean (dashed line). Significant periods are shaded.

Table 4.4

Episodes of regional Holocene river activity and stability in the North and South Islands, New Zealand based on analysis of ^{14}C-dated fluvial units.

Activity dates North Island (ages in cal. yr BP)	Activity dates South Island (ages in cal. yr BP)	Stability dates North Island (ages in cal. yr BP)	Stability dates South Island (ages in cal. yr BP)
	10,200–9500		
9500–9000			
8800–8400			
8200–7900			
7100–5900			
	5500–5300		
5100–4900		5100–4500	
	4800–4400		
4400–4000			
	4100–3900		4000–3300
	3700–3500		
3500–3200			
	3300–2900		
	2800–2100		
2200–1900			
		2000–1200	2000–1800
1800–1400			1600–1400
	1400–1300		
1200–1100			
		1000–900	1100–900
900–700			
	700–500	700–500	
500–0	300–100		

Table 4.5

Episodes of regional Holocene river activity in the six coherent precipitation variability regions of New Zealand based on analysis of ^{14}C-dated fluvial units.

Northern North Island (ages in cal. yr BP)	Southwestern North Island (ages in cal. yr BP)	Eastern North Island (ages in cal. yr BP)	Northern South Island (ages in cal. yr BP)	Western Southern South Island (ages in cal. yr BP)	Eastern South Island (ages in cal. yr BP)
				10,900–9600	
		9500–9000			
		8200–7800			
					5300–4300
					4200–3900
					3400–2800
			2800–2500	2700–2400	
1900–1400					
					1800–1300
1200–700		1000–800		1000–900	
	900–700				
			700–500	600–300	600–500
500–0	500–200		300–100	200–100	
		200–0			

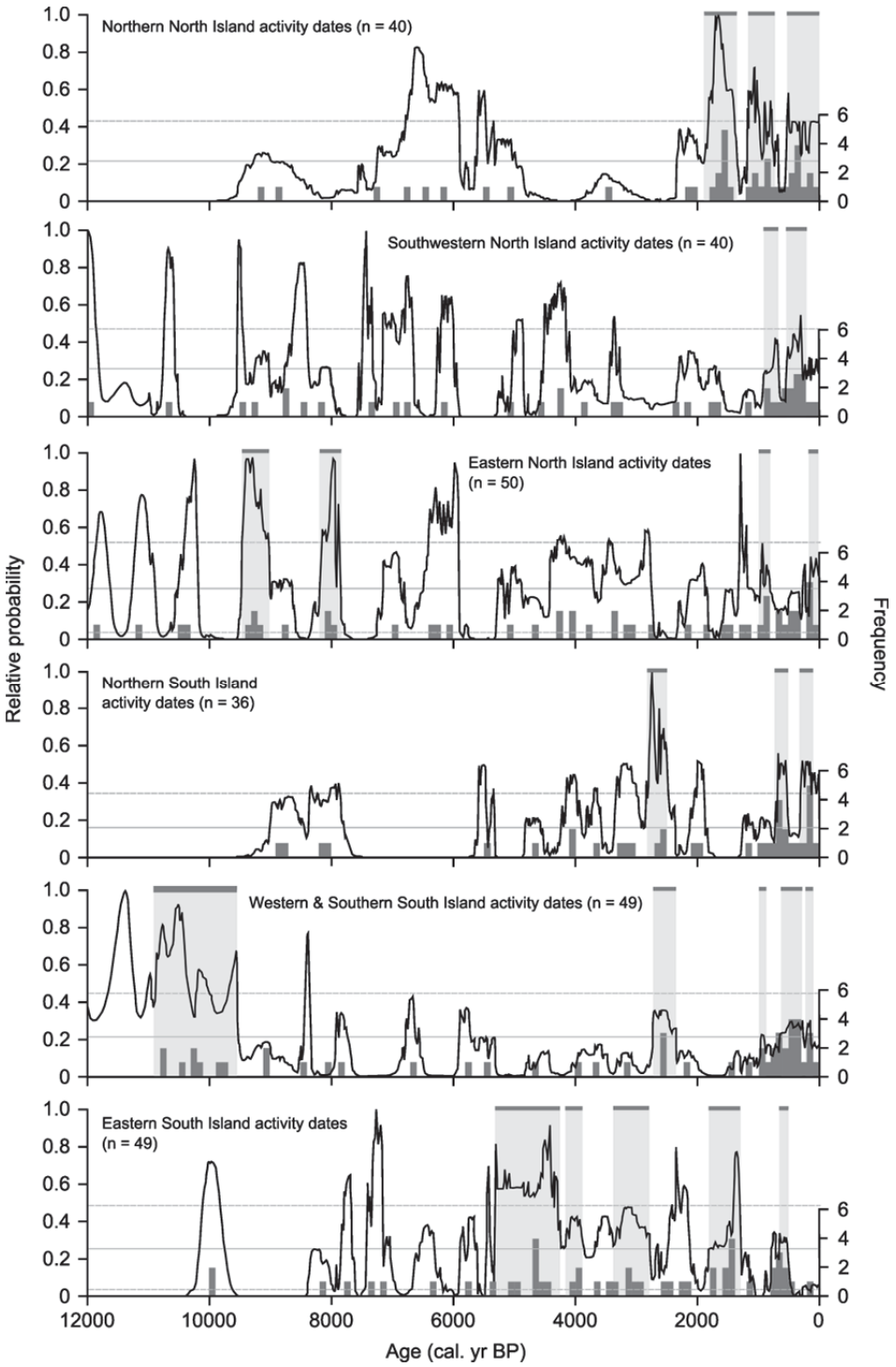

Fig. 4.10. Relative CPF plots of Holocene river 'activity' ^{14}C dates plotted with frequency of dates per 100 years from the coherent precipitation regions within New Zealand. Horizontal lines indicate the mean (solid line) and one standard deviation above and below the mean (dashed lines). Horizontal grey bars at the top of each plot indicate major river activity episodes.

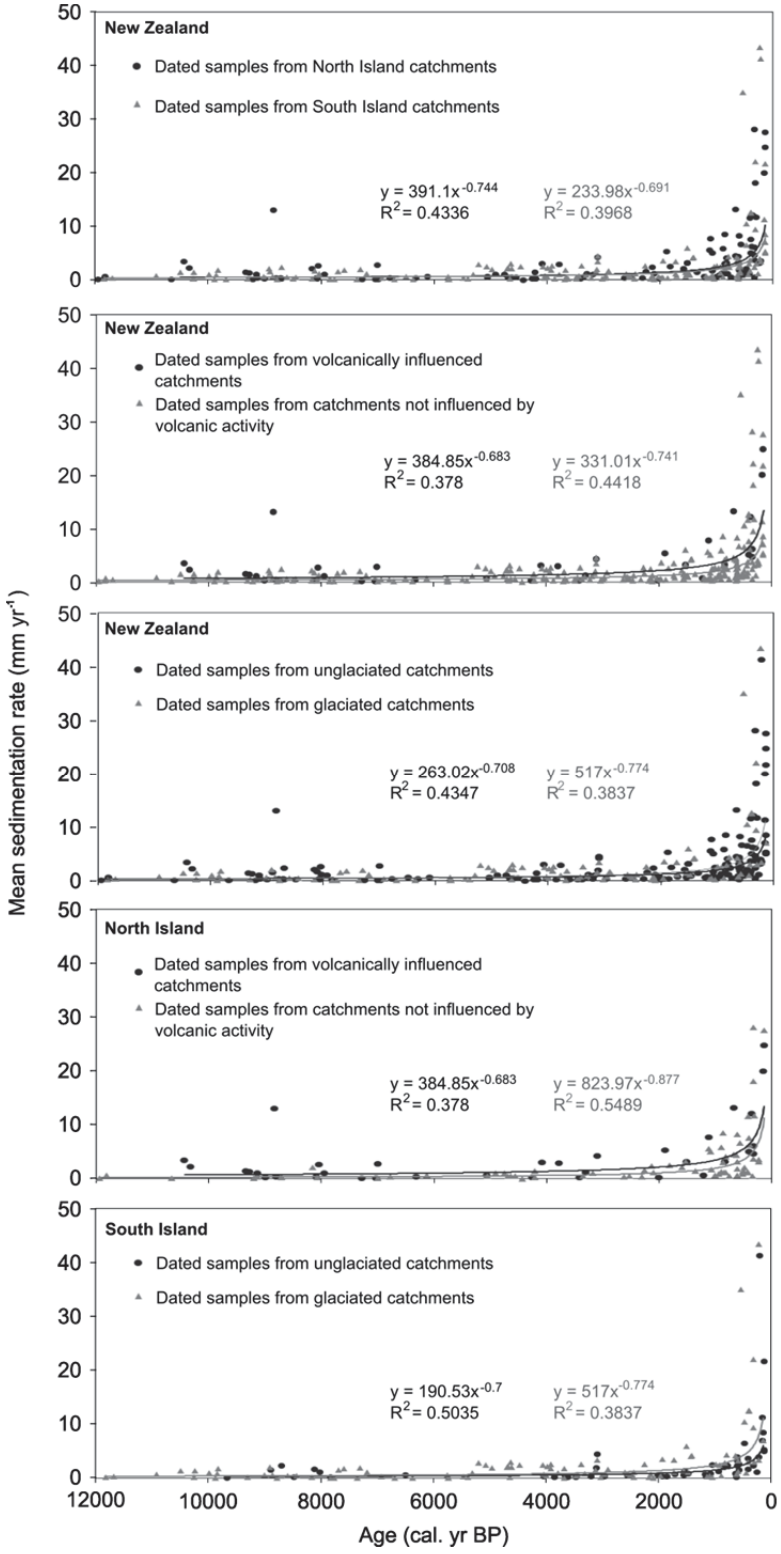

Fig. 4.11. Holocene floodplain sedimentation rates plotted for North and South Island catchments, New Zealand catchments influenced and not influenced by volcanic activity, New Zealand glaciated and unglaciated catchments, North Island catchments influenced and not influenced by volcanic activity and glaciated and unglaciated South Island catchments.

4.6 Discussion

4.6.1 River activity and regional climate change

The geography of New Zealand, spanning 13 degrees of latitude, orientated perpendicular to the prevailing Southern Hemisphere circumpolar westerlies, and with major axial ranges in both North and South Islands, ensures a high degree of regional climate complexity (Ummenhofer and England, 2007). Kidson (2000) and Mullan (1998) identify six homogenous precipitation regions (Fig. 4.1), some with contrasting surface climate variability. The divisions between these homogenous climate districts are largely the result of interactions between the dominant westerly flow and orography, with strong north–south and east-west contrasts in temperature and precipitation. To add to the regional complexity, individual river systems although located in one homogenous climate region may not reflect the climate of that region if the majority of the flow originates from a different climate region. A lack of ^{14}C dates in some regions mean that a full probability-based reconstruction of activity, stability and flooding cannot be carried out for each of the coherent precipitation regions, or North and South Island east-west comparisons. However, an analysis of ^{14}C 'activity' dates identifies a number of multi-centennial length phases of river activity, concentrated in the later part of the Holocene, with all regions registering increased fluvial activity at some stage in the last 600 years (Fig. 4.10 and Table 4.5).

Compilation of fluvial records from northern and southern precipitation regions (North and South Islands) show that, in terms of episodes of river activity, the two regions have exhibited a predominantly out-of-phase relationship (Figs. 4.7 and 4.9), primarily reflecting regional climate complexity and contrasting response to circulation changes (Kidson, 2000; Lorrey et al., 2008). New Zealand climate is strongly influenced by the operation of the tropical ENSO and extratropical SAM, with their relative influence showing latitudinal gradation (Ummenhofer and England, 2007). During El Niño (La Niña) phases of ENSO equatorial sea-surface temperatures (SST) are anomalously warm (cool) in the eastern and central Pacific and cool (warm) in the western Pacific. Precipitation patterns in New Zealand are influenced by the oscillation of ENSO through its influence on the position of the South Pacific Convergence Zone (Folland et al., 2002), the strength of the subtropical and polar front jet streams and migration of the mid-latitude storm tracks (Yuan, 2004).

Teleconnections between ENSO and streamflow have been detected in many catchments globally, including strong connections in New Zealand and Australia (Chiew and McMahon, 2002). In New Zealand the hydrological response to ENSO and the associated circulation

changes is consistent with climate effects, and is most notable in the rivers of northern and eastern North Island and the South Island axial ranges (Mosley, 2000). In these regions the influence of ENSO on the frequency and duration of rain-bearing atmospheric flow (northeasterly circulation in the northern and eastern North Island and westerly flow in the South Island) combined with topography has an influence on streamflow, although there is considerable variability between catchments and within ENSO events (Mosley, 2000).

Kidson (2000) defined 12 synoptic weather types and classified three regimes in New Zealand (trough, zonal and blocking regimes), the occurrence of which is associated with the oscillation of ENSO and SAM. Synoptic-climatological analysis has found that during El Niño there is an increase in zonal regime synoptic types and more blocking types during La Niña phases (Renwick, 2011) (Fig. 4.12). The positive mode of the SAM has been linked to increased frequency of blocking and zonal types and more trough types during negative SAM (Renwick, 2011) (Fig. 4.12).

The Southern Annular Mode (SAM) has been described as the leading mode of interannual variability in extratropical circulation in the Southern Hemisphere (Thompson and Wallace, 2000; Marshall, 2007). The SAM essentially defines the large-scale zonally-symmetric transfer of atmospheric mass, resulting in synchronous pressure anomalies of opposite signs between the mid- and high-latitudes (Gong and Wang, 1999; Thompson and Wallace, 2000). The positive (negative) phase of the SAM is characterised by warmer (cooler) surface temperatures in the Antarctic Peninsula region and cooler (warmer) temperatures in East Antarctica, an intensified (weakened) polar vortex, a southward (northward) shift in the extratropical storm tracks and subpolar westerlies (Thompson and Wallace, 2000; Kwok and Comiso, 2002; Marshall, 2003, 2007) (Fig. 4.12). During the negative (positive) phase of the SAM westerly flow across New Zealand is enhanced (reduced) and southern New Zealand experiences increased (decreased) precipitation, while in the North Island a more northeasterly flow regime during the positive mode of the SAM leads to increased moisture transport onto northern New Zealand (Ummenhofer and England, 2007).

Models have shown that the North Island climate is most influenced by ENSO and the tropical Pacific region, while in the South Island, precipitation is regulated by atmospheric circulation associated with the position of the subpolar westerlies and the operation of the SAM (Ummenhofer and England, 2007). Gomez et al's. (2011) synthesis of Pacific Southern palaeoclimate records (Figs. 4.13, 4.14 and 4.15) indicate that the operation of ENSO and SAM has fluctuated at millennial scales throughout the Holocene in response to precessional forcing. There is also evidence to suggest that the phase relationship of the two

leading climate modes has an impact on the strength of ENSO extratropical teleconnections (e.g., Gomez et al., 2011) (Figs. 4.13, 4.14 and 4.15).

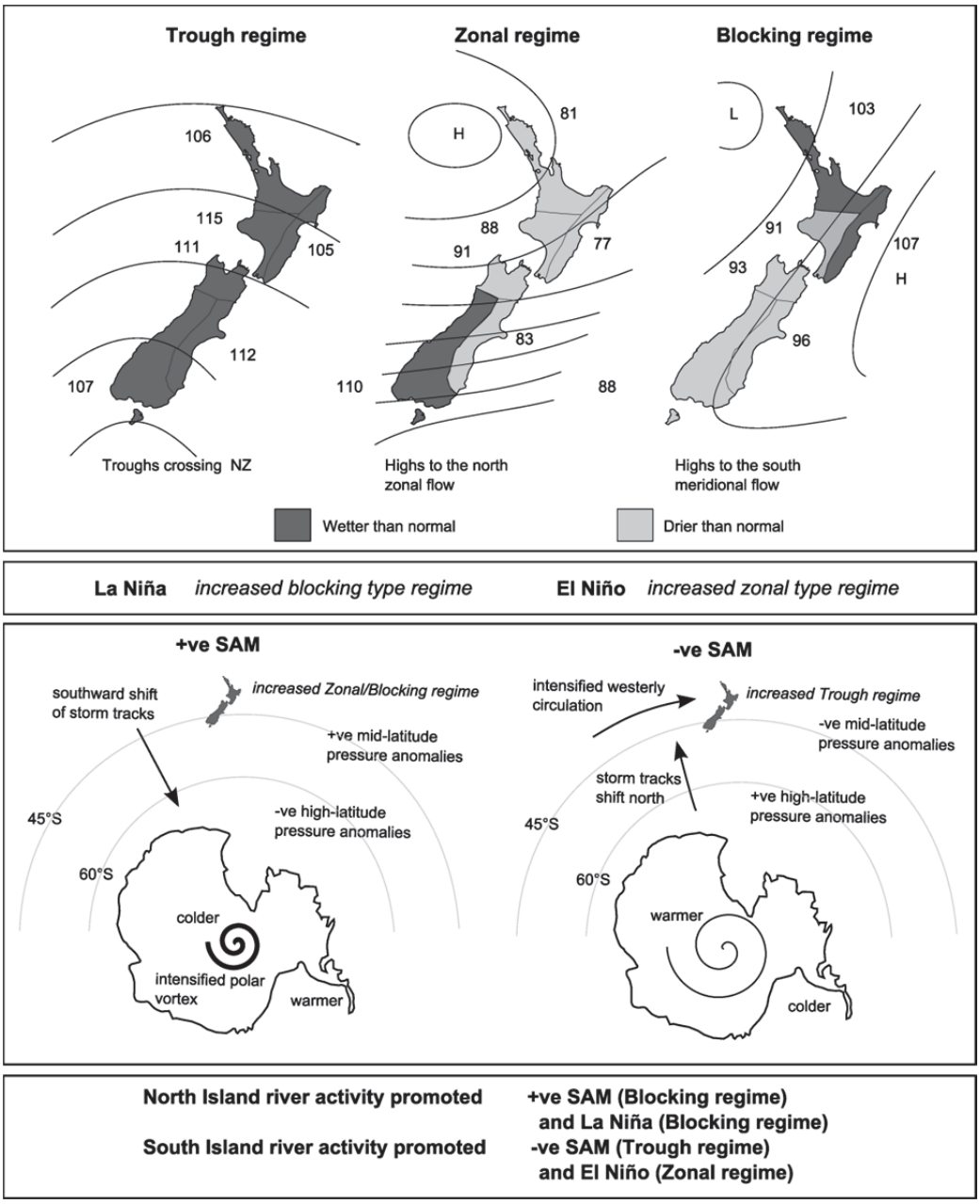

Fig. 4.12. New Zealand's three weather regimes displayed with an example of an associated synoptic pattern (Kidson, 2000) and annotated with average regional precipitation anomalies, based on monthly averages (Renwick, 2011). Rainfall figures for each of the coherent precipitation regions are percent of normal. The influence of the ENSO cycle and the polarity of the SAM on the relative frequency of occurrence of the synoptic types and associated regimes are indicated. The main features of the SAM and a summary of the effect of SAM and ENSO on North and South Island river activity are also included.

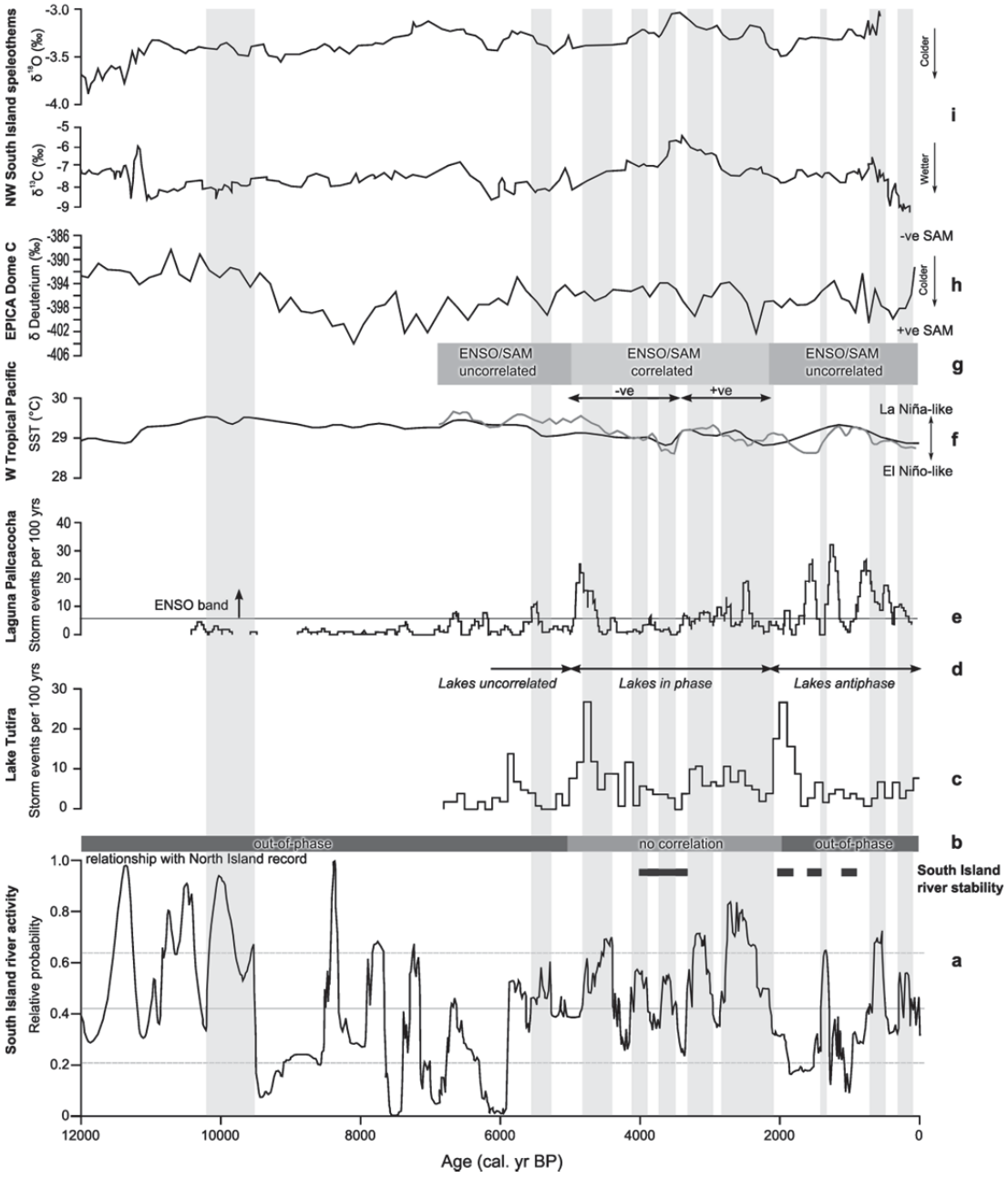

Fig. 4.13. Regional palaeoclimate proxy records for the Holocene. (a) Relative CPF plot of Holocene river activity in South Island, New Zealand, based on analysis of ^{14}C-dated Holocene fluvial units. Black horizontal bars indicate periods of South Island river stability based on ^{14}C-dated Holocene fluvial units. Vertical light grey bars indicate significant periods of South Island river activity. (b) Relationship between North and South Island river activity records. (c) Lake Tutira storm frequency record (Gomez et al., 2011). (d) Relationship between Lake Tutira and Laguna Pallcacocha sedimentation records (Gomez et al., 2011). (e) Event time series (100-yr overlapping windows) for the number of storm events from a record of sedimentation in Laguna Pallcacocha, southern Ecuador (Moy et al., 2002). (f) Western Tropical Pacific (WTP) Mg/Ca palaeoSST reconstruction derived for

cores MD81, MD76, MD70 and ODP806 (black line - stacked average) and cores MD81 and MD76 only (grey line) (Stott et al., 2004). (g) Relationship between Antarctic surface temperatures (SAM) and WTP temperature records (ENSO) (Gomez et al., 2011). (h) δ deuterium record (‰) from EPICA Dome C ice core, Antarctica (Jouzel, 2004). (i) $\delta^{13}C$ and $\delta^{18}O$ records (‰) from north-west South Island speleothems (Williams et al., 2010) 5 pt. running mean.

The early to mid Holocene (12,000 to 5000 cal. yr BP) has been identified as a period when ENSO was weak or non-operational (Sandweiss et al., 2001; Moy et al., 2002) and operating with reduced precipitation teleconnections (Shulmeister et al., 2006). Gomez et al. (2011) identified the period 6800 to 4900 cal. yr BP as a time when ENSO and SAM were uncorrelated and there was reduced connectivity between the high- and mid-latitudes (Fig. 4.15). SAM proxy records from east Antarctica reveal a strong dominance of negative SAM in the early Holocene switching to positive polarity for the period ~ 9000 to 6000 cal. yr BP (Fig. 4.15). Cross-correlation analysis of North and South Island river activity records during the early to mid Holocene (12,000 to 5000 cal. yr BP) shows that the timing of river activity in the North and South Islands is significantly (statistically) different, with river activity in the southern regions preceding North Island systems, suggesting climate was being more influenced by the operation of the high-latitude climate mode (SAM) at a time of weak ENSO influence and low or no connectivity between SAM and ENSO (Fig. 4.15).

Perhaps the most obvious difference between the North and South Island river activity records during the early to mid Holocene is that North Island phases of river activity were more prominent between ~ 9500 and 5900 cal. yr BP, and only one significant period of river activity was identified from the South Island record at 10,200–9500 cal. yr BP (Figs. 4.13, 4.14 and 4.15). Regional reconstructions of palaeohydroclimatic conditions using speleothem stable isotope records have proved useful in determining past centennial-scale circulation and climate regime changes in New Zealand (e.g., Lorrey et al., 2008; Williams et al., 2010). Evidence from these records suggests that cooler periods are associated with a trough regime and enhanced westerly circulation (promoted by El Niño conditions in northern New Zealand and negative phases of the SAM in southern New Zealand), while subtropical influences characterised by stronger northerly and easterly circulation (blocking regime) are linked to warmer temperatures (promoted under La Niña conditions and the positive phase of the SAM) (Lorrey et al., 2008) (Fig. 4.12). In the early to mid Holocene the only significant period of South Island river activity occurred during a period identified

as wet from the north-west South Island speleothem record, and at a time of warmer Antarctic temperatures (Figs. 4.13 and 4.15), signifying a dominance of negative SAM conditions and enhanced zonal atmospheric flow in southern regions (Fig. 4.12). In contrast, rivers in the North Island showed more evidence of activity and flooding in the later part of the first half of the Holocene when positive SAM conditions dominated (Figs. 4.14 and 4.15). Central-west North Island $\delta^{18}O$ records show no straightforward relationship between phases of river activity and the climatic changes detected in the record, although a phase of North Island river activity at 7100–5900 cal. yr BP corresponds to a prominent wet period when temperatures were declining in the speleothem record (Fig. 4.14). The behaviour of New Zealand rivers in the first half of the Holocene supports the idea that the SAM had a greater influence on mid-latitude climate at a time of weak ENSO (e.g., Fogt and Bromwich, 2006), suggesting that during this period the SAM, through its influence on westerly atmospheric flow, was driving New Zealand river activity (Fig. 4.12).

Between 5000 and 2000 cal. yr BP there is no significant correlation between the North and South Island river activity records. This period has been identified as a time of enhanced ENSO variability and intensification (Sandweiss et al., 2001; Shulmeister et al., 2006; Donders et al., 2008), strengthened ENSO teleconnections, with a phased relationship between ENSO and SAM (Gomez et al., 2011) (Figs. 4.13, 4.14 and 4.15) River activity in the South Island was associated with a warming and drying trend during this period, which peaks around 3500 cal. yr BP (Figs. 4.13 and 4.15). In contrast, the North Island exhibited less river activity in the mid to late Holocene, with some evidence from the central-west speleothem record that the climate during this time was exhibiting a cooling trend (Williams et al., 2010) (Figs. 4.14 and 4.15). We suggest that the Holocene river activity records from southern and northern New Zealand during the mid to late Holocene reflect changes in the relative dominance of the two major oscillatory climate modes, with the mid to late Holocene characterised by more complex interactions and teleconnections between ENSO and SAM.

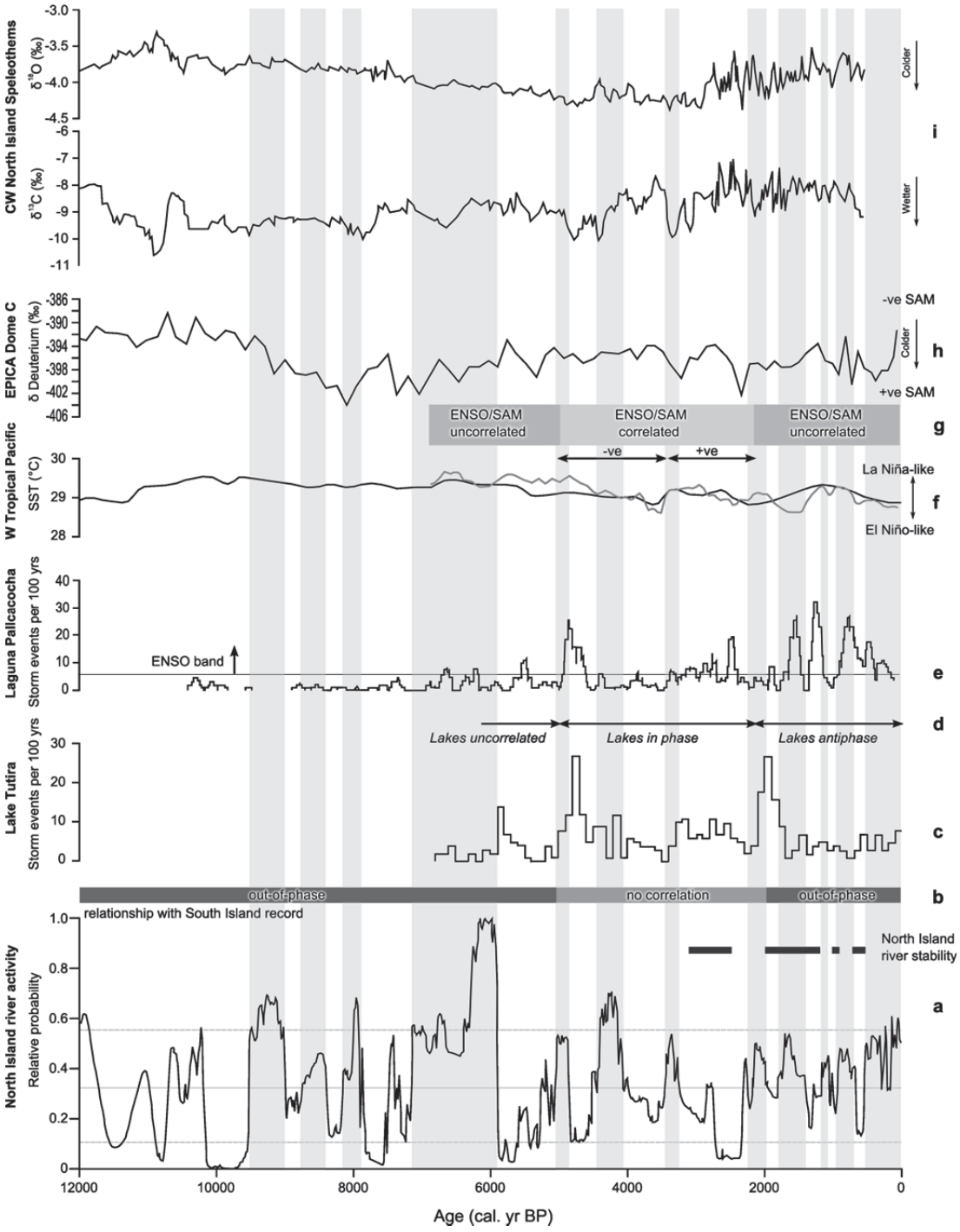

Fig. 4.14. Regional palaeoclimate proxy records for the Holocene. (a) Relative CPF plot of Holocene river activity in the North Island, New Zealand, based on analysis of ^{14}C–dated Holocene fluvial units. Black horizontal bars indicate periods of river stability based on ^{14}C-dated Holocene fluvial units. Vertical light grey bars indicate significant periods of North Island river activity. (b) Relationship between North and South Island river activity records. (c) Lake Tutira storm frequency record (Gomez et al., 2011). (d) Relationship between Lake Tutira and Laguna Pallcacocha sedimentation records (Gomez et al., 2011). (e) Event time

series (100-yr overlapping windows) for the number of storm events from a record of sedimentation in Laguna Pallcacocha, southern Ecuador (Moy et al., 2002). (f) Western Tropical Pacific (WTP) Mg/Ca palaeoSST reconstruction derived for cores MD81, MD76, MD70 and ODP806 (black line - stacked average) and cores MD81 and MD76 only (grey line) (Stott et al., 2004). (g) Relationship between Antarctic surface temperatures (SAM) and WTP temperature records (ENSO) (Gomez et al., 2011). (h) δ deuterium record (‰) from EPICA Dome C ice core, Antarctica (Jouzel, 2004). (i) $\delta^{13}C$ and $\delta^{18}O$ records (‰) from central-west North Island speleothems (Williams et al., 2010) 5 pt. running mean.

After 2000 cal. yr BP records from Kake Tutira and Laguna Pallcacocha suggest no correlation between ENSO and SAM (Gomez et al., 2011) (Figs. 4.13, 4.14 and 4.15). River activity records and cross-correlation analysis show that during this time river activity time-series for the North and South Islands are antiphased. River activity records also show that in the last 2000 years North Island rivers have been more active than South Island systems. Assessments of variability in New Zealand rainfall show that the North Island experiences anomalously dry conditions during the El Niño phases of ENSO (Ummenhofer and England, 2007) under an increased zonal synoptic regime (Renwick, 2011) (Fig. 4.12). North Island river activity is most likely to be associated with more meridional circulation patterns generated by a combination of La Niña phases of ENSO and the positive phase of the SAM, with increased frequency of storms and floods generated from the incursion of warm, moist subtropical air masses, which have been connected with major floods in historical records (Lorrey et al., 2008). It would appear that in the last 2000 years the positive phase of the SAM mode has dominated and has corresponded with warming (as highlighted in the central-western North Island speleothem records) (Fig. 4.14), adding support to the idea that North Island river activity is predominantly driven by enhanced sub-tropical airflow. A comparison of the South Island river activity record and Laguna Pallcacocha ENSO proxy records (Fig. 4.12), which indicate an increase in ENSO frequency over the last ~ 3000 years, shows that episodes of South Island river activity (at 2300–2100, 1400–1300, 700–500 and 300–100 cal. yr BP) occur during times of low ENSO frequency. The marked absence of river activity in the South Island with maximum ENSO activity during the Holocene is striking, suggesting this is not a key driver of river activity in this part of New Zealand at these times.

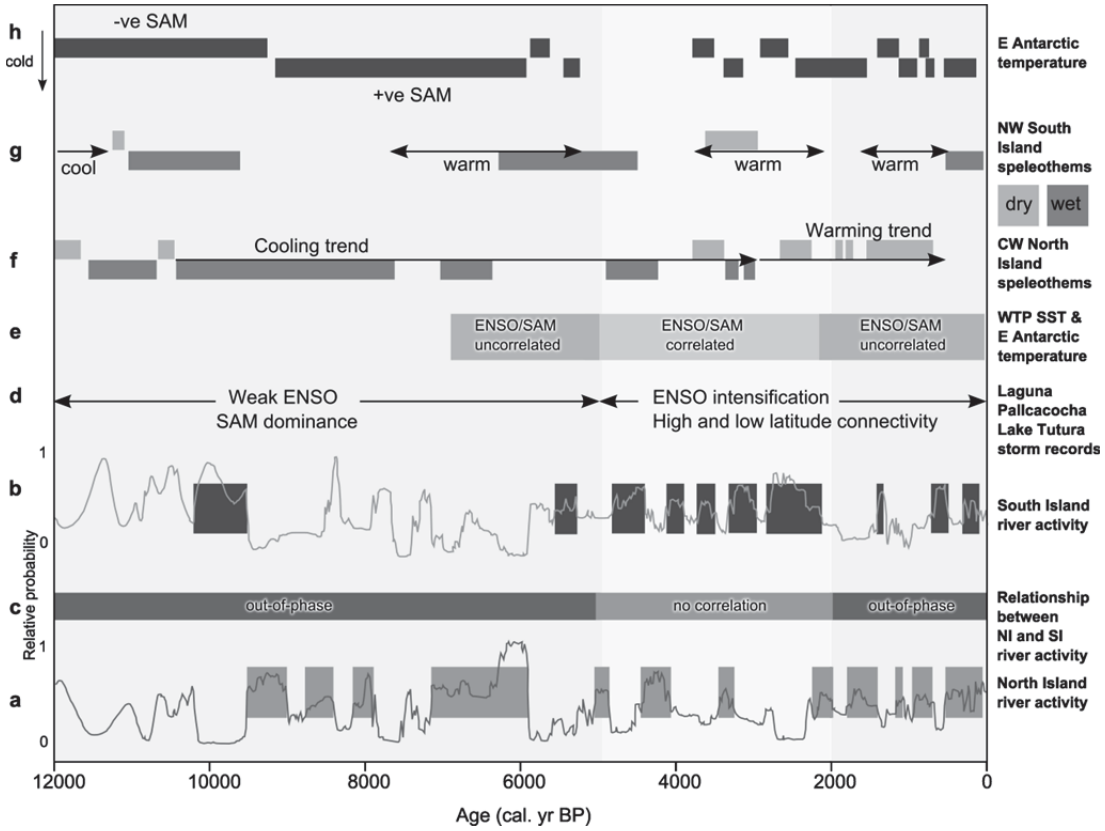

Fig. 4.15. Schematic of regional palaeoclimate, climate modes and major relationships for the Holocene. (a) Relative CPF plot of Holocene river activity in the North Island, New Zealand, based on analysis of ^{14}C-dated Holocene fluvial units. Grey horizontal bars indicate significant periods of river activity based on ^{14}C-dated Holocene fluvial units. (b) Relative CPF plot of Holocene river activity in the South Island, New Zealand, based on analysis of ^{14}C-dated Holocene fluvial units. Dark grey horizontal bars indicate significant periods of river activity based on ^{14}C-dated Holocene fluvial units. (c) Relationship between North and South Island river activity records. (d) Relative influence and intensity of ENSO and SAM determined from Lake Tutira, New Zealand (Gomez et al., 2011) and Laguna Pallcacocha, southern Ecuador (Moy et al., 2002), sedimentation records. (e) Relationship between Antarctic surface temperatures (SAM proxy) and WTP temperature records (ENSO proxy) (Gomez et al., 2011). (f) Temperature and precipitation inferred from central-west North Island speleothems (Williams et al., 2010). (g) Temperature and precipitation inferred from north-west South Island speleothems (Williams et al., 2010) (h) Polarity of the SAM inferred from East Antarctic temperature determined from the δ deuterium record from EPICA Dome C ice core (Jouzel, 2004).

4.6.2 Model of Holocene river activity

The out-of-phase river activity between North and South Islands strongly suggests a phased relationship between ENSO and SAM, and the relative dominance of the two modes may be responsible for driving Holocene river activity in New Zealand (Fig. 4.12). Holocene river activity in the North Island is likely to have been maximised during periods of increased occurrence of blocking regime synoptic type (favoured by positive SAM and La Niña conditions). This combination results in both weakening of the westerly winds across New Zealand and warming of the southwestern Pacific, placing an anomalously warm ocean in closer proximity to the North Island, providing conditions likely to generate large floods and episodes of enhanced river activity (wetter centuries). However, given the southward location of South Island, these conditions would have been less influential on river activity, and the bulk of the South Island would in contrast be less wet during these periods. Rather, river activity in the South Island would be maximised by enhanced westerly winds, steering storm tracks across the island from the Tasman Sea. These conditions would be favoured by an increased occurrence of the trough regime synoptic type (negative phase SAM-like circulation) and perhaps further enhanced by a more zonal regime (El Niño-like circulation conditions) (Fig. 4.12).

4.6.3 Holocene floodplain sedimentation rates

Reconstruction of New Zealand Holocene floodplain sedimentation rates, using sample depths and the midpoints of the 2 σ ranges of calibrated ^{14}C ages, shows a rapid increase in floodplain sedimentation in the last ~ 500 years (Fig. 4.11). A similar pattern of acceleration in sedimentation in the late Holocene has also been identified in both upland and lowland UK (Macklin et al., 2010), and Ireland (Turner et al., 2010). The late arrival of humans in New Zealand means that anthropogenic impacts on catchment erosion and floodplain sedimentation are confined to the last few centuries. It is most likely recent rapid sedimentation rates detected in the New Zealand fluvial record can be attributed to the deforestation that began in some parts of New Zealand shortly after the deposition of the Kaharoa Tephra (ca. 1314 AD) (Alloway et al., 2007). However, because of the episodic nature of aggradation at a point and preservation bias that favours younger deposits we would expect to see higher sedimentation rates in the most recent period. Sedimentation rates for many of the older dates may reflect a few centuries of continued sedimentation at that location after deposition of the dated sample, and then an absence of further deposition up until the present. Also the number of samples recording very high sedimentation rates during the recent period is small (10 samples exceed 15 mm yr^{-1}).

Sedimentation rates for glaciated/unglaciated catchments and catchments potentially affected by volcanic factors also show a similar transition from low sedimentation rates throughout the Holocene with increased sedimentation rates in the last few hundred years (Fig. 4.11). In this analysis glaciated catchment were catchments that presently have glaciated headwaters or have been glaciated during the LGCP. Unglaciated catchments are those catchments that have never had glacial ice cover. Volcanically influenced catchments are those catchments that are in proximity to the Taupo and Taranaki Volcanic zones, including catchments that were within the zone of tephra airfall. It is difficult to isolate the impacts that glaciation and volcanic activity have had on floodplain sedimentation in New Zealand as the subset of unglaciated catchments includes volcanically influenced catchments and the subset of catchments without volcanic influence includes glaciated catchments. As all glaciated catchments are located in the South Island and all catchments potentially influenced by volcanic activity are located in the North Island, analysis of the North Island data for the effects of volcanic activity and South Island data for the influence of glaciation, provides a clearer picture as to the effects that these factors have on floodplain sedimentation. There is evidence to suggest that floodplain sedimentation rates in North Island catchments potentially influenced by volcanic activity are higher (rates of ~ 1–2 mm yr^{-1} higher in the last ~ 4000 years) than for those catchments distally located from volcanic activity (Fig. 4.11). The impact of glaciation has not had an overriding effect on floodplain sedimentation in the South Island catchments.

4.7 Conclusion

A meta-analysis of ^{14}C-dated fluvial units in New Zealand obtained from published papers and unpublished reports has produced the first probability-based reconstructions of Holocene river behaviour in New Zealand. Records of river activity reveal a pattern of multi-centennial-length episodes of increased fluvial activity throughout the Holocene and that river activity in the North and South Islands is predominantly out of phase. Southern New Zealand has experienced episodes of river activity in response to enhanced westerly circulation, coinciding with the more trough regime synoptic types (negative phase SAM-like circulation). In the North Island river activity is most likely driven by increased meridional atmospheric circulation associated with more blocking regime synoptic types (La Niña-like and positive SAM-like circulation). At the resolution afforded by this study, it appears that during the Holocene, variability in atmospheric circulation is the key driver of river activity. Further work and data are needed to assess river activity at the scale of the coherent precipitation region. This will be further enhanced by beginning to fill geographical gaps in the ^{14}C database, such as in far northern New Zealand (Northland) (cf. Fig. 4.1). The

fluvial sedimentary archive also points to rapid acceleration in floodplain sedimentation after ~ 500 cal. yr BP, following commencement of anthropogenic deforestation. These results demonstrate the value of using fluvial archives to reconstruct past environmental conditions, and the potential for high resolution regional palaeoclimate reconstruction.

Acknowledgements

This work was funded by a Tertiary Education Commission Top Achiever Doctoral Scholarship awarded to JR. MGM and AFJ wish to thank HEFCW for financial support that enabled the compilation and analysis of the New Zealand ^{14}C dated Holocene fluvial database and MGM is especially grateful to Massey University for an International Visitor Research Fund award that greatly facilitated the development of this project. NJL's contribution was funded by PGSF Contract CO5X0705.

Chapter 5

The role of valley floor confinement as a control on Holocene floodplain development: an example from Northland, New Zealand

5.1 General introduction

Chapter 4 applied meta-analysis techniques to 401 fluvial ^{14}C-dated fluvial units in New Zealand to produce a probability-based reconstruction of Holocene river behaviour in response to environmental change (including climate) for New Zealand. Records of river activity indicate a pattern of multi-centennial-length episodes of increased fluvial activity throughout the Holocene, which is predominantly out of phase for northern (North Island) and southern (South Island) regions, driven by variability in atmospheric circulation. Chapter 4 concluded that further work and data were required to assess river activity at the scale of the coherent precipitation region and noted that Northland river systems were among the least researched catchments in New Zealand, with a lack of ^{14}C-dated fluvial units located in this region. Chapter 5 addresses this knowledge gap by reconstructing the fluvial history at eight floodplain sites located across the Northland region. In addition, Northland's tectonic and volcanic stability (in New Zealand terms) means river behaviour will be more directly driven by climate change for the majority of the Holocene. Thus, the focus of the chapter is to elucidate the role that climate and late Holocene anthropogenic impacts have had on Northland floodplain development in a range of valley floor configuration settings.

Chapter 5 is contained within the manuscript: J.M. Richardson, I.C. Fuller, K.A. Holt, N.J. Litchfield, M.G. Macklin: The role of valley floor confinement as a control on Holocene floodplain development: an example from Northland, New Zealand, which is in review in the journal *Geomorphology*. In this chapter the fluvial history at eight sites, from a range of valley floor settings and located across the Northland region, is reconstructed. A regional model for Holocene fluvial behaviour is proposed in Section 5.7.2 and the mechanisms involved in floodplain formation are discussed in Section 5.7.3. Finally, the model of Northland floodplain evolution through the Holocene is compared with floodplain development in other regions globally.

As part of the investigation into the floodplain development of Northland, the use of optically stimulated luminescence (OSL) dating to provide ages for Holocene fluvial sediments was also assessed. In order to test the technique in the Northland fluvial setting, five samples from sections previously ^{14}C-dated units were submitted for OSL dating. The results are presented and discussed in Appendix B and suggest that partial bleaching remains a major obstacle to reliable luminescence dating of fluvial sediments in Northland. Stratigraphic logs for the cores presented in this chapter are attached as Appendix C and result sheets for ^{14}C ages are contained in Appendix D.

5.2 Abstract

Valley floor mapping, sedimentology and ^{14}C-dating have been used to reconstruct the fluvial history at eight floodplain sites spread throughout Northland, New Zealand, a region removed from the main areas of tectonic and volcanic activity. We propose a regional model for Holocene floodplain evolution and fluvial behaviour based on a continuum of valley confinement settings. An absence of early to mid Holocene valley-fills (pre ~ 6500 cal. yr BP) coinciding with a warmer wetter climate suggests limited sediment sequestration due to enhanced discharge and reduced sediment loads during this time. Region-wide floodplain alluviation through the mid to late Holocene in response to climatically driven increases in sediment supply, was followed by a period of valley floor entrenchment and floodplain erosion beginning after ~ 2000 cal. yr BP. In partly confined valley settings this was followed by the aggradation of a lower Holocene floodplain surface, with rapid rates of vertical accretion in response to post-settlement catchment disturbance. The results of this study indicate that valley floor configuration has played a major role in controlling Northland floodplain development, accounting for differences in the specific fluvial unit assemblages between sites. Variations in sediment flux in response to climate change, and

more recently anthropogenic catchment perturbation, are the primary controls on Northland floodplain geomorphology.

5.3 Introduction

With increased hydro-climate variability predicted for the future (IPCC, 2007), developing a better understanding of long-term valley floor evolution and river behaviour will be vital for determining the impacts of future environmental change on river systems. Studies examining alluvial sequences have been successful in identifying the sensitivity of fluvial systems to environmental perturbation, and those taking a basin-wide (e.g., Macklin et al., 1992a; Taylor et al., 2000) or regional (e.g., Cohen and Nanson, 2007; Jones et al., 2010a) approach have been able to elucidate the primary controls on Holocene-scale fluvial landform development. The key geomorphic drivers of river behaviour include external factors such as land use, climate and tectonics, as well as intrinsic threshold controls operating within the boundary conditions imposed by geology (Cohen and Nanson, 2008; Brierley, 2010). Much of the late twentieth century research from the Northern Hemisphere examining river response to Holocene environmental change has focused on the role of climate and anthropogenic impacts in driving change (e.g., Starkel, 1983; Knox, 1993; Macklin and Lewin, 1993; Rumsby and Macklin, 1996).

More recent research has emphasised the role of climate as a driver of Holocene river behaviour, with sedimentary records demonstrating that phases of river activity and increased flooding have occurred in response to centennial-scale climate change throughout the Holocene (Starkel et al., 2006; Thorndycraft and Benito, 2006b; Hoffmann et al., 2008; Macklin et al., 2010), and have been linked to hydro-climatic changes associated with shifts in atmospheric circulation patterns (Knox, 2000; Macklin et al., 2006; Harden et al., 2010; Macklin et al., 2010; Richardson et al., 2013). However these records also show that episodes of alluviation within the last few hundred years are more likely to be a response to anthropogenic impacts associated with agricultural expansion and catchment land-use changes (Starkel et al., 2006; Hoffmann et al., 2008; Macklin et al., 2010; Richardson et al., 2013).

In New Zealand there has also been a strong emphasis on climate as the dominant forcing mechanism of change in river systems (e.g., Grant, 1985; Vella et al., 1988; Marden and Neall, 1990; Berryman et al., 2000). Evidence preserved in alluvial terrace sequences from North Island catchments suggests that the predominant response to climate amelioration during the Holocene was degradational, with sensitivity exhibited in association with more

subtle climate shifts (Clement and Fuller, 2007). However, New Zealand's active tectonic setting means that tectonics (e.g., Berryman et al., 2000; Litchfield and Berryman, 2005; Litchfield and Berryman, 2006; Berryman et al., 2010) and volcanic activity (e.g., Manville, 2002; Manville et al., 2005) are also major controls influencing river and floodplain dynamics (Clement and Fuller, 2007), and accordingly have formed a significant component of the fluvial research in New Zealand.

Adding to the complexity of interpreting the alluvial sedimentary record is the operation of autogenic fluvial processes in the channel and hillslope domain, which can result in non-uniform landscape responses to external perturbation (e.g., Cohen and Nanson, 2007). This reflects the major influence that variables such as valley floor width, accommodation space and sediment flux have on Holocene floodplain development and contemporary landscape forming processes (e.g., Brierley, 2010). Valley confinement is identified as a major determinant of floodplain morphology (Brierley and Fryirs, 2005), through its control on floodplain and reworking processes (e.g., Nanson and Croke, 1992). Brierley and Fryirs (2005) describe valley confinement as the degree to which the channel impinges on the valley margin. River types vary across a continuum ranging from confined valley setting rivers with no floodplain, through partly confined river valley settings, comprising discontinuous floodplain, to fully laterally unconfined alluvial systems (Brierley and Fryirs, 2005). The style of floodplain development in partly confined systems commonly involves floodplain reworking processes that lead to the polycyclic formation of terraces and floodplains, with similar morphology (and topography) but with different alluvial chronologies and stratigraphy (e.g., Cohen and Nanson, 2008; Stinchcomb et al., in press). The complexity of floodplain evolution in partly confined systems has created opportunities for reconstruction of river behaviour in response to palaeoenvironmental and palaeoclimate change (Cohen and Nanson, 2008; Stinchcomb et al., in press). To date, in New Zealand, there has been no fluvial research that has examined the role that valley floor confinement has on floodplain evolution and the spatial and temporal changes in Holocene river behaviour.

Analysis of Holocene fluvial radiocarbon records from New Zealand (Richardson et al., 2013) has highlighted the geographical gaps in New Zealand Holocene fluvial research. The majority of New Zealand studies have been catchment specific with limited chronological control, and some regions remain completely unexamined in terms of their Holocene fluvial history. The river systems of Northland (Fig. 5.1), the most northern region of New Zealand, are among the least researched catchments, and very little is known about their behaviour during the Holocene. Northland's distance from the main zone of plate convergence between

the Australian and Pacific plates and the Taupo Volcanic Zone (Fig. 5.1) allows us to focus on the impact that environmental change and valley floor configuration has had on sediment flux and sediment storage within the alluvial landscape, without the complications of tectonic- and volcanically-driven catchment disturbance. In addition, New Zealand's short history of human settlement, with a preferred first settlement date of ca. 800 years BP (Prickett, 2002), means that for the majority of the Holocene anthropogenic impacts on catchments will be absent. This is in sharp contrast to most other countries, where the impacts of past human activities have influenced landscape morphology, process and sediment fluxes for thousands of years (e.g., Foulds and Macklin, 2006).

Northland, New Zealand, therefore represents an ideal opportunity to examine river behaviour and floodplain evolution at a regional scale, and to elucidate the role that climate and late Holocene anthropogenic impacts have had on systems in a range of valley floor configuration settings. In this study we use geomorphological and sedimentological investigations to reconstruct Holocene floodplain development and river behaviour at eight sites in six Northland catchments. These sites sample a spectrum of local valley floor confinement settings in order to account for potential non-uniform landscape responses due to autogenic fluvial processes (cf. Cohen and Nanson, 2007). New ^{14}C-dated evidence is presented and we discuss valley floor evolution at eight sites. We explore the influence of the major controls on river behaviour in Northland and propose a regional model for floodplain evolution during the Holocene.

5.4 Regional setting

Northland, a narrow peninsula 300 km in length, comprises the most northern region of New Zealand (Fig. 5.1). It lies between latitudes 34°S and 37°S, 400–700 km northwest of the Hikurangi subduction margin between the Australian and Pacific plates. It is an area of low seismicity (http://www.geonet.org.nz/; Anderson and Webb, 1994), with no known active faults (http://data.gns.cri.nz/af/; Beetham et al., 2004), and is widely regarded as having been tectonically stable throughout the Quaternary (e.g., Brothers, 1954; Cotton, 1957; Gibb, 1986; Pillans, 1986; Brook, 1999; Marra and Alloway, 2006).

5.4.1 Geology

The geology of Northland is complex (Fig. 5.2), comprising uplifted blocks of Mesozoic greywacke, Tertiary to Quaternary volcanics (including scoria cones and lava flows) and Tertiary to Quaternary sedimentary sequences. In addition, large parts are underlain by an

allochthonous sequence of Cretaceous to Miocene strata (Northland Allochthon) emplaced during a major thrusting event in the early Miocene (Isaac, 1996; Edbrooke and Brook, 2009). Exposed basement rocks form the hills of northern and eastern Northland and the topography is moderate to very dissected hill country, with elevations up to 500 m. The moderately to very dissected major ranges of northwest and central Northland, including the highest point Te Raupua (781 m) in the Waima range, are formed in the allochthonous strata (Isaac, 1996). Central Northland is characterised by moderately dissected rolling hill country underlain by the deeply weathered sedimentary rocks of the Northland Allochthon (Edbrooke and Brook, 2009). In the west, Tutumoe (770 m) is the highest elevation of the Tutumoe Range, which has formed on a partly dissected early Miocene volcanic plateau (Edbrooke and Brook, 2009). There are currently no active volcanoes in Northland, and the most recent volcanic activity in the Holocene (1500–1800 years BP) has been primarily low-volume monogenetic basaltic eruptions of intraplate type (Smith et al., 1993).

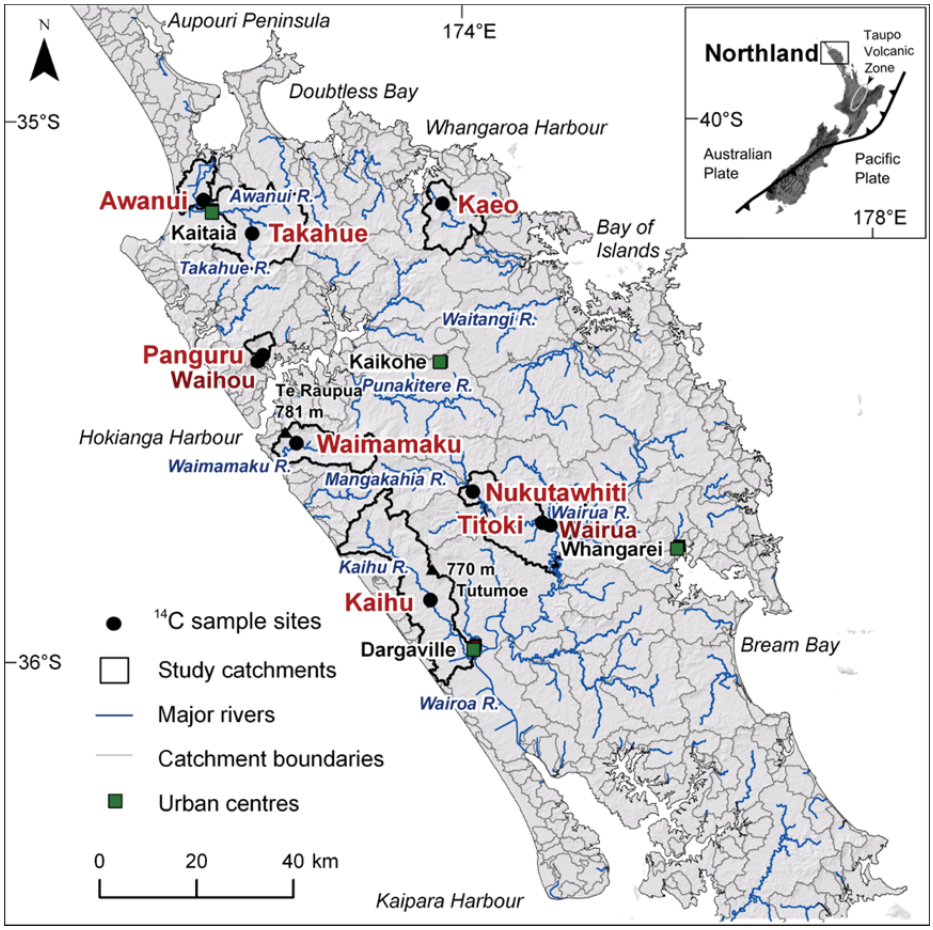

Fig. 5.1. Location map of study sites, catchment boundaries, major rivers and urban centres in Northland, New Zealand. Inset shows New Zealand tectonic setting.

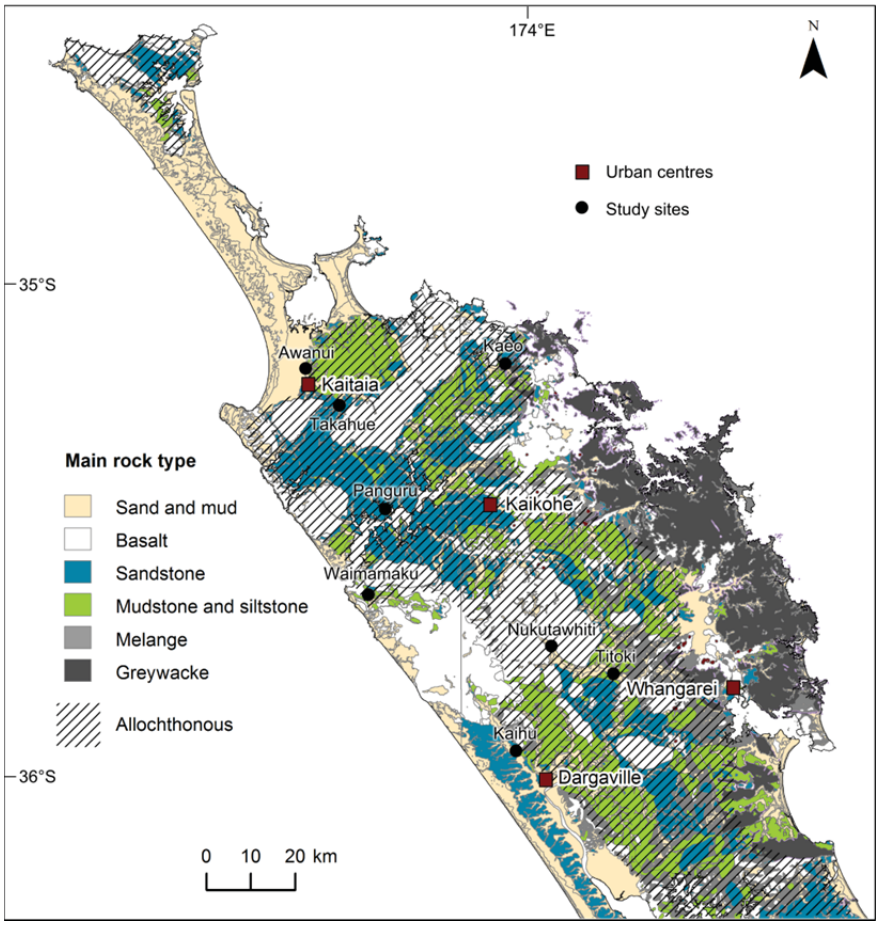

Fig. 5.2. Map showing the main rock types of Northland and the Northland Allochthon (data source: Isaac, 1996; Edbrooke and Brook, 2009). Quaternary aged rock types are predominantly sand and mud, with limited areas of Quaternary basalt near Whangarei and northeast of Kaikohe. Autochronous basalts and sandstones are predominantly Tertiary aged. Allochthonous rock types are Tertiary to Mesozoic age. Rock type in eastern Northland is predominantly Mesozoic greywacke.

Northland's relatively subdued topography, low latitude position and proximity to the ocean ensures a mild, humid and moderately windy climate (Moir et al., 1986). Rainfall, ranging from between 1200 and 2500 mm, occurs all year round in the region, but exhibits seasonal variability due to the influence of the migration of the sub-tropical high pressure belt (Moir et al., 1986). Summers generally experience less rainfall and occasional dry spells, with rainfall maxima recorded during winter months. Periods of intense rainfall associated with the incursion of tropical depressions and moist northeasterly flows are common. Northland's rivers are susceptible to severe flooding during these intense rainfall events due to small catchment sizes and enhanced runoff from steep slopes with impervious soils (Cathcart,

1978). While the majority of the Northland Peninsula comprises small catchments with short rivers (Fig. 5.1), Northland's largest river, the Wairoa River flowing into northern Kaipara Harbour, has a catchment area of 3652 km^2, draining one third of the total area of Northland (Poole, 1983).

5.4.2 Bioclimatic history

Regional pollen records show that in contrast to the rest of New Zealand, Northland remained forested throughout the Last Glacial Coldest Period (LGCP; ~ 28,000–18,000 cal. yr BP as defined by Alloway et al. (2007)), with *Agathis australis*-podocarp-hardwood forest coverage on the Aupouri Peninsular and *Nothofagus*-dominant forest south of Kaitaia (Newnham, 1990; Newnham et al., 1993). Palynological and sedimentological evidence from Northland swamps and lakes indicate there have been four broad climatic periods during the Holocene. The Holocene subdivision time-frames below are informal zones that have been formulated to discuss the Northland palaeoclimate record presented here. These zones straddle the Early-Middle Holocene Boundary at 8.2 ka BP and Middle-Late Holocene boundary at 4.2 ka BP (both linked to a Global Stratotype Section and Point) recently proposed by Walker et al. (2012).

Zone 1: early Holocene (~ 12,000–10,000 cal. yr BP). During this time, cool climate taxa including *Nothofagus* (beech) are well represented in Northland pollen records, indicating the Northland climate during this time was slightly colder than present day (Newnham, 1992; Striewski et al., 1996; Elliot, 1998).

Zone 2: early to mid Holocene (~ 10,000–5000 cal. yr BP). This period is characterised by the warmest and most mesic environment of the last 17,000 years based on vegetation records from far northern New Zealand (Dodson et al., 1988). Pollen abundance of species with a preference for warmer moister conditions, such as *Agathis* and *Metrosideros*, increased, while cooler elements declined (Dodson et al., 1988; Newnham, 1992; Striewski et al., 1996; Elliot, 1998; Elliot et al., 2005).

Zone 3: mid to late Holocene (~ 5000–2000 cal. yr BP). This period was subject to disturbance and deterioration in climate. Vegetation response in both eastern and western Northland includes declines in warmth-loving taxa and the expansion of hardy podocarps and other cool climate taxa (Dodson et al., 1988; Kershaw and Strickland, 1988; Elliot et al., 1995; Elliot et al., 2005). Seral trends, as indicated by increased abundance of pioneering species, and evidence of enhanced catchment erosion in the mid to late Holocene, were also

noted at a number of Northland sites (Striewski et al., 1996; Elliot et al., 1997; Elliot et al., 1998). These pollen records suggest that there was a shift to a more seasonal climate regime in the mid to late Holocene involving summer drought, more natural fires and increased cyclonic activity.

Zone 4: late Holocene to present (from ~ 2000 cal. yr BP). Prior to human arrival, records from this period show evidence of a milder wetter climate in the late Holocene (e.g., Elliot et al., 1995; Elliot, 1998). In New Zealand anthropogenic landscape impacts are restricted to the last ~ 800 years, with the settlement of New Zealand occurring in two phases, first by Polynesians immigrants, followed by European colonisation within the last 200 years. Although contentious, the date of first settlement by Māori is thought to have occurred ca. 800 years BP (Prickett, 2002; Sutton et al., 2008), with dates from seeds gnawed by the introduced Pacific rat pointing to a slightly later date of Polynesian colonisation at ~ 1280 AD (Wilmshurst et al., 2008). During Polynesian settlement of New Zealand there was extensive deforestation by intentional burning in order to encourage the establishment of *Pteridium esculentum* (bracken fern), an important source of carbohydrate (McGlone et al., 2005). Palaeovegetation reconstructions from Northland have used increases in *Pteridium* spores and charcoal to identify the first anthropogenic landscape disturbance, reporting dates ranging from ca. 1000 yr BP to 500 yr BP (Elliot et al., 1995; Elliot et al., 1997; Elliot et al., 1998; Ogden et al., 2003). Abrupt changes in physical and geochemical properties and an influx of catchment derived minerogenic material in the sediments of Lake Pupuke, located in Auckland, northern New Zealand, dates the onset of prehistoric Polynesian colonisation at ca. 610 cal. yr BP (Striewski et al., 2009). European settlement commenced in ~ 1830 AD and was followed by widespread forest clearance (e.g., Kershaw and Strickland, 1988).

The dominant land use in the Northland region today includes farming, horticulture and exotic forestry (Isaac, 1996; Edbrooke and Brook, 2009), while indigenous forest cover of podocarp-conifer-hardwood associations including *Agathis australis* (kauri) is mainly restricted to upland remnants (Elliot et al., 1997).

5.5 Method

5.5.1 Floodplain and terrace morphology

Eight sites were chosen from across the Northland region, each reflecting variations in bedrock lithology and control, channel slope and the degree of valley confinement. In this study we define a river as ‘partly confined’ when the convex channel bank abuts a bedrock

margin and there is genetic floodplain on the convex bend (sensu Brierley et al., 2002; Cohen and Nanson, 2007, 2008). In this work, sites which are strongly partly confined are classified as 'more confined' in this context, for ease of description. Sites which tend toward laterally unconfined on the confinement continuum are classified as 'less confined'.

The selected sites sample a range of different valley confinement settings in order to capture an overall picture of regional Holocene valley floor evolution which is not restricted by local factors. Catchment areas range from 545 km^2 to 19 km^2 (Table 5.1), while valley floor widths range from over 500 m at the Kaihu and lower Awanui sites to 150 m at the more confined Titoki site. Valley floor morphology was mapped using the NZTM2000 projection and topographic data obtained from NZTopo50 contour data LiDAR, supplied by Northland Regional Council (accuracy $\leq$ 0.15 m), and real-time kinematic (RTK) dGPS surveys (accuracy $\leq$ 0.05 m). Elevations tied to mean sea level are limited to the accuracy of the least accurate NZTopo50 contour data (vertical accuracy $\leq$ 10 m).

5.5.2 Sedimentology and radiocarbon chronology

At each site the major alluvial surfaces were cored using a hydraulic percussion system along a cross-valley transect to determine the underlying stratigraphy (Fig. 5.3 to Fig. 5.10). Cores and cutbank exposures were logged according to grain size and colour, with major facies boundaries noted.

Organic material (where present) was sampled from prominent stratigraphic boundaries interpreted to reflect changes in the depositional environment and flooding events. This organic material was then submitted for ^{14}C dating. The majority of samples consisted of wood (however short-lived organic material such as twigs or leaves were preferred) and the remainder were organic rich sediments and a single charcoal sample (Table 5.1). Samples were prepared by the University of Waikato Radiocarbon Dating Laboratory (New Zealand) and the ^{14}C activity in larger quantity samples was determined by radiometric analysis (liquid scintillation counting). The remaining samples were graphitized and analysed on the Keck Radiocarbon Dating Laboratory (University of California, USA) accelerator mass spectrometer (AMS). Results were reported as percent modern carbon following Stuvier and Pollack (1977), and based on the Libby half-life of 5568 yr with correction for isotopic fractionation applied. Radiocarbon ages less than 11,000 years BP were calibrated using OxCal version 4.1 (Bronk Ramsey, 2009) and the Southern Hemisphere calibration dataset SHCal04 (McCormac et al., 2004). Determinations older than 11,000 BP were calibrated using the international calibration dataset IntCal04 (Reimer et al., 2004). The results are

summarised in Table 5.1 and all ages are quoted as calibrated ages before present (the year 1950 AD) with 95% confidence interval uncertainties (cal. yr BP 2σ confidence).

5.6 Results

For each site we present a map of the geomorphology and a cross-valley section of the stratigraphic logs, as well as key stratigraphy, geomorphology and ^{14}C-dating results. The results for each site of the eight sites are presented in order from the least confined valley setting to the more confined site.

5.6.1 Awanui River

The Awanui River, north of Kaitaia, meanders across a wide coastal floodplain before flowing into Rangaunu Harbour (Fig. 5.1 and 5.3a). The valley is up to 6000 m wide in parts and is bounded in the east by Taipa mudstone of the Northland Allochthon, and Pliocene age mudstone and sandstone (Fig. 5.2) (Isaac, 1996). The western margin of the Awanui floodplain is bounded by Early Pleistocene coastal foredunes comprising uncemented to moderately cemented and partly consolidated sand (Isaac, 1996).

Topographical data from this site reveals a single continuous floodplain surface with evidence of numerous palaeochannels (Fig. 5.3). Three ^{14}C samples from a core near the Awanui River indicate that in this location the Holocene floodplain rests on an organic rich palaeosol aged 18,870–18,560 cal. yr BP at a depth of 3.5 m (Table 5.1 and Fig. 5.3c). Above this layer are interbedded silt and silty clay units, with organic rich flood deposits that returned dates of 3570–3380 cal. yr BP and 3240–2880 cal. yr BP (Table 5.1 and Fig. 5.3c).

5.6.2 Kaihu River

The Kaihu River, with a catchment area of 358 km^2 meanders across a wide (~ 5000 m) floodplain (Fig. 5.4) which is bounded in the east by allochthonous mudstone and mélange (Fig. 5.2). The valley margin on the western side comprises Pliocene dune-bedded sandstone and mudstone (Edbrooke and Brook, 2009). Figure 5.4a and b shows the planform and cross-section of the Kaihu River site north of Dargaville, where the Kaihu River joins the Wairoa River before entering northern Kaipara Harbour.

Remnant terraces of estimated early to Middle Pleistocene age (Edbrooke and Brook, 2009) form an elevated surface up to 4 m above the Holocene floodplain. The stratigraphy of the

Holocene floodplain comprises a thick peat unit at 4 m below the contemporary floodplain surface. The peat is overlain by vertically accreted silt and silty clay sequences, with flood deposits dated at 3820–3560 cal. yr BP and 4420–4160 cal. yr BP (KH2 in Fig. 5.4c and Table 5.1).

5.6.3 Panguru, Whakarapa Stream

Whakarapa Stream near Panguru, is located at the northern end of the Hokianga Harbour (Fig. 5.1) and forms part of the drainage of a small (19 m^2) catchment (Fig. 5.5a). At this site the small gravel bed stream flows across a topographically uniform low floodplain (Fig. 5.5b) within a valley incised into low mountain ranges (maximum elevation of 720 m) comprised of massive to well-bedded quartzofeldspathic sandstone of the Northland Allochthon (Fig. 5.2).

A terrace surface 16 m above the modern floodplain forming part of the valley floor margin (Fig. 5.5b) is of estimated Early to Middle Pleistocene age (Isaac, 1996). A cutbank exposure shows that the floodplain stratigraphy comprises interbedded silts, gravel and silty sand units (P2 in Fig. 5.5c). Charcoal within vertically accreted silts ~ 2 m below the floodplain surface returned a ^{14}C age of 460–310 cal. yr BP (P2 in Fig. 5.5c).

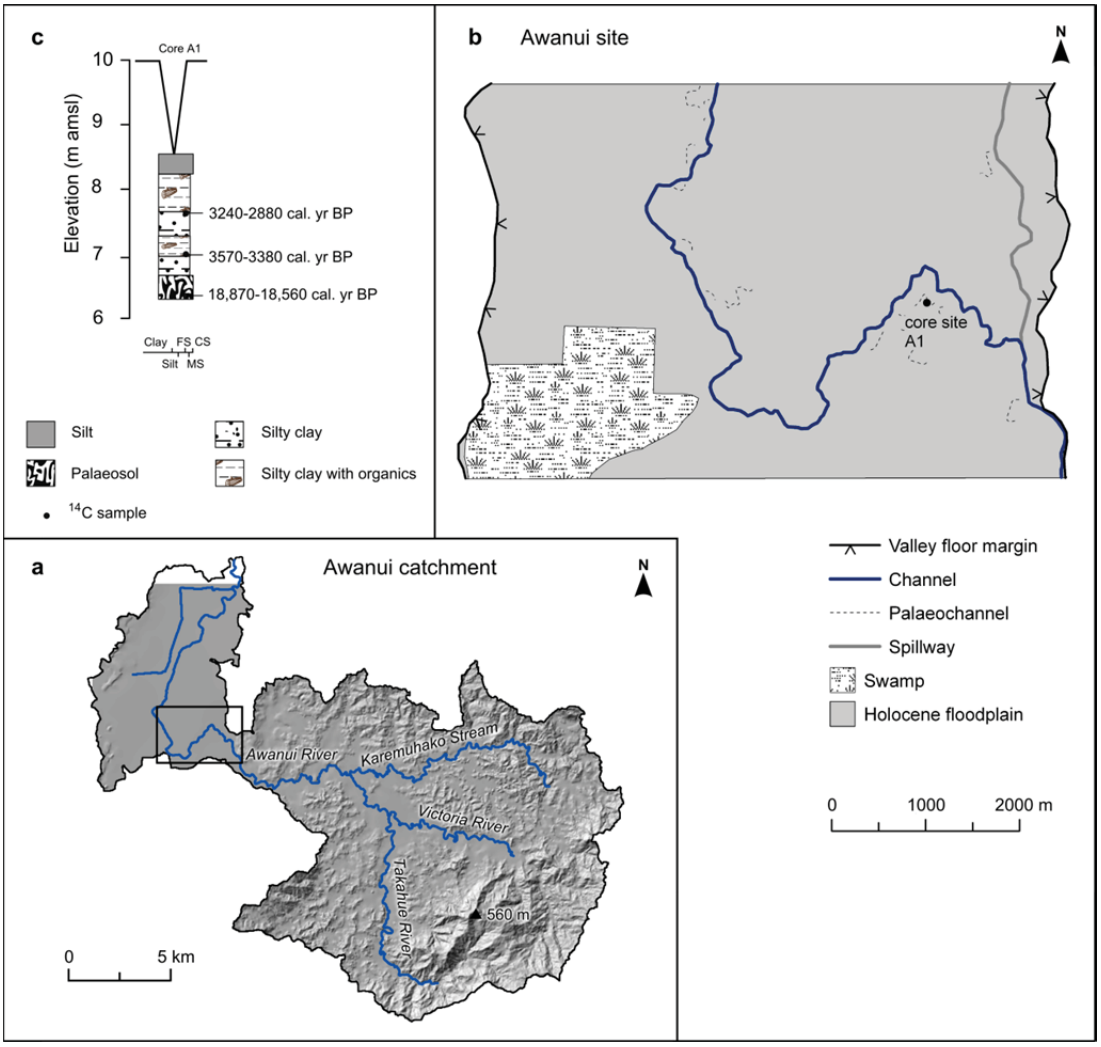

Fig. 5.3. (a) Hillshade DEM of the Awanui catchment (see Fig. 5.1 for location) showing the major rivers, maximum catchment elevation and study site location. (b) Awanui study site planform map showing major geomorphological features and core site location. (c) Chronostratigraphy at the core site.

5.6.4 Waimamaku River

The Waimamaku catchment is located on the western coast of Northland (Fig. 5.1 and Fig. 5.6a) and here the Waimamaku river has incised into plateau-forming Miocene aged flood basalts and muddy sandstones (Fig. 5.2). Large areas of Pleistocene landslides flank either side of the Waimamaku River in the mid to upper catchment (Isaac, 1996). At this site the gravel bed river flows through a valley that is bedrock-controlled, with valley floor widths less than 300 m, and is underlain by three major alluvial units (Fig. 5.6b and c).

The highest surface is gravels, dated at 20,170–19,570 cal. yr BP, suggesting this surface is a Late Pleistocene terrace remnant (W8 in Table 5.1 and Fig. 5.6c). The gravels are overlain by silty sand and clay sediments. A high Holocene floodplain sits ~ 4 m below the Late Pleistocene terrace and the stratigraphy is 2 m of vertically accreted silty sands lying on gravel deposits dated at 3160–2890 cal. yr BP (W9 in Table 5.1 and Fig. 5.6c). The lowest surface comprises massive silt overlying sand and gravel facies at ~ 3 m below the lowest floodplain surface (Fig. 5.6c). Chronostratigraphy of the low floodplain units at this site indicate that up to 3 m of sediment has been deposited within the last ~ 1000 cal. BP (W1 and W4 in Table 5.1 and Fig. 5.6c).

5.6.5 Takahue River

The Takahue River, a tributary of the Awanui River within the Awanui catchment (Figs. 5.1, 5.3 and 5.7) incises into Punakitere sandstone of the Northland Allochthon (Fig. 5.2) (Isaac, 1996). Three major surfaces are also recognised at the partly confined site (Fig. 5.7b and c). The highest surface is estimated to be of Early to Middle Pleistocene age (Isaac, 1996) and is elevated ~ 3 m above the high Holocene floodplain (Fig. 5.7c).

Figure 5.7c shows the chronostratigraphy of the Holocene floodplain surfaces at the Takahue River site. The high Holocene floodplain comprises vertically accreted silty sand, sand and gravel facies. Deposits within these units were dated at 6660–6490 cal. yr BP and 2000–1870 cal. yr BP (T2 in Table 5.1 and Fig. 5.7c). Chronostratigraphy of a palaeochannel in the high floodplain surface indicates a lower energy depositional environment with basal gravels aged 2760–2870 cal. yr BP, overlain by ~ 3 m of silty sediment that has been deposited in the last ~ 1300 years (T3 in Table 5.1 and Fig. 5.7c). The lower floodplain is less than 3 m below the high Holocene terrace, and comprises sediment dominated by gravel facies interbedded with thin silt and sand deposits (Fig. 5.7c). Wood in the basal matrix-supported gravels 4.58 m below the contemporary floodplain surface was dated at 13,300–13,090 cal. yr BP (T1 in Table 5.1 and Fig. 5.7c).

Table 5.1

Summary of ^{14}C data, sample code and description, core name, depositional environment and location of samples used in this study.

Site	Sample code	Core	Lab. No.	Sample material	Depositional environment	Sample depth (m)	Uncal-ibrated date (BP)	Calibrated date (cal. yr BP 2σ confidence)	Measure-ment
Awanui Catchment (area = 545 km^2)									
Awanui	Awan1c	A1	Wk-27970	Silt organics	Palaeochannel	3.8	15,495 ± 84	18,870–18,560	Radio-metric
Awanui	Awan1b	A1	Wk-28764	Silt organics	Palaeochannel	1.5	3299 ± 35	3570–3380	AMS
Awanui	Awan 1a	A1	Wk-28765	Silt organics	Palaeochannel	0.74	2962 ± 55	3240–2880	Radio-metric
Upper Awanui Catchment (area = 240 km^2)									
Takahue	Taka2e	T2	Wk-30434	Wood	Floodplain	4.62	5828 ± 25	6660–6490	AMS
Takahue	Taka2d	T2	Wk-30435	Wood	Floodplain	3.69	2033 ± 25	2000–1870	AMS
Takahue	Taka1c	T1	Wk-31570	Wood	Floodplain	3.55	13,192 ± 102	13,300–13,090	AMS
Takahue	Taka3g	T3	Wk-30764	Wood	Palaeochannel	3.58	2770 ± 25	2870–2760	AMS
Takahue	Taka3d	T3	Wk-31571	Silt organics	Palaeochannel	2.31	1381 ± 25	1300–1180	AMS
Kaeo Catchment (area = 114 km^2)									
Kaeo	Kaeo1b	K1	Wk-27971	Silt organics	Floodplain	4.85	691 ± 35	660–560	AMS
Kaeo	Kaeo4a	K4	Wk-30440	Wood	Floodplain	4.02	4769 ± 25	5580–5320	AMS
Kaeo	Kaeo4c	K4	Wk-30443	Silt organics	Floodplain	4.6	6820 ± 26	7680–7570	AMS
Kaihu Catchment (area = 358 km^2)									
Kaihu	Kaih2b	KH2	Wk-31573	Wood	Floodplain	2.32	3457 ± 28	3820–3560	AMS
Kaihu	Kaih2f	KH2	Wk-31574	Wood	Floodplain	3.6	3933 ± 28	4420–4160	AMS
Mangakahia Catchment (area = 253 km^2)									
Nukutawhiti	Nuku4a	M4	Wk-30441	Wood	Floodplain	3.44	> 48,000		AMS
Nukutawhiti	Nuku2a	M2	Wk-31576	Silt organics	Floodplain	1.47	3287 ± 30	3560–3380	AMS
Nukutawhiti	Mang2g	M5	Wk-27966	Wood	Palaeochannel	3.05	291 ± 35	450–150	AMS
Titoki	Mang1a	TI1	Wk-27967	Silt organics	Floodplain	7.4	850 ± 39	790–670	Radio-metric
Panguru Catchment (area = 19 km^2)									
Panguru	Pang2a	P2	Wk-27963	Charcoal	Floodplain	2.3	353 ± 30	460–310	AMS
Waimamaku Catchment (area = 133 km^2)									
Waimamaku	Waim4c	W4	Wk-30438	Wood	Floodplain	2.56	780 ± 25	730–650	AMS
Waimamaku	Waim9a	W9	Wk-31577	Wood	Floodplain	3.38	2947 ± 27	3160–2890	AMS
Waimamaku	Waim1c	W1	Wk-27968	Wood	Floodplain	3.3	1138 ± 41	1070–920	Radio-metric
Waimamaku	Waim8b	W8	Wk-30762	Silt organics	Floodplain	2.82	16,730 ± 32	20,170–19,570	AMS

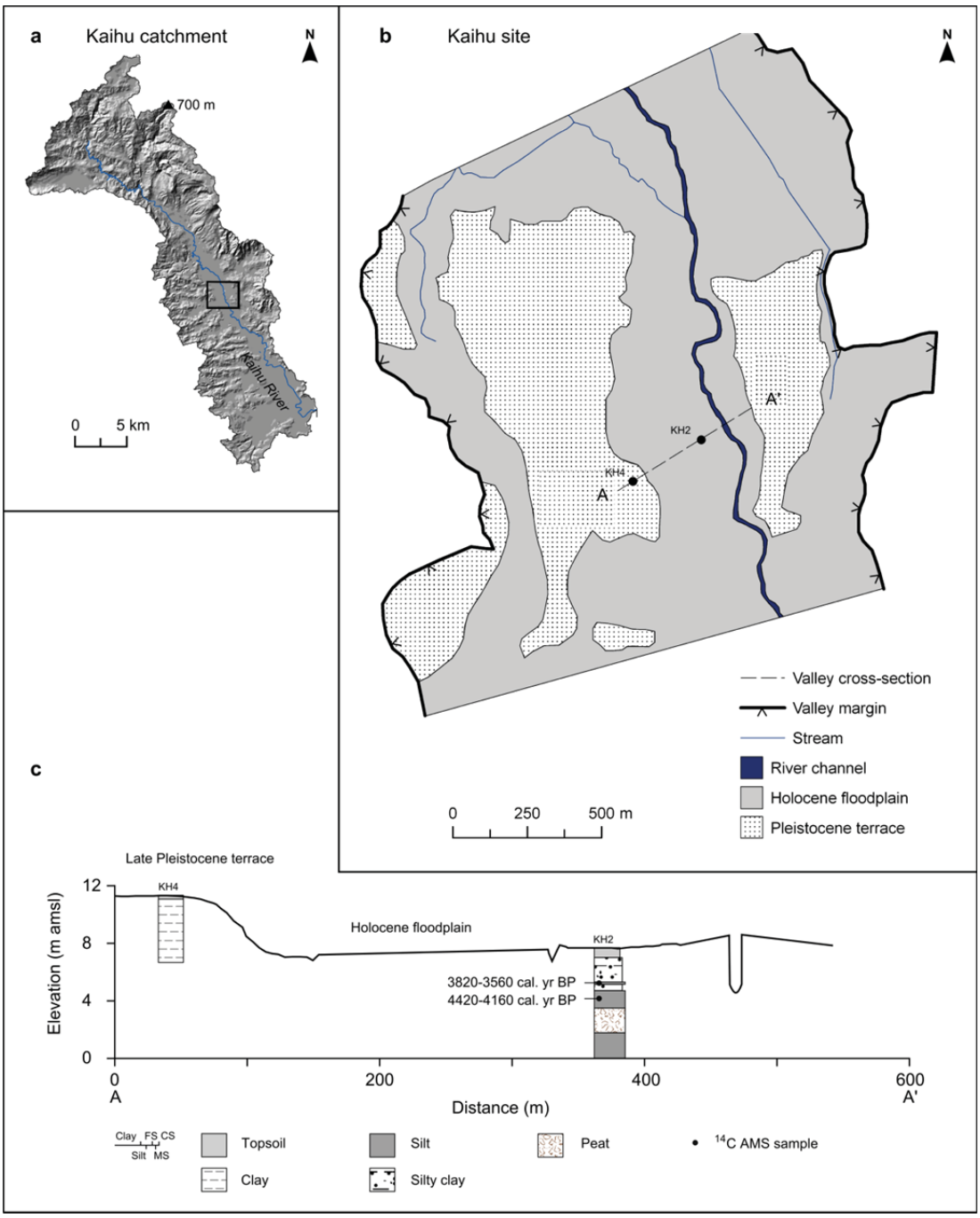

Fig. 5.4. (a) Hillshade DEM of the Kaihu catchment (see Fig. 5.1 for location) showing the major rivers, maximum catchment elevation and study site location. (b) Kaihu study site planform map showing major geomorphological features and core site locations. (c) Valley cross-sections showing topography and chronostratigraphy at the core sites.

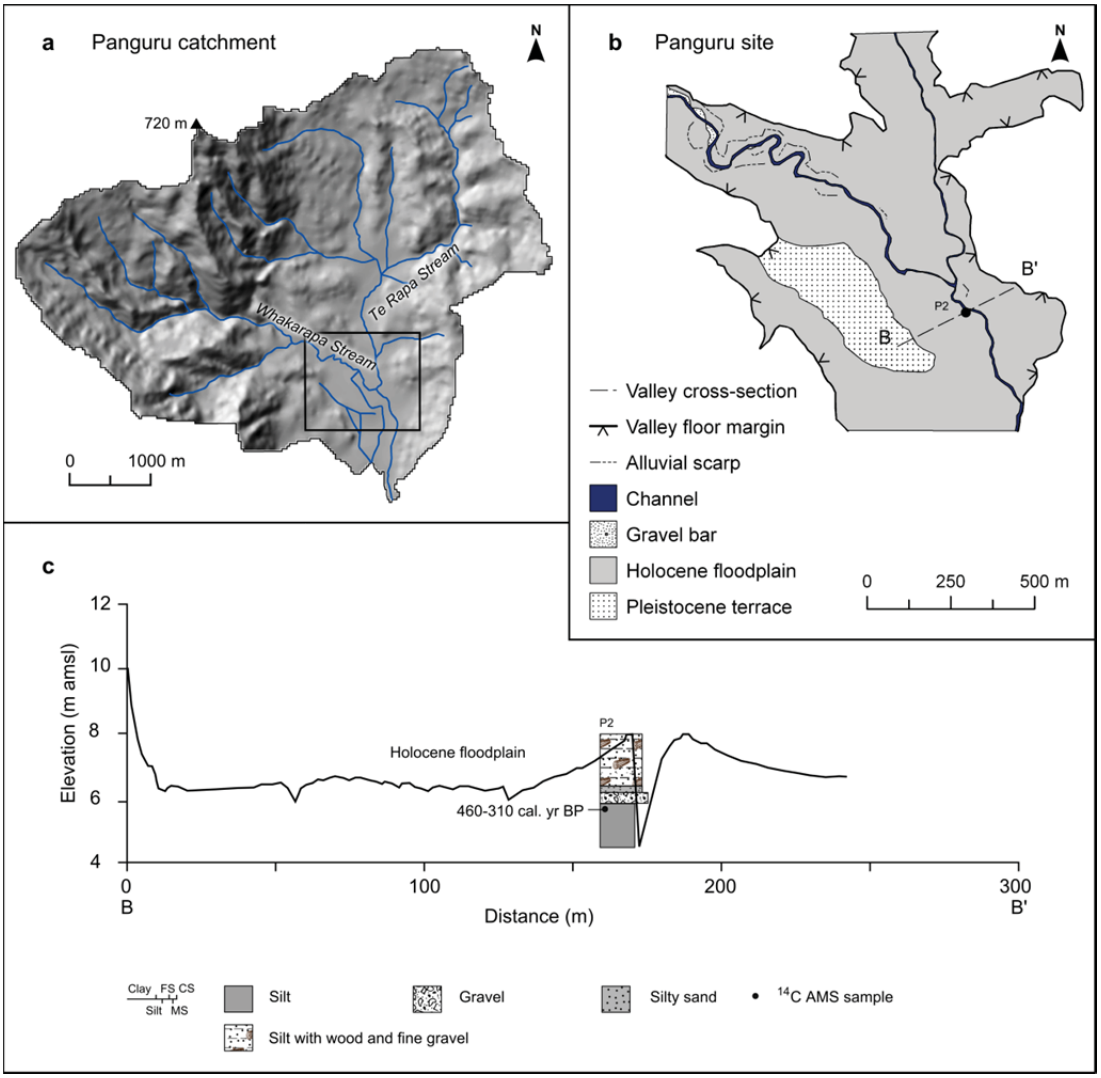

Fig. 5.5. (a) Hillshade DEM of the Panguru catchment (see Fig. 5.1 for location) showing the major streams, maximum catchment elevation and study site location. (b) Panguru study site planform map showing major geomorphological features and core site location. (c) Valley cross-section showing topography and chronostratigraphy at the core site.

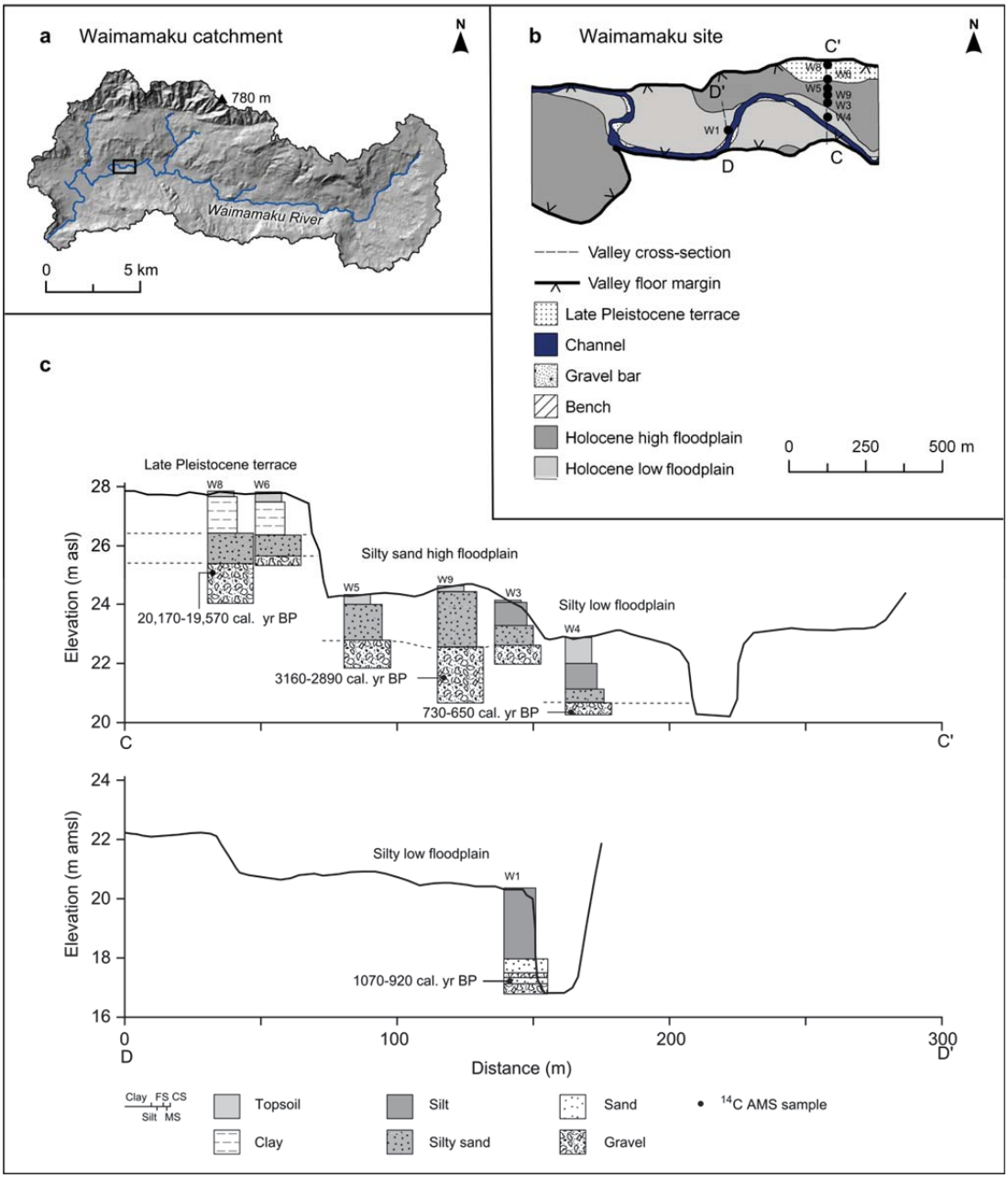

Fig. 5.6. (a) Hillshade DEM of the Waimamaku catchment (see Fig. 5.1 for location) showing the major river and streams, maximum catchment elevation and study site location. (b) Waimamaku study site planform map showing major geomorphological features and core site locations. (c) Valley cross-section showing topography and chronostratigraphy at the core sites.

5.6.6 Nukutawhiti, Mangakahia River

The Mangakahia River in central Northland (Figs. 5.1 and 5.8) occupies a similar geological setting to the Takahue site. Here a single thread gravel bed river cuts into allochthonous sandstone, draining ranges of Tangihua complex volcanic rock types and the eastern Tutamoe Range (Fig. 5.2) (Edbrooke and Brook, 2009).

The Holocene floodplain is laterally constrained at the valley margins by remnants of a Pleistocene terrace, with an AMS radiocarbon sample from this unit indicating an age older than 48,000 cal. yr BP, representing a minimum age at the limit of ^{14}C dating (M4 in Table 5.1 and Fig. 5.8c). The high Holocene floodplain at this site comprises up to 4 m of silt and silty sand (Fig. 5.8c). A flood deposit at 1.47 m below the high floodplain surface returned an age of 3560–3380 cal. yr BP (M2 in Table 5.1 and Fig. 5.8c). At this site there is also a relatively extensive area of low floodplain, 1–2 m below the high Holocene floodplain, with topographical evidence of palaeochannels, accretionary benches and lateral mobility (Fig. 5.8b and c). The sedimentology and geochronology of a palaeochannel fill indicates that this low floodplain has aggraded rapidly, with 3 m of upward fining sedimentation since 450–150 cal. yr BP (M5 in Table 5.1 and Fig. 5.8c).

5.6.7 Kaeo River

Figure 5.9 shows the catchment DEM, planform and cross-sections from the Kaeo River located in eastern Northland (Fig. 5.1). Here the gravel bed river is confined between outcrops of Waipapa Group lithic volcaniclastic sandstone and argillite and Northland Allochthon mudstone and sandstone (Fig. 5.2) (Edbrooke and Brook, 2009). Topographical data shows the valley floor comprises a single continuous Holocene floodplain and only a small remnant Pleistocene terrace, with valley floor widths varying between 100 and 600 m (Fig. 5.9b).

A bank exposure indicates accumulation rates of interbedded sands and silts since 660–560 cal. yr BP, in the order of 7 mm yr^{-1} (derived from sample Kaeo1b at K1, Table 5.1 and Fig. 5.9c). Farther down-valley, chronostratigraphy data indicate commencement of terrestrial deposition at 7680–7570 cal. yr BP (K4 in Table 5.1 and Fig. 5.9c).

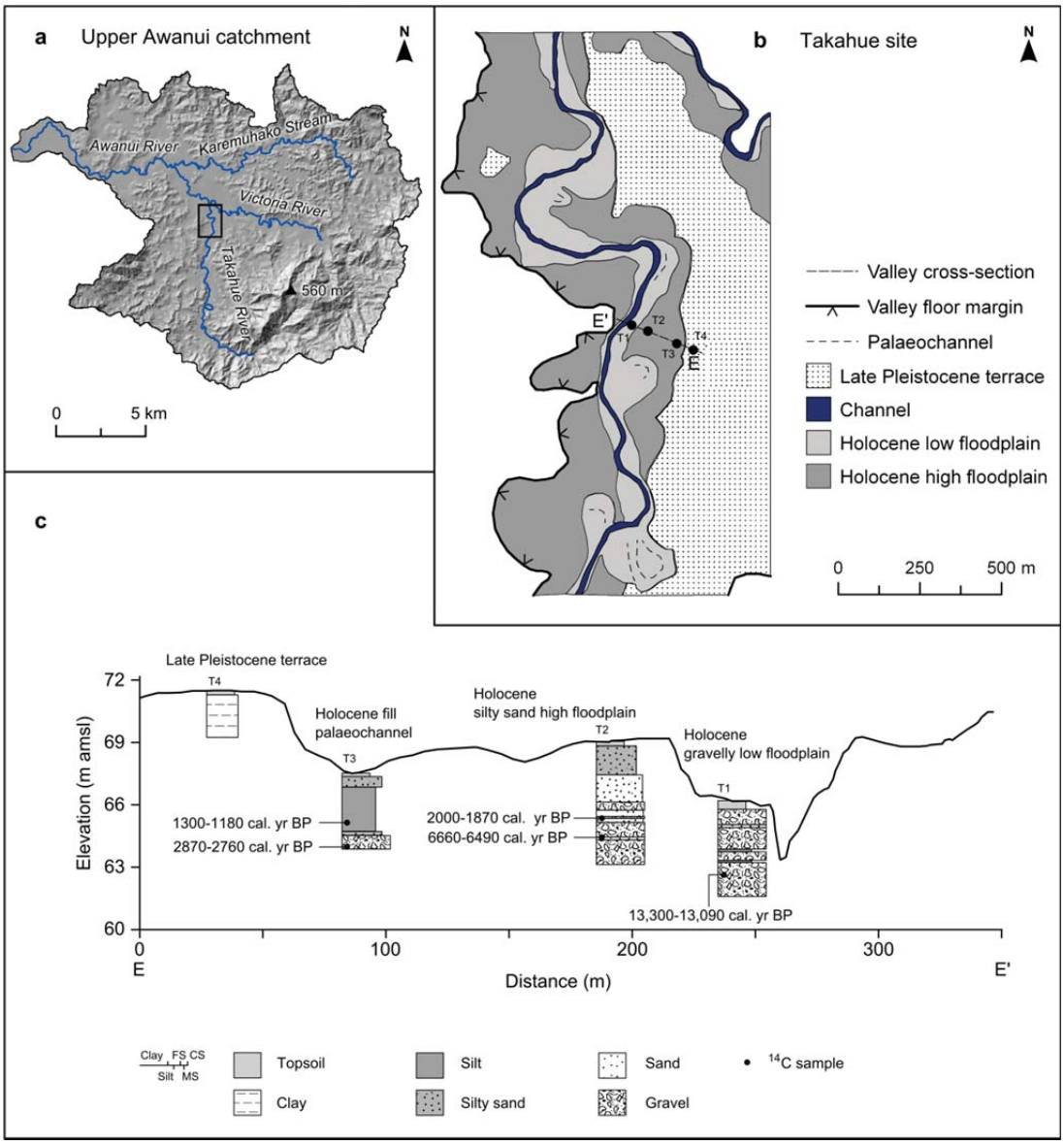

Fig. 5.7. (a) Hillshade DEM of the upper Awanui catchment (see Fig. 5.1 for location) showing the major rivers, maximum catchment elevation and study site location. (b) Takahue study site planform map showing major geomorphological features and core site locations. (c) Valley cross-section showing topography and chronostratigraphy at the core sites.

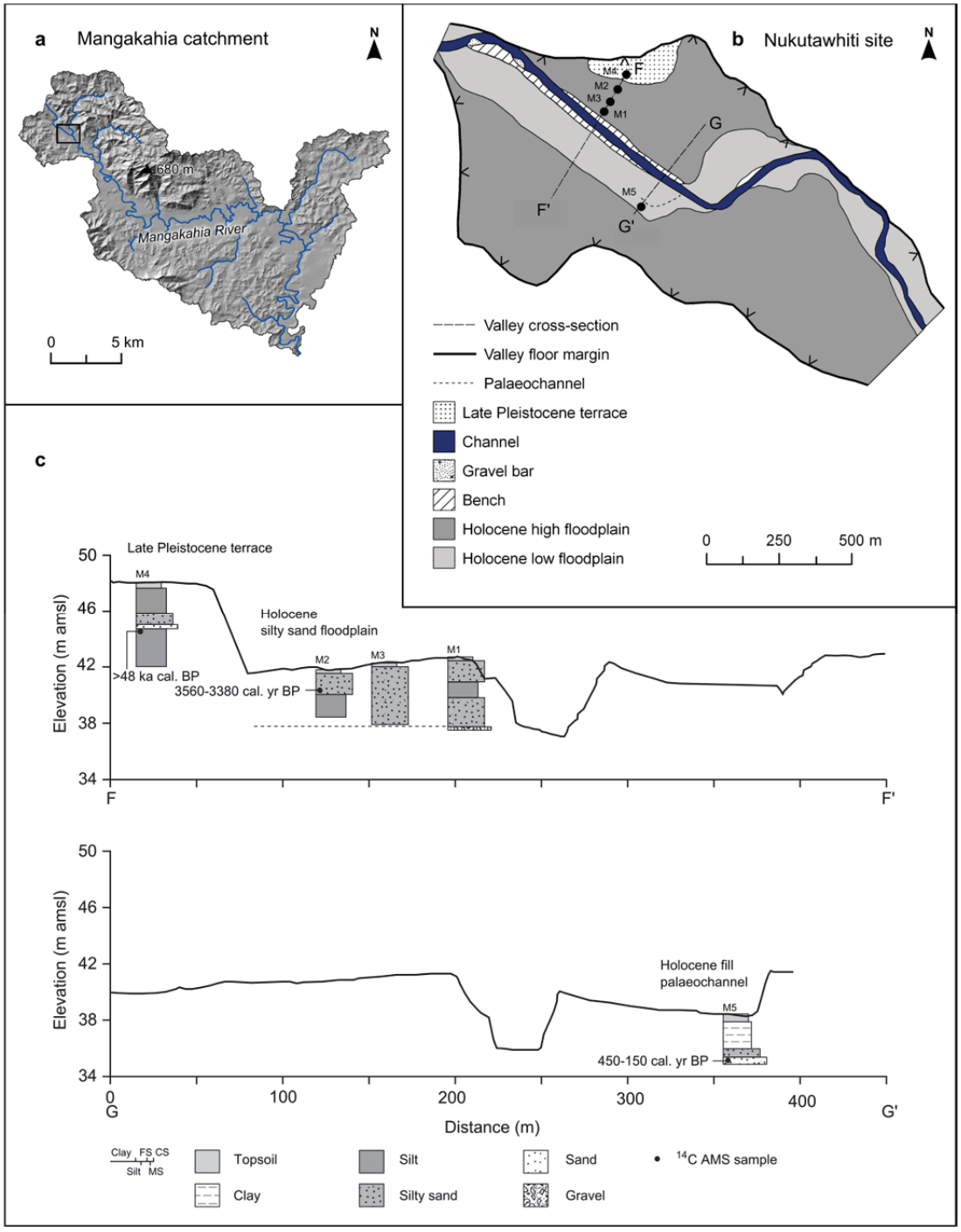

Fig. 5.8. (a) Hillshade DEM of the Mangakahia catchment (see Fig. 5.1 for location) showing the major rivers, maximum catchment elevation and study site location. (b) Nukutawhiti study site planform map showing major geomorphological features and core site locations. (c) Valley cross-section showing topography and chronostratigraphy at the core sites.

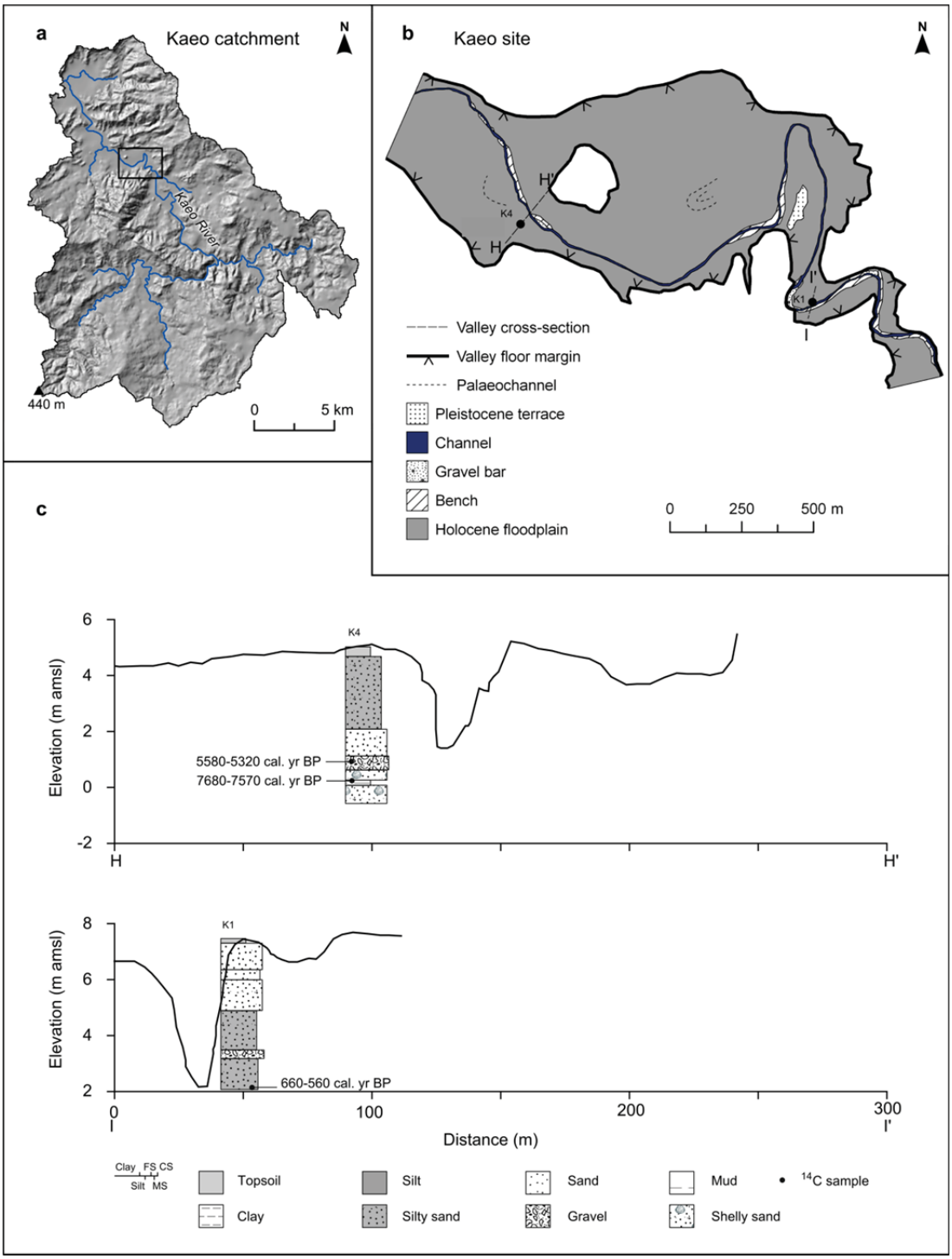

Fig. 5.9. (a) Hillshade DEM of the Kaeo catchment (see Fig. 5.1 for location) showing the major rivers, maximum catchment elevation and study site location. (b) Kaeo study site planform map showing major geomorphological features and core and exposure site locations. (c) Valley cross-section showing topography and chronostratigraphy at the core and exposure sites.

5.6.8 Titoki, Mangakahia River

Figure 5.10a and b shows the Mangakahia catchment and the geomorphology of the study site in the lower part of the catchment near Titoki in central Northland (Fig. 5.1). At this site the Mangakahia river has cut a narrow valley (~ 250 m wide) through Pleistocene basalt lava flows. Geomorphology and chronostratiphy indicate the presence of a single Holocene floodplain surface with the aggradation of over 7 m of alluvium, comprising silty sand, since 790–670 cal. yr BP (TI1 in Table 5.1 and Fig. 5.10c).

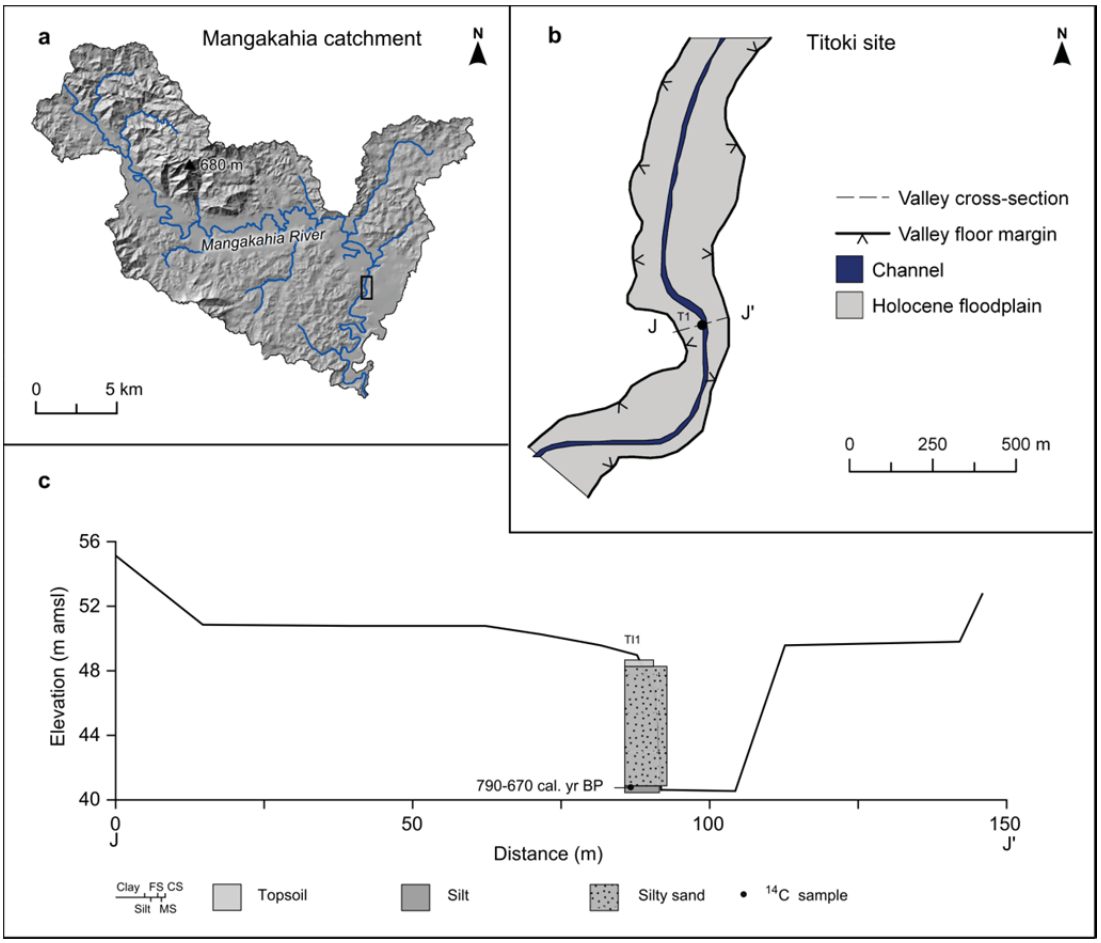

Fig. 5.10. (a) Hillshade DEM of the Mangakahia catchment (see Fig. 5.1 for location) showing the major rivers, maximum catchment elevation and study site location. (b) Titoki study site planform map showing major geomorphological features and exposure site location. (c) Valley cross-section showing topography and chronostratigraphy at the exposure site.

5.7 Discussion

5.7.1 Holocene valley floor evolution

What is immediately evident when looking across all Northland sites is the influence that bedrock configuration has on valley floor geomorphology and the assemblage of fluvial units. Planform maps and cross-sections from eight Northland sites (Figs. 5.3 to 5.10) show the geomorphological diversity expressed within the fluvial environment of these rivers. Each site has an assemblage of fluvial units (i.e., terraces, floodplains, palaeochannel fills) within boundaries imposed by bedrock configuration. Nanson and Croke's (1992) classification of different floodplain types was largely based on the differentiation of floodplain forming processes, recognising that floodplain morphology and genesis is the result of variations in stream power and sediment texture. Across the Northland sites floodplain morphology and evolution strongly reflects the dominant floodplain forming and floodplain reworking processes involved (see Fig. 5.11 for morphological examples of floodplain reworking processes).

The least confined valley settings (Awanui, Panguru and Kaihu sites) are characterised by a single broad Holocene age floodplain comprising vertically accreted silt and sand sequences derived from suspended sediment in overbank flows. At the Awanui site these floodplain deposits overlie peat or organic rich palaeosol deposits formed during the LGCP. At the Kaihu site Holocene flood deposits also overlie an undated peat unit. At the Panguru and Kaihu sites, the Holocene floodplain surface is bounded in part by the remnants of a high (> 10 m), undated, but presumed Pleistocene age terrace. Radiocarbon dates from the contemporary floodplain at Panguru suggest that there have been high sedimentation rates in the last few hundred years (~ 2 m of alluviation since 460–310 cal. yr BP (P2 in Table 5.1 and Fig. 5.5c). Thus, for these relatively unconfined sites, valley floor evolution has involved the infilling of incised valleys after the LGCP and during the Holocene. Floodplain geomorphology indicates that the dominant floodplain forming process has been vertical accretion and there is also evidence of reworking, involving lateral migration and cutoffs, leading to the formation of palaeochannels. In the last few hundred years anthropogenic deforestation and catchment disturbance have resulted in rapid sedimentation rates within the study catchments, draping young sediments across wide swaths of the Holocene floodplain surface in the unconfined valley setting.

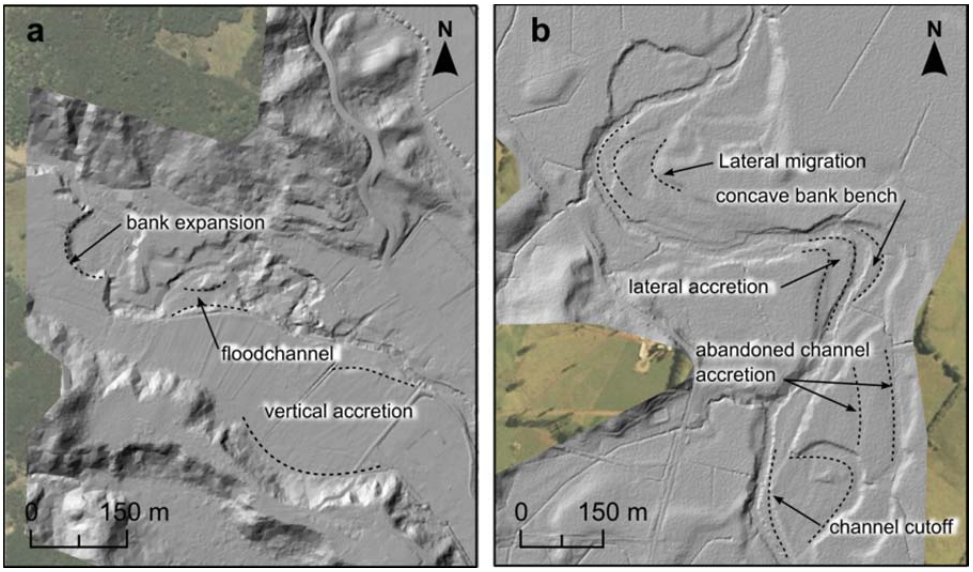

Fig. 5.11. LiDAR derived DEM hillshades overlying aerial images and showing morphological examples of floodplain forming and reworking processes. (a) Upper Whakarapa Stream, Panguru and (b) Takahue River.

The Nukutawhiti, Takahue and the Waimamaku sites are examples of more confined settings, where relatively narrow valleys are bounded by bedrock and remnant Pleistocene terraces. Two different Holocene floodplain surfaces can be identified, with the highest Holocene floodplain elevated ~ 2–4 m above the lower floodplain surface. The stratigraphy of the high Holocene floodplain generally comprises gravel overlain by 2–4 m of vertically accreted sand and silt, and with sedimentation rates in the order of 1.9 mm yr^{-1} or less (derived from T2 in Table 5.1 and Fig. 5.7c). Sediments of the low floodplain surface are finer grained silt and clay, with the exception of Takahue, where the low floodplain unit is a sequence of (fine) gravels (Fig. 5.7c). In these more confined valleys, floodplain evolution has comprised the vertical aggradation of a high Holocene floodplain surface by large-volume overbank flood flows. Dating at the Takahue site suggests that sometime after 2000–1870 cal. yr BP this high Holocene floodplain surface has been incised and then subsequently refilled by younger finer sediments at rates of around 1.9 mm yr^{-1} (derived from T3 in Table 5.1 and Fig. 5.7c). Sedimentation rates of 3.7 mm yr^{-1} at the Waimamaku site (derived from W4 in Table 5.1 and Fig. 5.6c) and 10 mm yr^{-1} at the Nukutawhiti site (derived from M5 in Table 5.1 and Fig. 5.8c) suggest rapid aggradation of the lower floodplain and palaeochannel has occurred in last few hundred years. Floodplain reworking processes in these more confined valley setting typically show evidence of channel expansion, lateral migration and floodchannels,

and also depositional forms at the channel margins (inset units), infilling of abandoned channels and vertically accreted floodplains (Fig. 5.11).

The Kaeo and Titoki sites represent the most confined sites and here the valley floor morphology is one of a single floodplain surface. At Kaeo, ^{14}C dates indicate valley floor infilling from 7570–7680 cal. yr BP, with fluvial sedimentation rates of less than 1 mm yr^{-1} (derived from K4 in Table 5.1 and Fig. 5.9c). Radiocarbon chronology at these most confined sites indicate that under conditions of limited accommodation space the Holocene floodplain has accumulated at a faster rate (7 mm yr^{-1} in Kaeo and 9.5 mm yr^{-1} at the Titoki site, derived from K1 in Fig. 5.9c and TI1 in Fig. 5.10c, and Table 5.1) in the last several hundred years, most likely in response to anthropogenic land-use change.

5.7.2 Regional model for Holocene fluvial behaviour

Figure 5.12 shows a schematic model for floodplain development in Northland for a continuum of valley floor confinement. A single continuous Holocene floodplain develops under conditions of both high and low levels of valley confinement. On the confinement continuum, the limited accommodation space for sediment storage, afforded by the more confined valley setting (Kaeo and Titoki sites), means that the rate of alluviation has been relatively rapid, burying older Holocene deposits and geomorphological evidence of floodplain reworking processes. In less confined valley settings (Kaihu, Panguru and Awanui) sediment is stored over a greater area and the geomorphology associated with floodplain reworking processes, such as lateral migration, is often better preserved. In partly confined valley settings (Nukutawhiti, Takahue, Waimamaku) the geomorphology is more complex, with multiple Holocene floodplain surfaces and evidence of floodplain reworking. Here the model of floodplain development is one of floodplain alluviation during the mid to late Holocene followed by destabilisation and incision sometime after ~ 2000 cal. yr BP and then rapid floodplain aggradation in response to anthropogenic catchment disturbance. The role of climate in floodplain development is discussed in Section 5.7.3.

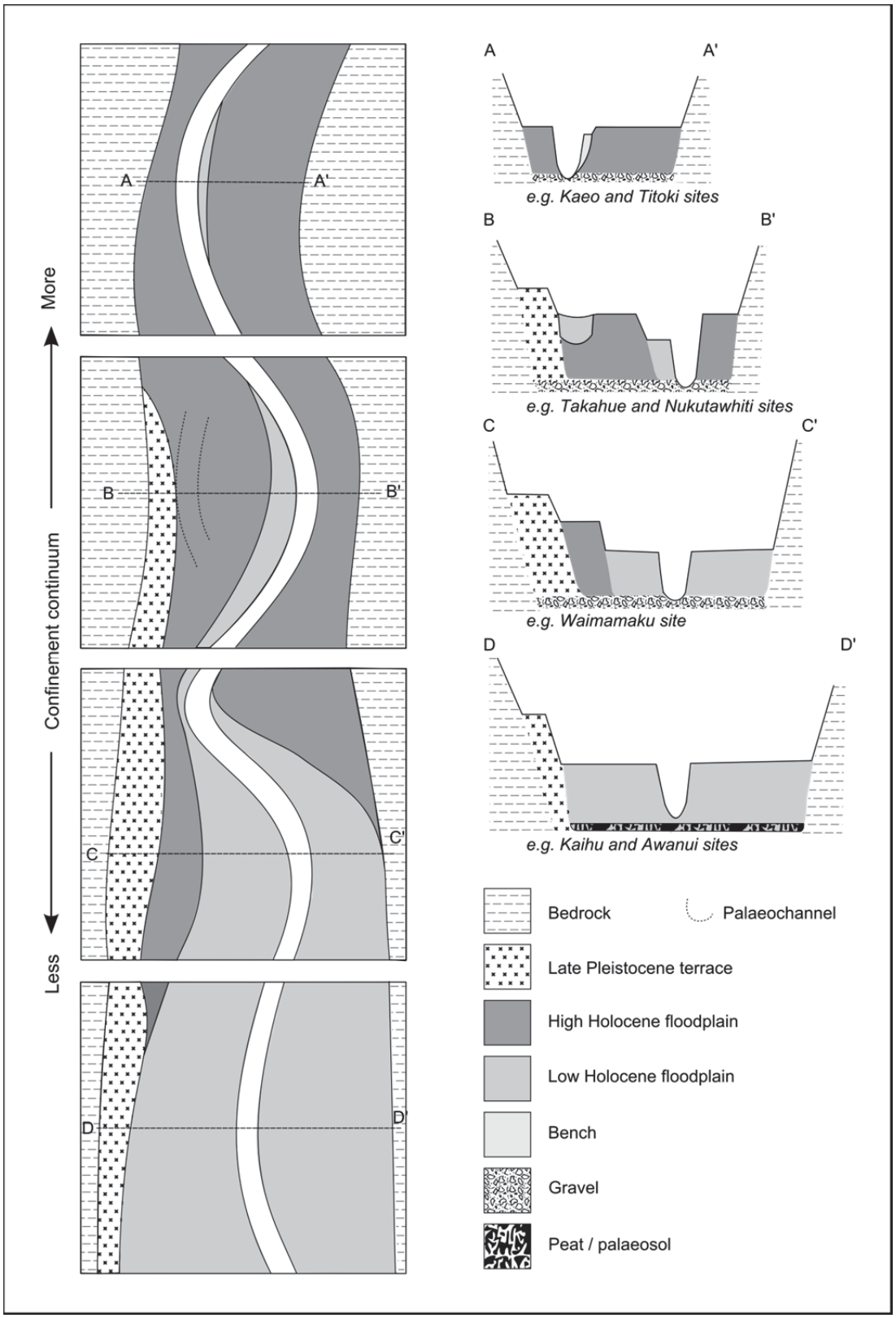

Fig. 5.12. Stylised schematic model for Holocene floodplain development in different valley confinement settings.

5.7.3 Mechanisms of floodplain formation

In the Northland alluvial record there is an absence of early to mid Holocene valley-fill deposits, with the oldest deposit from the high Holocene surface at partly confined sites aged 6660–6490 cal. yr BP. This gap in the alluvial record may be due to preservation factors (Lewin and Macklin, 2003) and the difficulties in sampling, or there may be a genuine gap in the sedimentary record due to a climatically driven phase of floodplain reworking and incision. A distinctive gap in the alluvial record of southeastern Australia between 8000 and 4000 cal. yr BP was detected by Cohen and Nanson (2007), and interpreted as representing an early to mid Holocene climatic optimum involving a period of increased discharge and low sediment yields, termed the *Nambucca Phase*. The chronostratigraphic evidence for reduced sediment loads in the early to mid Holocene in Northland is supported by additional proxy climate records, with palaeovegetation records suggesting more mesic climatic conditions (Dodson et al., 1988; Striewski et al., 1996; Elliot, 1998). It is therefore reasonable to infer that Northland catchments experienced a similar phase of enhanced river activity, albeit with an earlier cessation, to that reported in southeastern Australia (Cohen and Nanson, 2007). A warmer and wetter climate that prevailed at this time would be likely to produce higher discharges with lower sediment yields from stable well-vegetated catchments, resulting in the reduction of temporary sediment storage and potentially increased reworking of floodplain sediments.

The formation of different floodplain surfaces within partly confined valleys, as exemplified by the Takahue, Nukutawhiti and Waimamaku River sites, also suggest climate-driven changes in catchment sediment flux and/or discharge regime are responsible for the patterns of sediment storage. Radiocarbon dates from the high Holocene terrace at partly confined sites indicate that this surface aggraded around the mid to late Holocene with dates from gravels and flood deposits ranging from between 6660–6490 cal. yr BP and 2000–1870 cal. yr BP. As Cohen and Nanson (2007) pointed out the existence of an elevated terrace above a floodplain can be a result of: an increased channel-forming discharge and sediment load: increased discharge and decreased sediment load: reduced discharge and increased sediment concentration: or a more complex scenario. In Northland the mid to late Holocene phase of floodplain aggradation coincides with the climatic deterioration identified from pollen studies, and thus it is most likely a response to increased sediment supply and discharge resulting from extreme precipitation events and storm-driven vegetation disturbance. In addition, the Mangakahia, Takahue and Waimamaku catchments drain the steep slopes of the highest ranges in central and western Northland and are therefore more likely to be more responsive to changing hydrological conditions due to higher levels of catchment

connectivity here (cf. Harvey, 2001; Fryirs et al., 2007). The Waimamaku river is also flanked by large Pleistocene landslide deposits which ensure an abundant and easily remobilised sediment supply from the catchment slopes (cf. Korup et al., 2010).

After ~ 2000 cal. yr BP there appears to have been a second period of lateral channel destabilisation and erosion of the high Holocene floodplain at the partly confined sites. This phase of floodplain erosion broadly corresponds with a gap in the New Zealand alluvial record centred on ~ 1300 cal. yr BP identified by Richardson et al. (2013), where an absence of fluvial ^{14}C dates from all sedimentary environments representing both stability and activity in the New Zealand fluvial record point to a phase of erosion at this time. Vegetation records from the Northland region suggest that around the late Holocene there was some degree of climate amelioration, with peaks in abundance of warmth-loving species such as *Agathis australis* (Elliot et al., 1995; Elliot et al., 1997). We argue that this phase of incision in the fluvial record is a response to increased discharge and reduced sediment loads from stable catchments associated with a warmer, wetter and less seasonal climate regime. Basal ages for the low Holocene terrace indicate the lower floodplain at the partly confined fluvial sites started to accumulate after 1180–1300 cal. yr BP. We suggest rapid sedimentation of fine-grained alluvium, forming a lower floodplain surface, has occurred in response to anthropogenically driven catchment disturbance.

5.7.4 Northland floodplain development in a global context

The Northland model of floodplain evolution during the Holocene is in broad agreement with many other floodplain development models from other regions which describe Holocene floodplain formation in terms of phases of alluviation relating to climatic and anthropogenic forcing factors. The British Holocene episodic activity/preservation model developed by Macklin and Lewin (1993; 2003) and expanded by (Lewin et al., 2005) emphasised the episodic nature of Holocene sedimentation, involving factors such as cold-phase sediment exhaustion and secondary para-glacial effects (in the early Holocene), climatic episodes and anthropogenic factors (in the mid to late Holocene). One difference with the British model however, is because Northland remained forested throughout the LGM (e.g., Newnham, 1992) some of the sedimentary responses associated with the inheritance and reworking of Pleistocene sediments are not apparent in the Northland setting.

Another important distinction between Northland and models of Holocene sedimentation from other global regions is the nature and timing of anthropogenic impacts. Holocene floodplain sedimentation in the Rhine was found to be strongly influenced by human

impacts from ~ 3000 cal. yr BP (Hoffmann et al., 2009). Again in the British record, anthropogenic sedimentation involved extended time periods (thousands of years) in response to the introduction and expansion of agriculture, and more recently river engineering and drainage (Lewin et al., 2005). In the southern Cape region of South Africa two phases of anthropogenic floodplain sedimentation were discerned: an initial phase was initiated by the degradation of natural vegetation due to pastoral farming after 400 AD: and was followed by a second period of floodplain alluviation following European settlement (Damm and Hagedorn, 2010). In Northland, the sedimentary response to anthropogenic catchment disturbance is rapid and intense due to the short period of human settlement in the region, with less than 800 years of Polynesian settlement (Prickett, 2002) and ~ 170 years of European colonisation. Although, the sequential impacts of two settlement phases on floodplain sedimentation cannot be differentiated in the Northland record.

Reconstruction of fluvial behaviour of the partly confined middle Delaware River, USA also identifies a phase of fluvial activity associated with the onset of European (Euroamerican) settlement, which has followed several climatically driven phases of floodplain and terrace reworking during the early and middle Holocene (Stinchcomb et al., in press). This floodplain development model emphasised the role of floodplain and reworking processes leading to the formation of inset units comprising palaeochannel fills, oblique and lateral accretionary deposits, resulting in a similar geomorphology to landforms with an alternative development history (Stinchcomb et al., in press). This polycyclic mode of floodplain evolution identified in partly confined systems in Australia (Cohen and Nanson, 2008) and USA (Stinchcomb et al., in press) is also evident in the Northland partly confined sites, where the high Holocene terrace has undergone mid Holocene reworking and subsequent formation of a lower late Holocene surface that is regularly inundated by overbank flows.

In contrast to the partly confined sites in this study, the topography of both the more confined and least confined valleys sites is similar in that they comprise a single Holocene floodplain surface. Although subject to the same regional climatic drivers the different fluvial sites exhibit non-uniform landscape responses to changes in the catchment sediment flux and/or flow regime that can be largely explained by differences in valley confinement, through its control on accommodation space and floodplain forming and reworking processes. In southeastern Australian systems, the formative controls on floodplain development for partly confined settings were found to be quite different to unconfined valley settings (Cohen and Nanson, 2008), with the dominant controls on sediment storage patterns postulated to be a combination of intrinsic thresholds and Holocene climate change (Cohen and Nanson, 2007). Northland's partly confined rivers, like southeastern Australian

partly confined rivers, with their greater level of geomorphological complexity appear to offer greater opportunities for reconstructing alluvial histories and deciphering the dominant drivers of fluvial change in tectonically stable environments.

5.8 Conclusion

Valley floor mapping, sedimentology and ^{14}C dating at eight sites in Northland have been used to develop a model of Holocene floodplain development for different valley settings. An absence of early to mid Holocene valley-fills coinciding with a warmer wetter climate suggests a period of enhanced discharge and reduced sediment load resulting in increased limited sediment sequestration during this time. In the mid to late Holocene a single Holocene floodplain surface formed in less confined and more confined valley settings, often bounded by elevated remnant Pleistocene terraces, in response to episodic overbank deposition. In partly confined valley systems two Holocene terraces can be discerned. In the mid to late Holocene, aggradation of the higher surface has occurred in response to climatic deterioration, with the occurrence of large storms and floods, which has disturbed catchments, increasing the sediment supply from the catchment. After ~ 2000 cal. yr BP there has been a phase of degradation, coinciding with a transition to a warmer, wetter and less disturbed climate regime identified in the regional pollen records. This period of incision was then followed by rapid sedimentation of fine-grained alluvium resulting from anthropogenic driven catchment disturbance and the formation of a lower late Holocene floodplain surface.

Northland Holocene floodplain development and valley floor morphology reflect the interplay between valley configuration and accommodation space (geologically controlled) within the fluvial system, sediment supply, fluctuation in climate, and anthropogenic factors in the last several hundred years. This study shows that valley floor confinement has played a major role in controlling Northland floodplain development, accounting for differences in the specific fluvial unit assemblages between sites. Variations in sediment flux in response to climatic, and more recently anthropogenic, catchment disturbance, is the primary control on Northland floodplain geomorphology. The results of this work also highlight the opportunities that partly confined valley settings offer for reconstructing alluvial histories and expanding the New Zealand fluvial record.

Acknowledgements

This work was funded by a Tertiary Education Commission Top Achiever Doctoral Scholarship awarded to JR. Radiocarbon dating was supported by the Massey University Research Fund (to ICF). NJL's contribution was funded by PGSF Contract CO5X0705. Field assistance was provided by David Feek and landowners are thanked for permitting access to the sites described.

Chapter 6

Regional river activity in the Holocene: Northern New Zealand rivers as sensitive recorders of centennial-scale climate change

6.1 General introduction

Chapter 5 reconstructed the fluvial history at eight sites in Northland and developed a model of Holocene floodplain development for different valley settings in the region. The main aspects of the model were: an absence of early to mid Holocene valley-fills coinciding with a warmer wetter climate, the aggradation of a higher Holocene terrace in partly confined valleys during the mid to late Holocene, followed by a phase of degradation and subsequent rapid sedimentation of fine-grained alluvium resulting from anthropogenic driven catchment disturbance. This targeted field research in Northland produced additional fluvial radiocarbon (^{14}C) dates that were added to the New Zealand fluvial ^{14}C database, thereby addressing the lack of ^{14}C-dated fluvial units in northern New Zealand identified in Chapter 4. It is the aim of the following Chapter 6 to apply meta-analysis techniques to an expanded New Zealand fluvial ^{14}C database.

The following chapter presents a revised meta-analysis of 422 ^{14}C-dated Holocene fluvial units in New Zealand (meta-analysis data is included in Appendix A). In Section 6.3 probability-based records of river activity for Northland, the six coherent precipitation

regions, northern and southern regions combined, and probability-based records of river stability and activity for New Zealand are presented. The record of Holocene river activity for the North and South Islands and the northern new Zealand precipitation region are compared in Section 6.4 with other palaeoclimate proxy data representing tropical and polar influences on climate. Finally, the impact of the addition of 20 new fluvial activity ^{14}C dates (core logs and ^{14}C results are attached as Appendix C and D respectively) to the Fluvial database is examined and discussed in terms of the model proposed in Chapter 4, that suggests atmospheric circulation is the key driver of river activity in New Zealand.

6.2 Introduction

Meta-analysis of the New Zealand fluvial ^{14}C database in Chapter 4 revealed the sensitivity of New Zealand river systems to short-term and rapid Holocene climate variations. Atmospheric circulation change, involving the oscillation of the major Southern Hemisphere climate modes, the Southern Annular Mode (SAM) and El Niño Southern Oscillation (ENSO), emerged as a key driver of river activity in New Zealand. An out-of -phase pattern in the timing of river activity between the northern and southern regions of New Zealand dominates the Holocene record. River activity in the South Island generally responds to enhanced westerly atmospheric circulation associated with a predominance of trough regime synoptic type (negative SAM-like circulation). In the North Island episodes of river activity are generally driven by increased meridional atmospheric circulation associated with blocking regime synoptic conditions (La Niña-like and positive SAM-like circulation).

The analysis of the New Zealand fluvial ^{14}C database in Chapter 4 identified geographic gaps in the record, particularly far northern (Northland) and far southern (Southland) New Zealand. In addition the relatively small number of ^{14}C dates in each coherent precipitation region (compared to the UK dataset) prevented an assessment of river behaviour at this regional scale. New Zealand has a strongly regionalised climate, primarily due to orography and interaction with the prevailing westerly wind circulation (Chapter 2). More fluvial ^{14}C dates from across the regions, particularly Northland and Southland, would improve the resolution at the coherent precipitation region scale and present opportunities for reconstructing past atmospheric circulation regimes (e.g., Lorrey et al., 2007). Fluvial records form Northland are of particular value for palaeoclimate reconstruction, as the region has been tectonically and volcanically stable throughout the Holocene, potentially preserving a purer climate signal in the record.

This chapter presents a meta-analysis of 422 ^{14}C-dated Holocene fluvial units in New Zealand obtained from targeted field research in Northland (Chapter 5), published papers

and unpublished data. Essentially, this chapter performs the analysis described within Chapter 4 but with the addition of Northland data acquired from Chapter 5. The revised analysis provides a more geographically extensive probability-based reconstruction of Holocene river behaviour in New Zealand. In an extension to the approach in Chapter 4, episodes of river activity in the North and South Islands, and the coherent precipitation regions, including northern New Zealand, are identified and compared with alternative regional palaeoclimate records. The impact of 20 new ^{14}C dates, representing river activity in Northland, is examined and discussed in light of the model presented in Chapter 4, which suggests atmospheric circulation is the key driver of river activity in New Zealand.

6.3 Method

Twenty one fluvial ^{14}C ages (20 representing river activity) from the Northland region (Chapter 5) were added to the New Zealand fluvial ^{14}C database (Macklin et al., 2012a) analysed in Chapter 4. The New Zealand fluvial ^{14}C database contains 401 fluvial ^{14}C ages and was compiled from published papers, unpublished reports and unpublished data from the GNS Science Fossil Records Database (FRED) and New Zealand Rock Catalogue and geoanalytical database (PETLAB). Figure 6.1 shows the location of the ^{14}C-dated fluvial sites in New Zealand within the six precipitation zones, and the location of 21 new Northland fluvial ^{14}C ages. Table 6.1 shows the sample details, depositional environment and ^{14}C data for the 21 Northland fluvial ^{14}C ages. Of the 21 Northland ^{14}C dates, 20 were interpreted as representing fluvial activity and one ^{14}C date from the Kaihu catchment was obtained from a palaeosol unit deposited under stable conditions. The majority of the ^{14}C ages were from floodplain depositional environments, with four ^{14}C ages obtained from fluvial units deposited within palaeochannels.

Database ^{14}C ages were calibrated using SHCAL04 (McCormac et al., 2004) and the individual probabilities summed using the radiocarbon calibration programme OxCal version 4.1 (Bronk Ramsey, 2001) to produce cumulative probability function (CPF) plots at a 5-year resolution. CPF probabilities associated with subsets of the database (i.e., regional groupings or ^{14}C ages representing river activity or stability) were divided by the probability calculated for the CPF of the entire dataset to produce relative probability plots, removing the influence of preservation bias toward younger units (Hoffmann et al., 2008). The different groups were then normalised by dividing each value in the relative probability curve by the highest probability in the entire dataset. Probability peaks above the mean probability produced by at least three ^{14}C dates in a 200 year period were used to identify the most significant phases of river activity or stability (cf. Macklin et al., 2010; Richardson et al., 2013).

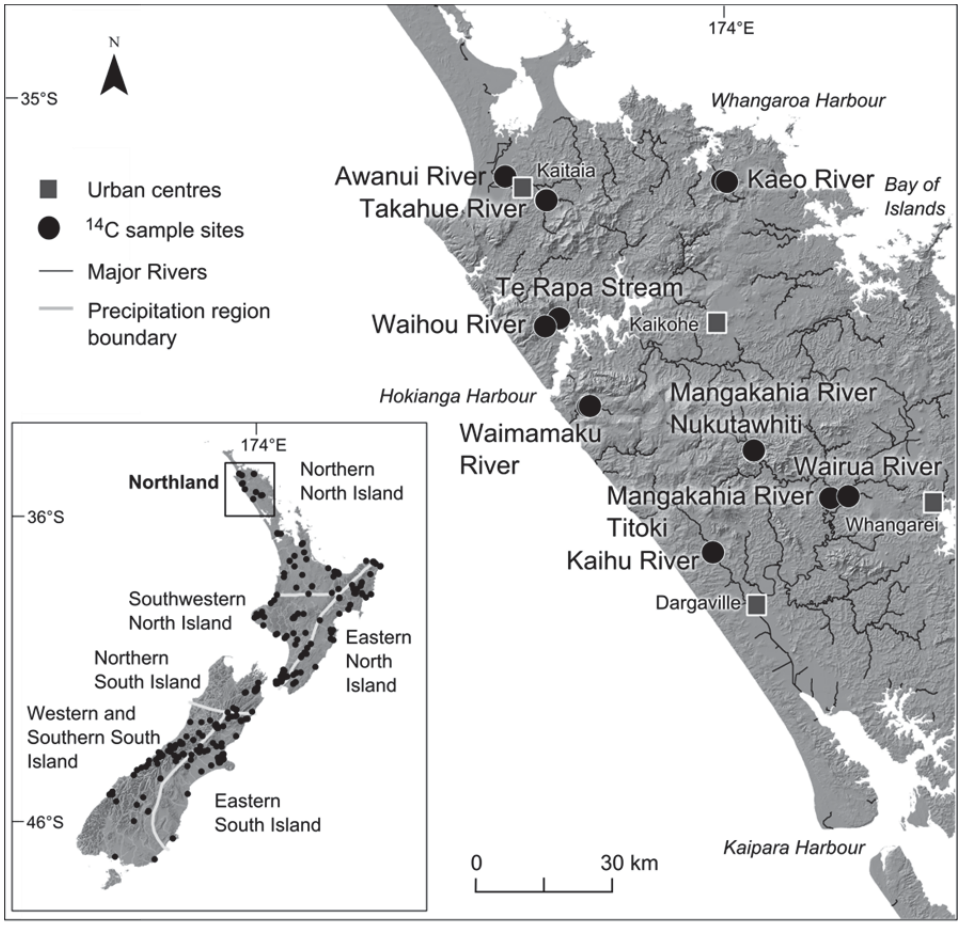

Fig. 6.1. The location of fluvial ^{14}C sample sites included in the New Zealand fluvial ^{14}C database and the location of Northland ^{14}C-dated fluvial units. The six coherent precipitation variability regions in New Zealand (Mullan, 1998) are also labelled.

6.4 Results

Figure 6.2 shows the CPF for the 21 Northland ^{14}C ages (a), the New Zealand Holocene fluvial ^{14}C database before the addition of the Northland ^{14}C ages (b) and the entire New Zealand Holocene fluvial ^{14}C database containing 422 fluvial ^{14}C dates (c). The New Zealand CPF plot shows a progressive increase in probabilities after ~ 2000 cal. yr BP due to the effect of preservation bias on the distribution of fluvial ^{14}C ages. The CPF curve constructed from Northland ^{14}C ages also reflects a preservation bias towards fluvial units younger than ~ 1000 cal. yr BP. The relative CPF plots of 'activity' and 'stability' for New Zealand and the CPF plot for new Northland 'activity' ^{14}C dates are shown in Fig. 6.3. From the meta-analysis of 284 ^{14}C ages representing fluvial activity and 112 ^{14}C ages representing stability, 13 major episodes of river activity and 9 episodes of river stability can be identified

in the New Zealand Holocene fluvial record (Table 6.2). In the Northland record two major episodes of river activity (3500–2800 and 800–600 cal. yr BP) are highlighted (Fig. 6.2 and Table 6.2).

Table 6.1

Summary of sample location, sample details, radiocarbon data, depositional environment and whether or not the sample represents fluvial activity or stability.

Data-base ID	Sample	Lab no.	Depositional environment	Sample material	Sample depth (m)	Uncalibrated date (BP)	Calibrated date (cal. yr BP 2σ confidence)	Activity /stability
Awanui Catchment – Awanui River								
416	Awan1b	Wk-28764	Palaeo-channel	Silt organics	1.5	3299 ± 35	3570–3380	Activity
417	Awan1a	Wk-28765	Palaeo-channel	Silt organic	0.74	2962 ± 55	3240–2880	Activity
Kaeo Catchment – Kaeo River								
414	Kaeo4a	Wk-30440	Floodplain	Wood	4.02	4769 ± 25	5580–5320	Activity
415	Kaeo4c	Wk-30443	Floodplain	Silt organics	4.6	6820 ± 26	7675–7570	Activity
423	Kaeo1b	Wk-27971	Floodplain	Silt organics	4.85	691 ± 35	660–560	Activity
Kaihu Catchment – Kaihu River								
412	Kaih2e	Wk-30436	Floodplain	Wood	2.3	3109 ± 25	3360–3170	Activity
428	Kaih2f	Wk-31574	Floodplain	Wood	3.6	3933 ± 28	4420–4160	Activity
427	Kaih2b	Wk-31573	Floodplain	Wood	2.86	3457 ± 28	3560–3820	Stability
Mangakahia Catchment – Mangakahia River								
420	Mang2g	Wk-27966	Palaeo-channel	Wood	3.05	291 ± 35	450–150	Activity
421	Mang1a	Wk-27967	Floodplain	Silt organics	7.4	850 ± 39	790–670	Activity
429	Nuku2a	Wk-31576	Floodplain	Silt organics	1.47	3287 ± 30	3560–3380	Activity
Panguru Catchment – Te Rapa Stream								
418	Pang2a	Wk-27963	Floodplain	Char-coal	2.3	353 ± 30	460–310	Activity
Upper Awanui Catchment – Takahue River								
410	Taka2e	Wk-30434	Floodplain	Wood	4.62	5828 ± 25	6660–6490	Actvity
411	Taka2d	Wk-30435	Floodplain	Wood	3.69	2033 ± 25	2000–1870	Activity
425	Taka3g	Wk-30764	Palaeo-channel	Wood	3.58	2770 ± 25	2870–2760	Activity
426	Taka3d	Wk-31571	Palaeo-channel	Silt organics	2.31	1381 ± 25	1300–1180	Activity
Waihou Catchment – Waihou River								
419	Waih3a	Wk-27964	Floodplain	Wood	5.5	5977 ± 47	6890–6640	Activity
Waimamaku Catchment – Waimamaku River								
413	Waim4c	Wk-30438	Floodplain	Wood	2.56	780 ± 25	730–650	Activity
430	Waim9a	Wk-31577	Floodplain	Wood	3.38	2947 ± 27	3160–2890	Activity
422	Waim1c	Wk-27968	Floodplain	Wood	3.3	1138 ± 41	1070–920	Activity
Wairua Catchment – Wairua River								
424	Poro4a	Wk-30763	Palaeo-channel	Silt organics	1.72	10,045 ± 31	10,110–9980	Activity

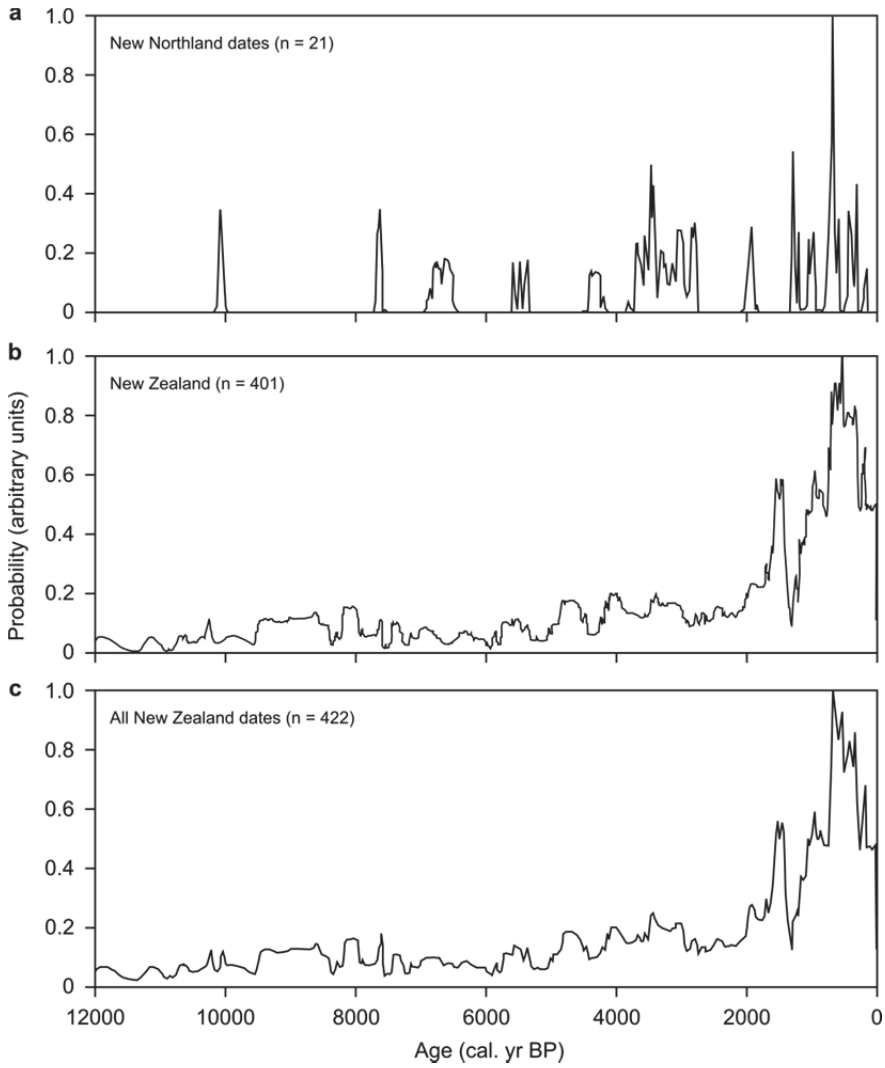

Fig. 6.2. Cumulative probability function (CPF) plots of ^{14}C-dated fluvial units in (a) Northland, (b) New Zealand before the addition of the Northland ^{14}C dates and (c) New Zealand after the addition of Northland ^{14}C ages.

New Zealand has a strongly regionalised climate due to interactions between orography and the dominant westerly flow (Chapter 2). The six coherent precipitation regions identified by Mullan (1998) (Fig. 6.1) are used as a basis for assessing regional river activity during the Holocene. Figure 6.4 and Table 6.3 display the results of a regional analysis of river activity and stability for the northern (North Island) and southern (South Island) precipitation regions. The North Island record is characterised by 13 episodes of increased river activity and four episodes of stability, three of which are recorded in the last 2000 years (Table 6.3). South Island rivers experienced 10 phases of increased fluvial activity and four stable periods

during the Holocene. The timing of the major phases of Holocene fluvial activity is predominantly out of phase between northern and southern New Zealand.

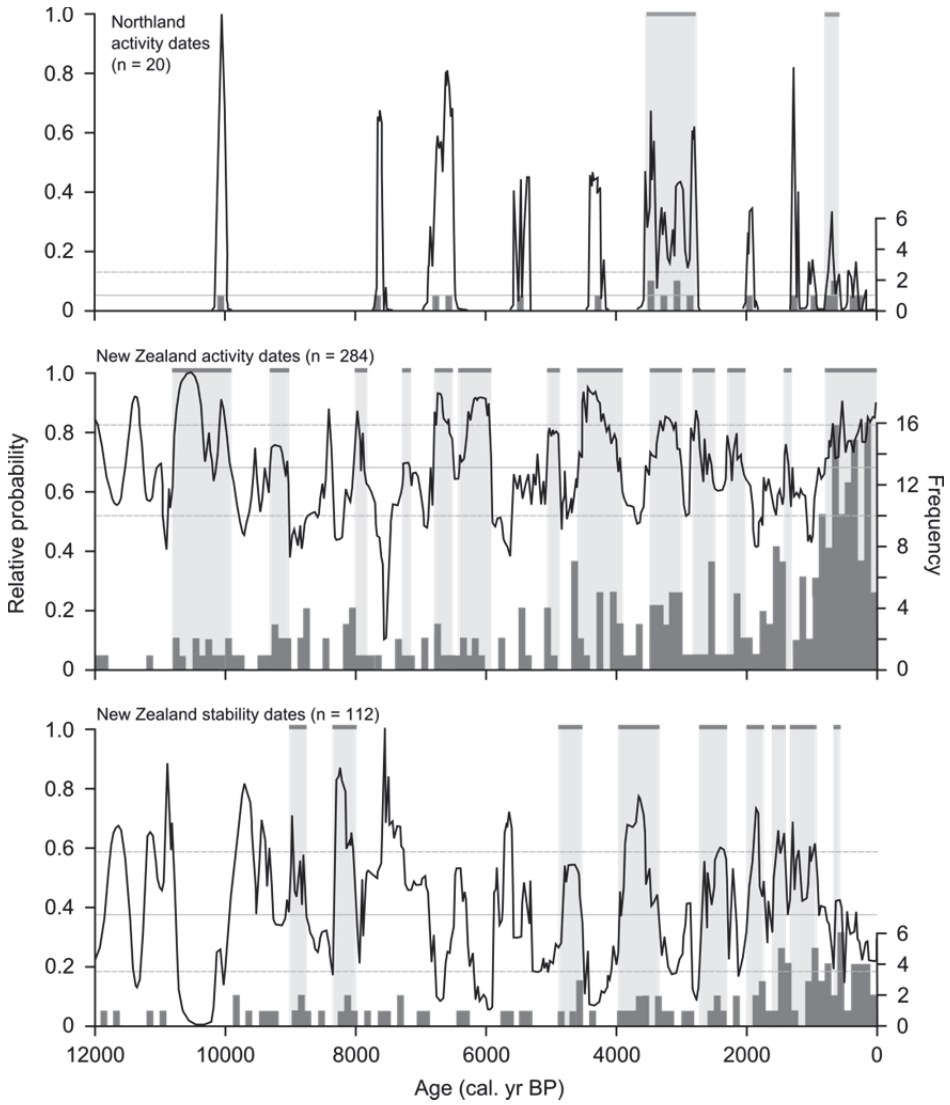

Fig. 6.3. Relative CPF plots of 'activity' and 'stability' ^{14}C dates plotted with frequency of dates per 100 years from New Zealand fluvial units. Horizontal lines indicate the mean (solid line) and one standard deviation above and below the mean (dashed lines). Horizontal grey bars at the top of each plot indicate major episodes of river activity or stability.

CPF's for river activity in the six coherent precipitation regions are shown in Fig. 6.5 and the most significant phases of activity, corresponding to probability peaks produced by at least three ^{14}C dates in a 200 year period, are summarised in (Table 6.4). Despite the data

thinning that has occurred in dividing the 'activity' ^{14}C dates into the six regions, the results show that all regions have experienced episodes of increased river activity. The timing of these episodes varies considerably across the six regions. Northern North Island experienced six phases of river activity, with the majority of river activity occurring in the last ~ 3500 years. By comparison, only two significant episodes of river activity in the late Holocene are identified in southwestern North Island (at 900–700 and 500–200 cal. yr BP). The river activity record for northern South Island comprises 36 ^{14}C dates, with all three significant phases of activity confined to within the last ~ 3000 years. In western and southern South Island a major phase of river activity occurred between 10,900 and 9600 cal. yr BP, and a further four episodes occurred after 2700 cal. yr BP. The Holocene river activity record for eastern South Island is characterised by five episodes of increased river activity after 5300 cal. yr BP.

Table 6.2

Episodes of Holocene river activity and stability in New Zealand and Northland based on analysis of ^{14}C-dated fluvial units.

Activity dates – Northland (ages in cal. yr BP)	Activity dates – NZ (ages in cal. yr BP)	Stability dates – NZ (ages in cal. yr BP)
	10,800–9900	
	9300–9000	
		9000–8800
		8400–8000
	8000–7800	
	7300–7200	
	6800–6500	
	6400–5900	
	5100–4900	
		4900–4500
	4600–3900	
		4000–3300
3500–2800	3500–3000	
		2700–2300
	2800–2500	
	2300–2100	
		2000–1700
		1600–1400
	1400–1300	
		1300–900
800–600		700–600
	800–0	

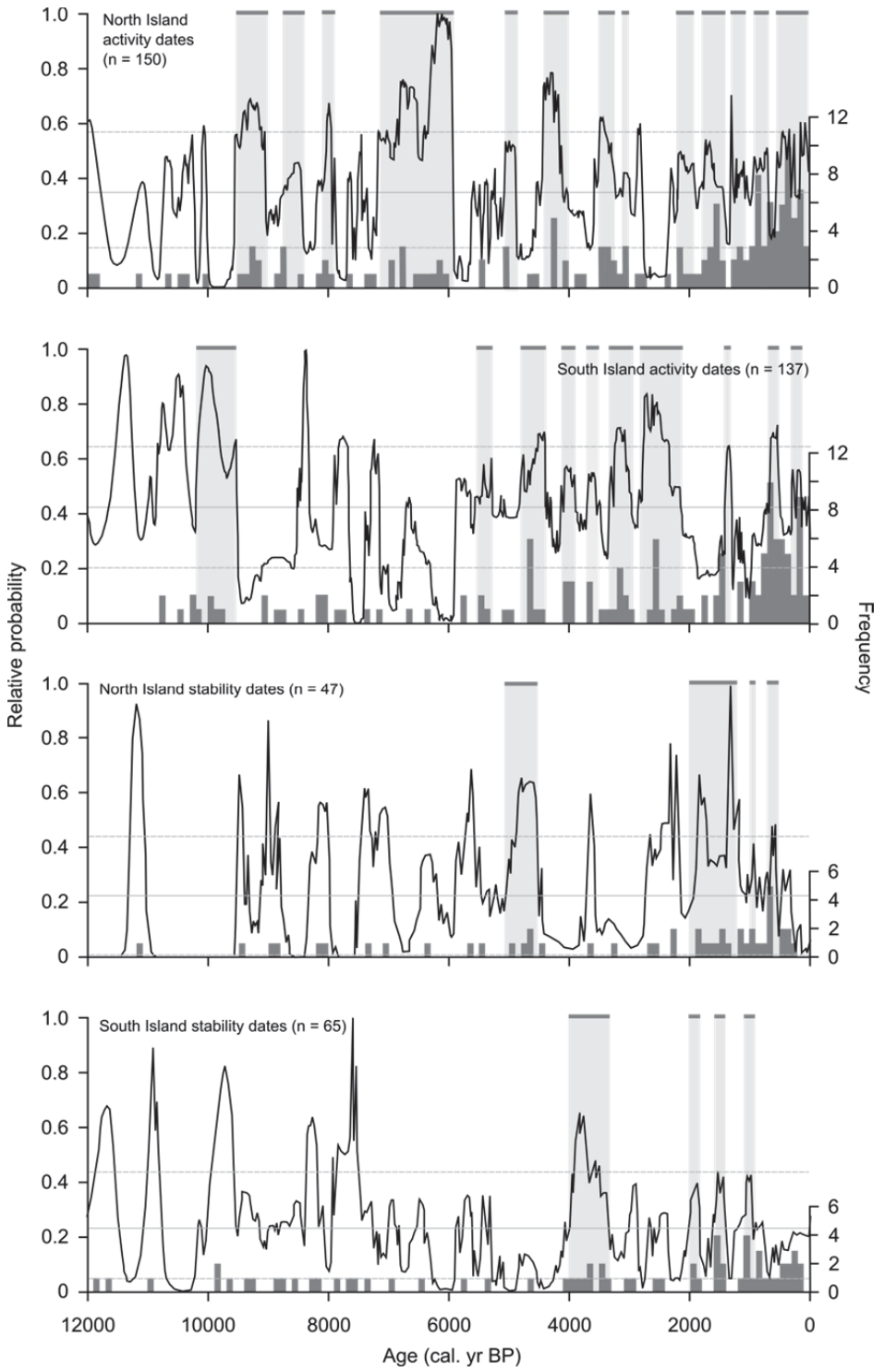

Fig. 6.4. Relative CPF plots of Holocene river 'activity and 'stability' ^{14}C dates plotted with frequency of dates per 100 years for the North and South Islands, New Zealand. Horizontal lines indicate the mean (solid line) and one standard deviation above and below the mean (dashed lines). Horizontal grey bars at the top of each plot indicate major episodes of river stability or activity.

Table 6.3

Episodes of regional Holocene river activity and stability in the North and South Islands, New Zealand, based on analysis of ^{14}C-dated fluvial units.

Activity dates North Island (ages in cal. yr BP)	Activity dates South Island (ages in cal. yr BP)	Stability dates North Island (ages in cal. yr BP)	Stability dates South Island (ages in cal. yr BP)
	10,200–9500		
9500–9000			
8800–8400			
8200–7900			
7100–5900			
	5500–5300		
5100–4900		5100–4500	
	4800–4400		
4400–4000			
	4100–3900		4000–3300
	3700–3500		
3500–3200			
3100–3000	3300–2900		
	2800–2100		
2200–1900			
		2000–1200	2000–1800
1800–1400			1600–1400
	1400–1300		
1300–1100			
		1000–900	1100–900
900–700			
	700–500	700–500	
500–0	300–100		

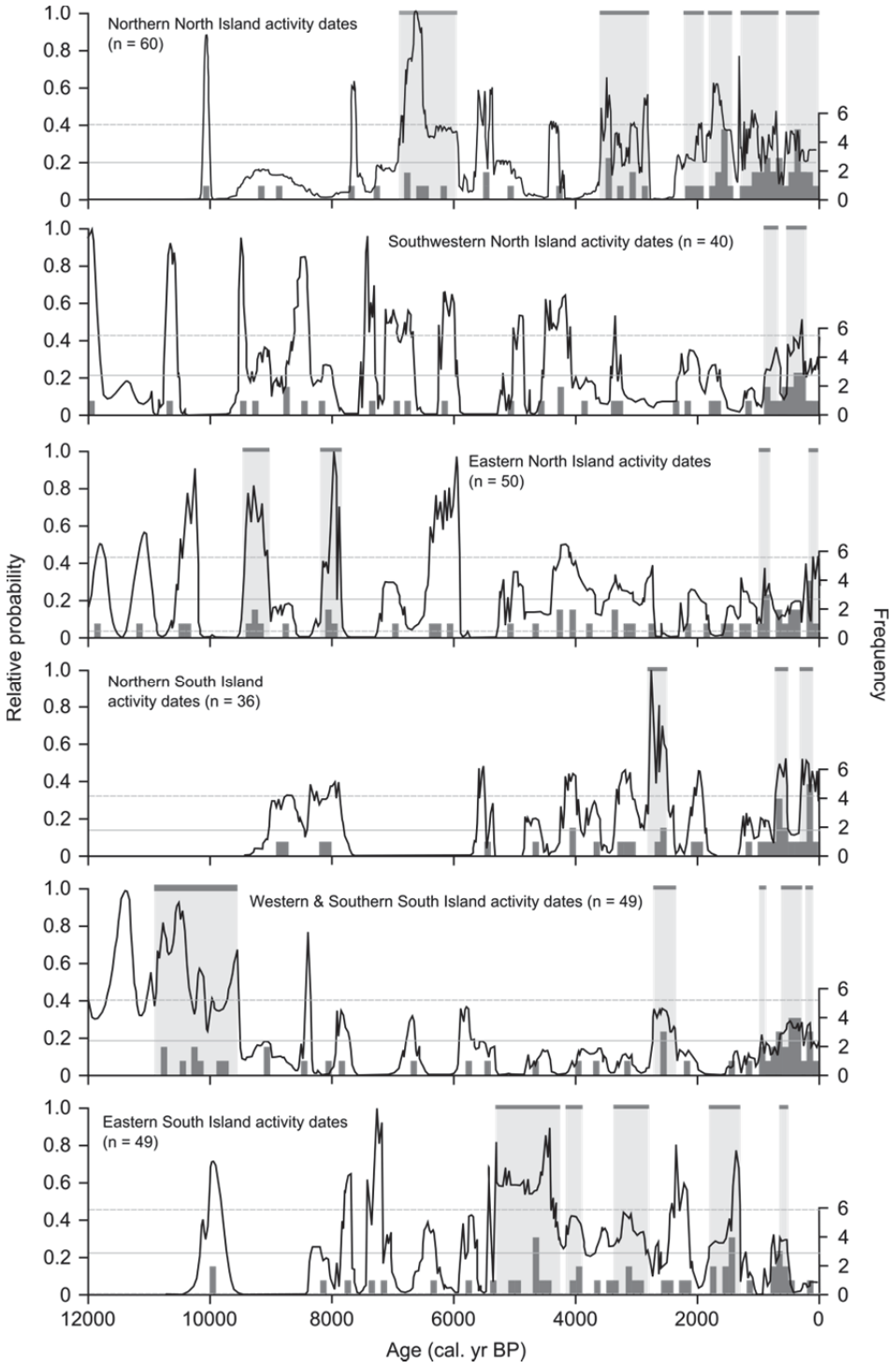

Fig. 6.5. Relative CPF plots of Holocene river 'activity' ^{14}C dates plotted with frequency of dates per 100 years from the coherent precipitation regions within New Zealand. Horizontal lines indicate the mean (solid line) and one standard deviation above and below the mean (dashed lines). Horizontal grey bars at the top of each plot indicate major river activity episodes.

Table 6.4

Episodes of regional Holocene river activity in the six coherent precipitation variability regions of New Zealand based on analysis of ^{14}C-dated fluvial units.

Northern North Island (ages in cal. yr BP)	Southwestern North Island (ages in cal. yr BP)	Eastern North Island (ages in cal. yr BP)	Northern South Island (ages in cal. yr BP)	Western Southern South Island (ages in cal. yr BP)	Eastern South Island (ages in cal. yr BP)
				10,900–9600	
		9500–9000			
		8200–7800			
6900–6000					
					5300–4300
					4200–3900
3600–2800					3400–2800
			2800–2500	2700–2400	
2200–1900					
1800–1400					1800–1300
1300–700		1000–800		1000–900	
	900–700				
			700–500	600–300	600–500
500–0	500–200		300–100	200–100	
		200–0			

6.5 Discussion

Re-analysis of the updated ^{14}C database has resulted in only very minor changes in the overall New Zealand fluvial activity record and North Island river activity record. In the original analysis in Chapter 4, two major phases of river activity identified in the New Zealand record at 6800–6600 cal. yr BP and 3400–3000 cal. yr BP have been extended by 100 years to 6800–6500 cal. yr BP and 3500–3000 cal. yr BP respectively (Table 6.2 and Fig. 6.3). For the North Island and South Island precipitation regions, the probability-based record of river activity remains almost identical to the original analysis, with only one period of river activity in the North Island at 1100–1200 cal. yr BP extended to 1300–1000 cal. yr BP (Table 6.3 and Fig 6.4).

The addition of 20 activity ^{14}C dates from Northland has, not surprisingly, had the largest impact on the river activity record constructed for the northern North Island precipitation zone, increasing the number of fluvial dated units in this region from 40 to 60 (Fig. 6.5). In contrast to most other parts of New Zealand, Northland has been tectonically and volcanically stable during the Holocene. This geological stability combined with a history of

human occupation confined to within the last ~ 800 years (Prickett, 2002) means that Northland catchment and river dynamics will be primarily driven by climate change. The original meta-analysis of northern New Zealand activity ^{14}C ages in Chapter 4, identified three significant phases of river activity for the region during the Holocene, at 1900–1400 cal. yr BP, 1200–700 cal. yr BP and 500–0 cal. yr BP. The 20 new ^{14}C dates from Northland has increased the number of phases of river activity (produced by a minimum of three ^{14}C dates in 200 years) to six, at 6900–6000 cal. yr BP, 3600–2800 cal. yr BP, 2200–1900 cal. yr BP, 1800–1400 cal. yr BP, 1300–700 cal. yr BP and 500–0 cal. yr BP (Fig. 6.5 and Table 6.4). The addition of data has dramatically improved the resolution of the northern North Island river activity record, with this region now containing the most ^{14}C dated fluvial units in the database.

The probability-based river activity record for the northern North Island precipitation region is compared with North and South Island river activity records and alternate regional palaeoclimate records in Fig. 6.6. Over the last ~ 2200 years, northern North Island rivers have, like North Island rivers, been particularly active. This activity in northern New Zealand has occurred at a time of enhanced connectivity between the mid and low latitudes (as detected in lake sedimentation records from Ecuador and eastern North Island), under predominantly positive SAM conditions and at a time when speleothem records from central-west North Island suggest warming and lower precipitation. Between ~ 5000 and 2200 cal. yr BP there has been one major multi-centennial length episode of increased river activity in northern North Island (3600–2800 cal. yr BP) and this was produced by a cluster of Northland ^{14}C dates (Figs. 6.3, 6.5 and 6.6). This prominent phase of river activity between 3500 and 2800 cal. yr BP in the Northland record coincided with a global Holocene cold event, at a time of enhanced climatic connectivity between the low and high latitudes, and when the major climate modes, El Niño Southern Oscillation (ENSO) and the Southern Annular Mode (SAM), were in phase (Chapter 7). Increased river activity in the Northland and northern New Zealand record also occurred during a period of enhanced river activity in the South Island and at a time when wet and cool conditions prevailed in central-west North Island (Fig. 6.6). A sixth multi-centennial phase of river activity in northern New Zealand, between 6000 and 6900 cal. yr BP, coincides with river activity in the North Island and a predominance of positive SAM-like circulation (Fig. 6.6).

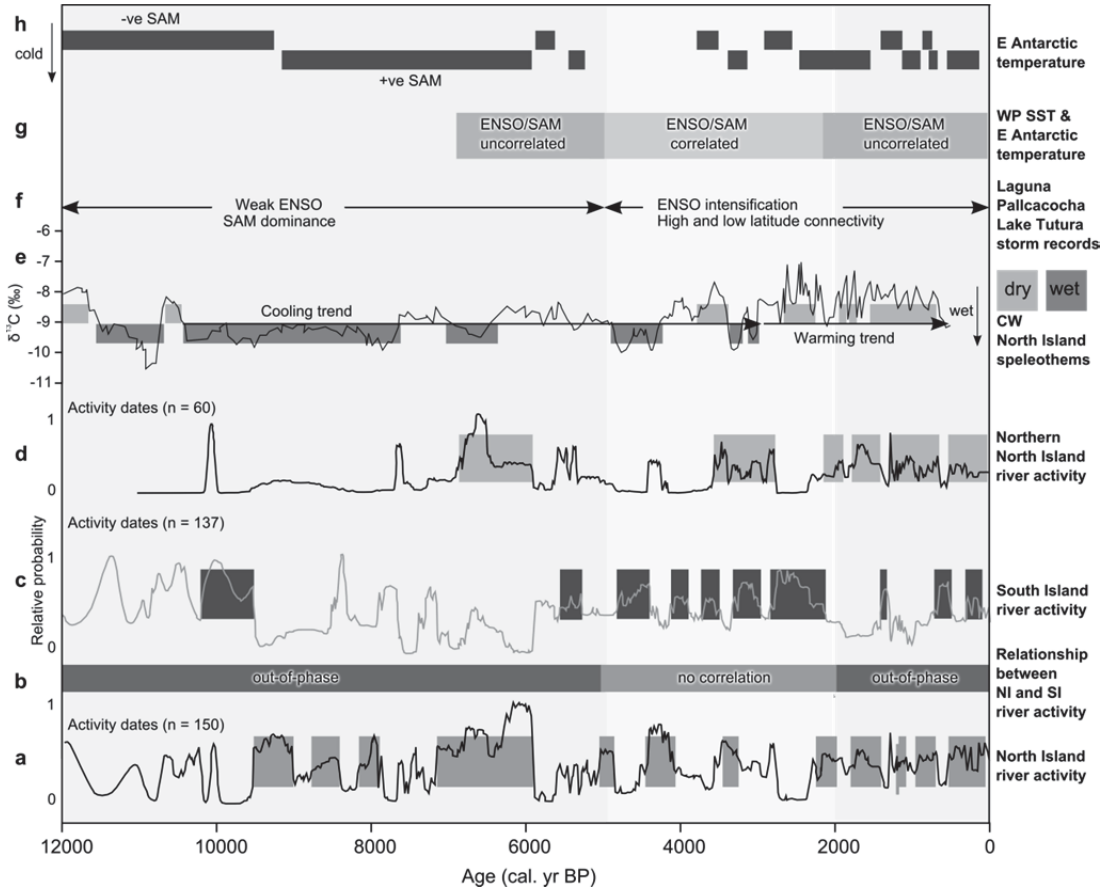

Fig. 6.6. Schematic of regional palaeoclimate proxy records, climate modes and major relationships for the Holocene. (a) Relative CPF plot of Holocene river activity in the North Island, New Zealand, based on analysis of ^{14}C-dated Holocene fluvial units. Grey horizontal bars indicate significant periods of river activity based on ^{14}C-dated Holocene fluvial units. (b) Relationship between North and South Island river activity records (Richardson et al., 2013). (c) Relative CPF plot of Holocene river activity in the South Island, New Zealand, based on analysis of ^{14}C-dated Holocene fluvial units. Dark grey horizontal bars indicate significant periods of river activity based on ^{14}C-dated Holocene fluvial units. (d) Relative CPF plot of Holocene river activity in northern North Island, New Zealand, based on analysis of ^{14}C-dated Holocene fluvial units. Grey horizontal bars indicate significant periods of river activity based on ^{14}C-dated Holocene fluvial units. (e) Temperature and precipitation inferred from central-west North Island speleothems (Williams et al., 2010). (f) Relative influence and intensity of ENSO and SAM determined from Lake Tutira (Gomez et al., 2011), New Zealand and Laguna Pallcacocha, southern Ecuador (Moy et al., 2002), sedimentation records. (g) Relationship between Antarctic surface temperatures (SAM proxy) and western Pacific sea-surface temperature records (ENSO proxy) (Gomez et al., 2011). (h) Polarity of the SAM inferred from East Antarctic temperature determined from the δ deuterium record from EPICA Dome C ice core (Jouzel, 2004).

The re-analysis of the New Zealand ^{14}C database confirms the model proposed in Chapter 4. Out-of-phase river activity between the North and South Islands suggests a phased relationship between ENSO and SAM, and the relative dominance of the two modes, may be responsible for driving Holocene river activity in New Zealand. Northern New Zealand has experienced episodes of river activity in response to enhanced meridional atmospheric circulation associated with La Niña-like and positive SAM-like circulation. In contrast, river activity in southern New Zealand is promoted by strengthened westerly circulation enhanced under negative phase SAM-like circulation conditions. Figure 6.5 shows that during the early to mid Holocene (12,000 to 5000 cal. yr BP) the timing of river activity in the North and South Islands is significantly different, suggesting climate was being more influenced by the operation of the high-latitude climate mode (SAM) at a time of weak ENSO and low or no connectivity between the SAM and ENSO. Between 5000 and 2000 cal. yr BP river activity records from southern and northern New Zealand are characterised by more complex interactions and teleconnections between ENSO and SAM, including a broadly synchronous river response to a globally extensive climate event (Chapter 7). In the last ~ 2000 years rivers in the North Island, Northland and the northern North Island coherent precipitation region have been more active than South Island systems, most likely driven by increased meridional atmospheric circulation associated with La Niña-like and positive SAM-like atmospheric patterns.

6.6 Conclusion

Twenty one ^{14}C dates from the Northland region have been added to the New Zealand fluvial ^{14}C database, filling a geographical gap in the record identified in an earlier analysis. Meta-analysis of the ^{14}C-dated fluvial deposits has produced a revised probability-based record of New Zealand river behaviour during the Holocene. The addition of the Northland ^{14}C dates to the fluvial sedimentary archive has improved the resolution of the river activity record for northern North Island, with six major multi-centennial phases of river activity identified. This study confirms the potential of using targeted field research to assess river activity at the coherent precipitation region scale. Rivers in Northern New Zealand, like North and South Island systems have exhibited sensitivity to short-term and rapid Holocene climate variations. The response of northern New Zealand rivers support the model suggesting river activity in New Zealand is predominantly influenced by atmospheric circulation variability and confirms the value of the fluvial archive for reconstructing past climate in this tectonically stable region.

Chapter 7

Fluvial records of Holocene climate variability and evidence of a 3500–2800 cal. yr BP cold event from northern New Zealand

7.1 General introduction

Chapter 6 presented a revised meta-analysis of the New Zealand fluvial radiocarbon (^{14}C) database. The addition of the Northland ^{14}C dates to the fluvial sedimentary archive has improved the resolution of the river activity record for the northern North Island coherent precipitation region and six significant phases of river activity have been identified for the Holocene. The pattern of river behaviour in northern New Zealand supports the model proposed in Chapter 4, that suggests river activity in New Zealand is predominantly influenced by atmospheric circulation variability. The following Chapter 7 focuses specifically on the fluvial record of Northland, comparing the probability-based record of river activity with a range of regional and global palaeoclimate records.

Chapter 7 is contained within the manuscript: J.M. Richardson, I.C. Fuller, K.A. Holt, N.J. Litchfield, M.G. Macklin: Fluvial records of Holocene climate variability and evidence of a 3500–2800 cal. yr BP cold event from northern New Zealand, which is in review in the journal *The Holocene*. In this chapter, meta-analysis techniques are applied to Holocene ^{14}C-dated fluvial units from Northland to provide a probability-based reconstruction of river

activity (Section 7.6). In section 7.7 the Northland river activity record is compared with published climate proxy records from Northland, elsewhere in New Zealand, and world-wide to establish the drivers of river activity and determine whether or not Northland rivers are in synchrony with global climate change.

7.2 Abstract

A meta-analysis of Holocene ^{14}C-dated fluvial units from Northland provides a probability-based reconstruction of river behaviour for the region. Comparison with a range of palaeoenvironmental records shows that stable climate, which prevailed under conditions of ENSO quiescence during the early to mid Holocene in Northland, promoted catchment stability that is reflected in the region's river systems. A prominent phase of river activity between 3500 and 2800 cal. yr BP coincided with a global Holocene cold event, at a time of enhanced climatic connectivity between the low and high latitudes, and when the major climate modes, El Niño Southern Oscillation (ENSO) and the Southern Annular Mode (SAM), were in phase. River activity in Northland is promoted by meridional atmospheric circulation (promoted under La Niña phases of ENSO and positive phases of the SAM) and occurred when climate was cooler and more seasonal, and at time when catchment vegetation was experiencing more disturbance.

7.3 Introduction

Climate has varied throughout the Holocene and has involved episodes of rapid climate change driven by a variety of factors and feedbacks such as solar variability, volcanic eruptions, melt-water flux, atmospheric and/or oceanic circulation changes and the operation of major climate modes (Bond et al., 2001; Mayewski et al., 2004; Gomez et al., 2011; Wanner et al., 2011). The impacts of these Holocene cold lapses, which are more subdued than the dramatic climatic fluctuations during the last glacial cycle, have been varied and widely reported (e.g., Mayewski et al., 2004; Alloway et al., 2007; Wanner et al., 2011). Perhaps the most influential evidence for Holocene cold events is the quasi-periodic Bond cycle attributed to the penetration of cooler ice-bearing surface water from the Nordic and Labrador Seas into warmer sub-polar waters (Bond et al., 2001). North Atlantic Holocene drift ice records preserve evidence for nine cold periods, possibly induced by solar driven changes in atmospheric and oceanic circulation (Bond et al., 2001).

Climate variability has also influenced glacier dynamics during the Holocene, with glacier advances in response to climate deterioration detected globally (e.g., Zhou et al., 1991;

Kirkbride and Dugmore, 2006; Hall, 2009; Ivy-Ochs et al., 2009; Schaefer et al., 2009; Putnam et al., 2012). Proxy records of temperature and precipitation from a plethora of sources (including, lake and ocean sediments, ice cores and speleothems) have also revealed the patterns and impacts of Holocene climate shifts (e.g., Mayewski et al., 2004; Alloway et al., 2007; Wanner et al., 2011), with many of these shifts correlated with one or more of the Bond cycles. A review of globally distributed palaeoclimate archive data from 30 published papers by Wanner et al. (2011) found that Bond cycles 2 (with a peak in drift ice index at ~ 3000 cal. yr BP) and 5 (with peaks in the drift ice index at ~ 7500 and ~ 8500 cal. yr BP) are the most commonly referred to Holocene climate episodes. Mayewski et al. (2004) also examined palaeoclimate records from across the globe, and although not all sites responded synchronously or with the same magnitude, six major globally extensive periods of rapid climate change (at 9000–8000, 6000–5000, 4200–3800, 3500–2500, 1200–1000, and 600–150 cal. yr BP) involving major changes in atmospheric circulation, cooler poles and tropically aridity, were identified. Present knowledge of Holocene climate variability and its impacts has been predominantly formed using palaeoclimate data from low latitudes and Northern Hemisphere locations (e.g., Mayewski et al., 2004; Wanner et al., 2011). Of the 81 palaeo-temperature and -humidity/precipitation archives examined by Wanner et al. (2011) in their review of Holocene climate, only 12 proxy records were from Southern Hemisphere locations. However, to fully explore the spatiotemporal patterns of Holocene climate variability, more Southern Hemisphere climate proxy records are required (Mayewski et al., 2004). New Zealand, spanning the mid-latitudes and orientated perpendicular to the prevailing circumpolar westerly atmospheric flow, is ideally placed to detect changes in Southern Hemisphere climate (Alloway et al., 2007).

Climate in New Zealand is affected by both polar and subtropical influences, including oscillations and teleconnections associated with the major climate modes, including El Niño-Southern Oscillation (ENSO; Mullan, 1995) and the Southern Annular Mode (SAM; Gong and Wang, 1999; Renwick and Thompson, 2006). A high level of regional climate complexity is created in New Zealand due to the interaction of these climate drivers, the latitudinal span, and the orography of the main axial ranges and mountains (Lorrey et al., 2012). In New Zealand the occurrence of three characteristic synoptic regimes (zonal, trough and blocking) have been identified (Kidson, 2000), and it is these different circulation regimes that are responsible for strongly differentiated regional patterns in temperature and precipitation. Alteration in the circulation regime, involving changes in the frequency or magnitude of the different synoptic types over decadal or longer timescales, produces distinctive spatial patterns detectable in palaeoclimate proxy records (Lorrey et al., 2008): providing information that can be used to reconstruct past circulation processes and

dynamics (Lorrey et al., 2007; 2012). This high level of regional differentiation is also reflected in New Zealand river systems (Richardson et al., 2013), where well-connected catchments respond rapidly to hydro-climatic forcing, without the lags associated with some alternate palaeoclimate archives.

Probability-based analysis of fluvial ^{14}C dates has been widely used in the Northern Hemisphere (Thorndycraft and Benito, 2006a; Hoffmann et al., 2008; Harden et al., 2010; Macklin et al., 2010; Turner et al., 2010), and recently in New Zealand (Macklin et al., 2012a; Richardson et al., 2013), to produce proxy records of hydro-climatic fluctuation at different spatial scales. This meta-analytical approach uses summed probability distributions associated with calibrated ^{14}C dates from fluvial units to produce cumulative probability functions (CPFs) and identify episodes of river activity, flooding or stability in the fluvial record. Interrogation of Northern Hemisphere datasets has revealed a strong underlying climate forcing of accelerated river activity (Thorndycraft and Benito, 2006a; Hoffmann et al., 2008; Harden et al., 2010; Macklin et al., 2010; Turner et al., 2010), and has also identified short-term hydro-climatic change not detected in alternative climate proxy records (e.g., Macklin et al., 2010). A clear anthropogenic signal has been recognised in late Holocene fluvial sedimentary archives, with accelerated floodplain sedimentation a response to catchment land-use changes (e.g., Thorndycraft and Benito, 2006b; Hoffmann et al., 2010; Macklin et al., 2010; Macklin et al., 2012a).

The New Zealand fluvial radiocarbon (^{14}C) database (Macklin et al., 2012a) has provided insights into the operation of the major oscillatory climate modes, El Niño Southern Oscillation (ENSO) and the Southern Annular Mode (SAM), in New Zealand throughout the Holocene (Richardson et al., 2013). Meta-analysis of the New Zealand database has shown that river activity in New Zealand has been driven by atmospheric circulation changes associated with SAM and ENSO, with the spatial and temporal patterns of river activity influenced by the phase relationship and relative dominance of these two major Southern Hemisphere climate modes. River activity in southern New Zealand is driven by enhanced westerly atmospheric circulation (promoted under the negative phase of the SAM), while episodes of river activity in the North Island Holocene fluvial record are a response to enhanced meridional atmospheric circulation (as occurs during La Niña phases of the Southern Oscillation and positive phases of the SAM). These synoptic conditions in northern New Zealand allow for generation of large floods associated with incursion of sub-tropical storms (Richardson et al., 2013). In the New Zealand fluvial record, the human influence on sediment flux and river activity have been restricted to the last ~ 500 years (Richardson et al., 2013).

The catchments of the Northland region of northern New Zealand are, in New Zealand terms, relatively distant from volcanic and tectonic factors that disturb catchments elsewhere in New Zealand, and in relatively close proximity to tropical climate influences (due to the northernmost location). These factors, combined with a short history of human disturbance, mean that in Northland river behaviour is most likely primarily driven by Holocene climate change. Recent reconstruction of the fluvial history at floodplain sites across the Northland region has shown that while valley floor configuration is a major control on floodplain geomorphology (Richardson et al., in review-b), sediment storage patterns within these systems reflect climatically forced changes in sedimentation. In Northland, a phase of floodplain aggradation in the mid to late Holocene occurred in response to climatically driven catchment disturbance and was followed by a phase of incision, prior to refilling in response to late Holocene anthropogenic catchment disturbance.

This paper applies meta-analysis techniques to new and published ^{14}C-dated Holocene fluvial deposits in Northland, located in the northern North Island precipitation region. Using these techniques we develop a probability-based record of Holocene fluvial behaviour for Northland that is compared with independent alternative palaeoclimate proxy records from Northland, elsewhere in New Zealand and globally.

7.4 Regional setting

Northland, the northernmost region of New Zealand, is a narrow peninsula 300 km long located between latitudes 34°S and 37°S, 400–700 km northwest of the active Hikurangi subduction margin between the Australian and Pacific plates (Fig. 7.1). The region is the most tectonically stable area of New Zealand, being the most distant from the Pacific plate boundary (cf. Fig. 7.1) with no known active faults (http://data.gns.cri.nz/af/; Beetham et al., 2004) and accordingly a low level of seismic activity (http://www.geonet.org.nz/; Anderson and Webb, 1994). In contrast to other regions of New Zealand, the topography of Northland is relatively subdued with the highest point being Te Raupua (781 m) located in the Waima Range, northwestern Northland.

The contemporary climate of Northland can be described as mild, humid and moderately windy (Moir et al., 1986), with a mean annual rainfall of 1200 mm in southwestern Northland and 1700 mm in northeastern Northland (climate summary data for the period 1969-1998 from http://www.Metservice.com), with winter season maximums in rainfall. Northland is part of the northern New Zealand coherent precipitation region, as defined by

Mullan (1998) using an analysis of New Zealand precipitation data to identify six homogenous climate regions (Fig. 7.1), which mainly reflects the interaction between the dominant westerly flow and orography of the main axial ranges of New Zealand.

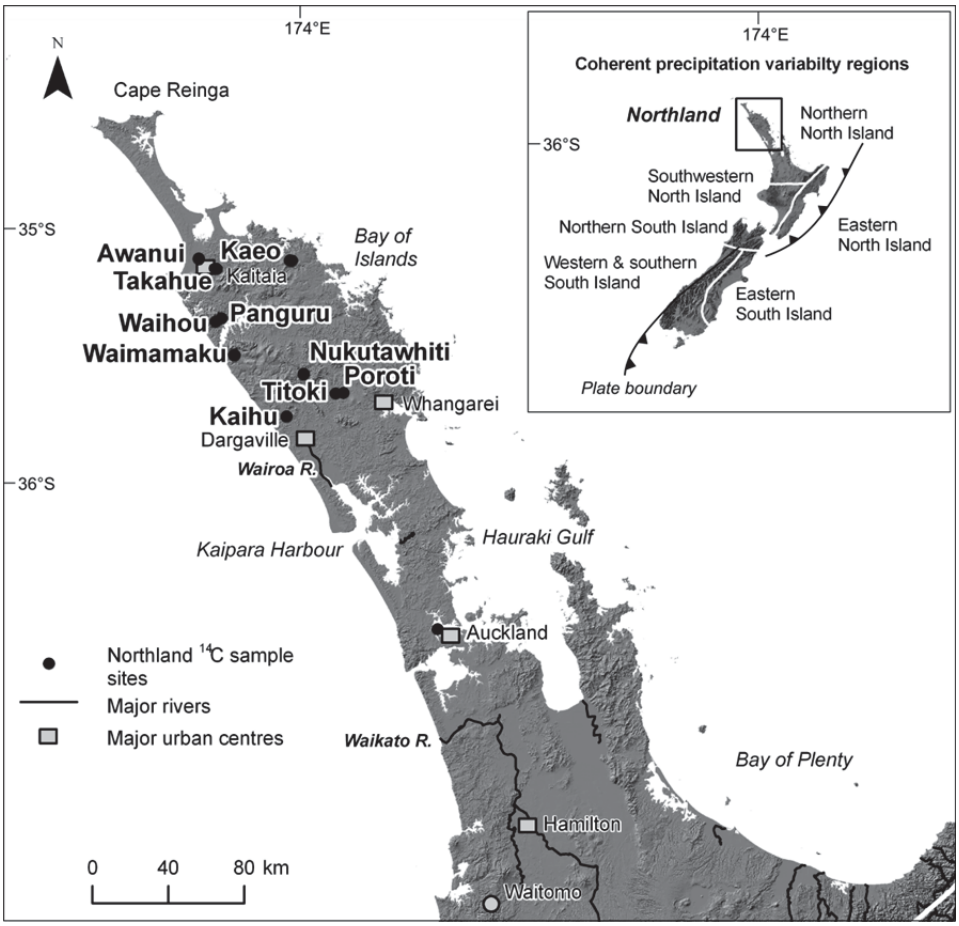

Fig. 7.1. Map showing the location of ^{14}C-dated Holocene fluvial unit sample sites in Northland, and major rivers and urban centres in northern New Zealand. Inset map shows the tectonic setting and six coherent precipitation variability regions (Mullan, 1998) of New Zealand.

In contrast to southern New Zealand, regional pollen records show that Northland remained forested throughout the Last Glacial Coldest Period (LGCP; ~ 28,000–18,000 cal. yr BP as defined by Alloway et al. (2007)). Holocene vegetation in the region was dominated by podocarp conifer-hardwood associations including *Agathis australis* (kauri), until widespread deforestation following Māori and European settlement after ~ 800 cal. yr BP (Prickett, 2002). Pollen records from the Northland region indicate four broad climatic

periods during the Holocene (Richardson et al., in review-b). These comprise: a cooler than present early Holocene (~ 12,000–10,000 cal. yr BP); a more mesic early to mid Holocene (~ 10,000–5000 cal. yr BP); a mid to late Holocene (~ 5000–2000 cal. yr BP) that was subject to more disturbance and climatic deterioration; and a late Holocene (from ~ 2000 cal. yr BP) which showed some evidence of climate amelioration prior to anthropogenic impact.

7.5 Methodology

7.5.1 Sedimentology and radiocarbon chronology

Ten fluvial sites from a range of catchment sizes and different valley confinement settings were selected from across the Northland region (Fig. 7.1). Sediment cores were collected using a percussion coring system, and along with suitable cutbank exposures, were logged and the sediment facies described. Details of the majority of these sites are contained within Richardson et al. (in review-b).

Organic material was sampled for ^{14}C-dating from sedimentary units deposited under conditions of fluvial activity and flooding (including fluvial gravel units, interbedded sands and silts and flood debris). Radiocarbon age determinations were carried out by the University of Waikato Radiocarbon Dating Laboratory (New Zealand) and Keck Radiocarbon Dating Laboratory (University of California, USA). Results were reported as percent modern carbon following Stuvier and Pollack (1977), and based on the Libby half-life of 5568 yr with correction for isotopic fractionation applied. Radiocarbon ages less than 11,000 BP were calibrated using OxCal v4.1 (Bronk Ramsey, 2009) and the Southern Hemisphere calibration dataset SHCal04 (McCormac et al., 2004). Determinations older than 11,000 BP were calibrated using the international calibration dataset IntCal04 (Reimer et al., 2004). Twenty ^{14}C-dated fluvial units from the Northland region were added to a New Zealand fluvial ^{14}C database containing 401 ^{14}C fluvial ages (Macklin et al., 2012a; Richardson et al., 2013). The database was compiled from published papers, unpublished reports and data from GNS Science using protocols described by Johnstone et al. (2006). Entries recorded in the database include information on the ^{14}C samples and locations, depositional environment and sedimentary context.

7.5.2 Radiocarbon data analysis

Following an approach developed by Macklin et al. (2010; 2012a), individual probabilities for the calibrated ^{14}C fluvial ages representing river activity in Northland were summed

using OxCal version 4.1 (Bronk Ramsey, 1995, 2001, 2009) to produce cumulative probability function (CPF) plots. Peaks in the CPF, created by the calibration curve and biases toward younger fluvial units due to preservation and sampling, were removed by dividing the Northland river activity subset by the entire New Zealand fluvial dataset to produce a relative probability plot. The curves were then normalised by dividing each value in the probability curve by the highest probability in the dataset.

Relative probabilities above the mean relative probability corresponding with a minimum of three dates within a 200 year period have been used to identify phases of flooding, river activity or stability in the New Zealand record (Macklin et al., 2012a; Richardson et al., 2013). This criterion could not be adhered to in this analysis due to the limited number of ^{14}C dates from Northland. In this case we have accepted the necessity for a lower level of confidence and have identified centennial-scale episodes of river activity where probabilities exceed the mean relative probability and are associated with a minimum of three ^{14}C dates within a 300 year period per activity episode.

Table 7.1 lists the details of the fluvial ^{14}C data from 11 sites in the Northland region. Twenty one fluvial ^{14}C dates representing river activity were obtained from 11 catchments ranging in area from the 14 km^2 (Panguru catchment in northwest Northland) to the 545 km^2 Awanui catchment located in the north of the region (Fig. 7.1). Of the 21 fluvial ^{14}C dates, 16 were recovered from floodplain sediments (as determined by the sedimentology and geomorphology), with the remaining obtained from fluvial units deposited in palaeochannels. Just over half the ^{14}C data came from wood samples with the remaining provided by determinations from silt organics and a single charcoal sample (Table 7.1).

7.6 Results

The raw CPF plots for the Northland fluvial 'activity' ^{14}C dates are shown in Fig. 7.2. There is an absence of dates from the early Holocene and gaps in the record, until an increase in probabilities after ~ 800 cal. yr BP. The small amount of data from the early Holocene may be due to preservation factors (cf. Lewin and Macklin, 2003) and the reduction in probabilities in the last ~ 200 years can be attributed to ^{14}C-dating limitations. Relative CPF plots of 'activity' ^{14}C dates for Northland show a number of peaks in the relative probability of river activity throughout the Holocene (Fig. 7.3). Three episodes, where probability peaks have been produced by at least three fluvial ^{14}C dates representing deposition within a 300 year timeframe of river activity, can be identified (3500–2800 cal. yr BP, 800–600 cal. yr BP and 500–300 cal. yr BP).

Table 7.1

Summary of sample location, sample details, depositional environment and radiocarbon data.

Site	Sample code	Data-base ID	Lab. No.	Sample material	Depositional environment	Sample depth (m)	Uncal-ibrated date (BP)	Calibrated date (cal. yr BP 2σ confidence)	Measure-ment
Awanui Catchment									
Awanui	Awan1b	416	Wk-28764	Silt organics	Palaeochannel	1.5	3299 ± 35	3570–3380	AMS
Awanui	Awan 1a	417	Wk-28765	Silt organics	Palaeochannel	0.74	2962 ± 55	3240–2880	Radio-metric
Upper Awanui Catchment – Takahue River									
Takahue	Taka2e	410	Wk-30434	Wood	Floodplain	4.62	5828 ± 25	6660–6490	AMS
Takahue	Taka2d	411	Wk-30435	Wood	Floodplain	3.69	2033 ± 25	2000–1870	AMS
Takahue	Taka3g	425	Wk-30764	Wood	Palaeochannel	3.58	2770 ± 25	2870–2760	AMS
Takahue	Taka3d	426	Wk-31571	Silt organics	Palaeochannel	2.31	1381 ± 25	1300–1180	AMS
Kaeo Catchment									
Kaeo	Kaeo1b	423	Wk-27971	Silt organics	Floodplain	4.85	691 ± 35	660–560	AMS
Kaeo	Kaeo4a	416	Wk-30440	Wood	Floodplain	4.02	4769 ± 25	5580–5320	AMS
Kaeo	Kaeo4c	415	Wk-30443	Silt organics	Floodplain	4.6	6820 ± 26	7680–7570	AMS
Kaihu Catchment									
Kaihu	Kaih2e	412	Wk-30436	Wood	Floodplain	2.3	3109 ± 25	3360–3170	AMS
Kaihu	Kaih2f	428	Wk-31574	Wood	Floodplain	3.6	3933 ± 28	4420–4160	AMS
Mangakahia Catchment									
Nukutawhiti	Nuku2a	429	Wk-31576	Silt organics	Floodplain	1.47	3287 ± 30	3560–3380	AMS
Nukutawhiti	Mang2g	420	Wk-27966	Wood	Palaeochannel	3.05	291 ± 35	450–150	AMS
Titoki	Mang1a	421	Wk-27967	Silt organics	Floodplain	7.4	850 ± 39	790–670	Radio-metric
Panguru Catchment – Te Rapa Stream									
Panguru	Pang2a	418	Wk-27963	Charcoal	Floodplain	2.3	353 ± 30	460–310	AMS
Te Atatu Peninsula Catchment – Whau River									
Whau River		351	NZ-497	Wood	Floodplain	1.0		620–320	Radio-metric
Waihou Catchment									
Waihou	Waih3a	419	Wk-27964	Wood	Floodplain	5.5	5977 ± 47	6890–6640	Radio-metric
Waimamaku Catchment									
Waimamaku	Waim4c	413	Wk-30438	Wood	Floodplain	2.56	780 ± 25	730–650	AMS
Waimamaku	Waim9a	430	Wk-31577	Wood	Floodplain	3.38	2947 ± 27	3160–2890	AMS
Waimamaku	Waim1c	422	Wk-27968	Wood	Floodplain	3.3	1138 ± 41	1070–920	Radio-metric
Wairua Catchment									
Wairua	Poro4a	424	Wk-30763	Silt organics	Palaeochannel	1.72	10,045 ± 31	10,110–9980	Radio-metric

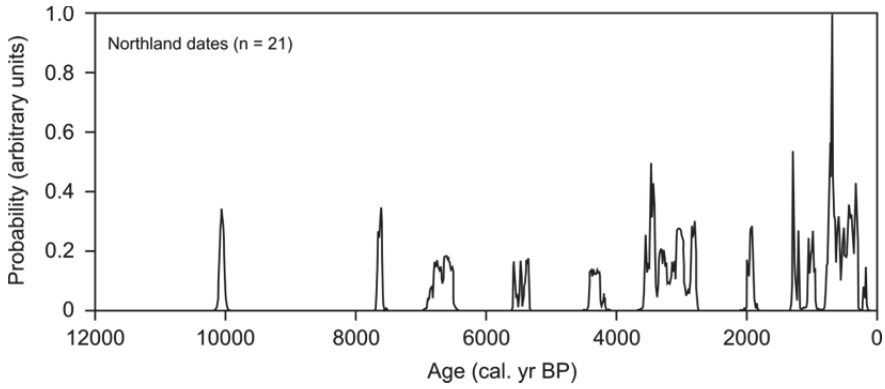

Fig. 7.2. Cumulative probability function (CPF) plot of ^{14}C-dated fluvial units in Northland.

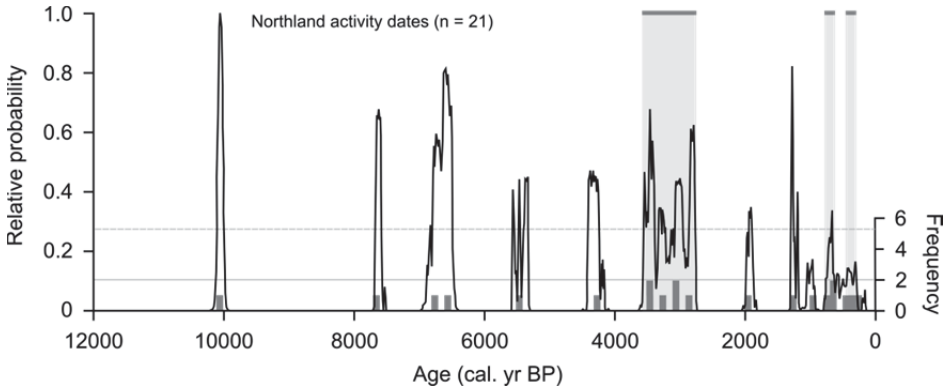

Fig. 7.3. Relative CPF plot of 'activity' ^{14}C dates plotted with frequency of dates per 100 years from Northland fluvial units. Horizontal lines indicate the mean (solid grey line) and one standard deviation above and below the mean (dashed grey line). Horizontal grey bars at the top of each plot indicate major episodes of river activity.

7.7 Discussion

The Northland Holocene river activity record offers a unique opportunity to provide insights into underlying climate forcing on river behaviour, with small well-connected responsive catchments that have been unaffected by tectonic and volcanic disturbances, and where anthropogenic impacts have been restricted to the last ~ 800 years (Prickett, 2002). Below

we compare the Northland records to published climate proxy records from Northland, elsewhere in New Zealand, and world-wide.

7.7.1 Early to mid Holocene

As Fig. 7.2 data show there is a low probability of significant river activity prior to 7000 cal. yr BP in the Northland region, with only two fluvial 'activity' ^{14}C dates reported for this time period. This is in contrast to the North Island record as a whole (Richardson et al., 2013). The absence of early to mid Holocene ^{14}C dates could be due to the preservation bias toward younger sediments in the alluvial domain, as fluvial sedimentation is episodic and older sediments are more likely to be removed or reworked (Lewin et al., 2005). However, palaeoclimate records from far northern New Zealand suggest relatively subdued climatic changes during this period, which may have also had an impact on sediment flux and discharge, leading to stable Northland river dynamics during the early to mid Holocene (~ 12,000–7000 cal. yr BP).

Palaeovegetation records from across the Northland region indicate an early to mid Holocene climate (~ 10,000–5000 cal. yr BP) which is stable, warmer and moister than at any other time during the Holocene (Fig. 7.4). The evidence from Northland pollen records suggests that warming in Northland occurred later than the general New Zealand pattern of ~ 11600–6500 cal. yr BP warming (Alloway et al., 2007). Pollen analysis from a number of Northland sites describe a trend of early Holocene replacement of cooler preference *Nothofagus* (beech)-podocarp-hardwood associations with the early to mid Holocene (~ 10,000–5000 cal. yr BP) expansion of *Agathis australis* (kauri)-podocarp-hardwood forest (Dodson et al., 1988; Elliot, 1998; Elliot et al., 2005). Pollen from swamp deposits near Dargaville showed little variation in the composition of the regional podocarp-broadleaf vegetation under stable climate conditions between 11,000 and 6800 cal. yr BP (D'Costa et al., 2009), and alternate palaeoclimate records from northern New Zealand also support a warmer moister early to mid Holocene, including high organic productivity in the maar lake Pupuke between 9500 and 7000 cal. yr BP (Horrocks et al., 2005). Speleothem records of palaeoprecipitation and palaeotemperature from Waitomo (Figs 7.1 and 7.4) indicate a warmer moister early to mid Holocene climate with a warm event peak at 10,800 cal. yr BP (Fig. 7.4) (Williams et al., 2010).

New Zealand climate variability is strongly influenced by the operation of the oscillatory climate modes; the tropical ENSO (e.g., Garreaud and Battisti, 1999) and the extratropical SAM (e.g., Gillett et al., 2006). Richardson et al. 92013) found that the key driver of New

Zealand river activity as a whole during the Holocene was variability in atmospheric circulation associated with ENSO and SAM, the phase relationship between the two modes, and the relative influence of the two modes which shows latitudinal gradation (Ummenhofer and England, 2007). In northern New Zealand the climate is more influenced by the tropical Pacific region and ENSO (Ummenhofer and England, 2007), and in northern New Zealand episodes of river activity are promoted by La Niña-like and positive SAM-like atmospheric circulation (Richardson et al., 2013). The absence of river activity in the Northland record prior to ~ 7000 cal. yr BP corresponds to a period when ENSO was weak or non-operational (Sandweiss et al., 2001; Moy et al., 2002), or subject to reduced precipitation teleconnections between distal regions and the tropical Pacific (Shulmeister et al., 2006). It is likely that the warm/moist stable climate that prevailed under conditions of ENSO quiescence during the early to mid Holocene (~ 10,000–5000 cal. yr BP) in Northland, promoted catchment stability which is reflected in the river systems, with an absence of valley floor filling (Richardson et al., in review-b) and limited evidence for floodplain sedimentation and river activity during this period.

7.7.2 Mid to late Holocene

In contrast to the stability of the early to mid Holocene (~ 10,000–5000 cal. yr BP), the mid to late Holocene (~ 5000–2000 cal. yr BP) involved ENSO intensification from ~ 7000 cal. yr BP (Moy et al., 2002) and the onset of active ENSO cyclicity (Donders et al., 2008). In Northland this period is characterised by an extended period of region-wide floodplain alluviation (Fig. 7.4) and floodplain terrace development (cutting and refilling of the valley floor) in partly confined valley floor settings in Northland (Richardson et al., in review-b). Three episodes of river activity have been identified in the Northland fluvial record, the most significant phase occurring between 3500 and 2800 cal. yr BP.

The majority of Northland palaeovegetation records detect some degree of climate change during the mid to late Holocene (Dodson et al., 1988; Kershaw and Strickland, 1988; Elliot et al., 1995; Striewski et al., 1996; Elliot et al., 1997; Elliot, 1998; Elliot et al., 1998; Elliot et al., 2005). Pollen evidence from swamp deposits in northwest Northland indicate increased seasonality, summer drought, wetter cooler winters and increased cyclonic activity, with declines in frost intolerant taxa and increases in the abundance of hardy podocarps between ~ 5000 and 2500 cal. yr BP (Fig. 7.4) (Elliot, 1998; Elliot et al., 2005). Pollen records from northern Northland show evidence of forest disturbance and seral trends after ~ 4000 cal. yr BP (Striewski et al., 1996), and in eastern Northland, climate after ~ 4000 cal. yr BP was considered cooler and drier with more intense cyclonic activity before climate

amelioration from ~ 2000 to 1600 cal. yr BP (Elliot et al., 1997). In eastern Northland palaeovegetation records from two sites indicate major change around ~ 3500 cal. yr BP, with signs of repeated forest disturbance and erosion, summer drought and cooling (Kershaw and Strickland, 1988; Elliot et al., 1998). Increase in the frequency of drought conditions was suggested as the cause of a decline in kauri in far northern New Zealand after ~ 3000 cal. yr BP (Dodson et al., 1988) and swamp deposits in western Northland show a pattern of kauri expansion and decline due to fluctuation in substrate wetness after ~ 3500 cal. yr BP (D'Costa et al., 2009). Other major changes detected in Northland records that correlate with the major phase of river activity (3500–2800 cal. yr BP) include increases in effective precipitation detected in swamp deposits near Whangarei, at 3400 cal. yr BP (Kershaw and Strickland, 1988) and around 3000–2000 years ago (Newnham, 1992).

The palaeoclimate proxy records from the Northland region suggest that the episode of river activity at 3500–2800 cal. yr BP was a climatically forced response to ENSO intensification, with evidence for increased seasonality and disturbance in the vegetation record around this time (Fig. 7.4). In addition, the phase relationship between SAM and ENSO may have also been playing a role in influencing river activity and amplifying ENSO teleconnections between the tropical Pacific and higher Southern Hemisphere latitudes. The cluster of fluvial ^{14}C dates and a peak in relative probability in the Northland river activity record between 3500 and 2800 cal. yr BP coincided with the general trend of a more disturbed and cooler mid to late Holocene climate regime, increases in El Niño frequency after ~ 3200–2800 yr BP (Sandweiss et al., 2001) and increased impacts in teleconnected regions from around 3000 cal. yr BP (Donders et al., 2008).

Storm records reconstructed from lake sediments in Ecuador and eastern North Island, New Zealand, indicate that between ~ 5000 and 2000 cal. yr BP storm frequencies were in phase (Gomez et al., 2011). This occurred at a time when tropical Pacific sea surface temperatures and central Antarctic surface temperatures signalled connectivity between the low and high latitudes and correlation between the SAM and ENSO climate modes (Gomez et al., 2011). The episode of Northland river activity coincides with a synchronised peak in storm activity at Laguna Pallcacocha and Lake Tutira (from 3300 to 3100 cal. yr BP), under La Niña-like conditions and during the positive phase of the SAM (Gomez et al., 2011). This reinforces the assertion that river activity in northern New Zealand is associated with a predominance of moisture bearing northeasterly atmospheric flow under a blocking synoptic regime (promoted by La Niña phases of the Southern Oscillation and positive phases of the SAM) (Richardson et al., 2013).

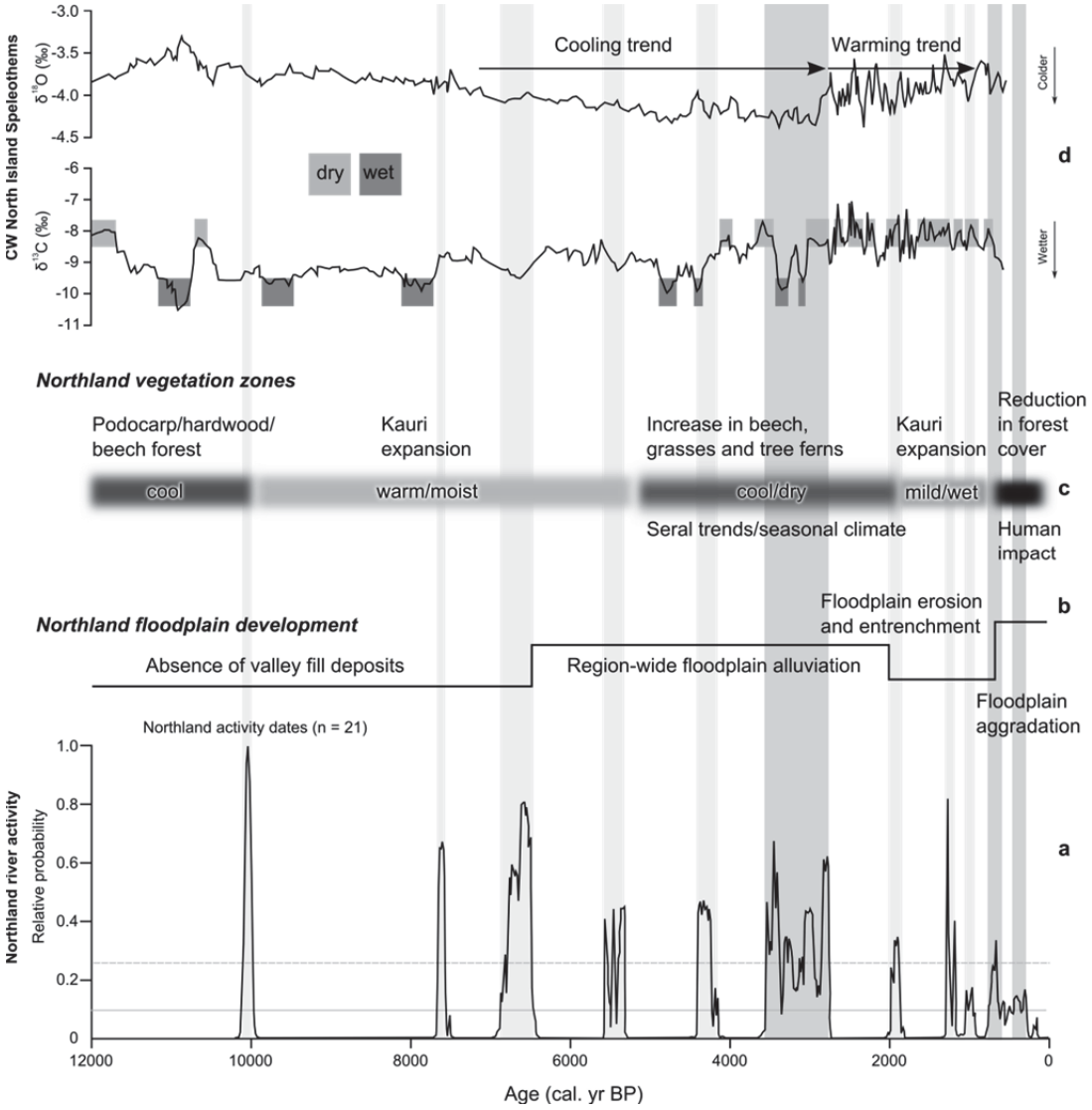

Fig. 7.4. Schematic of regional palaeoclimate, palaeovegetation and Northland river behaviour for the Holocene. (a) Relative CPF plot of Holocene river activity in Northland, New Zealand, based on analysis of ^{14}C-dated Holocene fluvial units. Vertical grey bars highlight episodes of river activity and vertical dark grey bars highlight the most significant episodes. (b) Summary of Northland Holocene floodplain development (Richardson et al., in review-b). (c) Northland palaeovegetation zones. (d) Temperature and precipitation inferred from composite curves of speleothem δ^{18}O and δ^{13}C for the Waitomo district of central-west North Island (Williams et al., 2010).

Circulation changes associated with the major climate modes influence rainfall patterns and the incidence of cyclonic activity in New Zealand, which in turn have an impact on

vegetation and sediment flux, and ultimately river system dynamics. It is most likely that the 3500–2800 cal. yr BP phase of river activity in the Northland record was a response to climatically driven catchment perturbation with potential amplification due to the unique nature of the Northland vegetation. A major component of the Holocene pre-settlement vegetation in far northern New Zealand was *Agathis australis* (kauri), the long-lived (> 600 years) emergent canopy tree which has a preference for a warm and moist climate (Ogden et al., 1992). Stand regeneration of kauri is episodic in nature and depends on large-scale disturbance (Ogden et al., 1992), creating a vulnerability toward cohort collapse if growth conditions deteriorate or through storm wind throw, potentially leading to large-scale catchment destabilisation.

Despite the fact that New Zealand has a high degree of regional climate variability (Ummenhofer and England, 2007), alternative palaeoclimate proxies and river activity records from other regions of New Zealand suggest that the climatic perturbation detected in the Northland river activity record at 3500–2800 cal. yr BP was not restricted to far northern New Zealand. Stable isotope speleothem data from Waitomo (Figs. 7.1 and 7.4 in central-west North Island (CWNI) provide a proxy record of Holocene palaeoprecipitation and palaeotemperature for the northern New Zealand coherent precipitation region (Williams et al., 2010). Northland river activity at 3500–2800 cal. yr BP corresponds to a remarkably cool phase (3400–2900 cal. yr BP) at the culmination of a gradual decline in temperature from the mid Holocene (Fig. 7.4). Speleothem records from northwestern South Island (NWSI) also a show negative excursion in $\delta^{18}O$ values concurrent with a glacier advance (mean moraine age of ~ 3200 years ago) in the Southern Alps (Schaefer et al., 2009; Williams et al., 2010). Peaks in $\delta^{13}C$ values at 3400 yr BP in both the CWNI and NWSI records suggest that the beginning of the phase of river activity in Northland occurred when these regions were dry as well as cool, although the CWNI speleothem data show considerable variation in precipitation during this time (Williams et al., 2010).

There is also evidence that this late Holocene cool event had a widespread impact on river systems in other regions of New Zealand, with river activity identified in five out of the six homogenous precipitation regions at ~ 3200 cal. yr BP (Richardson et al., 2013). Probability-based records of river activity for northern North Island, southwestern North Island, eastern North Island, northern South Island and eastern South Island (Richardson et al., 2013) show that in these climate regions rivers were also undergoing phases of river activity involving floodplain sedimentation at the same time as Northland systems. The only region that did not experience a significant phase of river activity during this time was the western and southern South Island climate region. Probability-based records of Holocene

river activity suggest that in the South Island increased river activity is a response to enhanced westerly atmospheric circulation associated with a predominance of trough regime synoptic type (negative SAM-like circulation) (Richardson et al., 2013). In the North Island episodes of river activity are driven by increased meridional atmospheric circulation associated with blocking regime synoptic conditions (La Niña-like and positive SAM-like circulation) (Richardson et al., 2013). The extent of river activity in New Zealand centred on the period ~ 3400–3000 cal. yr BP overrode a strong tendency toward an out-of-phase relationship between river activity in northern and southern regions (Richardson et al., 2013) and suggests that climate at the time was being more influenced by subtropical atmospheric influences.

Marked alteration in fluvial processes around the mid Holocene was also detected in eastern North Island floodplain, continental-shelf and continental-slope sediment records (Gomez et al., 2004). These sediment records preserve a textural change at ~ 4000 cal. yr BP, representing a shift in the sediment production process, from fluvial incision to a predominance of landslide derived material as a result of increased storms (Gomez et al., 2004). This mid Holocene climate change signal was interpreted as an intensification of atmospheric circulation and ENSO activity in the region (Gomez et al., 2004).

The episode of river activity detected in New Zealand and Northland records between 3500 and 2800 cal. yr BP also correlates with the well documented late Holocene cold event, one of six prominent cold periods, recognised in a number of palaeo-environmental records from around the globe (Wanner et al., 2011). The mechanism behind these Holocene cold relapses is thought to involve decreases in Boreal summer insolation and other processes, including volcanic eruptions, solar activity, melt-water flux and thermohaline circulation (Wanner et al., 2011). The Holocene cold event from 3300 to 2500 cal. yr BP (Wanner et al., 2011) and dry period (centred on ~ 3100 cal. yr BP) occurred during a time when summer insolation was increasing in the Southern hemisphere above that of the Northern Hemisphere (from ~ 4200 cal. yr BP to present). The cold relapse at 3300 to 2500 cal. yr BP exhibits the closest correlation with a Bond cycle, event 2 with a peak at ~ 3000 yr BP (Bond et al., 2001). Mayewski et al. (2004) also identified a global-scale rapid climate change event at 3500–2500 cal. yr BP, characterised by a pattern of cooler poles and tropical aridity, most likely forced by solar variability and changes in orbital insolation. This suggests that the Holocene event detected in the New Zealand river activity record and the Northland record between 3500 and 2800 cal. yr BP was globally extensive. It is therefore reasonable to assert that the phase of river activity and catchment destabilisation in Northland occurred in response to a solar forced global cold event during a period of rapid climate change.

7.7.3 Post-800 years

A further two probability based episodes of river activity (underlain by at least three fluvial 'activity' ^{14}C dates) are identified in the Northland record, at 800–600 cal. yr BP and 500–300 cal. yr BP (Figs. 7.3 and 7.4). These episodes occur during a period when anthropogenic impacts were likely to have played a major role in driving river dynamics in New Zealand. In Northland, floodplains have rapidly aggraded within the last ~ 1000 years (Richardson et al., in review-b) and sedimentation rates across New Zealand have show dramatic increases in the last ~ 500 years in response to widespread catchment disturbance (Page et al., 2000; Glade, 2003; Gomez et al., 2007; Kettner et al., 2007; Jones and Preston, 2012; Richardson et al., 2013). The increased sediment flux associated with widespread post-settlement deforestation has had a major impact on river dynamics, masking river response to any climate changes that may have occurred in the last few hundred years.

7.8 Conclusions

A probability based record of river behaviour in Northland, New Zealand, has been produced through the meta-analysis of Holocene ^{14}C-dated fluvial units and has revealed three significant phases of river activity at 3500–2800, 800–600 and 500–300 cal. yr BP. The record shows that river systems in the region have responded particularly strongly to a major global Holocene climatic perturbation centered at ~ 3000 cal. yr BP, and coincident with Bond cycle 2. It is likely that the warm/moist stable climate that prevailed during the early to mid Holocene in Northland promoted catchment stability which is reflected in the river systems, with an absence of valley floor filling and river activity. The phase of river activity at 3500–2800 cal. yr BP occurred in response to a globally extensive Holocene cold event at a time of enhanced connectivity between the low and high latitudes, correlation between the SAM and ENSO climate modes and ENSO intensification. In Northland, river activity is most likely driven by increased meridional circulation which brings a predominance of moist northeasterly atmospheric flow promoted by La Niña conditions and positive phases of the SAM. Evidence for increased seasonality and disturbance in the vegetation record coinciding with a significant phase of river activity suggests enhanced sediment supply linked with catchment disturbance, potentially involving widespread deforestation during storms in kauri dominated forests, has driven river activity in the region. Reconstruction of the Holocene fluvial record in Northland demonstrates the potential of using fluvial sedimentary archives to investigate Holocene climate dynamics.

Acknowledgements

This research was funded by a Tertiary Education Commission Top Achiever Doctoral Scholarship awarded to JR. Radiocarbon dating was supported by the Massey University Research Fund (to ICF). NJL's contribution was funded by PGSF Contract CO5X0705. The authors would like to thank the landowners for permitting access to the study sites and David Feek for his assistance in the field.

Chapter 8

Post-settlement fluvial response in Northland, New Zealand

8.1 General introduction

Chapter 7 presented a probability-based record of Holocene river behaviour in Northland, New Zealand, produced through the meta-analysis of ^{14}C-dated fluvial units from the region. Three significant phases of river activity at 3500–2800, 800–600 and 500–300 cal. yr BP were identified, with the earliest phase of enhanced river activity corresponding to a major global Holocene climatic perturbation and occurring during a time of enhanced seasonality and vegetation disturbance as detected in local palaeovegetation records. Phases of river activity within the last 1000 years are within the time-frame of human influence in New Zealand, and occurring when anthropogenic impacts were likely to have played major role in driving river dynamics. The following Chapter 8 focuses on reconstruction of the fluvial history and pre- and post-settlement alluviation at a site on the Kaeo River in eastern Northland.

Chapter 8 is contained within the manuscript: J.M. Richardson, I.C. Fuller, K.A. Holt, N.J. Litchfield, M.G. Macklin: Post-settlement fluvial response in Northland, New Zealand, which is in review in the journal *Catena*. In this chapter LiDAR data, sedimentology, ^{14}C chronology, XRF analysis and GPR techniques are used to examine pre- and post-settlement alluviation of the Kaeo River, where rapid rates of post-settlement floodplain aggradation have created considerable contemporary flooding issues. In Section 4 the geomorphology, stratigraphy, sedimentology and geochronology for the Kaeo site is examined and presented.

Section 5 outlines floodplain development, pre- and post-settlement sedimentation rates and anthropogenic impacts in this part of the Kaeo river valley.

8.2 Abstract

Many river systems, within New Zealand and globally, have experienced rapid acceleration in floodplain sedimentation in response to anthropogenic catchment disturbance, creating significant issues (i.e., flooding and water quality). Reconstruction of past river responses to environmental and anthropogenic-driven changes in sedimentation and erosion can provide valuable insights into these river dynamics. This research uses LiDAR data, sedimentology, radiocarbon chronology, XRF analysis and GPR to examine pre- and post-settlement alluviation of the Kaeo River and floodplain sedimentation in Northland, New Zealand. In Kaeo, rapid rates of post-settlement floodplain aggradation, equating to over 4 m of interbedded sand and silt alluvium in a confined valley setting, have created considerable contemporary flooding issues. Radiocarbon dates indicate that terrestrially sourced sedimentation commenced at 7680–7570 cal. yr BP, and continued at an average rate of < 4 mm yr^{-1}. Under conditions of limited accommodation space, the Holocene floodplain has accumulated at a faster average rate (~ 7.2 mm yr^{-1}) in the last several hundred years in response to anthropogenic catchment disturbance following Māori and European settlement. This response mirrors the general trend for Northland floodplains, which have seen a dramatic increase in the rate of floodplain accumulation in the last ~ 500 years. At the Kaeo site, floodplain aggradation associated with European deforestation has undergone a more than tenfold (from 0.7 to 42.2 mm yr^{-1}) increase above pre-human influenced sedimentation rates, producing a greater impact on floodplain morphology than any other environmental change in the last ~ 7500 years. These results have implications for future flood mitigation and land-use planning decisions in the area.

8.3 Introduction

Episodes of enhanced geomorphic activity in response to anthropogenic disturbance have been widely reported, (e.g., Passmore and Macklin, 1994; Schmidtchen and Bork, 2003; Foulds and Macklin, 2006). In some cases floodplain sedimentation rates have accelerated far beyond those rates induced by natural environmental changes such as climatic forcing (e.g., Brooks and Brierley, 1997; Knox, 2006). It is clear that human activities can have a major impact on river system dynamics, both directly (i.e., river engineering) and indirectly through human induced deforestation and land-use changes (e.g., Brierley and Fryirs, 2005; Syvitski et al., 2005; Gregory, 2006; Walling, 2006; Syvitski and Kettner, 2011). However,

the complexity of the fluvial system means that it is often not possible to differentiate between the relative influence of external drivers on runoff and sediment flux, with factors such as catchment sensitivity and catchment physiography also moderating catchment responses to environmental change. Despite this complexity, interrogation of large fluvial radiocarbon (^{14}C) datasets has proved to be valuable in terms of isolating the temporal and spatial patterns of climate change and anthropogenic impacts on fluvial systems (e.g., Starkel et al., 2006; Hoffmann et al., 2008; Harden et al., 2010; Macklin et al., 2010; Macklin et al., 2012a; Richardson et al., 2013).

In the British alluvial record a transition in river behaviour at ~ 4400 cal. yr BP, expressed as an increase in channel and floodplain sedimentation, has been related to widespread anthropogenic deforestation (Macklin et al., 2010). Also an acceleration in overbank sedimentation, occurring at much the same time in both Irish and British lowland and upland catchments at ~ 1000 cal. yr BP, is inferred to have occurred in response to advances in agricultural technology in the middle ages (Macklin et al., 2010; Turner et al., 2010). In British floodplains, anthropogenically driven increased soil erosion has resulted in the aggradation of mineralogically and lithologically distinct fine-grained sediments (e.g., Macklin and Lewin, 1986; Passmore and Macklin, 1994). These sediments have covered and buried more complex topography created by older Holocene channel and floodplain deposits, in some cases in a matter of only a few hundred years (e.g., Jones et al., 2010a). Other European river systems have also exhibited similar tendencies toward increased phases of floodplain aggradation in response to anthropogenic disturbance related to agricultural expansion and deforestation (e.g., Starkel et al., 2006; Thorndycraft and Benito, 2006b; Hoffmann et al., 2008).

In regions with a shorter history of anthropogenic landscape change, there is perhaps even more potential for analysing the cause and effect of anthropogenic activity on catchment dynamics. Research from regions with European colonial settlement restricted to the last few hundred years (e.g., Cohen, 2003; Knox, 2006; Damm and Hagedorn, 2010) show that there have been major and rapid human-induced impacts on river systems. The nature of river response, i.e., valley floor alluviation or channel incision, is determined largely by factors such as channel-hillslope connectivity, river type and valley confinement (e.g., Marutani et al., 1999; Fryirs and Brierley, 2001). The patterns of geomorphic response to European settlement vary from catchment to catchment, reflecting the ability of the fluvial system to source and transfer sediment. In some cases, variation in sediment supply and runoff, associated with changes in land use, settlement patterns and/or land conservation practises,

is characterised by different temporal phases of geomorphic adjustment (e.g., Cohen, 2003; Damm and Hagedorn, 2010).

In New Zealand, anthropogenic land-use changes are restricted to the last ~ 800 years, with the settlement of New Zealand occurring in two phases, first by Polynesians immigrants, and then followed by European colonisation within the last 200 years. Although contentious, the date of first settlement by Polynesians is thought to have occurred ~ 800 cal. yr BP (Prickett, 2002; Sutton et al., 2008), with dates from seeds gnawed by the introduced Pacific rat indicating a slightly later date of Polynesian arrival from ~ 670 cal. yr BP (Wilmshurst et al., 2008). Analysis of New Zealand ^{14}C-dated fluvial units suggests rapid acceleration in floodplain sedimentation after ~ 500 cal. yr BP, following commencement of anthropogenic deforestation (Richardson et al., 2013).

A review of North Island river behaviour by Grant (1985) identified eight major episodes of alluvial erosion and sedimentation in the last 1800 years, five of which occurred within the time-frame of human influence in New Zealand. The amount of floodplain alluviation was found to have varied considerably between sites, ranging from less than 3 m up to 14 m (Grant, 1985). Although there was local evidence that vegetation damage by fire increased sedimentation, there was no unequivocal evidence that disturbance by burning (anthropogenic or natural) had a broad-scale impact on erosion and sedimentation, lending support to the argument that climate was the primary control while vegetation damage only increased sediment availability (Grant, 1985). Increased storm frequency in response to variations in atmospheric circulation was postulated as the major mechanism influencing phases of erosion and alluvial sedimentation in New Zealand during the late Holocene (Grant, 1985).

Further insights to the impacts that both natural events and human induced deforestation have had on sediment flux and drainage basin processes in New Zealand are provided by research undertaken in the Waipaoa sedimentary system. The Waipaoa catchment is located in the actively uplifting eastern North Island, with regional uplift rates in the order of 0.5–1.1 mm yr^{-1} (Berryman et al., 2000). This active tectonic setting, combined with catchment geology and structure predisposed to landslides, has resulted in high rates of geomorphic activity and naturally high sediment yields (Gomez et al., 1999; Orpin, 2004; Jones and Preston, 2012). Catchment instability has been exacerbated by removal of the indigenous forest cover, initially to a limited extent by Polynesian settlement at ~ 650 cal. yr BP, and then more extensively with European settlement and the conversion of forest to pasture from the 1930's (Wilmshurst et al., 1999; Orpin, 2004; Jones and Preston, 2012). The geomorphic

impact of increased sediment flux on some sections of the Waipaoa River floodplain has been vertical accretion at an average rate (post-1850 AD) of ~ 60 mm yr^{-1}, although sedimentation rates resulting from individual floods can be several times higher than time-averaged rates (Gomez et al., 1999). Floodplain storage represented 5% of the suspended sediment load measured for an 11 year period (1979–1990) equating to 0.2–0.8 m of floodplain aggradation (Gomez et al., 1999). Terrigenous sediment accumulation on the continental shelf adjacent to the Waipaoa system suggests post-European colonisation increases in sediment yield in the order of four to five times greater than pre-settlement deposition rates (Foster and Carter, 1997). Modelled outputs of suspended sediment discharge for the Waipaoa River system have calculated increases of 140% after Polynesian arrival and 350% following European settlement (Kettner et al., 2007). These highlight the impact that anthropogenically-enhanced sediment delivery can have on the patterns and rates of sediment storage, with the conversion of forest to pasture effectively lowering the triggering threshold for slope instability and subsequent sediment conveyance to the stream system (Hicks et al., 2000; Jones and Preston, 2012).

Unlike the dynamic and large-scale Waipaoa catchment, catchments in the Northland region of New Zealand are situated relatively remotely (in New Zealand terms) from tectonic and volcanic factors which can disturb catchments. The Northland region is considered tectonically stable, with no uplift since at least the Quaternary (e.g., Brothers, 1954; Cotton, 1957; Gibb, 1986; Pillans, 1986; Brook, 1999; Marra and Alloway, 2006), low seismic activity (http://www.geonet.org.nz/; Anderson and Webb, 1994) and no known active faults (http://data.gns.cri/nz/af/; Beetham et al., 2004). The majority of Northland catchments are small and well-connected, offering a clear signal of Holocene climate variability and anthropogenic forcing on river system behaviour. In this part of New Zealand the pattern of floodplain development during the Holocene has involved a climatically forced period of mid to late Holocene floodplain aggradation followed by floodplain incision and finally rapid refilling in response to post-settlement catchment disturbance (Richardson et al., in review-b). Evidence from the meta-analysis of ^{14}C fluvial deposits in Northland floodplains has identified increased river activity at 800–600 cal. yr BP and 500–300 cal. yr BP, potentially representing two episodes of late Holocene fluvial activity in the region (Richardson et al., in review-a).

The aim of this paper is to examine floodplain sedimentation and river response to post-settlement catchment disturbance using data from the flood-prone Kaeo catchment in eastern Northland and ^{14}C data from eight other Northland floodplain sites (Fig. 8.1). Floodplain sediment coring, Ground Penetrating Radar (GPR) and Light Detection and Ranging

(LiDAR)-derived mapping is used to determine valley floor morphology and the valley fill stratigraphy at the Kaeo site. An investigation of post-settlement alluvium characteristics and chronology through high resolution multi-element X-ray fluorescence (XRF) analysis, particle size analysis and ^{14}C dating provides the detail needed to determine the nature and rates of Holocene floodplain alluviation, and offer some insight into sediment provenance. The resulting reconstruction of the floodplain morphology and Holocene floodplain sedimentation history contributes to an enhanced understanding of the river dynamics associated with anthropogenically-driven catchment disturbance. The results of this study provide information that can be used, along with projections of future climate change, to inform flood mitigation and land-use planning decisions.

8.4 Regional setting

8.4.1 Kaeo catchment physiography, geology and soils

The Kaeo River catchment, with an area of 114 km^2, is located on the east coast of the Northland Peninsula in far northern New Zealand (Fig. 8.1a). The landscape in this area comprises moderately dissected rolling hill country up to 440 m in elevation (Fig. 8.1b). Three major tributary streams drain the southwestern part of the catchment before joining the Kaeo River, which flows north into Whangaroa Harbour (Figs. 8.1b and 8.2b). The Kaeo River catchment straddles the present day eastern boundary of the Northland Allochthon, a series of Cretaceous to Oligocene age thrust sheets emplaced in the Early Miocene (Edbrooke and Brook, 2009). The main rock type through the central catchment is greywacke of Triassic and Jurassic age (Waipapa terrane), with allochthonous sandstone, mudstone and melange present over much of the remaining area (Edbrooke and Brook, 2009). The eastern and southeastern catchment also contain Early to Mid Miocene andesitic breccia and intrusions associated with the Wairakau Volcanic Centre (Edbrooke and Brook, 2009).

Soils of the Kaeo catchment floodplains comprise Whakapara silt and clay loams. The predominant soil types in the eastern and southeastern catchment are Te Ranga steepland silt and stony clay loams, and poorly drained rolling and hill land Waitotira clay soil. Soil type in the western catchment is mainly excessively drained gravelly clay (Tairaire) and well drained Bream clay loam and Haunga complex, with pockets of poorly drained Wharkohe silt loam and Otaha clay (soil data sourced from New Zealand Land Inventory, NZMS Sheet P04/05).

8.4.2 Northland climate

The climate of Northland (Fig. 8.1) can be described as mild, humid and moderately windy, (Moir et al., 1986), with a mean annual rainfall of 1200 mm in southwestern Northland and 1700 mm in northeastern Northland (climate summary data for the period 1969–1998 from http://www.Metservice.com). Summers are generally warm and humid, with less rainfall than during the mild and wetter winter months (Moir et al., 1986). However, the rainfall regime of Northland does exhibit a high degree of both year to year, and month to month variability (Moir et al., 1986). Periods of intense rainfall associated with moisture-bearing northeasterly flows and the incursion of tropical depressions are not uncommon (Moir et al., 1986).

Temperatures in the Kaeo area reach a maximum of 25°C in February and a minimum of 16°C in July (mean maximum daily temperatures calculated for the period 2002–2012 using data from the Kerikeri Ews climate station obtained from the NIWA National Climate database, http://cliflo.niwa.co.nz). Rainfall data from the Kaeo climate station (Fig. 8.1b) show a mean annual rainfall of 1596 mm (between 1981 and 2010), with a minimum in normal rainfall of 102 mm in January and a maximum of 199.5 mm in July (Kaeo climate station data obtained from the NIWA National Climate database, http://cliflo.niwa.co.nz).

Pollen records from the Northland region suggest that climate varied during the Holocene and can broadly be divided into four climatic zones. A cooler than present early Holocene (~ 12,000–10,000 cal. yr BP); a more mesic early to mid Holocene (~ 10,000–5000 cal. yr BP); a mid to late Holocene (~ 5000–2000 cal. yr BP) that was subject to more disturbance and climatic deterioration; and a late Holocene (from ~ 2000 cal. yr BP) which showed some evidence of climate amelioration prior to anthropogenic impact (Dodson et al., 1988; Newnham, 1992; Striewski et al., 1996; Elliot, 1998; Elliot et al., 2005).

8.4.3 Vegetation, land use and settlement history

Prior to human arrival indigenous forest cover in Northland comprised of predominantly mixed podocarp conifer-hardwood associations, including the long-lived emergent conifer *Agathis australis* (kauri) (e.g., Kershaw and Strickland, 1988; Elliot et al., 1998). During Polynesian settlement of New Zealand there was extensive deforestation by intentional burning in order clear land for settlements and trackways, and also to possibly encourage the establishment of *Pteridium esculentum* (bracken fern), an important source of carbohydrate (McGlone et al., 2005). Pollen records from lake sediments in central Bay of Islands identify a date of ~ 1000 cal. yr BP for the commencement of anthropogenic catchment disturbance,

characterised by a decline in all shrub and tree taxa, increases in charcoal and the abundance of *Pteridium* spores (Elliot et al., 1998).

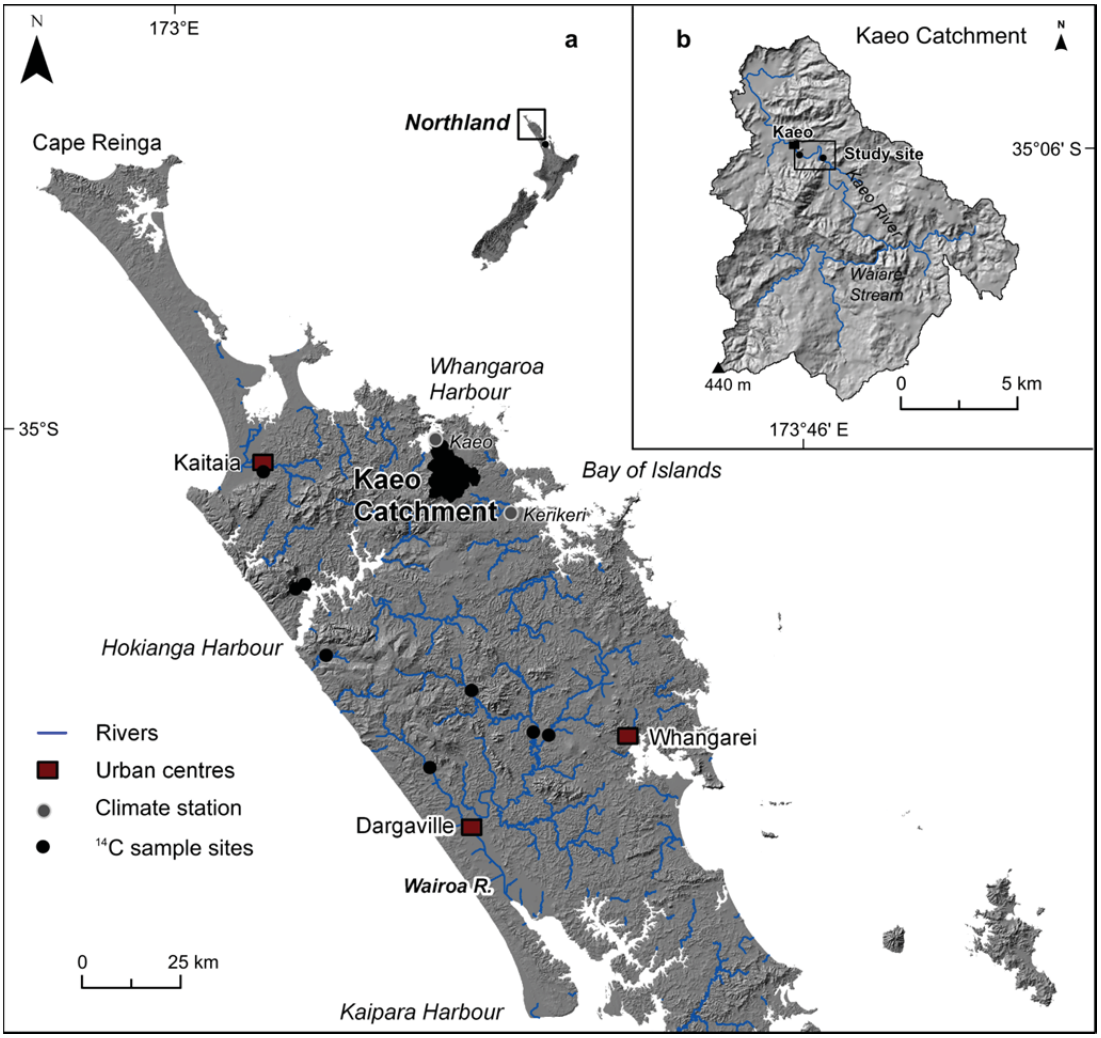

Fig. 8.1. (a) Location map of the Kaeo catchment in the Northland region of New Zealand showing the location of Holocene ^{14}C-dated floodplain sample sites, rivers and urban centres. (b) The study site location in the lower Kaeo catchment near the settlement of Kaeo (labelled).

Immediately prior to European settlement the northern North Island of New Zealand was the most heavily populated area in New Zealand (Metge et al., 1960), and large tracts of forest in Northland had already been cleared (Holloway, 1960). In the pollen record a decline in tree pollen and concurrent increases in herb pollen and the appearance of pollen of

introduced taxa, such as *Cupressus*, *Pinus* and European pasture herbs, marks the beginning of European influence on the vegetation within the last ~ 200 years (Elliot et al., 1995; 1998).

In the Kaeo area, Polynesian deforestation was restricted to small patches for gardens and tracks, with the major period of deforestation occurring after European settlement (M.M. Hayes, personal communication, 7 August, 2012). At the time when the first European ships began to visit Whangaroa Harbour to log kauri for ship spars (around 1820), the Māori settlement of Kaeo was concentrated around the Pohue Pa (Fig. 8.3), with the Kaeo River winding through a cultivated valley surrounded by forested hills (Sale, 1986). Earliest European settlement in Kaeo occurred in 1823, with the establishment of a Wesleyan mission, and in 1833 the first individual Europeans settled in the Whangaroa area (Sale, 1986). Kaeo became a major site for the extraction of kauri and the river was used to float logs down to the Whangaroa Harbour (Sale, 1986). By the late 1800's to early 1900's the kauri logging and gum industry had reached its peak and was followed by farming activities (Sale, 1986). Between 1910 and 1950 much of the remaining bush in the Kaeo River catchment was cleared for pasture and the establishment of small-scale dairy farms (M.M. Hayes, personal communication, 7 August, 2012). However, by the second half of the 20th century many of the farming operations were no longer economically viable and areas with poorer soils were left to regenerate to native bush or converted to exotic forest plantations, with dry stock farming restricted to the more fertile valleys (M.M. Hayes, personal communication, 7 August, 2012). Figure 8.2 shows the distribution of contemporary vegetation in the Kaeo River catchment. The majority of the catchment is covered with regenerated native forest and scrub, and there are some large areas of exotic forest planted in the southeast of the catchment. Areas of pasture are largely confined to the river valleys.

8.5 Methods

8.5.1 Geomorphology and stratigraphy

High resolution LiDAR topographic data (accurate to within ± 150 mm) supplied by the Northland Regional Council (NRC) and GIS were used to produce a digital elevation model (DEM) of the Kaeo River study site and floodplain (Fig. 8.3) using standard methodologies (cf. Jones et al., 2007). Floodplain sediment cores were extracted from the floodplain using a hydraulic percussion coring system and logged according to grain size, lithology and colour. Ground Penetrating Radar (GPR) surveys included in this study were conducted during dry conditions using a Sensors and Software pulseEKKO PRO radar system with Full Bistatic assembly. GPR profiling uses pulses of high frequency electromagnetic energy to detect

discontinuities in the dielectric properties of subsurface materials and the technique has been widely used in sedimentary research (cf. Neal, 2004). GPR data for KXS1 (Fig. 8.3) were acquired in two lines, both using 100 MHz antennas with a step spacing of 0.25 m. The choice of antenna frequency depends on the depth of penetration and resolution required, with depth of investigation increasing and spatial resolution decreasing as frequency decreases. As the main objective of the survey was to determine the overall structure and the bedrock-valley fill boundary, the 100 MHz antenna frequency was chosen. The use of 100 MHz antenna frequency in the floodplain environment has been shown to provide an approximation of floodplain stratigraphy for depths of alluvium up to 3 m (Nobes et al., 2001).

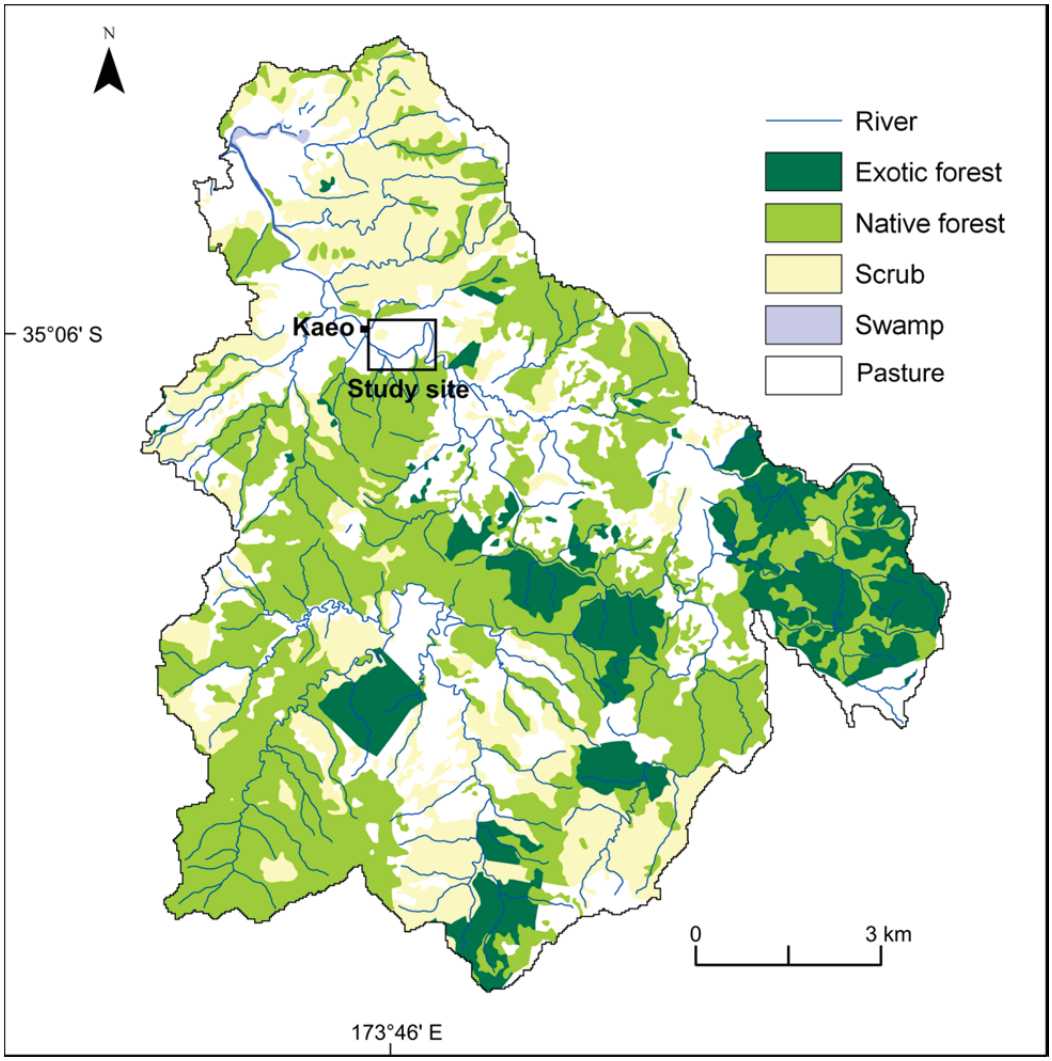

Fig. 8.2. Contemporary land cover map of the Kaeo catchment, Northland, New Zealand. (Data source: NZTopo50-AV28 geodata, www.linz.govt.nz, accessed 20 Nov 2011).

The most southern section of the KXS1 (Fig. 8.3) radar survey traverses the floodplain from the valley edge to the southern channel margin and includes 471 radar traces over a length of 117.5 m. A second 89.5 m line on KXS1, comprising 359 radar traces, was surveyed from the northern edge of the channel across a palaeochannel and floodplain, stopping at the base of a bedrock outcrop. Topographic surveying of the GPR line was carried out using RTK-dGPS at the time of GPR data acquisition. Subsurface images were produced using Sensors and Software EKKO View Delux GPR viewing and processing software. Images are displayed with the topography adjusted using RTK-dGPS topographical data, with the autogain function applied to the data set to compensate for the loss of signal with depth and highlight deeper reflections. Target depths are determined using a radar wave velocity and is dependent on the geologic material properties being surveyed. In this study a radar velocity of 0.1 m ns^{-1} was used to convert travel time to an estimate of depth as this value was quoted in the pulseEKKO Pro user guide as an appropriate value to use when there is uncertainty regarding the velocity of the material being surveyed. It also represents a mid-value between dry soil and sand (0.15 m ns^{-1}) and clay and wet sand (0.06 m ns^{-1}), which were the main sediments being surveyed.

8.5.2 Sedimentology and radiocarbon chronology

High resolution multi-element X-ray fluorescence (μXRF) analysis of Kaeo floodplain sediments was undertaken using an ITRAX μX-ray core scanner (IEGS, Aberystwyth University, UK) with a 3 kW molybdenum target tube operating at 30 kV and 30 mA (cf. Croudace et al., 2006). Reconstruction of the chemical stratigraphy of sediments preserved in alluvial environments can provide detailed information on changes in catchment hydrology, sediment sources and flux (e.g., Collins et al., 1997; Heath and Plater, 2010; Jones et al., 2010b). In this study, four sections of a floodplain core (K4 in Fig. 8.3) were scanned at a resolution of 500 μm with a count time of 10 seconds/increment and 28 elements were measured. XRF elemental data measured at 500 μm increments resulted in a data set of n = 5474 counts, representing 2.735 m of core (Appendix E).

Particle size analysis of floodplain sediments was carried out using a Horiba Partica LA-950v2 laser scattering particle size distribution analyser (Appendix A). Sediment samples for particle size analysis were pretreated with H_2O_2 to remove organic material. The refractive index was determined through X-ray diffraction (XRD) analysis on ground floodplain sediment samples (Appendix E). XRD spectra were obtained using a GBC

EMMA X-ray diffractometer operating at 35 kV and 20 mA using monochromatic Co Ka radiation. Scans parameters were 2o 2θ/min scan rate at steps of 0.1o 2θ.

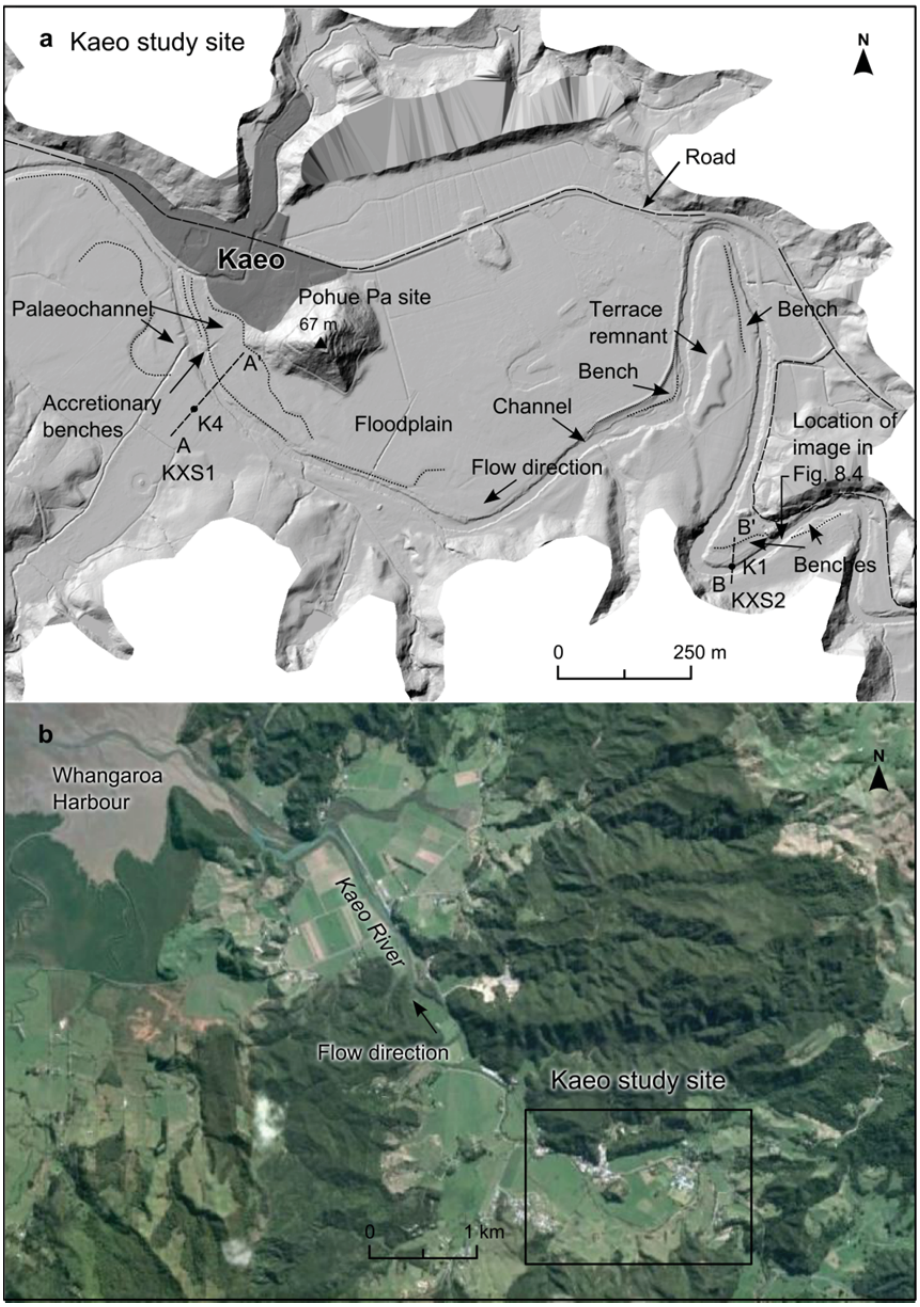

Fig. 8.3. (a) LiDAR derived digital elevation model hillshade of the Kaeo study site labelled with the main geomorphic features, location of cross-sections and sediment cores used in this study. (b) GoogleEarth™ aerial image of the lower Kaeo catchment with study site indicated.

Organic material collected from core sediments and fresh cutbank exposures were submitted to the University of Waikato Radiocarbon Dating Laboratory for preparation, and analysed on the Keck Radiocarbon Dating Laboratory (University of California) accelerator mass spectrometer (AMS). Results were reported as percent modern carbon following Stuvier and Pollack (1977), and based on the Libby half-life of 5568 years with correction for isotopic fractionation applied. Radiocarbon ages were calibrated using OxCal v4.1 (Bronk Ramsey, 2009) and the Southern Hemisphere calibration dataset SHCal04 (McCormac et al., 2004), and are reported in calibrated years before present (cal. yr BP) with 2 sigma uncertainties.

8.6 Results

8.6.1 Geomorphology and stratigraphy

In the eastern part of the study site the Kaeo River is partly confined within a narrow (~ 100 m) bedrock-controlled valley, before opening out into a broader valley setting where the floodplain is up to 750 m wide (Fig. 8.3). The low flow channel is less than 10 m in width and has a coarse-gravel bed ~ 3 m below the contemporary floodplain surface (Fig. 8.4). The assemblage of channel and floodplain geomorphic elements comprising the valley floor, including benches and palaeochannels (labelled in Fig. 8.3), represent the different reworking and formation processes operating in this part of the fluvial system.

Fig. 8.4. Kaeo River, Northland, New Zealand. Looking upstream in an eastward direction from a location labelled in Fig. 8.3. Approximate height of banks is 3 m (image: J Richardson, December 2009).

Investigation of the floodplain stratigraphy at the Kaeo site was undertaken using GPR and coring at cross-section KXS1 (Fig. 8.5) and examination of a cutbank exposure along KXS2 **(**Fig. 8.6). The characteristics of floodplain sedimentation between 0 and 120 m along KXS1 is one of laterally continuous vertical accretion units comprising fluvial silty sands, sand and gravel to a depth of 4.8 m. On the opposite side of the channel the profile shows a more complex stratigraphy, and a more varied geomorphology and topography is evident (Fig. 8.5b and c). The bench at 140 m along the profile is characterised by dipping reflectors interpreted as oblique accretionary units. The overall sedimentation pattern, incorporating the natural levee and infilled palaeochannel, is one of laterally continuous reflectors. Hyperbolic reflections at ~ 0 m elevation along the GPR line indicate subsurface objects and suggest a major stratigraphic boundary, interpreted as the base of the alluvial fill in this part of the valley floor.

The floodplain stratigraphy and topography at a more confined section of the Kaeo River is detailed in Fig. 8.6. Bank exposures in this part of the study site show over 4 m of massive sands and silty sands. The top 2.0 m of exposure K1 is characterised by interbedded sand and silt units overlying coarse grained sand, finer grained sandy silt deposits between 3.0 and 4.9 m, and a thin gravel unit at ~ 4 m below the floodplain surface (Fig. 8.6a).

8.6.2 Sedimentology and radiocarbon chronology

Although ITRAX geochemical data are considered semi-quantitative, with data output as peak area integrals for elements (count data), it does show the elemental variation with depth. Figure 8.7 displays the XRF 5 point smoothed peak area integral data for selected elements (Al, Si, P, K, Mn, Fe, Zn, and Pb) from Kaeo floodplain sediments obtained in core K4 (Fig. 8.5a). Elements selected for display (see Appendix A for XRF data and Appendix E for all element plots and the optical image of the scanned core) were the more common minerogenic elements or elements that exhibited a marked trend or peak in concentration (i.e., Pb). Data validity decreases toward the bottom of the core, most obviously in the lower-most 170 mm of the profile where this section of core comprises sand and gravel. Overall, all elements show some fluctuation around a mean value, and in the top 2.0 m of core the amount of Fe, Mn and Zn increases down the core as a result of post-depositional redox-related diagenesis processes. Mn and Zn also show a step change reduction in these two elements at 2 m, corresponding with a sediment colour change associated with a redox boundary. The only marked variation in an elemental profile is that of Pb, with peak area integral data showing elevated levels at depths between 1.20 and 1.50 m, peaking at 1.35 m.

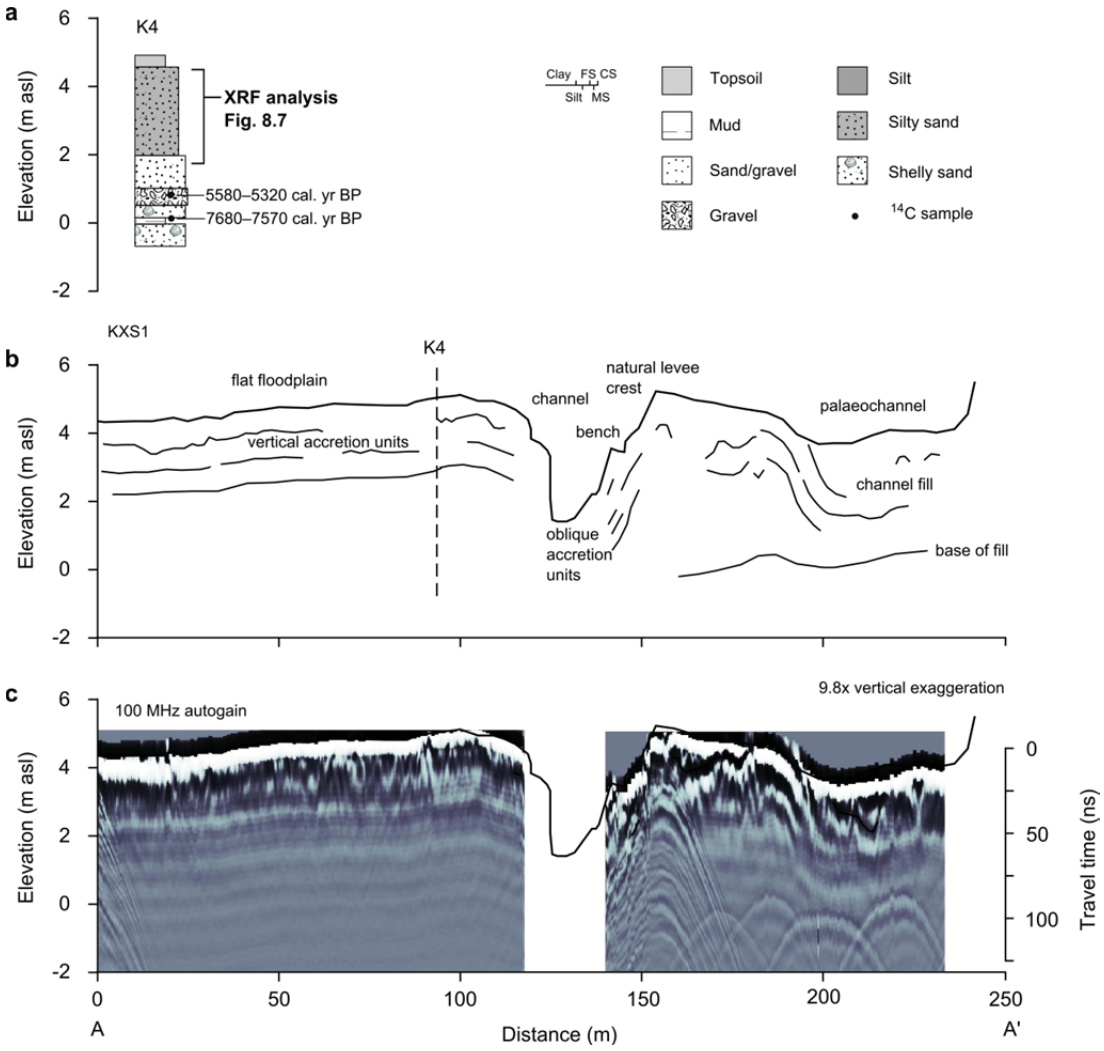

Fig. 8.5. (a) Log of floodplain core K4 displayed with lithology, grain size, radiocarbon chronology and reference to XRF analysis of the top 2.7 m of core. (b) Cross-section KXS1 showing location of core K4 and stratigraphical interpretation of the GPR profile. (c) GPR profile acquired with 100 MHz antennae and processed using the autogain function.

Grain size data for the sedimentary sequence of interbedded silty sands in the top 2.0 m of a bank exposure are shown in Fig. 8.6c (see Appendix A for complete data set). These vertically accreted overbank floodplain deposits are described as sand and silty sand and show considerable variability in grain size. Visually the coarser sandier units appear darker, while the deposits with greater silt and clay content are a lighter brown. The D_{50} value for each of the depositional units correlate well with visual assessments of grain size and also show a variation in sediment particle size in the top 2.0 m of exposed floodplain, ranging from between 600 µm (coarse sand dominated unit) and 11 µm (fine silt dominated unit).

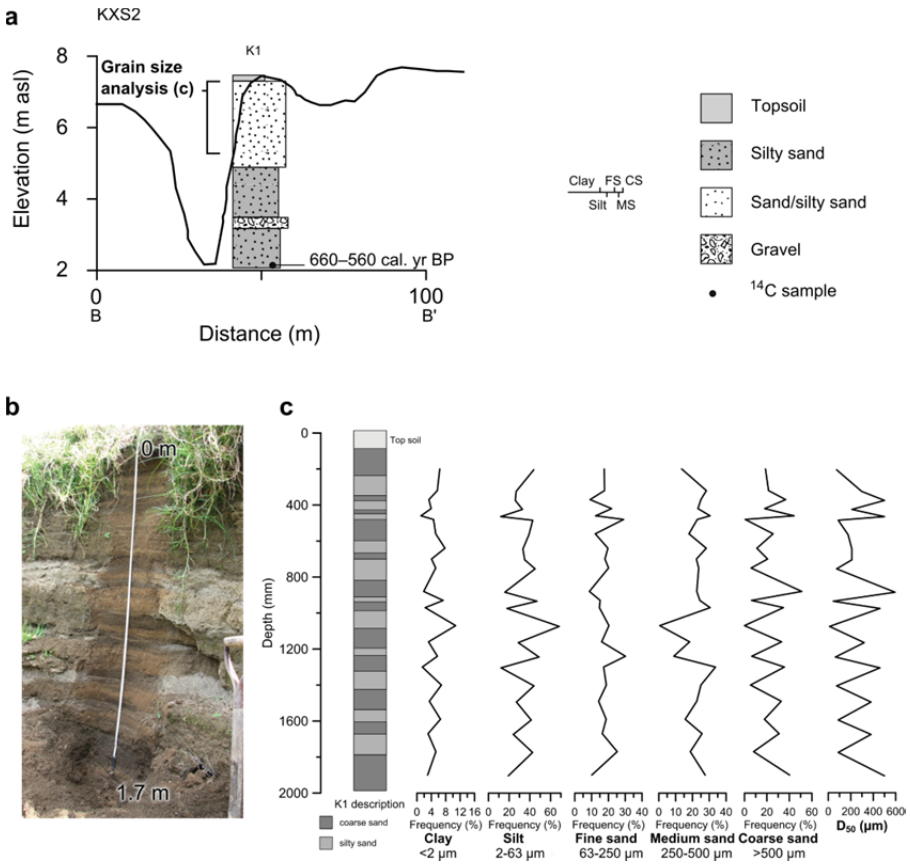

Fig. 8.6. (a) Floodplain exposure K1 displayed with lithology, grain size, radiocarbon chronology and reference to grain size analysis of the top 2.0 m of core. (b) Image of interbedded sand and silty sands in bank exposure K1 (image: J Richardson, Dec 2009). (c) Description, grain size frequency data and sediment D_{50} of top 2 m of exposure K1.

Figure 8.5a shows the ^{14}C data for core K4. The base of this core comprises medium to coarse-grained shell rich sand deposited in an estuarine environment, i.e., when Whangaroa Harbour extended much farther up-valley than present. An organic rich sandy silt unit immediately above the shell rich sand at 4.6 m dates the beginning of fluvial deposition at 7680–7570 cal. yr BP (Table 8.1). Wood in a fluvial sandy gravel unit at 4.0 m (above fine-grained organic rich deposits) returned an age of 5580–5320 cal. yr BP (Table 8.1). Above the sandy gravel is a very coarse-grained sand/gravel silt unit (1 m thick) and overlying this is 2.5 m of massive fine-grained sandy silt. Figure 8.6a shows the ^{14}C chronology for exposure K1 where organic material from a silty sand unit underlying 4.8 m of interbedded sand and silty sands returned a ^{14}C age of 660–560 cal. yr BP (Table 8.1).

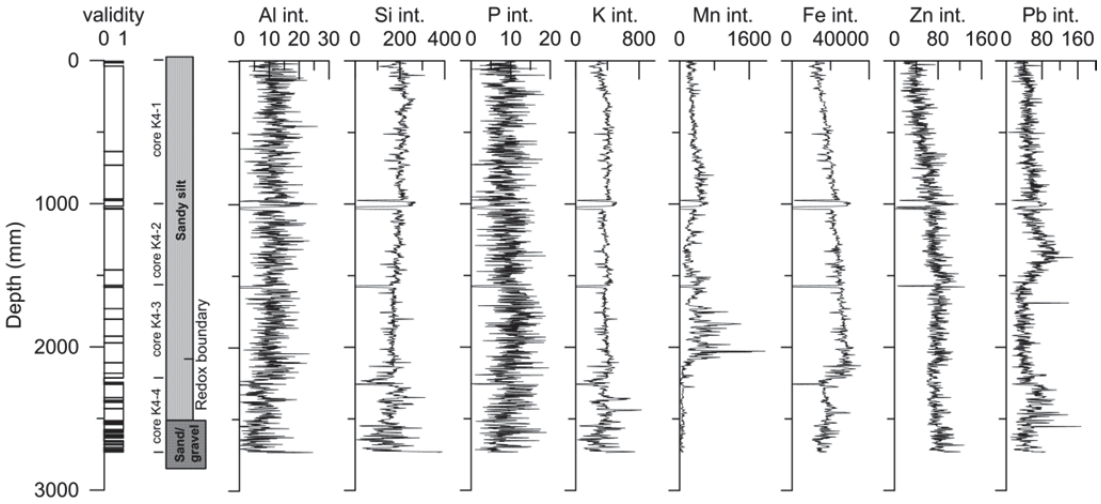

Fig. 8.7. Inorganic geochemical data from high resolution XRF scans (5 point smoothed peak area integral [int.] data) for selected elements and in Kaeo floodplain sediment (core K4 in Figs. 8.3a and 8.5a) and detector-sediment distance (validity) index (where 0 is invalid).

8.6.3 Northland floodplain sedimentation rates

^{14}C ages for Kaeo floodplain units were combined with data from seven other Northland catchments (Table 8.1) to produce Fig. 8.8. Holocene floodplain sedimentation rates were calculated using the depth of sample divided by the midpoint of the 2 σ calibrated ^{14}C age range, with the surface assumed to have an age of zero.

8.7 Discussion

Historical evidence suggests that the floodplain study site at Kaeo has undergone considerable morphological change in the last ~ 150 years, with longboats previously able to navigate up to a landing located in the township (M.M. Hayes, personal communication, 7 August, 2012). LiDAR derived maps and aerial imagery of the Kaeo study site indicate that the valley floor has been infilled, and a broad floodplain (up to 750 m wide) in the less-confined section of the valley has developed. Aerial imagery of the site taken in March 2012 (Fig. 8.9) following 146 mm of rain in 24 hours, an amount that exceeded the total average monthly rainfall normally recorded for March, shows that the floodplain is still extensively inundated, creating considerable contemporary flooding issues and indicating ongoing floodplain sedimentation.

Table 8.1

Summary of radiocarbon data, sample description and location of samples used in this study.

Core	Sample code	Lab. No.	Depositional environment	Sample material	Sample depth (m)	Uncalibrated date (BP)	Calibrated date (cal. yr BP 2σ confidence)	Measurement
Kaeo Catchment – Kaeo River								
K4	Kaeo4a	Wk-30440	Floodplain	Wood	4.02	4769 ± 25	5580–5320	AMS
K4	Kaeo4c	Wk-30443	Floodplain	Silt organics	4.6	6820 ± 26	7680–7570	AMS
K1	Kaeo1b	Wk-27971	Floodplain	Silt organic	4.85	691 ± 35	660–560	AMS
Kaihu Catchment – Kaihu River								
KH2	Kaih2e	Wk-30436	Floodplain	Wood	2.3	3109 ± 25	3360–3170	AMS
KH2	Kaih2f	Wk-31574	Floodplain	Wood	3.6	3933 ± 28	4420–4160	AMS
KH2	Kaih2b	Wk-31573	Floodplain	Wood	2.86	3457 ± 28	3560–3820	AMS
Mangakahia Catchment - Mangakahia River								
M1	Mang1a	Wk-27967	Floodplain	Silt organics	7.4	850 ± 39	790–670	Radiometric
M2	Nuku2a	Wk-31576	Floodplain	Silt organics	1.47	3287 ± 30	3560–3380	AMS
Panguru Catchment – Te Rapa Stream								
P2	Pang2a	Wk-27963	Floodplain	Charcoal	2.3	353 ± 30	460–310	AMS
Te Atatu Peninsula Catchment – Whau River (Grant-Taylor and Rafter, 1971)								
		NZ-497	Floodplain	Wood	1	494 ± 67	620–320	Radiometric
Upper Awanui Catchment – Takahue River								
T2	Taka2e	Wk-30434	Floodplain	Wood	4.62	5828 ± 25	6660–6490	AMS
T2	Taka2d	Wk-30435	Floodplain	Wood	3.69	2033 ± 25	2000–1870	AMS
Waihou Catchment – Waihou River								
WA3	Waih3a	Wk-27964	Floodplain	Wood	5.5	5977 ± 47	6890–6640	AMS
Waimamaku Catchment – Waimamaku River								
W4	Waim4c	Wk-30438	Floodplain	Wood	2.56	780 ± 25	730–650	AMS
W9	Waim9a	Wk-31577	Floodplain	Wood	3.38	2947 ± 27	3160–2890	AMS
W1	Waim1c	Wk-27968	Floodplain	Wood	3.3	1138 ± 41	1070–920	AMS

8.7.1 Floodplain development

At cross-section KXS1 the onset of fluvial sedimentation is dated at 7680–7570 cal. yr BP (Fig. 8.3 and Table 8.1). GPR profiles show the core stratigraphy is representative of the deposits underlying the wider floodplain and indicates that the base of alluvial fill in this location is ~ 1 m below the present channel bed. On the true left of the channel the dominant floodplain forming processes are vertical accretion of a flat floodplain surface, with the accumulation of sediment suspended in overbank flows characterised by horizontal reflectors in the GPR profile, similar to that described for other floodplain sites (Nobes et al.,

2001; Jones et al., 2010b). Floodplain chronostratigraphy at this core site indicates that average floodplain sedimentation rates were in the order of 0.3 mm yr^{-1} (Table 8.2) between ~ 7600 and 5500 cal. yr BP, with sediments dominated by coarse-grained/gravelly deposits. Average sediment rates in the last ~ 5500 years are 0.7 mm yr^{-1} (Table 8.2).

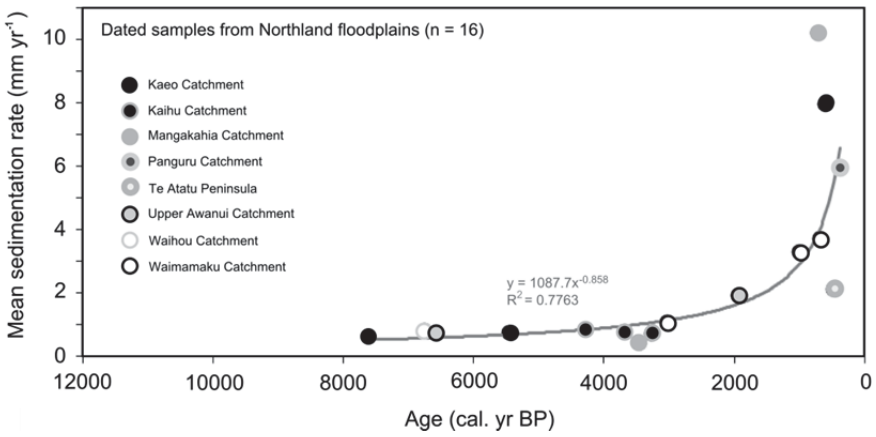

Fig. 8.8. Holocene floodplain sedimentation rates plotted for Northland catchments.

Fig. 8.9. Aerial image of flooding in Kaeo (19 March 2012) that occurred following 146 mm of rain in 24 hours. (Image: http://tvnz.co.nz/national-news/raw-video-aerial-view-northland-flooding-4784567, date accessed 2 February 2012).

On the true right bank channel margin, obliquely accreted deposits have formed an inset floodplain unit (in-channel bench), a step-like fluvial depositional feature that occurs at elevations between the major floodplain surface and the channel bed. The inset unit on the true right of the channel has been formed as result of sediment draping at the channel margin during different flood stages as has been described for other sites (cf. Brierley et al., 2002; Jones et al., 2010b). There is similar bench morphology on the left channel margin; however due to lack of GPR data the formation processes cannot be confirmed.

The top 2.5 m of floodplain sediment in core K4 is massive heavily oxidised fine-grained sandy silt grading down to mottled grey-blue silt. Geochemically this sediment is compositionally homogenous with only lead (Pb) and the redox-sensitive (Zn, Fe and Mn) and soluble (Sr and Rb) elements showing any significant variation in concentration in the profile (Fig. 8.7). Fe and Mn increase as a result of post-depositional diagenesis to a depth of 2.0 m, below which these elements decrease due to reduction and dissolution. Variation of Pb (which has low solubility) within the floodplain sediment most likely represents an anthropogenic source. In New Zealand lead alkyl petroleum additives were introduced in the 1920's to boost octane rating. Lead emissions increased between 1930 and 1975, before plateauing at a maximum between 1975 and 1986, and then rapidly reducing following the shift to unleaded petroleum (Pearson et al., 2010). Sub-surface peaks in Pb concentration coinciding with peak Pb emissions have been found in North Island lakes and have well exceeded concentrations resulting from naturally derived sources (e.g., volcanic tephras) (Pearson et al., 2010). Post-settlement floodplain sedimentation rates for the Kaeo floodplain, calculated using the depth of the Pb peak, equate to just over 40 mm yr^{-1} over the last 32 years (Table 8.2). This value vastly exceeds the average sedimentation rate of 0.7 mm yr^{-1} over the last ~ 5500 years (Table 8.2).

At cross-section KXS2, floodplain morphology reflects a greater degree of channel confinement, with a narrow valley floor and floodplain pockets that have accumulated on the concave margin of the channel bends. A radiocarbon age from wood (660–560 cal. yr BP) in a silty sand unit, at the base of a 4.8 m sedimentary sequence of interbedded sands and silty sands, indicates an average post-Polynesian settlement sedimentation rate in this part of the valley of 7.2 mm yr^{-1} (Table 8.2). Grain size data for this part of the catchment indicate that the top 2.0 m of floodplain comprises interbedded flood deposits of coarse-grained sand-dominated units (maximum grain size 600 μm) and fine sediment units dominated by clay and silt size fractions < 63 μm (Fig. 8.6c). This pattern of sedimentation is characteristic of overbank flood deposits, incorporating couplets of coarser material associated with deposition during peak discharge and finer suspended sediments deposited during waning

flows (Jones et al., 2010b). The laminated nature of sedimentation at this site differs from the floodplain sedimentation farther down the valley at KXS1, where the top 2.5 m of floodplain sediment comprises a massive lithologically homogenous silty sand unit. These sediments reflect a depositional environment that is more distal from the channel and where sedimentation is dominated by the lateral accretion of finer suspended material without heterolithic differentiation (e.g., Jones et al., 2010b).

Geomorphological and sedimentological data indicate the dominant fluvial response to increased sediment flux and limited accommodation space has been the vertical adjustment of the floodplain and infilling of the valley through vertical accretion processes, with evidence that there has been less than 1 m of vertical adjustment in the channel bed over the last ~ 7500 years. The presence of palaeochannels signifies channel changes involving channel cutoff, and these almost completely infilled channels are still likely to act as flood channels during overbank flows. Lateral channel adjustment processes have included lateral migration, bank erosion and channel expansion, most likely episodic rather than progressive (cf. Brierley and Fryirs, 2005), and subsequent contraction with the formation of accretionary benches.

Table 8.2

Kaeo floodplain sedimentation rates.

Floodplain unit	Sample age	Depth (mm)	Sedimentation duration (yrs)	Sedimentation depth (mm)	Sedimentation rate (mm yr^{-1})
Floodplain surface (K1)	0	0			
			672	4850	7.2
Flood deposit within inset unit (K1)	610 cal. yr BP (mean)	4850			
Floodplain surface (K4)	0	0			
			5514	4020	0.7
Fluvial gravel (K4)	5452 cal. yr BP (mean)	4020			
			2170	580	0.3
Fine grained mud (K4)	7622 cal. yr BP (mean)	4600			
Floodplain surface (K4)	0	0			
			32	1350	42.2
Pb peak in fine-grained silty sand (K4)	1980 AD (estimated)	1350			

8.7.2 Anthropogenic impacts

Figure 8.8 confirms that average floodplain sedimentation rates in Kaeo and seven other Northland catchments, follow a similar pattern to the wider New Zealand records (Richardson et al., 2013), with rapid increases in average floodplain sedimentation rates in the last ~ 500 years. Palaeovegetation reconstructions from Northland have used increases in *Pteridium* spores and charcoal to identify the first anthropogenic landscape disturbance, reporting dates ranging from ~ 1000 yr BP to 500 cal. yr BP (Elliot et al., 1995; Elliot et al., 1997; Elliot et al., 1998; Ogden et al., 2003). Abrupt changes in physical and geochemical properties and an influx of catchment derived minerogenic material in the sediments of Lake Pupuke located in Auckland, dates the onset of prehistoric Polynesian colonisation in northern New Zealand at ~ 610 cal. yr BP (Striewski et al., 2009). It is therefore likely that episodes of river activity and accelerated floodplain sedimentation in Northland after ~ 500 cal. yr BP are driven by increased sediment flux associated with widespread post-settlement deforestation rather than climatic forcing.

At the Kaeo site the response to anthropogenic catchment land-use change and catchment destabilisation has also been accelerated floodplain sedimentation. Of particular significance to the sediment budget of the lower Kaeo River are inset bench units. Bench deposits act as temporary sediment storage areas and can be responsible for large volumes of sediment exchange (Thoms and Olley, 2004), and hence can comprise a significant component of a river systems sediment budget. Although the character of in-channel bench units varies between fluvial systems there is evidence that in more dynamic environments formation can be cyclic, with erosion of benches occurring during low frequency high magnitude events and construction taking place as a result of more frequent but smaller floods (Erskine and Livingstone, 1999) or during drought-prone hydro-climatic conditions (Royall et al., 2010). In-channel benches are particularly significant in catchments that have undergone anthropogenically-driven increases in erosion and sedimentation (Fryirs and Brierley, 2001), with large volumes of sequestered sediment acting as secondary sediment sources vulnerable to reworking (Davis, 2009). The geomorphology of the Kaeo sites suggests that in-channel sediment storage in the form of inset benches are a feature of the fluvial system here, with the potential to contribute to continuing high rates of sediment supply to the lowland floodplain even after catchment stabilisation.

However, the geochemistry of floodplain sediments at the Kaeo site does not give any indication that secondary sediment sources such as inset units have become a more important component in the post-disturbance sediment budget or since catchment vegetation

regeneration. Post-settlement fluvial material shows no significant chemical heterogeneity and minimal lithological variation. However, a shift in the character of sediment supply may not necessarily be detectable within the floodplain sedimentary record as in-channel sediment stores would be essentially comprised of sediments from the same source (i.e., bank erosion or hillslope soil erosion),. The geomorphology of the lowland Kaeo floodplain does suggest that since European settlement there have been spatial changes in the distribution of sediment stores and sinks within the catchment, with the lowland Kaeo River floodplain becoming a major sediment accumulation zone. Such changes in the distribution of sediment stores and long-term sinks following European catchment disturbance are not unusual and have led to the conversion of the lowland floodplains from transfer zones to sites of sediment accumulation with large volumes of material transformed into transient stores (e.g., Fryirs and Brierley, 2001).

The geomorphic behaviour of the Kaeo catchment during the Holocene is consistent with observations from fluvial sites within New Zealand and globally. That is, low pre-settlement rates of floodplain accretion persisted until human-induced deforestation forced an acceleration in floodplain sedimentation rates. The geomorphic impact of increased sediment flux on the tectonically stable lower Kaeo catchment floodplain, although significant, is not as profound as sedimentation rates reported for reaches of the Waipaoa River, where there has been vertical accretion at an average rate (post-1850) of ~ 60 mm yr^{-1} (Gomez et al., 1999). In the Waipaoa sedimentary system, where active tectonics and geology predispose the region to high rates of geomorphic activity (Litchfield et al., 2008), vegetation disturbance caused by the Taupo eruption (~ 1.7 ka) and land clearance by Polynesian settlers, extreme storms and earthquakes, have all generated strong landscape responses (Gomez et al., 2007). However, it is European land clearance that has the greatest impact on the late Holocene depositional record (Gomez et al., 2007). Such findings mirror other studies which have found that indirect human induced catchment disturbance associated with European settlement has had profound effects on the hydrologic and sediment regimes of rivers, playing a greater role than climatic perturbation (e.g., Brooks and Brierley, 1997; Knox, 2006).

The role of climatic influences on catchment instability and enhancing sediment supply cannot be ruled out completely in post-settlement landscapes, as palaeohydrological research has shown that land-use change may act as a priming mechanism for catchment instability (Macklin and Lewin, 1993; Foulds and Macklin, 2006). In the Waipaoa sedimentary system, post-European deforestation has altered the landscape sensitivity to a range of sediment generating events (Gomez, 2007). In the lowland wetlands and floodplains of the Murray-

Darling Basin in southeastern Australia, pre-European sedimentation rates of between 0.1 and 1 mm yr^{-1} increased to an early post-settlement rate of up to 20 mm yr^{-1}, with the most recent rates of 10–30 mm yr^{-1} attributed to soil degradation and drought conditions in the catchment (Gell et al., 2009). In some cases, overbank sedimentation on floodplains has reduced in response to changes in land management practices (Knox, 1987), while at other sites massive anthropogenically driven increases in floodplain sedimentation and continued high sediment delivery has continued, regardless of improved land conservation measures (Knox, 2006). In Kaeo high rates of floodplain sedimentation rates (42 mm yr^{-1}) have continued in the last few decades, despite extensive catchment reforestation via the regeneration of native shrubland and exotic forest plantations.

8.7.3 Implications for flood management

The reconfiguration in the way sediment is stored and transferred within the Kaeo catchment and the transformation of the lowland floodplain to a major accumulation zone since European settlement has important implications in terms of sediment and flood management. The post European-settlement fluvial response has been rapid infilling of the lowland valley floor with aggradation of up to ~ 2–4 m (depending on accommodation space) of homogenous silty sand. Floodplain sedimentation rates have remained high despite reforestation of a large proportion of the Kaeo River catchment and flooding remains a major issue for the area. In light of predictions of more frequent extreme hydrological events, it is important that any flood mitigation or land-use decision consider the potential impacts of ongoing high rates of sediment accumulation in the lowland floodplain. More work should be undertaken to assess the nature of change in sediment source, transfer and accumulation since European settlement in the Kaeo catchment, and to quantify contemporary rates of the Kaeo River floodplain aggradation.

8.8 Conclusions

Geomorphological and sedimentological evidence from the Kaeo site show that post-European deforestation has had a greater influence on floodplain morphology and floodplain sedimentation than any other environmental change in the last 7500 years. Radiocarbon chronology indicates that fluvial sedimentation commenced around ~ 7500 cal. yr BP, with rates around the mid Holocene calculated to be in the vicinity of 0.3 mm yr^{-1}. Floodplain sedimentation rates in Kaeo and Northland have accelerated in the last ~ 500 years following Polynesian settlement, and in the more confined valley setting over 4.8 m of material has accumulated in less than 700 years, representing an average post-settlement rate of 7.2 mm yr^{-1}. But in Kaeo it has been extensive deforestation associated with European settlement

that has had the greatest impact on floodplain dynamics, with the Kaeo lowland floodplain now a major sediment accumulation zone. In the partly confined valley setting up to 2.5 m of lithologically and geochemically homogenous fine-grained material have accumulated on the floodplain, with recent sedimentation rates of up to 42.2 mm yr^{-1} within the last ~ 30 years.

Under conditions of limited accommodation space, high sediment supply from slopes destabilised by extensive post-European land clearance, a well-connected catchment and a low channel bed elevation, the model of floodplain development in the Kaeo area has been one of a stable channel bed and aggrading floodplain. Although more work is required to determine contemporary sedimentation rates, the relative position of the peak in anthropogenic lead within the floodplain alluvium suggests floodplain sedimentation has remained high in recent decades, despite increased cover of regenerated native forest and exotic plantation forests. Therefore, any flood protection measures or land-use decisions in the Kaeo area should consider the potential implications of ongoing high rates of floodplain sedimentation along with predictions of increased frequency of extreme hydrologic events.

Acknowledgements

This research was funded by a Tertiary Education Commission Top Achiever Doctoral Scholarship awarded to JR. Radiocarbon dating was supported by the Massey University Research Fund (to ICF). NJL's contribution was funded by PGSF Contract CO5X0705. The authors would like to thank the landowners for permitting access to the study sites and M. Hayes for supplying information on the early settlement of Kaeo. The authors would also like to acknowledge D. Feek for his technical support in the field and Dr H. Lamb (Aberystwyth University) for undertaking the XRF core scanning. LiDAR data was kindly supplied by the Northland Regional Council (B. Cathcart, J. Camuso, J. Santos and C. Anderson).

Chapter 9

Discussion

9.1 Introduction

This chapter provides additional discussion in support of the discussion sections in Chapters 4–8.

9.2 Spatial and temporal considerations

An overarching theme within geomorphology is the importance of the spatiotemporal scale under consideration when attempting to rationally 'order' what we see in the fluvial environment. More than ever before, geomorphologists are undertaking research across a wide range of spatial and temporal scales, underpinned by a extensive range of theoretical constructs and modes of explanation (Church, 1998). At the channel scale (10^4 m) and above, and a 30 year time scale (10^9 s), explanation of river behaviour is based on hydraulic geometry and engineering regime descriptions, where channel development is constrained both by endogenous (i.e., channel cut-off) and exogenous (i.e., climate) controls (Church, 1998). Exogenous controls on river behaviour are the most important at the largest scales (up to 10^6 m and 10^{12} s). While at timescales of between 30 and 9000 years both exogenous and endogenous constraints are influential (Macklin et al., 1998).

This research has examined river behaviour across a number of spatial scales within the timeframe of the Holocene, where development is constrained by both exogenous and endogenous factors. Chapter 4 looked at New Zealand wide records of river behaviour, finding ultimately that it was more appropriate to look at river activity at a smaller scale and

comprising the northern and southern regions. Nested within the fluvial records for New Zealand are the regional records, and Chapters 4, 5, and 7 focus on river behaviour in the Northland region. The regional fluvial record of Northland comprises reach-scale observations, with Chapter 8 reflecting the analysis of fluvial forms and processes at this smaller scale.

In addressing the question of whether or not Northland rivers are in synchrony with global climate it is necessary to reconstruct the fluvial history at a regional scale and compare this with global scale records of climate variability. This presents challenges as the Holocene climate record is extremely complex and contains a large amount of noise created by local-scale variability. The purpose of multi-proxy reconstructions for different regions is to identify major climate events that override local-scale variations. The analyses presented here highlight the spatial variation in river behaviour across New Zealand, which adds further complexity when attempting to determine the influence of Holocene climate change on river dynamics. Considering river behaviour at the level of the coherent precipitation region has gone some way towards dealing with the regional variability as driven by climate, but within and across these boundaries other environmental controls (i.e., tectonic activity) will be locally important.

Reconstructions of Holocene river behaviour at the regional level (in Northland) have been made using reach-scale data. Sediments preserved at this scale have been used to reconstruct the drainage basin history and the influence of environmental change. The development of a regional model that describes floodplain evolution in Northland is a way of meaningfully collating information from a range of different floodplain settings, and temporally bracketing regionally extensive episodes of fluvial change. Within the broad-scale patterns will be considerable variation between catchments, and also between reaches within the same catchment. This is illustrated by the way channel form changes from the steep gradient and confined reaches in the upper catchment, to the wide alluvial floodplains in the lowland part of the catchment.

Temporal considerations have also been important in this work. The analyses presented here have concentrated on developing a Holocene record of river behaviour at centennial resolution. Essentially, although the depositional record is dominated by event scale responses, more temporally extensive periods of climate variability can be detected as phases of floodplain deposition or incision. The temporal resolution of the New Zealand fluvial ^{14}C database analysis can be considered to be at a level of ‘wet century’ detection, rather than individual climatic events occurring over hours or days.

9.3 Limitations of radiocarbon dating and the fluvial radiocarbon database

The analyses and reconstructions of Holocene river behaviour presented in this thesis have been based on the geochronological information gained from fluvial sediments using the radiocarbon (^{14}C) dating technique: a method based on the premise that the amount of ^{14}C in organic matter can be used to determine the time elapsed since the death of the organism. The accuracy and precision of the ^{14}C dating technique relies on a number of fundamental physical assumptions. The method assumes that the concentration of ^{14}C has remained constant over time, that ^{14}C is homogenously distributed throughout the various reservoirs and that the ratios of carbon isotopes are not altered by any other factors except radioactive decay. Extensive research in the field of ^{14}C dating has proved that these basic assumptions are flawed, therefore, ^{14}C determinations must be corrected using calibration curves and offsets (Suess, 1955; Rafter and Ferguson, 1957; De Vries, 1958; Tans et al., 1979; Stuiver and Braziunas, 1989; Beck et al., 2001; Hughen et al., 2004; Fairbanks et al., 2005; Reimer et al., 2009). In this work, ^{14}C ages have been calibrated using the calibration curve SHCAL04 (McCormac et al., 2004), which is the most up-to-date consensus curve for the Southern Hemisphere, and individual probability distributions associated with each calibrated ^{14}C date have been summed using the ^{14}C calibration programme OxCal version 4.1 (Bronk Ramsey, 1995; 2009). The meta-analyses presented in this research are heavily reliant on the accuracy and precision of the underlying calibration data.

The accuracy and precision of any ^{14}C age assessment also relies on the accurate measurement of residual ^{14}C activity in a representative samples of organic matter. Both the accelerator mass spectrometer (AMS) and radiometric methods were used to determine the ^{14}C ages of the fluvial deposits in the New Zealand database and the Northland samples. A major advantage of radiocarbon dating with AMS is the reduction in the size of the sample required. However, the small sample size of AMS can make the method more vulnerable to low levels of sample or pre-treatment contamination if a unrepresentative portion of an inhomogeneous sample is selected. There will also be variable precision between ages obtained from measurement using AMS (more precise) and the radiometric method.

Robust age determination is dependent on careful sample selection and prevention of contamination from unrepresentative carbon. Material for dating can be contaminated by modern carbon in overlying sediments and organisms, which will result in younger than actual ^{14}C ages. Another major issue of particular significance when ^{14}C dating fluvial derived deposits is the possibility of redeposition and contamination by older isotopically

depleted organic material. Large dating errors can occur when there is a time lag between the death of the organism and deposition. Using charcoal to determine the age of deposition in the fluvial setting can be problematic as charcoal is particularly susceptible to reworking, resulting in ^{14}C ages that are too old (Blong and Gillespie, 1978). Caution must also be taken when using bulk sediments for age determinations as older transported material can produce erroneous ages for deposition.

In terms of the accuracy of ^{14}C ages included in the New Zealand fluvial database, the quality of the data is dependent on the care that individual researchers have taken in selecting representative samples. In addition, material sampled for dating will reflect the particular research agenda of individual projects (i.e., studies designed to determine uplift rates from terrace sequences), potentially creating sampling biases within the dataset. The lack of Northland and Southland ^{14}C dates in the database originally is an example of spatial bias possibly reflecting the tectonic stability of these regions. Temporal bias can also occur in the database when a significant sedimentary unit can be dated more easily by alternative means. In the New Zealand record the Taupo tephra is widespread and recognisable; negating the need for ^{14}C dating of associated fluvial deposits, thereby potentially creating a gap (absence of data) in the ^{14}C dated fluvial record that is not palaeoenvironmentally significant. Other criticisms of ^{14}C databases such as the New Zealand fluvial database are that, typically, case studies are underpinned by only a small amount of dates with no independent dating control, and that the databases incorporates many different types of environmental change (Chiverall et al., 2011).

Additional limitations of the ^{14}C database stem from issues associated with fluvial sediments, their geomorphological context and what they mean in the palaeoenvironmental record. The fluvial sedimentary record is fragmentary and sedimentation units can vary in both areal and temporal extent. A fluvial unit may relate to a single flood event or the sedimentary record may reflect multi-centennial continuous deposition. The fluvial sedimentary archive is also influenced by the extent to which individual units are preserved. Analysis of database of ^{14}C dates only highlights depositional episodes and does not identify phases of increased channel movement, floodplain incision or erosion (although a marked absence of dates can be interpreted as a result of erosion). Despite these limitations, New Zealand fluvial systems are sensitive recorders of environmental change, their sediments preserving a record of response to changes in sediment flux and/or hydrological regime, often without a lagged response that other palaeoenvironmental proxy record may exhibit (i.e., glacier behaviour).

In an effort to mitigate some of limitations associated with the ^{14}C dating technique, database compilation, and interpretation, each ^{14}C date included in the database has been scrutinised by an experienced fluvial geomorphologist. The sedimentary context has been examined by looking at the associated stratigraphic logs and an assessment as to what type of river behaviour each fluvial ^{14}C age is dating (i.e., active floodplain sedimentation) has been made. Ultimately the robustness of the CPF analyses and any palaeoenvironmental interpretations are reliant on the quality of the underlying ^{14}C data in the fluvial database. The CPF methodology should be considered exploratory, a way in which existing data can be utilised, and used to inform the direction of future fluvial research. The fluvial research in Northland provides a blueprint for how fluvial research aimed at expanding the NZ database can be approached in a way that addressed many of the limitations and considerations associated with the CPF and ^{14}C database approach.

9.4 Site selection

The methodological approach and site selection in Northland was driven by the need to avoid spatial and temporal bias in the reconstruction of river behaviour at the regional scale. Obviously, logistical considerations (such as ease of site access) were important, but the overarching consideration was achieving spatial coverage across the region (i.e., sites from east, west, north, south and central Northland). Sites were also selected from across a range of different floodplain types following Nanson and Croke's (1992) genetic classification of floodplains. The Northland sites reflect differences in the geological setting, degree of channel confinement, sediments, slope, bankfull discharge and specific stream power. All of the floodplain sites can be described as either high energy noncohesive floodplains (Class A) or medium energy noncohesive floodplains (Nanson and Croke, 1992). Table 9.1 summarises the floodplain classification and specific stream power for the Northland floodplain sites in Fig. 9.1 and described in Chapter 5. Typically, the more confined sites can be classified as high energy noncohesive floodplain environments with high specific stream power, while the less confined sites are medium energy noncohesive floodplains with low specific stream power (< 100 W m^{-2}). Floodplain type varies throughout the catchment, with the reaches in the upper catchments having higher stream powers, while reaches at the lowland sites are less confined with lower specific stream powers.

Fig. 9.1. Northland study sites. (a) Waimamaku River near Waimamaku. (b) Mangakahia River near Nukutawhiti. (c) Kaeo River near Kaeo. (d) Kaihu River near Maitahi. (e) Takahue River near Pamapuria. (f) Mangakahia River near Titoki. (g) Te Rapa Stream near Panguru. (h) Awanui floodplain near Awanui, Kaitaia. Images: J Richardson, December 2009.

Table 9.1

Floodplain classification and specific stream power for the Northland floodplain sites.

Site	Slope (m/m)	Class[a]/order	Type	specific stream power, ω (W m^{-2})
Awanui	0.0016257	B/B3	Meandering river, lateral-migration floodplain	97
Kaeo	0.0031776	B/B2	Wandering gravel-bed river floodplain	91
Kaihu	0.0009713	B/B3	Meandering river, lateral-migration floodplain	19
Nukutawhiti	0.0038222	A/A2	Confined vertical accretion floodplain	288
Panguru	0.0035135	B/B2	Wandering gravel-bed river floodplain	180
Takahue	0.0056725	B/B2	Wandering gravel bed river floodplain	79
Titoki	0.0057143	A/A2	Confined vertical accretion floodplain	722
Waimamaku	0.0053033	A/A2	Confined vertical accretion floodplain	509

[a] A: High energy noncohesive floodplains, B; Medium energy noncohesive floodplains (Nanson and Croke, 1992).

Another major consideration when selecting sites was the potential for sediment preservation. The more confined reaches in the upper parts of the catchment were typically steeper, bedrock and very coarse gravel/boulder channel beds, with limited sediment sequestration. On the other end of the spectrum, the sites in the lower catchment (i.e., Awanui) were less confined, with wide medium energy floodplains and relatively (compared to reaches in the upper catchment) low rates of floodplain reworking. The depositional records at these sites have a greater potential for preservation, and therefore offered a more temporally extensive record of river behaviour. The location of the reach within the catchment has a major influence on the likelihood of reworking and sediment preservation. Although sites were selected on the basis that they would be able to provide a sedimentary record, there was still an emphasis on sampling across a range of floodplain environments.

9.5 Discharge regime and the geomorphic effectiveness of flood events

A number of factors determine the hydrological response of a catchment, including: rainfall duration and intensity, channel characteristics and catchment physiographic characteristics, geology and soils, vegetation and land use. Climatic characteristics, including temperature and the annual distribution of precipitation, largely determine the discharge regime of river systems. Different regimes can be classified using the mean annual temperature and precipitation range along with the seasonal distribution pattern (Beckinsale, 1969). Based on this classification the discharge regime of Northland rivers can be classified as CS, denoting a warm moist temperate climate with marked summer low flow. Table 9.2 summarises flow statistics for the larger Northland rivers. Low flows are recorded during summer and

maximum historical flows are in the range of 1.5 to 2 times the annual flood flow. The coefficient of variability of discharge for Northland rivers, and indeed most of New Zealand rivers is low due to a temperate moist climate. This is in contrast to the discharge regime of rivers in arid zones where annual runoff can be low but discharge can be highly variable (high discharge coefficient) with extreme floods occurring. In the dynamic coastal sand-bed rivers of NSW Australia, where the coefficient of variability of discharge is large, channel and floodplain morphology is conditioned by alternating decadal scale phases of drought or flooding causing catastrophic floodplain stripping (Nanson and Erskine, 1988). The less-responsive gravel bed rivers of Northland with comparatively low discharge variability are less likely to undergo such catastrophic change. The model of floodplain development in Northland is one of progressive and gradual floodplain accretion and phases of floodplain erosion in response to climatically driven changes in the discharge regime.

The geomorphic effectiveness of floods has important implication in terms of the preservation or reworking along valley floors. Wolman and Gerson (1978) defined geomorphic effectiveness in terms of the ability of an event or combination of events to alter landscape morphology. The geomorphological effectiveness of flood events influences the production and persistence of landforms in the fluvial domain. The most geomorphic effective floods are of medium to long duration, with medium to large total energy expenditure, and large peak stream power per unit area (Costa and O'Connor, 1995). In Northland the geomorphic effectiveness of any given flood event will vary spatially. In the upper reaches of the catchments large stream power per unit area are created when channel are confined in narrow valleys or gorges. At these locations there is a large potential for sediment reworking and limited storage occurs. In contrast, the lower reaches are less confined, stream power is low and there is less potential for sediment erosion and transport.

Table 9.2

Flow statistics for major Northland rivers.

Site no.	River	Min flow ($l\ s^{-1}$)	Mean flow ($l\ s^{-1}$)	Max flow ($m^3\ s^{-1}$)	Annual flood ($m^3\ s^{-1}$)	Years record
1316	Awanui	322	6044	221	149	43
46611	Kaihu	526	4159	395	150	31
46618	Mangakahia (Nukutawhiti)	968	6928	1038	484	41
46626	Mangakahia (Titoki)	1567	25792	949	524	18
46644	Wairua	750	18510	313	205	41

9.5.1 The role of riparian vegetation

Riparian vegetation has a major influence on the hydrology and morphology of river systems (i.e., Hupp and Osterkamp, 1996). Riparian and floodplain vegetation has been shown to play a role in bar and island formation, bank strength and flow hydraulics (Hickin, 1984). The influence of vegetation (both living and dead material) can be stabilising through root reinforcement of banks and flow resistance (Webb and Erskine, 2003) or destabilising due to flow changes and instigation of local scour (Hupp and Osterkamp, 1996). In southeastern Australia, major channel changes (i.e., incision and channel widening) have occurred in response to anthropogenic catchment clearance, the removal of riparian vegetation and desnagging programmes (Brooks and Brierley, 1997; Lester and Boulton, 2008), independent of any change in the flood regime. The impact of riparian vegetation removal in Australian fluvial systems has been to increase the geomorphic effectiveness of flood events, although the timing and pattern of river response varies (Brooks and Brierley, 1997). In recent decades, river managers are increasingly looking to reinstate riparian vegetation in an attempt to restore river system ecological health and geomorphic diversity (Erskine and Webb, 2003).

In New Zealand and Northland, unlike in Australia, there has been no *widespread* concerted management plan to intentionally remove riparian vegetation or large woody debris from river channels to improve flood conveyance. The removal of vegetation from the riparian zones in Northland has largely been a result of the clearance of land for agriculture. The consequence of the lack of riparian vegetation at many sites in recent years is increased geomorphic effectiveness of floods and bank erosion (Fig. 9.2). It is unlikely that riparian vegetation played a major role in conditioning differences in the geomorphic response under climatically driven changes in the hydrologic regime prior to human settlement in Northland. The removal or damage of riparian vegetation would have been restricted to catchment- or reach-scale disturbance, as would occur following channel proximal landsides or storm events. Landslide deposits in the upper Waimamaku River valley provide an example of a pre-anthropogenic geomorphic perturbation that would have potentially damaged riparian vegetation, leading to elevated sediment supply until the catchment vegetation recovered. Wide-spread damage to riparian vegetation in New Zealand since human settlement, and particularly since European settlement, has influenced river behaviour, making it difficult to gauge river response to other environmental changes (i.e., climate) that may have occurred in the late Holocene.

Fig. 9.2. Bank erosion caused by the Mangakahia River, Nukutawhiti, Northland. Image: J Richardson, December 2009.

9.6 Sea-level history of Northland

Knowledge of the timing and extent of Holocene sea-level change in New Zealand is still being developed. Early eustatic sea-level curves constructed for New Zealand showed that present mean sea level (PMSL) was attained ca. 6500 years BP, with a ca. -0.4 m regression at between 5000–4500 years BP and a ca. + 0.6–2.0 m rise above PMSL from ca. 4500-3500 years BP (Gibb, 1986). A more recent composite New Zealand sea-level curve developed for New Zealand suggested that PMSL was attained at ca. 7500 years BP, and continued rising to reach a maxima at ca. +1.0 m above PMSL at ca. 4000 years BP, followed by only minor sea level fluctuation around PMSL until ca. 2000 years BP (Hayward et al., 2010). After ca. 2000 years BP there was a gradual regression to ca. -0.4 m below PMSL at ca. 500 years BP, culminating in a final rise to PMSL (Hayward et. al. 2010). Sea-level curves for the Auckland-Northland region suggest that sea level rose from ca. -3 m below PMSL at ca. 8000 cal. yr BP to attain PMSL by ca. 7700 cal. yr BP (Clement, 2011). Sea level continued to rise to reach a peak +0.9 m above PMSL between 6300 and 5600 cal. yr BP, before falling gradually to reach PMSL by ca. 1600 cal. yr BP (Clement, 2011).

9.6.1 Northland river response to sea-level change

In the early Holocene the rivers systems of Northland would have been graded to a lower sea level (-3 m below PMSL at ca. 8000 cal. yr BP). After attainment of PMSL at ca. 7700 cal. yr BP (Clement, 2011) there appears to have been only gradual sea-level fluctuations within the range of +0.9 m (Clement, 2011), which would have involved minor and gradual adjustments in the river gradients. The transition from estuarine to fluvial deposition at the Kaeo site (the closest site to the present day coast) occurred at 7675–7570 cal. yr BP, which is in agreement with the timing of the attainment of PMSL at ca. 7700 cal. yr BP as identified by Clement (2011). The depositional record at Kaeo highlights the fact that for the more coastal sites, the fluvial depositional record will be limited to within the last ca. 7700 cal yr BP, with the evidence for any prior fluvial deposition buried beneath estuarine deposits. The preservation potential of early Holocene fluvial deposits is low at coastal proximal locations and therefore any palaeoclimate inferences made based on the lack of sedimentation during this period must be made with caution.

In the Northland fluvial deposition record the absence of evidence for floodplain sedimentation does coincide with both a cooler early Holocene and the transition to a warmer and wetter climate from ~10,000 cal. yr BP, with the potential for reduced sediment storage, However, issues associated with the preservation and retrieving early Holocene sediments makes it difficult to decipher the early Holocene fluvial record. In terms of the impact of fluctuation in sea-level after ca. 7700 cal yr BP, there is no indication from the sedimentary record obtained from Kaeo (i.e., fluvial to estuarine transitions or knickpoint recession), or indeed any of the other sites examined in Northland, that gradual and minor sea-level changes had an impact on river behaviour.

A comprehensive description of river response to the transition from the sea-level lowstand during the LGCP to the attainment of PMSL is hampered by a lack of dating control in the Northland region. The existence of Pleistocene terraces at a number of sites suggest that they were formed when river systems were graded to a much lower base-level as occurred during the LGCP. On the geological maps of Northland (Qmap series published by GNS Science), these deposits are classified as Holocene and Pleistocene aged unconsolidated to poorly consolidated sand, mud, peat, and shell deposits of estuarine, lacustrine, swamp, alluvial, and colluvial origins (Q1a), based on minimal (if any) geochronology (Isaac, 1996; Edbrooke and Brook, 2009). Radiocarbon dates obtained in this study obtained from the presumed Pleistocene terraces suggest that deposition was occurring at > 48,000 years ago at the central Northland Nukutawhiti site and at 20,170–19,720 cal yr BP at the western Northland Waimamuku site. Based on these ^{14}C dates, and in the absence of any other

chronology for these terrace surfaces from other published sources, it can be concluded that downcutting of the river to its present position began sometime after 20,170–19,720 cal. yr BP at Waimamaku and after 48,000 years BP at the latest at the Nukutawhiti site. Aggradation river terrace development in New Zealand during the period ca. 30,000–10,000 is thought to be driven by climate change, tectonics and volcanic activity, with the complex terrace sequences preserved as a result of tectonic uplift (Clement and Fuller, 2007). The tectonic stability of Northland throughout the Quaternary (e.g., Brothers, 1954; Cotton, 1957; Gibb, 1986; Pillans, 1986; Brook, 1999; Marra and Alloway, 2006), with some studies suggesting tectonic stability since the Miocene (e.g., Gage 1953; Eiby 1955; Lensen 1975), has resulted in a less complex terrace geomorphology in Northland than other less tectonically stable regions of New Zealand. Without more climate and chronological data for the Northland region it is difficult to determine whether Pleistocene terrace aggradation was purely a response to lower sea-level or whether climatic controls were also involved.

9.7 The Anthropocene and the New Zealand fluvial record

The concept of an 'Anthropocene' initially proposed by Crutzen and Stoermer (2000), and used to describe the present time within the Geological time scale in which Earth system processes are being altered by human activities, is gaining momentum in the scientific literature. Although not yet formally recognised, an 'Anthropocene' working group is considering a proposal to formally accept the term 'Anthropocene' to describe a defined geological unit within the Geological Time Scale, either as a separate Epoch following the Holocene or as a subdivision of the Holocene Epoch. The timing of the beginning of the 'Anthropocene' is a matter for debate (Crutzen and Steffen, 2003), with Crutzen and Stoermer (2000) originally proposing that the start of the 'Anthropocene' followed the invention of the steam engine in 1784. In terms of New Zealand river behaviour, there is clear evidence of human impact on the fluvial stratigraphic record after ~500 cal. yr BP. And in Northland, anthropogenic catchment disturbance after ~1000 cal. yr BP altered the patterns of sediment erosion, transport and deposition in fluvial systems. The deposition of a widespread fine-grained post-settlement alluvium is most likely a response to vegetation clearance following European settlement. Therefore, the New Zealand fluvial record supports the concept of the Anthropocene, with human activities responsible for alterations in fluvial processes after ~500 cal. yr BP, and most notably in Northland since the arrival of Europeans in the early 19th Century.

9.7.1 Disequilibrium associated with human activity

Fluctuations in the sediment supply and hydrology over time mean that a channel must be continually adjusting through the erosion, reworking and deposition of sediments within constraints imposed by the boundary conditions (i.e., geology). A channel can be defined as in equilibrium (steady state) when its form continually fluctuates around an average condition over time (Schumm, 1977). When a landform that tends towards equilibrium is undergoing progressive change in form or output, as can occur in response to environmental change, a state of disequilibrium prevails (Renwick, 1992). Human disturbance is a source of change in the fluvial environment that can lead to disequilibrium (i.e., Renwick, 1992), and the response time will determine the duration of disequilibrium.

The fluvial records of New Zealand and Northland show that human settlement has had a profound effect on river behaviour, with a dominant response of rapid acceleration in floodplain aggradation. It is most likely that catchment disturbance resulting from deforestation increased sediment loads, promoting disequilibrium in New Zealand Fluvial systems. Due to a lack of detailed information on the contemporary behaviour of these rivers, it is not possible to determine whether or not they have returned to equilibrium conditions. Sedimentation rates from Kaeo and other Northland sites suggest that the dominant response to anthropogenic induced land-use change has been rapid infilling of the valley floor. In Kaeo, stratigraphical and geomorphologic data indicates that the river may still be responding to catchment vegetation changes and still in disequilibrium. Sedimentation rates in the lowland valley remain high despite catchment revegetation, and sediment stored in the channel and floodplain are important components of the sediment budget.

9.7.2 Management implications

Flooding and sediment management are key issues for catchment management in Northland. A feature in many of the small settlements in Northland is that the old churches, and indeed the older dwellings, are located well above the contemporary floodplain (i.e., in Panguru on the Late Pleistocene terrace), while more recent buildings (from ~1940) are more inclined to be built on less elevated sites. This suggests that flooding (at least since European settlement) in many parts of Northland has been a regular occurrence, and that only in the most recent decades pressure for suitable land (and possibly a reduced occurrence of large floods?) has resulted in more development on the Holocene floodplain.

The sites most at risk from flooding in Northland are the less confined lowland floodplain sites (i.e., Kaihu) and the most confined sites (i.e., Kaeo), where there is only a single

Holocene floodplain surface. At partly confined sites such as Waimamaku River and Takahue River the presence of a Holocene terrace has provided an elevated surface, and most of the building and infrastructure is located here. The issue with a temporally limited documented flood record and only a short history of human settlement is that the flood magnitude and frequency record is only relatively short compared with the entire Holocene period. However, the reconstructed flood history shows that these high Holocene surfaces have been inundated in the past, and although flooding at this level represents a extremely high magnitude low frequency event, flooding to this extent could potentially occur in the future. The fact that extreme floods have occurred in the past, combined with the predictions of future climate change, and the potential for a greater frequency for extreme events (the most likely to cause high magnitude flood events), makes some Northland floodplain locations particularly vulnerable to inundation. Any future development on the contemporary floodplain, especially at lowland floodplain sites and confined settings, should consider the potential flood risk calculated for more than just the historical flood record.

The most vulnerable sites to flooding at present in Northland (i.e., Kaeo) face more immediate issues of how to protect infrastructure and homes from more frequent but lower magnitude events. Flood protection engineering is an expensive option and before this level of investment is made the longer term trajectory of river behaviour should be understood, along with the implications of ongoing river adjustment to past environmental change and the potential impact of predicted future climate change. Once again, it is important to consider the flood frequency and magnitude record over a time-scale longer than European settlement. Cost benefit analysis of flood protection works should consider the potential for more frequent floods and extreme floods in future scenarios, and future development on the most flood prone sites should be restricted.

Chapter 10

Synthesis and conclusions

10.1 Introduction

This thesis has aimed to determine the influence of Holocene climate change on river behaviour in New Zealand and more specifically Northland, by reconstructing Holocene river response to environmental change at the national and regional scale. This has been achieved through the integration of meta-data analysis of a New Zealand fluvial radiocarbon (^{14}C) database with targeted field research in catchments across the Northland region. The first section in this chapter synthesises the research, drawing together several strands, including: Holocene climate change, river response to Holocene environmental change, New Zealand river response to Holocene environmental change, Northland floodplain development and Northland Holocene fluvial history. Following the synthesis, the main conclusions addressing the specific objectives stated in Section 1.2 are summarised. Finally, the research implications and potential direction of future research are outlined.

10.2 Synthesis

The review of Holocene climate in Chapter 2 presents the evidence for a variable climate during the Holocene. Although Holocene climate change has not been of the magnitude observed during the Last Glacial period, climate variability has influenced human societies and ecosystems (e.g., Mayewski et al., 2004). Solar variability, due to orbital precessional changes and cosmic ray flux, is thought to be the key driver of millennial- to centennial-scale Holocene climate change. However, a number of different forcing factors, feedbacks and teleconnections, operating across a range of spatial and temporal scales within the interconnected ocean-atmosphere-cryosphere system, are also involved in Holocene climate change.

Comprehensive reviews of globally-distributed palaeoclimate proxy data have identified broad patterns of globally extensive major periods of rapid climate change, or cold climate events, overprinting complex regional patterns of climate variability (e.g., Mayewski et al., 2004; Wanner et al. 2011). Although these reviews have provided evidence for global climate forcing, they are dominated by Northern Hemisphere records and a lack of well-dated high-resolution palaeoclimate records from the Southern Hemisphere is preventing a more comprehensive understanding of global climate dynamics (e.g., Denton and Broecker, 2008; Wanner et al., 2011). It is this knowledge gap that this research has addressed, by applying meta-analysis techniques to ^{14}C-dated Holocene fluvial units in New Zealand and Northland; producing the first centennial-scale probability-based reconstruction of river response to environmental (including climate) change in this region.

Since fluvial systems respond to environmental changes, and preserve a sedimentary record of river response to those changes, they offer considerable potential for reconstructing centennial-scale hydro-climatic change (e.g., Macklin and Lewin, 2003; Johnstone et al., 2006; Harden et al., 2010; Hoffmann et al., 2008; Macklin et al., 2010; 2012; Turner et al., 2010). Chapter 3 outlined the key mechanisms involved in driving Holocene river behaviour, the nature of river response to environmental perturbation, the way in which fluvial systems record environmental changes and the state of knowledge as to how New Zealand rivers have responded to environmental change during the Holocene. This demonstrated that New Zealand rivers, like river systems globally, have responded to environmental changes during the Holocene. Climate variability associated with atmospheric circulation change has influenced erosion and sedimentation in New Zealand river systems (Grant 1985). However, New Zealand's active tectonic setting means that tectonic and volcanic drivers also play a role in New Zealand river dynamics (e.g., Manville, 2002; Litchfield and Berryman, 2005). Anthropogenic impacts on sediment flux have been confined to the last several hundred years (e.g., Grant 1985). To date however, there has been limited research on river behaviour in New Zealand at the regional- or national-scale, with investigations largely restricted to the catchment- and reach-scale. Chapter 4 addressed this gap in the research using the recently compiled New Zealand fluvial ^{14}C database (Macklin et al., 2012) and the meta-analysis approach to aggregate and analyse data from individual fluvial studies, thereby, providing the first truly regional assessment of New Zealand Holocene river behaviour.

This was achieved by applying meta-analysis techniques to a database (Macklin et al., 2012a) of 401 ^{14}C-dated Holocene fluvial units in New Zealand to produce a probability-based reconstruction of Holocene river behaviour at the national and regional scales. These records

of river activity, which do not include any Northland data, reveal a pattern of multi-centennial-length episodes of increased fluvial activity throughout the Holocene, with 12 multi-centennial length episodes of river activity and flooding identified in the North Island, and 11 episodes identified in the South Island record. Thus, episodes of river activity in northern and southern regions have exhibited a predominantly out-of-phase relationship. This is driven by the phase relationship between El Niño Southern Oscillation (ENSO) and the Southern Annular Mode (SAM), and the relative dominance of the two modes. This is consistent with research that indicates northern New Zealand is predominantly affected by atmospheric circulation in the tropical Pacific and the operation of ENSO, while the South Island is most affected by circulation changes associated with the subpolar westerlies and the oscillation of the SAM (Ummenhofer and England, 2007).

Therefore, this meta-analysis suggests large-scale atmospheric changes are involved in driving major episodes of river activity in New Zealand, and at least at the regional scale, have overridden any forcing due to base-level, tectonic or volcanic influences. The emerging pattern of river activity in New Zealand is one of increased river activity in the South Island primarily in response to enhanced westerly atmospheric circulation, associated with a predominance of trough regime synoptic type promoted by negative SAM-like circulation. In the North Island, episodes of river activity are primarily driven by increased meridional atmospheric circulation associated with blocking regime synoptic conditions enhanced by La Niña-like and positive SAM-like circulation.

In addition to strong north-south hydro-climatic contrasts in New Zealand, interactions between the prevailing westerly circulation and axial ranges in both islands ensure strong east-west regional contrasts. Although the meta-analysis found that all regions had experienced phases of river activity during the Holocene, a comprehensive regional assessment of river behaviour was not possible due to a lack of ^{14}C-dated fluvial units, most markedly in far northern (Northland) and far southern (Southland) New Zealand. The absence of fluvial research and ^{14}C-dated fluvial units in the Northland region is addressed in Chapters 5 to 8, because the river systems of Northland, the most northern region of New Zealand, are among the least researched rivers in the country, and very little is known about their behaviour during the Holocene. Northland's distance from the main zone of plate convergence between the Australian and Pacific plates and the Taupo Volcanic Zone, and New Zealand's short history of human settlement, means that the complications of tectonically- and volcanically-driven catchment disturbance are absent from Northland river systems, while anthropogenic impacts are restricted to the late Holocene. Northland therefore represented an ideal opportunity to examine river behaviour at a regional scale, and

to further elucidate the role that climate and late Holocene anthropogenic impacts have had on New Zealand rivers.

In Chapter 5, valley floor mapping, sedimentology and ^{14}C dating reconstructed the Holocene fluvial history at eight floodplain sites spread throughout Northland to develop a model of Holocene floodplain development for different valley settings which demonstrated: i) an absence of early to mid Holocene valley-fills (pre ~ 6500 cal. yr BP), ii) region-wide floodplain alluviation through the mid to late Holocene, iii) valley floor entrenchment and floodplain erosion beginning after ~ 2000 cal. yr BP, and iv) rapid rates of vertical accretion in response to post-settlement catchment disturbance. The absence of early to mid Holocene valley-fills, coincided with a warmer, wetter climate detected in the fossil pollen record, suggesting that during this period enhanced discharge and reduced sediment loads resulted in limited floodplain sediment storage. By contrast, in the mid to late Holocene, a single Holocene floodplain surface formed in less confined and more confined valley settings, often bounded by elevated remnant Pleistocene terraces, in response to episodic overbank deposition. The limited accommodation space for sediment storage, afforded by the more confined valley setting (Kaeo and Titoki sites), means that the rate of alluviation has been relatively rapid here, burying older Holocene deposits. In the less confined valley settings (Kaihu, Panguru and Awanui sites) sediment was stored over a greater area and the geomorphology associated with floodplain reworking processes is often better preserved.

At partly confined valley sites (Waimamaku and Takahue sites), which represent an intermediate position between the less confined and more confined sites (where only a single Holocene surface is found), two Holocene terraces were discerned. Aggradation of the higher floodplain surface occurred during the mid to late Holocene in response to climatic deterioration, with the occurrence of large storms and floods, which disturbed catchments and increased sediment supply. After ~ 2000 cal. yr BP, a phase of degradation coincided with a transition to a warmer, wetter and less disturbed climate regime identified in the regional pollen records. This period of incision was then followed by rapid sedimentation of fine-grained post-settlement alluvium, resulting from anthropogenically-driven catchment disturbance, leading to the development of a lower late Holocene floodplain surface.

Chapter 5 demonstrated that in Northland variations in sediment flux in response to climatic, and more recently anthropogenic, catchment disturbance, is the primary control on Northland floodplain geomorphology. Valley floor confinement has also played a major role in controlling floodplain development, accounting for differences in the specific fluvial unit assemblages between sites, and therefore conditioning the precise fluvial response. These

results also highlight the opportunities that partly confined valley settings in particular, offer for reconstructing fluvial histories, preserving ^{14}C-dated fluvial units that contributed to the expansion of the New Zealand fluvial record. Accordingly, 21 new fluvial ^{14}C ages obtained from the Northland region were added to the New Zealand fluvial ^{14}C database to revise the probability-based centennial-scale record of Holocene New Zealand river behaviour. This improved the resolution of the record of river activity for the northern New Zealand precipitation region. Importantly, results showed that rivers in northern New Zealand, like other North and South Island rivers have exhibited sensitivity to short-term and rapid Holocene climate variations. This finding then supports the model developed in Chapter 4, that river activity in New Zealand is predominantly influenced by atmospheric circulation variability in spite of tectonic and volcanic influences. These findings demonstrated the value of using targeted field research to assess river activity at the coherent precipitation region scale and highlight the significance of climate control in New Zealand catchments during the Holocene.

In order to assess the phase relationship between global and regional climate changes and river behaviour in Northland during the Holocene, meta-analysis was applied to 21 fluvial ^{14}C dates representing river activity (Chapter 7). Focusing on Northland inevitably thinned the data available for analysis, but three significant phases (underlain by at least three fluvial 'activity' ^{14}C dates) of river activity at 3500–2800, 800–600 and 500–300 cal. yr BP were identified. The phase of river activity occurring between 3500–2800 cal. yr BP was responsible for Holocene floodplain aggradation and the development of the high Holocene floodplain surface in partly confined valley settings discussed in Chapter 5. Comparison of the probability-based record of river activity with independent regional and global palaeoclimate proxy records indicates that this phase of river activity occurred in response to a globally extensive Holocene cold event (Chapter 7). This period also coincided with a time of enhanced connectivity between the low and high latitudes, correlation between the SAM and ENSO climate modes and ENSO intensification. Evidence for increased seasonality and disturbance in the regional pollen record coeval with this significant phase of river activity suggests enhanced sediment supply linked with catchment disturbance, potentially involving widespread canopy disturbance during storms in kauri dominated forests, has driven river activity in the region. This pattern of river behaviour in Northland is consistent with models developed in Chapter 4 and 5 that suggested river activity in northern New Zealand is most likely driven by increased meridional circulation, which brings a predominance of moist northeasterly atmospheric flow, and promoted by La Niña conditions and positive phases of the SAM.

The episodes of river activity identified in the Northland record, at 800–600 cal. yr BP and 500–300 cal. yr BP occurred during a period when anthropogenic impacts (Māori and European settlement and forest clearance) were likely to have played a major role in river behaviour. Floodplain sedimentation rates have undergone rapid acceleration in the last ~ 500 years, most likely as response to human-induced deforestation and widespread catchment disturbance (Chapter 4). Variation in sediment flux in response to anthropogenic catchment perturbation was the primary control on Northland floodplain geomorphology within the last ~ 1000 years. In partly confined valley settings a period of floodplain erosion (sometime after ~ 2000 cal. yr BP) was followed by the aggradation of a low Holocene floodplain surface, associated with rapid vertical accretion of post-settlement alluvium.

In confined sites such as Kaeo in eastern Northland, rapid acceleration in floodplain sedimentation in response to anthropogenic catchment disturbance has created significant catchment management issues (i.e., flooding and water quality). At Kaeo terrestrially-sourced sedimentation commenced at 7675–7570 cal. yr BP, and continued at an average rate of < 4 mm yr^{-1} until human occupation. However, in the last several hundred years, under conditions of limited accommodation space, the floodplain accumulated at a faster average rate (~ 7.2 mm yr^{-1}) in response to anthropogenic catchment disturbance following Māori and European settlement. Floodplain aggradation associated with European deforestation has undergone a more than tenfold (from 0.7 to 42.2 mm yr^{-1}) increase above pre-human influenced sedimentation rates, producing a greater impact on floodplain morphology than any other environmental change in the last ~ 7500 years, including, hitherto the primary driver of climate. This demonstrates the scale of perturbation and disequilibrium associated with human activity in these fluvial systems.

This thesis has produced a new probability-based centennial-scale palaeohydro-climate proxy record for the New Zealand, located in the land-sparse mid-latitudes of the Southern Hemisphere; providing an important and rich data-source. It has integrated the reconstruction of the first fluvial histories in the Northland region with a recently compiled New Zealand ^{14}C database and demonstrated that prior to human settlement, Holocene river behaviour in New Zealand has been primarily driven by regional centennial-scale climate variability, with atmospheric circulation playing a key role. The work has shown that despite the complexity afforded by tectonic and volcanic disturbance, and a strongly regionalised climate due to New Zealand's latitudinal span and interactions between orography and the prevailing westerly flow, New Zealand's rivers are sensitive respondents to and recorders of climate change. In fact, regional climate complexity provides opportunities for palaeoclimate and palaeocirculation (atmospheric) reconstruction, with this research

demonstrating the value of targeted field research for improving the resolution of the fluvial record at the coherent precipitation region level.

Finally, in addressing the question, "are the Northland rivers of New Zealand in synchrony with global Holocene climate change?", this research finds that yes, prior to human disturbance, Northland rivers were in synchrony with global Holocene climate change. While there is a high level of regional climate complexity in New Zealand and river behaviour is primarily driven by regional climate forcing, evidence from Northland rivers suggests that a globally extensive abrupt climate change signal can promote a synchronous fluvial response, overprinting complex regional patterns of Holocene river behaviour.

10.3 Conclusions addressing the thesis aims

10.3.1 The influence of Holocene climate change on river behaviour in New Zealand

The first aim of this research was to determine the influence of Holocene climate change on river behaviour in New Zealand. Probability-based records of river activity in New Zealand show a pattern of multi-centennial-length episodes of increased fluvial activity throughout the Holocene. During the Holocene, 12 multi-centennial length episodes of river activity and flooding were identified in the North Island, and in the South Island record 11 periods exceed the mean relative probability of activity. Out-of-phase river activity between the North and South Islands suggests a phased relationship between ENSO and SAM, and the relative dominance of the two modes, may be responsible for driving Holocene river activity in New Zealand. The northern precipitation region and Northland experienced episodes of river activity primarily in response to enhanced meridional atmospheric circulation associated with La Niña-like and positive SAM-like circulation. In contrast, river activity in southern New Zealand is promoted by strengthened westerly circulation enhanced under negative phase SAM-like circulation conditions. At the resolution afforded by this study, it appears that during the Holocene, variability in atmospheric circulation is the key driver of river activity in New Zealand.

10.3.2 Chronology of river activity and the fluvial history of Northland catchments during the Holocene

This research also aimed to develop a chronology of river activity and reconstruct the fluvial history at selected sites across the Northland region. Reconstruction of the fluvial history at

eight sites has been used to develop a model of Holocene floodplain development for different valley confinement settings. An absence of early to mid Holocene valley-fills, coinciding with a warmer and wetter climate, suggests a period of enhanced discharge, reduced sediment load and limited sediment storage during this time. At the least and most confined sites a single Holocene floodplain surface aggraded during the mid to late Holocene. In partly confined valley settings two Holocene floodplain surfaces can be identified. In the mid to late Holocene, aggradation of the higher surface has occurred in response to climatic deterioration, which has disturbed catchments and increased the sediment supply from the catchment. After ~ 2000 cal. yr BP there was a phase of degradation, coinciding with a transition to a warmer, wetter and less disturbed climate regime identified in the regional pollen records. This phase of degradation was followed by rapid sedimentation of fine-grained alluvium resulting from anthropogenic driven catchment disturbance and the formation of a lower late Holocene floodplain surface.

Northland Holocene floodplain development and valley floor morphology reflects the interplay between valley configuration and accommodation space (geologically controlled) within the fluvial system, sediment supply, fluctuation in climate, and anthropogenic factors in the last several hundred years. Variations in sediment flux in response to climatic, and more recently anthropogenic, catchment disturbance, is the primary control on Northland floodplain geomorphology. Valley floor confinement accounts for differences in the specific fluvial unit assemblages between sites.

10.3.3 The degree of synchrony between global climate change and river behaviour in Northland during the Holocene

It was the aim of this research to apply meta-data analysis techniques to new radiocarbon ages from Northland catchments and address the question as to whether climate change in Northland is in synchrony, or out of phase with global climate change. Meta-analysis of Holocene ^{14}C-dated fluvial units from Northland identified three significant phases of river activity at 3500–2800, 800–600 and 500–300 cal. yr BP. The phase of river activity at 3500–2800 cal. yr BP occurred in response to a globally extensive Holocene cold event at a time of enhanced connectivity between the low and high latitudes, correlation between the SAM and ENSO climate modes and ENSO intensification. In Northland, river activity is most likely enhanced by meridional circulation and moisture laden northeasterly atmospheric flow, promoted by La Niña conditions and positive phases of the SAM. Enhanced sediment supply due to climatically driven catchment disturbance is a key driver of river activity in the region. In the last ~ 800 years increased sediment flux associated with widespread post-settlement deforestation has had a major impact on Northland river dynamics. Thus, at the resolution of

the study it can be concluded that prior to human colonisation rivers in Northland were in synchrony with global climate change.

10.3.4 Human impacts on catchment stability following Māori and European settlement in Northland

The final aim of the research was to identify human impacts on catchment stability following Māori and European settlement in Northland. Analysis of New Zealand ^{14}C-dated fluvial units indicate rapid acceleration in floodplain sedimentation after ~ 500 cal. yr BP following commencement of anthropogenic deforestation. In Northland, the pattern of floodplain development during the Holocene has involved a climatically forced period of mid to late Holocene floodplain aggradation followed by floodplain incision and finally rapid refilling in response to post-settlement catchment disturbance. Meta-analysis of ^{14}C-dated fluvial deposits in Northland floodplains identified increased river activity at 800–600 cal. yr BP and 500–300 cal. yr BP, potentially representing two episodes of late Holocene fluvial activity in the region within the timeframe of human settlement. Floodplain sedimentation rates in Kaeo accelerated in the last ~ 500 years following Polynesian settlement. However, at the Kaeo site, post-European deforestation has had a greater influence on floodplain morphology and floodplain sedimentation than any other environmental change in the last 7500 years. Floodplain sedimentation has remained high in recent decades, despite increased cover of regenerated native forest and exotic plantation forests.

10.4 Research implications

This research has made an original contribution to palaeohydro-climate research through the use of targeted fluvial research in Northland and the recently compiled New Zealand fluvial ^{14}C database, to elucidate the role that climate change and anthropogenic impacts have had on New Zealand river behaviour. The results suggest that at the centennial-scale, regional atmospheric circulation change is the key driver of river behaviour for most of the Holocene, with anthropogenic catchment disturbance responsible for enhanced river activity and floodplain aggradation in the last ~ 500 years. It is therefore likely that any climate change involving a shift in the atmospheric circulation regime will impact on river behaviour in New Zealand. More specifically, increased incidence or strength in meridional flow as promoted by positive phases of the SAM and La Niña will tend to enhance river activity in Northern regions of New Zealand, while river activity in southern New Zealand will be enhanced by strengthened westerly flow (promoted under negative SAM and El Niño phases). However, at the catchment- or reach-scale, river response will be largely

determined by local controls such as sediment supply and accommodation space, with these factors largely moderated by the post-settlement fluvial history.

10.5 Future research

The interrogation of the New Zealand fluvial ^{14}C database has proved to be valuable in terms of isolating the temporal and spatial patterns of climate change and anthropogenic impacts on fluvial systems, despite the complexity afforded by tectonics and a strongly regionalised climate. This research has also demonstrated the value of targeted field research in improving the resolution of the database at the regional level, thereby contributing to an improved understanding of palaeocirculation patterns and regional hydro-climate dynamics. There is considerable potential for future research aimed at improving the spatial and temporal resolution of the New Zealand fluvial ^{14}C database, with special attention paid to geographical gaps in the record (i.e., northwestern and southern South Island).

A second area of focus for future research should be post-settlement alluviation. This research has highlighted the massive impact that post-settlement alluviation, particularly post-European settlement, has had on Northland river systems. Floodplain sediment rates have accelerated far beyond those induced by other environmental change in the Holocene, including climate. More work is required to improve the knowledge around post-European settlement sedimentation rate dynamics and controls (i.e., have high sedimentation rates following initial European land clearance remained high, or tailed off, and what controls are involved). In addition more information is required in terms of assessing and modelling the ongoing impacts of post-settlement alluviation and the potential interactions with climate change. An improved understanding could make a contribution to the future management of floodplain environments, especially in light of predicted future anthropogenically forced rapid climate change.

References

Adams, K. D. (2012). Response of the Truckee River to lowering base level at Pyramid Lake, Nevada, based on historical air photos and LiDAR data. Geosphere, 8, 607–627.

Alley, R. B., Mayewski, P. A., Sowers, T., Stuiver, M., Taylor, K. C., Clark, P. U. (1997). Holocene climatic instability: A prominent, widespread event 8200 yr ago. Geology, 25, 483–486.

Alloway, B. V., Lowe, D. J., Barrell, D. J. A., Newnham, R. M., Almond, P. C., Augustinus, P. C., Bertler, N. A. N., Carter, L., Litchfield, N. J., McGlone, M. S., Shulmeister, J., Vandergoes, M. J., Williams, P. W. (2007). Towards a climate event stratigraphy for New Zealand over the past 30 000 years (NZ-INTIMATE project). Journal of Quaternary Science, 22, 9–35.

Anderson, E., Harrison, S., Passmore, D. G., Mighall, T. M., Wathan, S. (2004). Late Quaternary river terrace development in the Macgillycuddy's Reeks, southwest Ireland. Quaternary Science Reviews, 23, 1785–1801.

Anderson, H., Webb, T. (1994). New Zealand seismicity patterns revealed by the upgraded national seismograph network. New Zealand Journal of Geology and Geophysics, 37, 477–493.

Angell, J. K., Korshover, J. (1985). Surface temperature changes following six major volcanic episodes between 1780 and 1980. Climate and Applied Meteorology, 24, 937–951.

Arz, H. W., Gerhardt, S., Pätzold, J., Röhl, U. (2001). Millennial-scale changes of surface- and deep-water flow in the western tropical Atlantic linked to Northern Hemisphere high-latitude climate during the Holocene. Geology, 29, 239–242.

Ashworth, P. J., Best, J. L., Jones, M. (2004). Relationship between sediment supply and avulsion frequency in braided rivers. Geology, 32, 21–24.

Augustinus, P., Bleakley, N., Deng, Y. B., Shane, P., Cochran, U. (2008). Rapid change in early Holocene environments inferred from Lake Pupuke, Auckland City, New Zealand. Journal of Quaternary Science, 23, 435–447.

Augustinus, P., Cochran, U., Kattel, G., D'Costa, D., Shane, P. (2012). Late Quaternary paleolimnology of Onepoto maar, Auckland, New Zealand: Implications for the drivers of regional paleoclimate. Quaternary International, 253, 18–31.

Augustinus, P., D'Costa, D., Deng, Y., Hagg, J., Shane, P. (2011). A multi-proxy record of changing environments from ca. 30 000 to 9000 cal. a BP: Onepoto maar palaeolake, Auckland, New Zealand. Journal of Quaternary Science, 26, 389–401.

Barber, D. C., Dyke, A., Hillaire-Marcel, C., Jennings, A. E., Andrews, J. T., Kerwin, M. W., Bilodeau, G., McNeely, R., Southon, J., Morehead, M. D., Gagnon, J. M. (1999). Forcing of the cold event of 8,200 years ago by catastrophic drainage of Laurentide lakes. Nature, 400, 344–348.

Barrell, D. J. A., Almond, P. C., Vandergoes, M. J., Lowe, D. J., Newnham, R. M. (2013). A composite pollen-based stratotype for inter-regional evaluation of climatic events in New Zealand over the past 30,000 years (NZ-INTIMATE project). Quaternary Science Reviews.

Basher, L. R., Lynn, I. H., Whitehouse, I. E. (1995). Geomorphology of the Wairau floodplain and implications for floodplain management planning, Landcare Research Science Series No. 11 (pp. 42). Lincoln.

Beck, J. W., Richards, D. A., Edwards, R. L., Silverman, B. W., Smart, P. L., Donahue, D. J., Hererra-Osterheld, S., Burr, G. S., Calsoyas, L., Jull, A. J. T., Biddulph, D. (2001). Extremely Large Variations of Atmospheric 14C Concentration During the Last Glacial Period. Science, 292, 2453–2458.

Becker, B., Schirmer, W. (1977). Palaeoecological study on the Holocene valley development of the River Main, southern Germany. Boreas, 6, 303–321.

Beckinsale, R. P. (1969). River Regimes. In R. J. Chorley (Ed.), *Introduction to Physical Hydrology* (pp. 176). London: Methuen.

Beetham, R. D., McSaveney, M., Dellow, G., Rosenberg, M., Johnston, D., Smith, W. (2004). A review of natural hazards information for Northland region, IGNS Science Report 2004/2006. Lower Hutt: GNS.

Bentley, M. J., Hodgson, D. A., Smith, J. A., Cofaigh, C. Ó., Domack, E. W., Larter, R. D., Roberts, S. J., Brachfeld, S., Leventer, A., Hjort, C., Hillenbrand, C.-D., Evans, J. (2009). Mechanisms of Holocene palaeoenvironmental change in the Antarctic Peninsula region. The Holocene, 19, 51–69.

Berger, A., Loutre, M. F. (1991). Insolation values for the climate of the last 10 million years. Quaternary Science Reviews, 10, 297–317.

Berryman, K., Marden, M., Eden, D. N., Mazengarb, C., Ota, Y., Moriya, I. (2000). Tectonic and paleoclimatic significance of Quaternary river terraces of the Waipaoa River,

east coast, North Island, New Zealand. New Zealand Journal of Geology and Geophysics, 43, 229–245.

Berryman, K., Marden, M., Palmer, A., Wilson, K., Mazengarb, C., Litchfield, N. (2010). The post-glacial downcutting history in the Waihuku tributary of Waipaoa River, Gisbourne district: implications for tectonics and landscape evolution in the Hikurangi subduction margin. Marine Geology, 270, 55–71.

Bianchi, G. G., McCave, I. N. (1999). Holocene periodicity in North Atlantic climate and deep-ocean flow south of Iceland. Nature, 397, 515–517.

Björck, S., Walker, M. J. C., Cwynar, L. C., Johnsen, S., Knudsen, K.-L., Lowe, J. J., Wohlfarth, B. (1998). An event stratigraphy for the Last Termination in the North Atlantic region based on the Greenland ice-core record: a proposal by the INTIMATE group. Journal of Quaternary Science, 13, 283–292.

Blong, R. J., Gillespie, R. (1978). Fluvially transported charcoal gives erroneous 14C ages for recent deposits. [10.1038/271739a0]. Nature, 271, 739-741.

Bond, G., Kromer, B., Beer, J., Muscheler, R., Evans, M. N., Showers, W., Hoffmann, S., Lotti-Bond, R., Hajdas, I., Bonani, G. (2001). Persistent solar influence on North Atlantic climate during the Holocene. Science, 294, 2130–2136.

Bond, G., Showers, W., Cheseby, M., Lotti, R., Almasi, P., deMenocal, P., Priore, P., Cullen, H., Hajdas, I., Bonani, G. (1997). A pervasive millenial-scale cycle in North Atlantic Holocene and glacial climates. Science, 278, 1257–1266.

Boswijk, G., Fowler, A., Lorrey, A., Palmer, J., Ogden, J. (2006). Extension of the New Zealand kauri (Agathis australis) chronology to 1724 BC. The Holocene, 16, 188–199.

Brackenridge, G. R. (1980). Widespread episodes of stream erosion during the Holocene and their climatic cause. Nature, 283, 655–656.

Bradley, R. S. (1988). The explosive volcanic eruption signal in Northern Hemisphere continental temperature records. Climatic Change, 12, 221–243.

Brazier, V., Whittington, G., Ballantyne, C. K. (1988). Holocene debris cone evolution in Glen Etive, Western Grampien Highlands, Scotland. Earth Surface Processes and Landforms, 13, 525–531.

Brierley, G. J. (2010). Landscape memory: the imprint of the past on contemporary landscape forms and processes. Area, 42, 76–85.

Brierley, G. J., Fryirs, K., Outhet, D., Massey, C. (2002). Application of the River Styles framework as a basis for river management in New South Wales, Australia. Applied Geography, 22, 91–122.

Brierley, G. J., Fryirs, K. A. (2005). Geomorphology and river management: applications of the River Styles Framework (pp. 398). Oxford, UK: Blackwell Publishing.

Brodie, J. W. (1957). Late Pleistocene beds, Wellington Peninsula. New Zealand Journal of Science and Technology, B38, 623–643.

Bronk Ramsey, C. (1995). Radiocarbon calibration and analysis of stratigraphy: the OxCal program. Radiocarbon, 37, 425–430.

Bronk Ramsey, C. (2001). Development of the radiocarbon calibration program OxCal. Radiocarbon, 43, 355–363.

Bronk Ramsey, C. (2009). Bayesian analysis of radiocarbon dates. Radiocarbon, 51, 337-360.

Brönnimann, S., Xoplaki, E., Casty, C., Pauling, A., Luterbacher, J. (2007). ENSO influence on Europe during the last centuries. Climate Dynamics, 28, 181–197.

Brook, E. J., Sowers, T., Orchado, J. (1996). Rapid variations in atmospheric methane concentration during the past 110,000 years. Science, 273, 1087–1091.

Brook, F. J. (1999). Stratigraphy and landsnail faunas of Late Holocene coastal dunes, Tokerau Beach, northern New Zealand. Journal of the Royal Society of New Zealand, 29, 337–359.

Brooks, A. P., Brierley, G. J. (1997). Geomorphic responses of lower Bega River to catchment disturbance 1851–1926. Geomorphology, 18, 291–304.

Brothers, R. N. (1954). The relative Pleistocene chronology of the South Kaipara District, New Zealand. Transactions of the Royal Society of New Zealand, 82, 677–694.

Brown, L. J. (1995). Holocene shoreline depositional processes at Poverty Bay, a tectonically active area, northeastern North Island, New Zealand. Quaternary International, 26, 21–33.

Buckland, P. C., Amorosi, T., Barlow, L. K., Dugmore, A. J., Mayewski, P. A., McGovern, T. H., Ogilvie, A. E. J., Sadler, J. P., Skidmore, P. (1995). Bioarchaeological evidence and climatological evidence for the fate of Norse farmers in medieval Greenland. Antiquity, 70, 88–96.

Bull, W. B. (1990). Stream-terrace genesis: implications for soil development. Geomorphology, 3, 351–367.

Bull, W. B. (1991). Geomorphic responses to climate change. New York: Oxford University Press.

Campbell, J. K., Nicol, A., Howard, M. E. (2003). Long-term changes to river regimes prior to late Holocene coseismic faulting, Canterbury, New Zealand. Journal of Geodynamics, 36, 147–168.

Carter, L. (2001). Currents of change. Water and Atmosphere, 9, 15–17.

Cathcart, R. W. (1978). Soil conservation and erosion control, in R.C Holland (ed.) Northland regional resources survey: Northland Regional Development Council in

partnership with Northland Regional Planning Authority. Northland Regional Development Council: Northland Regional Planning Authority, Whangarei. 438 pp.

Changnon, S. A. (1983). Trends in floods and related climate conditons in Illinois. Climatic Change, 5, 341–363.

Charles, C. D., Lynch-Stieglitz, J., Ninnemann, U. S., Fairbanks, R. G. (1996). Climate connections between the hemispheres revealed by deep sea sediment core/ice core correlations. Earth and Planetary Science Letters, 142, 19–27.

Charman, D. J. (2010). Centennial climate variability in the British Isles during the mid–late Holocene. Quaternary Science Reviews, 29, 1539–1554.

Chatfield, C. (2004). The analysis of time series (6th ed.). Boca Raton: Chapman and Hall.

Chiew, F. H. S., McMahon, T. A. (2002). Global ENSO streamflow teleconnection, streamflow forecasting and interannual variability. Hydrological Sciences Journal, 47, 505–522.

Chiverrell, R. C., Thorndycraft, V. R., Hoffmann, T. O. (2011a). Cumulative probability functions and their role in evaluating the chronology of geomorphological events during the Holocene. Journal of Quaternary Science, 26, 76–85.

Chiverrell, R. C., Thorndycraft, V. R., Hoffmann, T. O. (2011b). Reply to Comment: Cumulative probability functions and their role in evaluating the chronology of geomorphological events during the Holocene. [Chiverrell et al. (2011)]. Journal of Quaternary Science, 26, 241–244.

Church, M. (1998). Space, time and the mountain - how do we order what we see? In B. L. Rhoads C. E. Thorn (Eds.), *The scientific nature of geomorphology: Proceedings of the 27th Binghamton Symposium in Geomorphology held 27–29 September 1996* (pp. 147–170): John Wiley & Sons Ltd.

Clark, P. U., Alley, R. B., Pollard, D. (1999). Northern Hemisphere ice-sheet Influences on global climate change. Science, 286, 1104–1111.

Claussen, M., Gayler, V. (1997). The greening of Sahara during the mid-Holocene: results of an interactive atmosphere-biome model. Global Ecology and Biogeography Letters, 6, 369–377.

Clement, A. J. H. (2011). Holocene sea-level change in the New Zealand Archipelago and the geomorphic evolution of a Holocene coastal plain incised-valley system: the lower Manawatu valley, North Island, New Zealand. Unpublished PhD thesis, Masssey University, New Zealand.

Clement, A. J. H., Fuller, I. C. (2007). Fluvial responses to environmental change in the North Island, New Zealand, during the past c. 30 ka recorded in river terrace sequences: a review and model for river behaviour. New Zealand Journal of Geology and Geophysics, 50, 101–116.

Coelho, C. A. S., Uvo, C. B., Ambrizzi, T. (2002). Exploring the impacts of the tropical Pacific SST on the precipitation patterns over South America during ENSO periods. Theoretical and Applied Climatology, 71, 185–197.

Cohen, T. J. (2003). Late Holocene floodplain processes and Post-European channel dynamics in a partly confined valley of New South Wales, Australia, PhD thesis, University of Wollongong, Australia.

Cohen, T. J., Nanson, G. C. (2007). Mind the gap: an absence of valley-fill deposits identifying the Holocene hypsithermal period of enhanced flow regime in southeastern Australia. The Holocene, 17, 411–418.

Cohen, T. J., Nanson, G. C. (2008). Topographically associated but chronologically disjunct late Quaternary floodplains and terraces in a partly confined valley, south-eastern Australia. Earth Surface Processes and Landforms, 33, 424–443.

Collins, A. L., Walling, D. E., Leeks, G. J. L. (1997). Use of the geochemical record preserved in floodplain deposits to reconstruct recent changes in river basin sediment sources. Geomorphology, 19, 151–167.

Collins, B., Dunne, T. (1986). Erosion of tephra from the 1980 eruption of Mount St. Helens. Geological Society of America Bulletin, 97, 905–986.

Collins, W. D., Ramaswamy, V., Schwarzkopf, M. D., Sun, Y., Portmann, R. W., Fu, Q., Casanova, S. E. B., Dufresne, J. L., Fillmore, D. W., Forster, P. M. D., Galin, V. Y., Gohar, L. K., Ingram, W. J., Kratz, D. P., Lefebvre, M. P., Li, J., Marquet, P., Oinas, V., Tsushima, Y., Uchiyama, T., Zhong, W. Y. (2006). Radiative forcing by well-mixed greenhouse gases: Estimates from climate models in the Intergovernmental Panel on Climate Change (IPCC) Fourth Assessment Report (AR4). Journal of Geophysical Research, 111, D14317.

Costa, J. E. (1974). Response and recovery of a piedmont watershed from tropical storm Agnes, June 1972. Water Resources Research, 10, 106–112.

Costa, J. E., O'Connor, J. E. (1995). Geomorphically effective floods. In J. E. Costa (Ed.), *Natural and Anthropogenic Influences in Fluvial Geomorphology, Geophys. Monogr. Ser.* (Vol. 89, pp. 45–56). Washington DC: AGU.

Cotton, C. A. (1957). Pleistocene shorelines on the compound coast of Otago. New Zealand Journal of Science and Technology, 38B, 750–762.

Coulthard, T. J., Lewin, J., Macklin, M. G. (2005). Modelling differential catchment response to environmental change. Geomorphology, 69, 222–241.

Coulthard, T. J., Van De Wiel, M. J. (2007). Quantifying fluvial non linearity and finding self organized criticality? Insights from simulations of river basin evolution. Geomorphology, 91, 216–235.

Crosby, B. T., Whipple, K. X. (2006). Knickpoint initiation and distribution within fluvial networks: 236 waterfalls in the Waipaoa River, North Island, New Zealand. Geomorphology, 82, 16–38.

Croudace, I. W., Rindby, A., Rothwell, G. (2006). ITRAX: description and evaluation of a new multi-function X-ray core scanner. In R. G. Rothwell (Ed.), *New Techniques in Sediment Core Analysis* (pp. 51-63). London: The Geological Scociety of London, Special Publications.

Crowley, T. J., Zielinski, G., Vinther, B., Udisti, R., Kreutz, K., Cole-Dai, J., Castellano, E. (2008). Volcanism and the Little Ice Age. PAGES News, 16, 22–23.

Crutzen, P. I., Stoermer, E. F. (2000). The Anthropocene. IGBP Newsletter, 41, 17–18.

Crutzen, P. J., Steffen, W. (2003). How long have we been in the Anthropocene Era? Climatic Change, 61, 251–257.

D'Costa, D., Boswijk, G., Ogden, J. (2009). Holocene vegetation and environmental reconstructions from swamp deposits in the Dargaville region of the North Island, New Zealand: implications for the history of kauri (*Agathis australis*). The Holocene, 19, 559–574.

Dadson, S. J., Hovius, N., Chen, H., Dade, W. B., Lin, J.-C., Hsu, M.-L., Lin, C.-W., Horng, M.-J., Chen, T.-C., Milliman, J., Stark, C. P. (2004). Earthquake-triggered increase in sediment delivery from an active mountain belt. Geology, 32, 733–736.

Damm, B., Hagedorn, J. (2010). Holocene floodplain formation in the southern Cape region, South Africa. Geomorphology, 122, 213–222.

Davis, L. (2009). Sediment entrainment potential in modified alluvial streams: implications for re-mobilization of stored in-channel sediment. Physical Geography, 30, 249–268.

de Noblet-Ducoudré, N., Claussen, M., Prentice, C. (2000). Mid-Holocene greening of the Sahara: first results of the GAIM 6000 year BP experiment with two asynchronously coupled atmosphere/biome models. Climate Dynamics, 16, 643–659.

De Vries, H. (1958). Atomic Bomb Effect: Variation of Radiocarbon in Plants, Shells, and Snails in the Past 4 Years. Science, 128, 250-251.

Dean, W. E., Forester, R. M., Bradbury, J. P. (2002). Early Holocene change in atmospheric circulation in the Northern Great Plains: an upstream view of the 8.2 ka cold event. Quaternary Science Reviews, 21, 1763–1775.

Debret, M., Bout-Roumazeilles, V., Grousset, F., Desmet, M., McManus, J. F., Massei, N., Sebag, D., Petit, J.-R., Copard, Y., Trentesaux, A. (2007). The origin of the 1500–year climate cycles in Holocene North-Atlantic records. Climate of the Past, 3, 569–575.

deMenocal, P., Ortiz, J., Guilderson, T., Adkins, J., Sarnthein, M., Baker, L., Yarusinsky, M. (2000). Abrupt onset and termination of the African Humid Period: rapid climate responses to gradual insolation forcing. Quaternary Science Reviews, 19, 347–361.

Denton, G. H., Broecker, W. S. (2008). Wobbly ocean conveyor circulation during the Holocene? Quaternary Science Reviews, 27, 1939–1950.

Denton, G. H., Karlén, W. (1973). Holocene climatic variations - their pattern and possible cause. Quaternary Research, 3, 155–205.

Deutsch, M., Ruggles, F. (1974). Optical data processing and projected applications of the ERTS-1 imagery covering the 1973 Mississippi river valley floods. Water Resources Bulletin, 10, 1023–1039.

Dijkstra, H. (2008). Antarctic Circumpolar Current *Dynamical Oceanography* (pp. 327–350). Berlin Heidelberg: Springer

Dodson, J. R., Enright, N. J., McLean, R. F. (1988). A late Quaternary vegetation history for far northern New Zealand. Journal of Biogeography, 15, 647–656.

Donders, T. H., Wagner-Cremer, F., Visscher, H. (2008). Integration of proxy data and model scenarios for the mid-Holocene onset of modern ENSO variability. Quaternary Science Reviews, 27, 571–579.

Douglass, D. H., Knox, R. S. (2005). Climate forcing by the volcanic eruption of Mount Pinatubo. Geophysical Research Letters, 32, L05710.

Duplessy, J.-C., Ivanova, E., Murdmaa, I., Paterne, M., Labeyrie, L. (2001). Holocene paleoceanography of the northern Barents Sea and variations of the northward heat transport by the Atlantic Ocean. Boreas, 30, 2–16.

Edbrooke, S. W., Brook, F. J. (2009). Geology of the Whangarei area. Institute of Geological & Nuclear Sciences 1:250 000 map 2. 1 sheet + 68 p. Lower Hutt, New Zealand. GNS Science.

Eden, D. N., Palmer, A. S., Cronin, S. J., Marden, M., Berryman, K. R. (2001). Dating the culmination of river aggradation at the end of the last glaciation using distal tephra compositions, eastern North Island, New Zealand. Geomorphology, 38, 133–151.

Elliot, M., Neall, V., Wallace, C. (2005). A Late Quaternary pollen record from Lake Tangonge, far northern New Zealand. Review of Palaeobotany and Palynology, 136, 143–158.

Elliot, M. B. (1998). Late Quaternary pollen records of vegetation and climate change from Kaitaia Bog, far northern New Zealand. Review of Palaeobotany and Palynology, 99, 189–202.

Elliot, M. B., Flenley, J. R., Sutton, D. G. (1998). A late Holocene pollen record of deforestation and environmental change from the Lake Tauanui catchment, Northland, New Zealand. Journal of Paleolimnology, 19, 23–32.

Elliot, M. B., Striewski, B., Flenley, J. R., Kirkman, J. H., Sutton, D. G. (1997). A 4300 year palynological and sedimentological record of environmental change and human impact from Wharau Road Swamp, Northland, New Zealand. Journal of the Royal Society of New Zealand, 27, 401–418.

Elliot, M. B., Striewski, B., Flenley, J. R., Sutton, D. G. (1995). Palynological and Sedimentological evidence for a radiocarbon chronology of environmental change and Polynesian deforestation from Lake Taumatawhana, Northland, New Zealand. Radiocarbon, 37, 899–916.

Ely, L. L., Enzel, Y., Baker, V. R., Cayan, D. R. (1993). A 5000-year record of extreme floods and climate change in the southwestern United States. Science, 262, 410–412.

Erskine, W. D. (1994). Sand slugs generated by catastrophic floods on the Goulburn River, New South Wales. In L. J. Olive, R. J. Loughran J. A. Kesby (Eds.), *Variability in Stream Erosion and Sediment Transport* (Vol. 224, pp. 143–151). Wallingford, UK: IAHS Publication.

Erskine, W. D. (2011). Geomorphic controls on historical channel planform changes on the Lower Pages River, Hunter Valley, Australia. Australian Geographer, 42, 289–307.

Erskine, W. D., Livingstone, E. A. (1999). In-channel benches: the role of floods in their formation and destruction on bedrock-confined rivers. In A. J. Miller A. Gupta (Eds.), *Varieties of fluvial form* (pp. 445–475). Chichester, UK: John Wiley & Sons.

Erskine, W. D., Webb, A. A. (2003). Desnagging to resnagging: new directions in river rehabilitation in southeastern Australia. River Research and Applications, 19, 233–249.

Eskine, W. D., Warner, R. F. (1998). Further assessment of flood- and drought-dominated regimes in south-eastern Australia. Australian Geographer, 29, 257–261.

Evans, J. L., Allan, R. J. (1992). El Nino/southern oscillation modification to the structure of the monsoon and tropical cyclone activity in the Australasian region. International Journal of Climatology, 12, 611–623.

Fairbanks, R. G., Mortlock, R. A., Chiu, T.-C., Cao, L., Kaplan, A., Guilderson, T. P., Fairbanks, T. W., Bloom, A. L., Grootes, P. M., Nadeau, M.-J. (2005). Radiocarbon calibration curve spanning 0 to 50,000 years BP based on paired $^{230}Th/^{234}U/^{238}U$ and ^{14}C dates on pristine corals. Quaternary Science Reviews, 24, 1781–1796.

Fan, K., Wang, H. J. (2004). Antarctic Oscillation and the dust weather frequency in North China. Geophysical Research Letters, 31, L10201.

Fan, K. E. (2007). Zonal asymmetry of the Antarctic Oscillation. Geophysical Research Letters, 34, L02706.

Fleitmanna, D., Burns, S. J., Mangini, A., Mudelsee, M., Kramers, J., Villaa, I., Neff, U., Al-Subbary, A. A., Buettner, A., Hippler, D., Matter, A. (2007). Holocene ITCZ and

Indian monsoon dynamics recorded in stalagmites from Oman and Yemen (Socotra). Quaternary Science Reviews, 26, 170–188.

Fogt, R. L., Bromwich, D. H. (2006). Decadal variability of the ENSO teleconnection to the high-latitude South Pacific governed by coupling with the Southern Annular Mode. Journal of Climate, 19, 979–996.

Foley, J. A., Kutzbach, J. E., Coe, M. T., Levis, S. (1994). Feedbacks between climate and boreal forests during the Holocene epoch. Nature, 371, 52–54.

Folland, C. K., Renwick, J. A., Salinger, M. J., Mullan, A. B. (2002). Relative influences of the Interdecadal Pacific Oscillation and ENSO on the South Pacific Convergence Zone. Geophysical Research Letters, 29, 1643.

Foster, G., Carter, L. (1997). Mud sedimentation on the continental shelf at an accretionary margin-Poverty Bay, New Zealand. New Zealand Journal of Geology and Geophysics, 40, 157–173.

Foulds, S. A., Macklin, M. G. (2006). Holocene land-use change and its impact on river basin dynamics in Great Britain and Ireland. Progress in Physical Geography, 30, 589–604.

Fowler, A., Lorrey, A., Crossley, P. (2005). Seasonal growth characteristics of Kauri. Tree-Ring Research, 61, 3–19.

Fowler, A. M., Boswijk, G., Gergis, J., Lorrey, A. (2008a). ENSO history recorded in *Agathis australis* (kauri) tree rings. Part A: kauri's potential as an ENSO proxy. International Journal of Climatology, 28, 1–20.

Fowler, A. M., Boswijk, G., Lorrey, A. M., Gergis, J., Pirie, M., McCloskey, S. P. J., Palmer, J. G., Wunder, J. (2012). Multi-centennial tree-ring record of ENSO-related activity in New Zealand. [10.1038/nclimate1374]. Nature Clim. Change, advance online publication.

Fowler, A. M., Palmer, J., Fenwick, P. (2008b). An assessment of the potential for centennial-scale reconstruction of atmospheric circulation from selected New Zealand tree-ring chronologies. Palaeogeography, Palaeoclimatology, Palaeoecology, 265, 238–254.

Fraedrich, K. (1994). An ENSO impact on Europe? Tellus A, 46, 541–552.

Fryirs, K., Brierley, G. J. (2001). Variability in sediment delivery and storage along river courses in Bega catchment, NSW, Australia: implications for re-mobilization of stored in-channel sediment. Geomorphology, 38, 237–265.

Fryirs, K. A., Brierley, G. J., Preston, N. J., Kasai, M. (2007). Buffers, barriers and blankets: The (dis)connectivity of catchment–scale sediment cascades. Catena, 70, 49–67.

Fuller, I. C. (2008). Geomorphic impacts of a 100-year flood: Kiwitea Stream, Manawatu catchment, New Zealand. Geomorphology, 98, 84–95.

Fuller, I. C., Macklin, M. G., Lewin, J., Passmore, D. G., Wintle, A. G. (1998). River response to high-frequency climate oscillations in southern Europe over the past 200 k.y. Geology, 26, 275–278.

Garreaud, R. D., Battisti, D. S. (1999). Interannual (ENSO) and interdecadal (ENSO-like) variability in the Southern Hemisphere tropospheric circulation. Journal of Climate, 12, 2113–2123.

Gell, P., Fluin, J., Tibby, J., Hancock, G., Harrison, J., Zawadzki, A., Haynes, D., Khanum, S., Little, F., Walsh, B. (2009). Anthropogenic acceleration of sediment accretion in lowland floodplain wetlands, Murray-Darling Basin, Australia. Geomorphology, 108, 122–126.

Gibb, J. B. (1986). A New Zealand regional Holocene eustatic sea-level curve and its application to determination of vertical tectonic movements. Royal Society of New Zealand Bulletin, 24, 377–395.

Gillett, N. P., Kell, T. D., Jones, P. D. (2006). Regional climate impacts of the Southern Annular Mode. Geophysical Research Letters, 33, L23704.

Glade, T. (2003). Landslide occurrence as a response to land use change: a review of evidence from New Zealand. Catena, 51, 297–314.

Gomez, B., Carter, L., Orpin, A. R., Cobb, K. M., Page, M. J., Trustrum, N. A., Palmer, A. S. (2011). ENSO/SAM interactions during the middle and late Holocene. The Holocene, 22, 23–30.

Gomez, B., Carter, L., Trustrum, N. A. (2007). A 2400 yr record of natural events and anthropogenic impacts in intercorrelated terrestrial and marine sediment cores: Waipaoa sedimentary system, New Zealand. Geological Society of America Bulletin, 119, 1415–1432.

Gomez, B., Carter, L., Trustrum, N. A., Palmer, A. S., Roberts, A. P. (2004). El Niño-Southern Oscillation signal associated with middle Holocene climate change in intercorrelated terrestrial and marine sediment cores, North Island, New Zealand. Geology, 32, 653–656.

Gomez, B., Eden, D. N., Hicks, D. M., Trustrum, N. A., Peacock, D. H., Wilmshurst, J. M. (1999). Contribution of floodplain sequestration to the sediment budget of the Waipaoa River, New Zealand. The Geological Society of London, Special Publications, 163, 69–88.

Gomez, B., Phillips, J. D. (1999). Deterministic uncertainty in bed load transport. Journal of Hydraulic Engineering, 125, 305–308.

Gong, D., Wang, S. (1999). Definition of Antarctic oscillation index. Geophysical Research Letters, 26, 459–462.

Gow, A. J., Williamson, T. (1971). Volcanic ash in the Antarctic ice sheet and its possible climatic implications. Earth and Planetary Science Letters, 13, 210–213.

Grant-Taylor, T. L., Rafter, T. A. (1963). New Zealand natural radiocarbon measurements I - V. Radiocarbon, 5, 118-162.

Grant-Taylor, T. L., Rafter, T. A. (1971). New Zealand radiocarbon age measurements - 6. New Zealand Journal of Geology and Geophysics, 14, 364–402.

Grant, P. (1981). Recently increased tropical cyclone activity and inferences concerning coastal erosion and inland hydrological regimes in New Zealand and eastern Australia. Climatic Change, 3, 317–332.

Grant, P. (1985). Major periods of erosion and alluvial sedimentation in New Zealand during the late Holocene. Journal of the Royal Society of New Zealand, 15, 67–121.

Gregory, K. J. (2006). The human role in changing river channels. Geomorphology, 79, 172–191.

Hall, A., Visbeck, M. (2002). Synchronous variability in the Southern Hemisphere atmosphere, sea ice, and ocean resulting from the Annular Mode. Journal of Climate, 15, 3043–3057.

Hall, B. L. (2009). Holocene glacial history of Antarctica and the sub-Antarctic islands. Quaternary Science Reviews, 28, 2213–2230.

Harden, T., Macklin, M. G., Baker, V. (2010). Holocene flood histories in south-western USA. Earth Surface Processes and Landforms, 35, 707–716.

Harvey, A. M. (2001). Coupling between hillslopes and channels in upland fluvial systems: implications for landscape sensitivity illustrated from the Howgill Fells, northwest England. Catena, 42, 225–250.

Harvey, A. M., Miller, S. Y., Wells, S. G. (1995). Quaternary soil and river terrace sequences in the Aguas/Feos river systems: Sorbas basin, southeast Spain. In J. Lewin, M. G. Macklin J. C. Woodward (Eds.), *Mediterranean Quaternary river environments* (pp. 263–281). Rotterdam: A. A. Balkema.

Harvey, A. M., Oldfield, F., Baron, A. F., Pearson, G. W. (1981). Dating of post-glacial landforms in the central Howgills. Earth Surface Processes and Landforms, 6, 401–412.

Hayes, S. K., Montgomery, D. R., Newhall, C. G. (2002). Fluvial sediment transport and deposition following the 1991 eruption of Mount Pinatubo. Geomorphology, 45, 211–224.

Hayward, B. W., Grenfell, H. R., Sabaa, A. T., Kay, J., Daymond-King, R., Cochran, U. (2010). Holocene subsidence at the transition between strike-slip and subduction on the Pacific-Australian plate boundary, Marlborough Sounds, New Zealand. Quaternary Science Reviews, 29, 648–661.

Heath, S. K., Plater, A. J. (2010). Records of pan (floodplain wetland) sedimentation as an approach for post-hoc investigation of the hydrological impacts of dam impoundment: The Pongolo river, KwaZulu-Natal. Water Research, 44, 4226–4240.

Hendy, E. J., Gagan, M. K., Lough, J. M. (2003). Chronological control of coral records using luminescent lines and evidence for non-stationary ENSO teleconnections in northeast Australia. The Holocene, 13, 187–199.

Hickin, E. J. (1984). Vegetation and river channel dynamics. The Canadian Geographer, XXVIII, 111–126.

Hickin, E. J., Nanson, G. C. (1975). The character of channel migration on the Beatton River, northeast British Columbia, Canada. Geological Society of America Bulletin, 86, 487–494.

Hicks, D. M., Gomez, B., Trustrum, N. A. (2000). Erosion thresholds and suspended sediment yields, Waipaoa River Basin, New Zealand. Water Resources Research, 36, 1129–1142.

Hodell, D. A., Brenner, M., Curtis, J. H., Guilderson, T. (2001a). Solar forcing of drought frequency in the Maya Lowlands. Science, 292, 1367–1370.

Hodell, D. A., Kanfoush, S. L., Shemesh, A., Crosta, X., Charles, C. D., Guilderson, T. P. (2001b). Abrupt cooling of Antarctic surface waters and sea ice expansion in the South Atlantic sector of the Southern Ocean at 5000 cal yr B.P. Quaternary Research, 56, 191–198.

Hoffmann, T., Erkens, G., Gerlach, R., Klostermann, J., Lang, A. (2009). Trends and controls of Holocene floodplain sedimentation in the Rhine catchment. Catena, 77, 96–106.

Hoffmann, T., Lang, A., Dikau, R. (2008). Holocene river activity: analysing 14C-dated fluvial and colluvial sediments from Germany. Quaternary Science Reviews, 27, 2031–2040.

Hoffmann, T., Thorndycraft, V. R., Brown, A. G., Coulthard, T. J., Damnati, B., Kale, V. S., Middelkoop, H., Notebaert, B., Walling, D. E. (2010). Human impact on fluvial regimes and sediment flux during the Holocene: Review and future research agenda. Global and Planetary Change, 72, 87–98.

Holloway, J. T. (1960). Pre-European vegetation of New Zealand. In A. H. McLintock (Ed.), *A descriptive atlas of New Zealand*. Wellington: Government Printer.

Hooke, J. (2003). River meander behaviour and instability: a framework for analysis. Transactions of the Institute of British Geographers, 28, 238–253.

Hooke, J. M. (2004). Cutoffs galore!: occurrence and causes of multiple cutoffs on a meandering river. Geomorphology, 61, 225–238.

Hooke, J. M., Yorke, L. (2011). Channel bar dynamics on multi-decadal timescales in an active meandering river. Earth Surface Processes and Landforms, 36, 1910–1928.

Horrocks, M., Augustinus, P., Deng, Y., Shane, P., Andersson, S. (2005). Holocene vegetation, environment, and tephra recorded from Lake Pupuke, Auckland, New Zealand. New Zealand Journal of Geology and Geophysics, 48, 85–94.

Hughen, K., Lehman, S., Southon, J., Overpeck, J., Marchal, O., Herring, C., Turnbull, J. (2004). 14C Activity and Global Carbon Cycle Changes over the Past 50,000 Years. Science, 303, 202-207.

Huijun, W. (2002). The instability of the East Asian summer monsoon-ENSO relations. Advances in Atmospheric Sciences, 19, 1–11.

Hume, T. M., Sherwood, A. M., Nelson, C. S. (1975). Alluvial sedimentology of the Upper Pleistocene Hinuera Formation, Hamilton Basin, New Zealand. Journal of the Royal Society of New Zealand, 5, 421–462.

Hupp, C. R., Osterkamp, W. R. (1996). Riparian vegetation and fluvial geomorphic processes. Geomorphology, 14, 277-295.

Hurst, H. E. (1944). A short account of the Nile basin. Physical Department Paper 45, Ministry of Public Works, Egypt.

Huybers, P., Langmuir, C. (2009). Feedback between deglaciation, volcanism, and atmospheric CO2. Earth and Planetary Science Letters, 286, 479-491.

IPCC. (2007). Climate Change 2007. Core writing team: Pachauri, R. K., Reisinger, A. Synthesis Report: Contribution of Working Groups I, II and III to the Fourth Assessment. Report of the Intergovernmental Panel on Climate Change (104pp). Geneva, Switzerland: IPCC.

Isaac, M. J. (1996). Geology of the Kaitaia area. Institute of Geological & Nuclear Sciences 1:250 000 geological map 1. 1 sheet + 44 p. Lower Hutt, New Zealand. GNS Science.

Ivy-Ochs, S., Kerschner, H., Maisch, M., Christl, M., Kubik, P. W., Schlüchter, C. (2009). Latest Pleistocene and Holocene glacier variations in the European Alps. Quaternary Science Reviews, 28, 2137–2149.

Johnstone, E., Macklin, M. G., Lewin, J. (2006). The development and application of a database of radiocarbon-dated Holocene fluvial deposits in Great Britain. Catena, 66, 14–23.

Jones, A. F., Brewer, P. A., Johnstone, E., Macklin, M. G. (2007). High-resolution interpretative geomorphological mapping of river valley environments using airborne LiDAR data. Earth Surface Processes and Landforms, 32, 1574–1592.

Jones, A. F., Brewer, P. A., Macklin, M. G. (2010a). Geomorphological and sedimentological evidence for variations in Holocene flooding in Welsh river catchments. Global and Planetary Change, 70, 92–107.

Jones, A. F., Lewin, J., Macklin, M. G. (2010b). Flood series data for the later Holocene: Available approaches, potential and limitations from UK alluvial sediments. The Holocene, 1123–1135.

Jones, G. A. (1994). Holocene climate and deep ocean circulation changes: evidence from accelerator mass spectrometer radiocarbon dated Argentine Basin (SW Atlantic) mudwaves. Paleoceanography, 9, 1001–1016.

Jones, K. E., Preston, N. J. (2012). Spatial and temporal patterns of off-slope sediment delivery for small catchments subject to shallow landslides within the Waipaoa catchment, New Zealand. Geomorphology, 141, 150–159.

Jouzel, J. (2004). EPICA Dome C Ice Cores Deuterium Data. IGBP PAGES, World Data Centre for Palaeoclimatology. Data Contribution Series #2004-038. NOAA/NGDC Paleoclimatology Program, Boulder CO, USA.

Julian, P. R., Chervin, R. M. (1978). A study of the Southern Oscillation and Walker Ciculation phenomenon. Monthly Weather Review, 106, 1433–1451.

Jungclaus, J. H., Lorenz, S. J., Timmreck, C., Reick, C. H., Brovkin, V., Six, K., Segschneider, J., Giorgetta, M. A., Crowley, T. J., Pongratz, J., Krivova, N. A., Vieira, L. E., Solanki, S. K., Klocke, D., Botzet, M., Esch, M., Gayler, V., Haak, H., Raddatz, T. J., Roeckner, E., Schnur, R., Widmann, H., Claussen, M., Stevens, B., Marotzke, J. (2010). Climate and carbon-cycle variability over the last millennium. Climate of the Past, 6, 723–737.

Kale, V. S. (2008). A half-a-century record of annual energy expenditure and geomorphic effectiveness of the monsoon-fed Narmada River, central India. Catena, 75, 154–163.

Karlén, W., Kuylenstierna, J. (1996). On solar forcing of Holocene climate: evidence from Scandinavia. The Holocene, 6, 359–365.

Kasting, J. F., Toon, O. B., Pollack, J. B. (1988). How climate evolved on the terrestrial planets. Scientific American, 258, 90–97.

Kershaw, A. P., Strickland, K. M. (1988). A Holocene pollen diagram from Northland, New Zealand. New Zealand Journal of Botany, 26, 145–152.

Kettner, A. J., Gomez, B., Syvitski, J. P. M. (2007). Modeling suspended sediment discharge from the Waipaoa River system, New Zealand: The last 3000 years. Water Resources Research, 43, W07411.

Kidson, J. W. (2000). An analysis of New Zealand synoptic types and their use in defining weather regimes. International Journal of Climatology, 20, 299–316.

Kirkbride, M. P., Dugmore, A. J. (2006). Responses of mountain lee caps in central Iceland to Holocene climate change. Quaternary Science Reviews, 25, 1692–1707.

Klitgaard-Kristensen, D., Sejrup, H., Haflidi Haflidason, H., Johnsen, S., Spurk, M. (1998). A regional 8200 cal. yr BP cooling event in northwest Europe, induced by final stages of the Laurentide ice-sheet deglaciation? Journal of Quaternary Science, 13, 165–169.

Knox, J. C. (1987). Historical Valley Floor Sedimentation in the Upper Mississippi Valley. Annals of the Association of American Geographers, 77, 224–244.

Knox, J. C. (1993). Large increases in flood magnitude in response to modest changes in climate. Nature, 361, 430–432.

Knox, J. C. (2000). Sensitivity of modern and Holocene floods to climate change. Quaternary Science Reviews, 19, 439–457.

Knox, J. C. (2006). Floodplain sedimentation in the Upper Mississippi Valley: Natural versus human accelerated. Geomorphology, 79, 286–310.

Kochel, R. C., Baker, V. R., Patton, P. C. (1982). Paleohydrology of southwestern Texas. Water Resources Research, 18, 1165–1183.

Korup, O., Densmore, A. L., Schlunegger, F. (2010). The role of landslides in mountain range evolution. Geomorphology, 120, 77–90.

Kundzewicz, Z. W., Mata, L. J., Arnell, N. W., DÖLl, P., Jimenez, B., Miller, K., Oki, T., ŞEn, Z., Shiklomanov, I. (2008). The implications of projected climate change for freshwater resources and their management. Hydrological Sciences Journal, 53, 3–10.

Kutzbach, J. E., Bonan, G., Foley, J., Harrison, S. P. (1996). Vegetation and soil feedbacks on the response of the African Monsoon to orbital forcing in the early to middle Holocene. Nature, 384, 623–626.

Kwok, R., Comiso, J. (2002). Spatial patterns of variability in Antarctic surface temperature: connections to the Southern Hemisphere Annular Mode and the Southern Oscillation. Geophysical Research Letters, 29, 1705.

Lachniet, M. S., Asmerom, Y., Burns, S. J., Patterson, W. P., Polyak, V. J., Seltzer, G. O. (2004). Tropical response to the 8200 yr B.P. cold event? Speleothem isotopes indicate a weakened early Holocene monsoon in Costa Rica. Geology, 32, 957–960.

Landsea, C. W. (2000). El Niño/Southern Oscillation and the seasonal predictability of tropical cyclones. In H. F. Diaz V. Markgraf (Eds.), *El Niño and the Southern Oscillation, Multiscale Variability and Global and Regional Impacts* (pp. 149–181). New York: Cambridge University Press.

Lane, E. W. (1955). The importance of fluvial morphology in hydraulic engineering. Proceedings of the American Society of Civil Engineers, 81, 1–17.

Langridge, R. M., Berryman, K. R., Van Dissen, R. J. (2005). Defining the segmentation and the Holocene slip rate of the Wellington Fault, New Zealand: the Pahiatua section. New Zealand Journal of Geology and Geophysics, 48, 591–607.

Lecointre, J. A., Neall, V. E., Palmer, A. S. (1998). Quaternary lahar stratigraphy of the western Ruapehu ring plain, New Zealand. New Zealand Journal of Geology and Geophysics, 41, 225–245.

Leopold, L. B. (1976). Reversal of erosion cycle and climatic change. Quaternary Research, 6, 557–562.

Leopold, L. B., Miller, J. P. (1954). A postglacial chronology for some alluvial valleys in Wyoming. Geological Survey Water-Supply Paper, 1261, Washington, United States.

Lester, R. E., Boulton, A. J. (2008). Rehabilitating agricultural streams in Australia with wood: A review. Environmental Management, 42, 310–326.

Lewin, J., Macklin, M. G. (2003). Preservation potential for Late Quaternary river alluvium. Journal of Quaternary Science, 18, 107–120.

Lewin, J., Macklin, M. G., Johnstone, E. (2005). Interpreting alluvial archives: sedimentological factors in the British Holocene fluvial record. Quaternary Science Reviews, 24, 1873–1889.

Litchfield, N. (2008). Using fluvial terraces to determine Holocene coastal erosion and Late Pleistocene uplift rates: An example from northwestern Hawke Bay, New Zealand. Geomorphology, 99, 369–386.

Litchfield, N., Berryman, K. (2006). Relations between postglacial fluvial incision rates and uplift rates in the North Island, New Zealand. Journal of Geophysical Research, 111, F02007.

Litchfield, N., Berryman, K., Brackley, H., Carter, L., Marden, M., Page, M., Trustrum, N. (2008). The Waipaoa Sedimentary System: research review and future directions. Sediment Dynamics in Changing Environments: Proceedings of a Symposium held in Christchurch, New Zealand, 325, IAHS Publication, pp. 408–416.

Litchfield, N., Dissen, R. V., Heron, D., Rhoades, D. (2006). Constraints on the timing of the three most recent surface rupture events and recurrence interval for the Ohariu Fault: trenching results from MacKays Crossing, Wellington, New Zealand. New Zealand Journal of Geology and Geophysics, 49, 57–61.

Litchfield, N., Dissen, R. V., Langridge, R., Heron, D., Prentice, C. (2004). Timing of the most recent surface rupture event on the Ohariu Fault near Paraparaumu, New Zealand. New Zealand Journal of Geology and Geophysics, 47, 123–127.

Litchfield, N., Rieser, U. (2005). Optically stimulated luminescence age constraints for fluvial aggradation terraces and loess in the eastern North Island, New Zealand. New Zealand Journal of Geology and Geophysics, 48, 581–589.

Litchfield, N. J., Berryman, K. R. (2005). Correlation of fluvial terraces within the Hikurangi Margin, New Zealand: implications for climate and baselevel controls. Geomorphology, 68, 291–313.

Ljung, G. M., Box, G. E. P. (1978). On a measure of a lack of fit in time series models. Biometrika, 65, 297–303.

Lorrey, A., Fowler, A. M., Salinger, J. (2007). Regional climate regime classification as a qualitative tool for interpreting multi-proxy palaeoclimate data spatial patterns: A New Zealand case study. Palaeogeography, Palaeoclimatology, Palaeoecology, 253, 407–433.

Lorrey, A., Williams, P., Salinger, J., Martin, T., Palmer, J., Fowler, A., Zhao, J.-x., Neil, H. (2008). Speleothem stable isotope records interpreted within a multi-proxy framework and implications for New Zealand palaeoclimate reconstruction. Quaternary International, 187, 52–75.

Lorrey, A. M., Vandergoes, M., Almond, P., Renwick, J., Stephens, T., Bostock, H., Mackintosh, A., Newnham, R., Williams, P. W., Ackerley, D., Neil, H., Fowler, A. M. (2012). Palaeocirculation across New Zealand during the last glacial maximum at ~21 ka. Quaternary Science Reviews, 36, 189–213.

Lowe, D. J., Blaauw, M., Hogg, A. G., Newnham, R. M. (2013). Ages of 24 widespread tephras erupted since 30,000 years ago in New Zealand, with re-evaluation of the timing and palaeoclimatic implications of the Lateglacial cool episode at Kaipo bog. Quaternary Science Reviews.

Lucchitta, I., Curtis, G. H., Davis, M. E., Davis, S. W., Turrin, B. (2000). Cyclic aggradation and downcutting, fluvial response to volcanic activity, and calibration of soil-carbonate stages in the western Grand Canyon, Arizona. Quaternary Research, 53, 23–33.

Macklin, M. G., Benito, G., Gregory, K. J., Johnstone, E., Lewin, J., Michczynska, D. J., Soja, R., Starkel, L., Thorndycraft, V. R. (2006). Past hydrological events reflected in the Holocene fluvial record of Europe. Catena, 66, 145–154.

Macklin, M. G., Fuller, I. C., Jones, A. F., Bebbington, M. (2012a). New Zealand and UK Holocene flooding demonstrates interhemispheric climate asynchrony. Geology, 40, 775–778.

Macklin, M. G., Fuller, I. C., Lewin, J., Maas, G. S., Passmore, D. G., Rose, J., Woodward, J. C., Black, S., Hamlin, R. H. B., Rowan, J. S. (2002). Correlation of fluvial

sequences in the Mediterranean basin over the last 200 ka and their relationship to climate change. Quaternary Science Reviews, 21, 1633–1641.

Macklin, M. G., Johnstone, E., Lewin, J. (2005). Pervasive and long-term forcing of Holocene river instability and flooding in Great Britain by centennial-scale climate change. The Holocene, 15, 937–943.

Macklin, M. G., Jones, A. F., Lewin, J. (2010). River response to rapid Holocene environmental change: evidence and explanation in British catchments. Quaternary Science Reviews, 29, 1555–1576.

Macklin, M. G., Jones, A. F., Lewin, J. (2011). Comment: Cumulative probability functions and their role in evaluating the chronology of geomorphological events during the Holocene. [Chiverrell et al. (2011)]. Journal of Quaternary Science, 26, 238–240.

Macklin, M. G., Lewin, J. (1986). Terraced fills of Pleistocene and Holocene age in the Rheidol Valley, Wales. Journal of Quaternary Science, 1, 21–34.

Macklin, M. G., Lewin, J. (1993). Holocene river alluviation in Britain. Zeitschrift für Geomorphologic Supplement-Band, 88, 109–122.

Macklin, M. G., Lewin, J. (2003). River sediments, great floods and centennial-scale Holocene climate change. Journal of Quaternary Science, 18, 101–105.

Macklin, M. G., Lewin, J., Woodward, J. C. (2012b). The fluvial record of climate change. Philosophical Transactions of the Royal Society A: Mathematical, Physical and Engineering Sciences, 370, 2143–2172.

Macklin, M. G., Passmore, D. G., Newson, M. D. (1998). Controls of short and long term river instability: processes and patterns in gravel-bed rivers, the Tyne basin, northern England. In P. E. Klingeman, R. L. Beschta, J. Bradley P. D. Komar (Eds.), *Gravel-bed Rivers in the Environment* (pp. 257–278). Colorado: Water resources publications.

Macklin, M. G., Passmore, D. G., Rumsby, B. T. (1992a). Climatic and cultural signals in Holocene alluvial sequences: the Tyne basin, northern England. In S. Needham M. G. Macklin (Eds.), *Alluvial archaeology in Britain* (pp. 123–135). Oxford: Oxbow Press.

Macklin, M. G., Passmore, D. G., Stevenson, A. C., Edwards, D. N., O'Brien, C. F. (1991). Holocene alluviation and land-use change on Callaly Moor, Northumberland, UK. Journal of Quaternary Science, 6, 225–232.

Macklin, M. G., Rumsby, B. T., Heap, T. (1992b). Flood alluviation and entrenchment: Holocene valley-floor development and transformation in the British uplands. Geological Society of America Bulletin, 104, 631–643.

Magilligan, F. J., Phillips, J. D., James, L. A., Gomez, B. (1998). Geomorphic and sedimentological controls on the effectiveness of an extreme flood. The Journal of Geology, 106, 87–96.

Maher, B. A., Hu, M. (2006). A high-resolution record of Holocene rainfall variations from the western Chinese Loess Plateau: antiphase behaviour of the African/Indian and East Asian summer monsoons. The Holocene, 16, 309–319.

Major, J. J. (2003). Post-eruption hydrology and sediment transport in volcanic river systems. Water Resources Impact, 5, 10–15.

Major, J. J., Pierson, T. C., Dinehart, R. L., Costa, J. E. (2000). Sediment yield following severe volcanic disturbance – a two decade erspective from Mount St. Helens. Geology, 28, 819–822.

Makaske, B., Smith, D. G., Berendsen, H. J. A., de Boer, A. G., van Nielen-Kiezebrink, M. F., Locking, T. (2009). Hydraulic and sedimentary processes causing anastomosing morphology of the upper Columbia River, British Columbia, Canada. Geomorphology, 111, 194–205.

Mantua, N. J., Hare, S. R. (2002). The Pacific Decadel Oscillation. Journal of Oceanography, 58, 35–44.

Manville, V. (2002). Sedimentary and Geomorphic Responses to Ignimbrite Emplacement: Readjustment of the Waikato River after the a.d. 181 Taupo Eruption, New Zealand. The Journal of Geology, 110, 519–541

Manville, V., Newton, E. H., White, J. D. L. (2005). Fluvial responses to volcanism: resedimentation of the 1800a Taupo ignimbrite eruption in the Rangitaiki River catchment, North Island, New Zealand. Geomorphology, 65, 49–70.

Manville, V., Wilson, C. J. N. (2004). The 26.5 ka Oruanui eruption, New Zealand: a review of the roles of volcanism and climate in the post-eruptive sedimentary response. New Zealand Journal of Geology and Geophysics, 47, 525–547.

Marden, M., Mazengarb, C., Palmer, A., Berryman, K., Rowan, D. (2008). Last glacial aggradation and postglacial sediment production from the non-glacial Waipaoa and Waimata catchments, Hikurangi Margin, North Island, New Zealand. Geomorphology, 99, 404–419.

Marden, M., Neall, V. (1990). Dated Ohakean terraces offset by the Wellington Fault near Woodville, New Zealand. Journal of Geology and Geophysics, 33, 449–453.

Marra, M. J., Alloway, B. V. (2006). Paleoenvironmental reconstruction of a well-preserved Stage 7 forest sequence catastrophically buried by basaltic eruptive deposits, northern New Zealand. Quaternary Science Reviews, 25, 2143–2161.

Marshall, G. J. (2003). Trends in the Southern Annular Mode from Observations and Reanalyses. Journal of Climate, 16, 4134–4143.

Marshall, G. J. (2007). Half-century seasonal relationships between the Southern Annular Mode and Antarctic temperatures. International Journal of Climatology, 27, 373–383.

Marutani, T., Kasai, M., Reid, L. M. (1999). Influence of storm-related sediment storage on the sediment delivery from tributary catchments in the upper Waipaoa River, New Zealand. Earth Surface Processes and Landforms, 24, 881–896.

Mason, S. J., Lindesay, J. A. (1993). A note on the modulation of Southern Oscillation-southern Africa rainfall associations with the Quasi-Biennial Oscillation. Journal of Geophysics Research, 98, 8847–8850.

Masson, V., Vimeux, F., Jouzel, J., Morgan, V., Delmotte, M., Ciais, P., Hammer, C., Johnsen, S., Lipenkov, V., Mosley-Thompson, E., Petit, J.-R., Steig, E. J., Stievenard, M., Vaikmae, R. (2000). Holocene climate variability in Antarctica based on 11 ice-core isotopic records. Quaternary Research, 54, 348–358.

Mayewski, P. A., Rohling, E. E., Stager, J. C., Karlen, W., Maasch, K. A., Meeker, L. D., Meyerson, E. A., Gasse, F., van Kreveld, S., Holmgren, K., Lee-Thorp, J., Rosqvist, G., Rack, F., Staubwasser, M., Schneider, R. R., Steig, E. J. (2004). Holocene climate variability. Quaternary Research, 62, 243–255.

McCabe, G. J., Dettinger, M. D. (1999). Decadal variations in the strength of ENSO teleconnections with precipitation in the western United States. International Journal of Climatology, 19, 1399–1410.

McCormac, F., Hoggs, A., Blackwell, P., Buck, C., Higham, T., Reimer, P. (2004). SHCAL04 Southern Hemishere Calibration, 0–11 cal kyr BP. Radiocarbon, 46, 1087–1092.

McGlone, M., Salinger, M., Moar, N. (Eds.). (1993). *Paleovegetation studies of New Zealand's climate since the Last Glacial Maximum*. Minneapolis: Univ. Minesota Press.

McGlone, M., Wilmshurst, J. M., Leach, H. (2005). An ecological and historical review of bracken (*Pteridium esculentum*) in New Zealand, and its cultural significance. New Zealand Journal of Ecology, 29, 165 –184.

McGlone, M. S., Basher, L. R. (1995). The deforestation of the upper Awatere catchment, Inland Kaikoura range, Marlborough, South Island, New Zealand. New Zealand Journal of Ecology, 19, 53–66.

McGlone, M. S., Nelson, C. S., Hume, T. M. (1978). Palynology, age and environmental significance of some peat beds in the Upper Pleistocene Hinuera Formation, South Auckland, New Zealand. Journal of the Royal Society of New Zealand, 8, 385–393.

McGuire, W. J., Howarth, R. J., Firth, C. R., Solow, A. R., Pullen, A. D., Saunders, S. J., Stewart, I. S., Vita-Finzi, C. (1997). Correlation between rate of sea-level change and frequency of explosive volcanism in the Mediterranean. Nature, 389, 473–476.

McKercher, A. I., Henderson, R. D. (2003). Shifts in flood and low-flow regimes in New Zealand due to interdecadal climate variations. Hydrological Sciences Journal, 48, 637–654.

Meneghini, B., Simmonds, I., Smith, I. N. (2007). Association between Australian rainfall and the Southern Annular Mode. International Journal of Climatology, 27, 109–121.

Metge, A. J., Golson, J., Biggs, B. G., Lewthwaite, G. R. (1960). The Maori settlement of New Zealand. In McLintock (Ed.), *A descriptive atlas of New Zealand*. Wellington: Government Printer.

Meyer, D. F., Martinson, H. A. (1989). Rates and processes of channel development and recovery following the 1980 eruption of Mount St. Helens, Washington. Hydrological Sciences Journal, 34, 115–127.

Miller, A. J. (1995). Valley morphology and boundary conditions influencing spatial patterns of flood flow. In J. E. Costa, A. J. Miller, K. W. Potter P. R. Wilcock (Eds.), *Natural and Anthropogenic Influences in Fluvial Geomorphology. Geophysical Monograph, vol. 89* (pp. 57–81): American Geophysical Union.

Miller, G. H., Geirsdóttir, Á., Zhong, Y., Larsen, D. J., Otto-Bliesner, B. L., Holland, M. M., Bailey, D. A., Refsnider, K. A., Lehman, S. J., Southon, J. R., Anderson, C., Björnsson, H., Thordarson, T. (2012). Abrupt onset of the Little Ice Age triggered by volcanism and sustained by sea-ice/ocean feedbacks. Geophysical Research Letters, 39, L02708.

Moir, R. W., Collen, B., Thompson, C. S. (1986). The climate and weather of Northland. New Zealand Meteorological Service (37pp). Government Printer, Wellington.

Moog, D. B., Whiting, P. J. (1998). Annual hysteresis in bed load rating curves. Water Resources Research, 34, 2393–2399.

Moreno, P. I., François, J. P., Villa-Martínez, R. P., Moy, C. M. (2009). Millennial-scale variability in Southern Hemisphere westerly wind activity over the last 5000 years in SW Patagonia. Quaternary Science Reviews, 28, 25–38.

Moros, M., Andrews, J. T., Eberl, D. D., Jansen, E. (2006). Holocene history of drift ice in the northern North Atlantic: Evidence for different spatial and temporal modes. Paleoceanography, 21, PA2017.

Mosley, M. P. (2000). Regional differences in the effects of El Niño and La Niña on low flows and floods. Hydrological Sciences Journal, 45, 249–267.

Moy, C. M., Seltzer, G. O., Rodbell, D. T., Anderson, D. M. (2002). Variability of El Niño/Southern Oscillation activity at millennial timescales during the Holocene epoch. Nature, 420, 162–165.

Mullan, A. B. (1995). On the linearity and stability of Southern oscillation-climate relationships for New Zealand. International Journal of Climatology, 15, 1365–1386.

Mullan, A. B. (1998). Southern hemisphere sea-surface temperatures and their contemporary and lag association with New Zealand temperature and precipitation. International Journal of Climatology, 18, 817–840.

Nanson, G. C. (1986). Episodes of vertical accretion and catastrophic stripping: a model of disequilibrium floodplain development. Geological Society of America Bulletin, 97, 1467–1475.

Nanson, G. C., Croke, J. C. (1992). A genetic classification of floodplains. Geomorphology, 4, 459-486.

Nanson, G. C., Erskine, W. D. (1988). Episodic changes of channels and floodplains in New South Wales. In R. F. Warner (Ed.), *Fluvial Geomorphology of Australia* (pp. 201–221). Sydney: Academic Press.

Nanson, G. C., Price, D. M., Short, S. A., Young, R. W., Jones, B. G. (1991). Comparative uranium-thorium and thermoluminescence dating of weathered quaternary alluvium in the tropics of Northern Australia. Quaternary Research, 35, 347–366.

Neal, A. (2004). Ground-penetrating radar and its use in sedimentology: principles, problems and progress. Earth-Science Reviews, 66, 261–330.

Newnham, R., McGlone, M., Moar, N., Wilmshurst, J., Vandergoes, M. (in press). The vegetation cover of New Zealand at the Last Glacial Maximum. Quaternary Science Reviews.

Newnham, R. M. (1990). Late Quaternary palynological investigations into the history of vegetation and climate in northern New Zealand. Unpublished PhD thesis, University of Auckland, New Zealand.

Newnham, R. M. (1992). A 30,000 year pollen, vegetation and climate record from Otaikairangi (Hikurangi), Northland, New Zealand. Journal of Biogeography, 19, 541–554.

Newnham, R. M., Lowe, D. J., Green, J. D., Turner, G. M., Harper, M. A., McGlone, M. S., Stout, S. L., Horie, S., Froggatt, P. C. (2004). A discontinuous ca. 80 ka record of Late Quaternary environmental change from Lake Omapere, Northland, New Zealand. Palaeogeography, Palaeoclimatology, Palaeoecology, 207, 165–198.

Newnham, R. M., Ogden, J., Mildenhall, D. (1993). A vegetation history of the far north of New Zealand during the Late Otira (Last) Glaciation. Quaternary Research, 39, 361–372.

Newnham, R. M., Vandergoes, M. J., Sikes, E., Carter, L., Wilmshurst, J. M., Lowe, D. J., McGlone, M. S., Sandiford, A. (2012). Does the bipolar seesaw extend to the terrestrial southern mid-latitudes? Quaternary Science Reviews, 36, 214–222.

Newson, M. D. (2002). Geomorphological concepts and tools for sustainable river ecosystem management. Aquatic Conservation: Marine and Freshwater Ecosystems, 12, 365–379.

Nicholls, N. (1983). Predicting Indian monsoon rainfall from sea-surface temperature in the Indonesia-north Australia area. Nature, 306, 576–577.

Nicholson, S. E., Entekhabi, D. (1986). The quasi-periodic behavior of rainfall variability in Africa and its relationship to the Southern Oscillation. Archiv für Meteorologie, Geophysik und Bioklimatologie, A34, 311–348.

Nicholson, S. E., Flohn, H. (1980). Climatic Change, 2, 313–348.

Nicol, A., Campbell, J. K. (2001). The impact of episodic fault-related folding on late Holocene degradation terraces along Waipara River, New Zealand. New Zealand Journal of Geology and Geophysics, 44, 145–156.

Nielsen, S. H. H., Koç, N., Crosta, X. (2004). Holocene climate in the Atlantic sector of the Southern Ocean: Controlled by insolation or oceanic circulation? Geology, 32, 317–320.

Nobes, D. C., Ferguson, R. J., Brierley, G. J. (2001). Ground-penetrating radar and sedimentological analysis of Holocene floodplains: insight from the Tuross valley, New South Wales. Australian Journal of Earth Science, 48, 347–355.

O'Brien, S. R., Mayewski, P. A., Meeker, L. D., Meese, D. A., Twickler, M. S., Whitlow, S. I. (1995). Complexity of Holocene climate as reconstructed from a Greenland ice core. Science, 270, 1962–1064.

Ogden, J., Deng, Y., Boswijk, G., Sandiford, A. (2003). Vegetation changes since early Maori fires in Waipoua Forest, Northern New Zealand. Journal of Archaeological Science, 30, 753–767.

Ogden, J., Wilson, A., Hendy, C., Newnham, R. M., Hogg, A. G. (1992). The Late Quaternary history of kauri (*Agathis australis*) in New Zealand and its climatic significance. Journal of Biogeography, 19, 611–622.

Orpin, A. R. (2004). Holocene sediment deposition on the Poverty-slope margin by the muddy Waipaoa River, East Coast New Zealand. Marine Geology, 209, 69–90.

Ota, Y., Berryman, K. R., Hull, A. G., Miyauchi, T., Iso, N. (1988). Age and height distribution of Holocene transgressive deposits in eastern North Island, New Zealand. Palaeogeography, Palaeoclimatology, Palaeoecology, 68, 135–151.

Ota, Y., Hull, A. G., Iso, N., Ikeda, Y., Moriya, I., Yoshikawa, T. (1992). Holocene marine terraces on the northeast coast of North Island, New Zealand, and their tectonic significance. New Zealand Journal of Geology and Geophysics, 35, 273–288.

Page, M., Trustrum, N., Gomez, B. (2000). Implications of a century of anthropogenic erosion for future land use in the Gisborne-East Coast region of New Zealand. New Zealand Geographer, 56, 13–24.

Page, M. J., Trustrum, N. A., Orpin, A. R., Carter, L., Gomez, B., Cochran, U. A., Mildenhall, D. C., Rogers, K. M., Brackley, H. L., Palmer, A. S., Northcote, L. (2010). Storm frequency and magnitude in response to Holocene climate variability, Lake Tutira, North-eastern New Zealand. Marine Geology, 270, 30–44.

PAGES. (2013). Continental-scale temperature variability during the past two millennia. [Progress Article]. Nature Geoscience, 6, 339-346.

Palmer, J., Lorrey, A., Turney, C. S. M., Hogg, A., Baillie, M., Fifield, K., Ogden, J. (2006). Extension of New Zealand kauri (*Agathis australis*) tree-ring chronologies into Oxygen Isotope Stage (OIS) 3. Journal of Quaternary Science, 21, 779–787.

Passmore, D. G., Macklin, M. G. (1994). Provenance of fine grained alluvium and late Holocene land-use change in the Tyne basin, northeast England. Geomorphology, 9, 127–142.

Passmore, D. G., Macklin, M. G., Stevenson, A. C., O'Brien, C. F., Davis, B. A. S. (1992). A Holocene alluvial sequence in the lower Tyne Valley, northern Britain: a record of river response to environmental change. The Holocene, 2, 138–147.

Pearson, L. K., Hendy, C. H., Hamilton, D. P., Pickett, R. C. (2010). Natural and anthropogenic lead in sediments of the Rotorua lakes, New Zealand. Earth and Planetary Science Letters, 297, 536–544.

Pearson, R. G., Dawson, T. P. (2003). Predicting the impacts of climate change on the distribution of species: are bioclimate envelope models useful? Global Ecology and Biogeography, 12, 361–371.

Petit, J. R., Jouzel, J., Raynaud, D., Barkov, N. I., Barnola, J.-M., Basile, I., Bender, M., Chappellaz, J., Davis, M., Delaygue, G., Delmotte, M., Kotlyakov, V. M., Lipenkov, V., Lorius, C., Pepin, L., Ritz, C., Saltzman, E., Stievenard, M. (1999). Climate and atmospheric history of the last 420,000 years from the Vostok ice core, Antarctica. Nature, 399, 429–436.

Pezzi, L. P., Cavalcanti, I. F. A. (2001). The relative importance of ENSO and tropical Atlantic sea surface temperature anomalies for seasonal precipitation over South America: a numerical study. Climate Dynamics, 17, 205–212.

Phillips, J. D. (2003). Sources of nonlinearity and complexity in geomorphic systems. Progress in Physical Geography, 27, 1–23.

Pielke, R. A., Vidale, P. L. (1995). The boreal forest and the polar front. Journal of Geophysical Research, 100, 25755–25758.

Pillans, B. (1986). A late Quaternary uplift map for North Island, New Zealand. Royal Society of New Zealand, 24, 409–417.

Pittock, A. B. (1983). Recent climatic change in Australia: Implications for a C02-warmed earth. Climatic Change, 5, 321–340.

Poole, A. L. (1983). Catchment control in New Zealand. Water and Soil Miscellaneous Publication No. 48, National Water and Soil Conservation Organisation, Wellington. 185.

Poole, A. L., Adams, N. M. (1986). Trees and Shrubs of New Zealand. Wellington, New Zealand: Government Printing Office.

Power, S., Casey, T., Follland, C., Colman, A., Mehta, V. (1999). Inter-decadal modulation of the impact of ENSO on Australia. Climate Dynamics, 15, 319–324.

Power, S. B., Smith, I. N. (2007). Weakening of the Walker Circulation and apparent dominance of El Niño both reach record levels, but has ENSO really changed? Geophysical Research Letters, 34, L18702.

Prickett, N. (2002). First settlement date and early rats: an opinion poll. Archaeology in New Zealand, 45, 288–292.

Pullar, W. A., Patel, R. N. (1972). Identification of tree stumps and driftwood associated with tephra layers in alluvium, peat, and dune sands. New Zealand Journal of Botany, 10, 605–614.

Pullar, W. A., Penhale, H. R. (1970). Periods of recent infilling of the Gisborne Plains Basin. New Zealand Journal of Science, 13, 410–434.

Putnam, A. E., Schaefer, J. M., Denton, G. H., Barrell, D. J. A., Finkel, R. C., Andersen, B. G., Schwartz, R., Chinn, T. J. H., Doughty, A. M. (2012). Regional climate control of glaciers in New Zealand and Europe during the pre-industrial Holocene. Nature Geoscience, 5, 627–630.

Quigley, M. C., Sandiford, M., Cupper, M. L. (2007). Distinguishing tectonic from climatic controls on range-front sedimentation. Basin Research, 19, 491–505.

Rafter, T. A., Ferguson, G. J. (1957). Atom bomb effect-recent increase in the carbon-14 content of the atmosphere, biosphere, and surface water of the oceans. New Zealand Journal of Science and Technology, 38, 871-873.

Rasmusson, E. M., Wallace, J. M. (1983). Meteorological aspects of El Niño/Southern Oscillation. Science, 222.

Rattenbury, M. S., Cooper, A. F., Norris, R. J. (1988). Recent Alpine Fault thrusting at Kaka Creek, central westland, New Zealand. New Zealand Journal of Geology and Geophysics, 31, 117–120.

Reason, C. J. C., Rouault, M. (2005). Links between the Antarctic Oscillation and winter rainfall over western South Africa. Geophysical Research Letters, 32, L022419.

Reeves, J. M., Barrows, T. T., Cohen, T. J., Kiem, A. S., Bostock, H. C., Fitzsimmons, K. E., Jansen, J. D., Kemp, J., Krause, C., Petherick, L., Phipps, S. J. (2013). Climate variability over the last 35,000 years recorded in marine and terrestrial archives in the Australian region: an OZ-INTIMATE compilation. Quaternary Science Reviews.

Reid, I., Frostick, L. (1994). Fluvial sediment transport and deposition. In K. Pye (Ed.), *Sediment Transport and Depositional Processes* (pp. 89–155). Oxford: Blackwell.

Reimer, P. J., Baillie, M. G. L., Bard, E., Bayliss, A., Beck, J. W., Bertrand, C. J. H., Blackwell, P. G., Buck, C. E., Burr, G. S., Cutler, K. B., Damon, P. E., Edwards, R. L., Fairbanks, R. G., Friedrich, M., Guilderson, T. P., Hogg, A. G., Hughen, K. A., Kromer, B., McCormac, G., Manning, S., Ramsey, C. B., Reimer, R. W., Remmele, S., Southon, J. R., Stuiver, M., Talamo, S., Taylor, F. W., Plicht, J. V. D., Weyhenmeyer, C. E. (2004). IntCal04 terrestrial radiocarbon age calibration, 0–26 cal kyr BP. Radiocarbon, 46, 1029–1058.

Reimer, P. J., Baillie, M. G. L., Bard, E., Bayliss, A., Beck, J. W., Blackwell, P. G., Ramsey, C. B., Buck, C. E., Burr, G. S., Edwards, R. L., Friedrich, M., Grootes, P. M., Guilderson, T. P., Hajdas, I., Heaton, T. J., Hogg, A. G., Hughen, K. A., Kaiser, K. F., Kromer, B., McCormac, F. G., Manning, S. W., Reimer, R. W., Richards, D. A., Southon, J. R., Talamo, S., Turney, C. S. M., van der Plicht, J., Weyhenmeyer, C. E. (2009). IntCal09 and Marine09 radiocarbon age calibration curves, 0-50,000yeats cal BP. Radiocarbon, 51(4), 1111-1150.

Reinhardt, L. J., Bishop, P., Hoey, T. B., Dempster, T. J., Sanderson, D. C. W. (2007). Quantification of the transient response to base-level fall in a small mountain catchment: Sierra Nevada, southern Spain. Journal of Geophysical Research, 112, F03S05.

Renwick, J., Thompson, D. (2006). The Southern Annular Mode and New Zealand climate. Water and Atmosphere, 14, 24–25.

Renwick, J. A. (2011). Kidson's Synoptic weather types and surface climate variability over New Zealand. Weather and Climate, 31, 3–23.

Renwick, W. H. (1992). Equilibrium, disequilibrium, and nonequilibrium landforms in the landscape. Geomorphology, 5, 265–276.

Richardson, J. M., Fuller, I. C., Holt, K. A., Litchfield, N. J., Macklin, M. G. (in review-a). Fluvial records of Holocene climate variability and evidence of a 3500–2800 cal. yr BP cold event from northern New Zealand.

Richardson, J. M., Fuller, I. C., Holt, K. A., Litchfield, N. J., Macklin, M. G. (in review-b). The role of valley floor confinement as a control on Holocene floodplain development: an example from Northland, New Zealand.

Richardson, J. M., Fuller, I. C., Macklin, M. G., Jones, A. F., Holt, K. A., Litchfield, N. J., Bebbington, M. (2013). Holocene river behaviour in New Zealand: response to regional centennial-scale climate forcing. Quaternary Science Reviews, 69, 8-27.

Risebrobakken, B., Jansen, E., Andersson, C., Mjelde, E., Hevrøy, K. (2003). A high-resolution study of Holocene paleoclimatic and paleoceanographic changes in the Nordic Seas. Paleoceanography, 18, 1017.

Robertson-Rintoul, M. S. E. (1986). A Quantitative soil-stratigraphic approach to the correlation and dating of Post-glacial river terraces in Glen Feshie, Western Cairngorms. Earth Surface Processes and Landforms, 11, 605–617.

Robock, A. (2000). Volcanic eruptions and climate. Review of Geophysics, 38, 191-219.

Rohling, E. J., Palike, H. (2005). Centennial-scale climate cooling with a sudden cold event around 8,200 years ago. Nature, 434, 975–979.

Ronghui, H., Yifang, W. (1989). The influence of ENSO on the summer climate change in China and its mechanism. Advances in Atmospheric Sciences, 6, 21–32.

Ropelewski, C. F., Halpert, M. S. (1986). North American Precipitation and Temperature Patterns Associated with the El Niño/Southern Oscillation (ENSO). Monthly Weather Review, 114, 2352–2362.

Rother, H., Shulmeister, J. (2006). Synoptic climate change as a driver of late Quaternary glaciations in the mid-latitudes of the Southern Hemisphere. Climate of the Past, 2, 11–19.

Royall, D., Davis, L., Kimbrow, D. R. (2010). In-channel benches in small watersheds: examples from the Southern Piedmont. Southeastern Geographer, 50, 445–467.

Ruddiman, W. F. (2003). The anthropogenic greenhouse era began thousands of years ago Climatic Change, 61, 261–293.

Rumsby, B. T., Macklin, M. G. (1994). Channel and floodplain response to recent abrupt climate change: the Tyne basin, northern England. Earth Surface Processes and Landforms, 19, 499–515.

Rumsby, B. T., Macklin, M. G. (1996). River response to the last neoglacial (the 'Little Ice Age') in northern, western and central Europe. Geological Society, London, Special Publications, 115, 217–233.

Sale, E. V. (1986). Whangaroa. Kaeo: Whangaroa Book Committee.

Salinger, M. J. (1980a). New Zealand climate: I. Precipitation patterns. Monthly Weather Review, 108, 1892–1904.

Salinger, M. J. (1980b). New Zealand climate: II. Temperature patterns. Monthly Weather Review, 108, 1905–1912.

Salinger, M. J., Renwick, J. A., Mullan, A. B. (2001). Interdecadal Pacific Oscillation and South Pacific climate. International Journal of Climatology, 21, 1705–1721.

Sallun, A. E. M., Sallun Filho, W., Suguio, K., Babinski, M., Gioia, S. M. C. L., Harlow, B. A., Duleba, W., De Oliveira, P. E., Garcia, M. J., Weber, C. Z., Christofoletti, S. R., Santos, C. d. S., Medeiros, V. B. d., Silva, J. B., Santiago-Hussein, M. C., Fernandes, R. S. (2012). Geochemical evidence of the 8.2 ka event and other Holocene environmental changes recorded in paleolagoon sediments, southeastern Brazil. Quaternary Research, 77, 31–43.

Salzer, M. W., Hughes, M. K. (2007). Bristlecone pine tree rings and volcanic eruptions over the last 5000 yr. Quaternary Research, 67, 57–68.

Sandiford, A., Newnham, R., Alloway, B., Ogden, J. (2003). A 28 000–7600 cal yr BP pollen record of vegetation and climate change from Pukaki Crater, northern New Zealand. Palaeogeography, Palaeoclimatology, Palaeoecology, 201, 235–247.

Sandweiss, D. H., Maasch, K. A., Burger, R. L., Richardson, J. B., III, Rollins, H. B., Clement, A. (2001). Variation in Holocene El Niño frequencies: Climate records and cultural consequences in ancient Peru. Geology, 29, 603–606.

Schaefer, J. M., Denton, G. H., Kaplan, M., Putnam, A., Finkel, R. C., Barrell, D. J. A., Andersen, B. G., Schwartz, R., Mackintosh, A., Chinn, T., Schluchter, C. (2009). High-frequency Holocene glacier fluctuations in New Zealand differ from the northern signature. Science, 324, 622–625.

Schmidtchen, G., Bork, H.-R. (2003). Changing human impact during the period of agriculture in central Europe: the case study Biesdorfer Kehlen, Brandenburg, Germany. In A. Lang, R. Dikau K. Hennrich (Eds.), *Long term hillslope and fluvial system modelling* (Vol. 101, pp. 183-200). Berlin: Springer Berlin / Heidelberg.

Schulz, M., André, P., Timmermann, A. (2004). Glacial-interglacial contrast in climate variability at centennial-to-millennial timescales: observations and conceptual model. Quaternary Science Reviews, 23, 2219–2230.

Schumm, S. A. (1977). The fluvial system. New York: John Wiley & Sons.

Schumm, S. A. (1979). Geomorphic thresholds: the concept and its applications. Transactions of the Institute of British Geographers, NS4, 485–515.

Schumm, S. A. (1993). River response to baselevel change: implications for sequence stratigraphy. The Journal of Geology, 101, 279–294.

Schumm, S. A., Parker, R. S. (1973). Implications of complex response of drainage systems for Quaternary alluvial stratigraphy. Nature Physical Science, 243, 99–100.

Segschneider, B., C.A., L., L., W. J. D., N., W. C. J., Manville, V. (2002). Resedimentation of the 1.8 ka Taupo Ignimbrite in the Mohaka and Ngaruroro river catchments, Hawke's Bay, New Zealand. New Zealand Journal of Geology and Geophysics, 45, 85–102.

Shulmeister, J., Goodwin, I., Renwick, J., Harle, K., Armand, L., McGlone, M. S., Cook, E., Dodson, J., Hesse, P. P., Mayewski, P., Curran, M. (2004). The Southern Hemisphere westerlies in the Australasian sector over the last glacial cycle: a synthesis. Quaternary International, 118–119, 23–53.

Shulmeister, J., Rodbell, D. T., Gagan, M. K., Seltzer, G. O. (2006). Inter-hemispheric linkages in climate change: paleo-perspectives for future climate change. Climate of the Past, 2, 167–185.

Sigurdsson, H. (1990). Evidence of volcanic loading of the atmosphere and climate response. Palaeogeography, Palaeoclimatology,Palaeoecology (Global and Planetary Change Section), 89, 277–289.

Sijp, W. P., England, M. H. (2009). Southern Hemisphere westerly wind control over the ocean's thermohaline circulation. Journal of Climate, 22, 1277–1286.

Silvestri, G. E., Vera, C. S. (2003). Antarctic Oscillation signal on precipitation anomalies over southeastern South America. Geophysical Research Letters, 30, 2115.

Smith, I. E. M., Okada, T., Itaya, T., Black, P. M. (1993). Age relationships and tectonic implications of late Cenozoic basaltic volcanism in Northland, New Zealand. New Zealand Journal of Geology and Geophysics, 36, 385–394.

Speich, S., Blanke, B., Cai, W. (2007). Atlantic meridional overturning circulation and the Southern Hemisphere supergyre. Geophysical Research Letters, 34, L23614.

Starkel, L. (1983). The reflection of hydrologic changes in the fluvial environment of the temperate zone during the last 15,000 years. In K. J. Gregory (Ed.), *Background to Palaeohydrology: A Perspective* (pp. 213–235). Chichester: Wiley and Sons.

Starkel, L., Soja, R., Michczynska, D. J. (2006). Past hydrological events reflected in Holocene history of Polish rivers. Catena, 66, 24–33.

Stenchikov, G., Delworth, T. L., Ramaswamy, V., Stouffer, R. J., Wittenberg, A., Zeng, F. (2009). Volcanic signals in oceans. Journal of Geophysical Research, 114, D16104.

Stenseth, N. C., Ottersen, G., Hurrell, J. W., Mysterud, A., Lima, M., Chan, K.-S., Yoccoz, N. G., Ådlandsvik, B. (2003). Studying climate effects on ecology through the use of climate indices: the North Atlantic Oscillation, El Niño Southern Oscillation and beyond. Proceedings - Royal Society of London. Biological sciences, 270, 2987–2096.

Stephens, T., Atkin, D., Augustinus, P., Shane, P., Lorrey, A., Street-Perrott, A., Nilsson, A., Snowball, I. (2012). A late glacial Antarctic climate teleconnection and variable

Holocene seasonality at Lake Pupuke, Auckland, New Zealand. Journal of Paleolimnology, 48, 785–800.

Stinchcomb, G. E., Driese, S. G., Nordt, L. C., Allen, P. M. (in press). A mid to late Holocene history of floodplain and terrace reworking along the middle Delaware River valley, USA. Geomorphology.

Stølum, H.-H. (1996). River Meandering as a Self-Organization Process. Science, 271, 1710–1713.

Stott, L., Cannariato, K., Thunell, R., Haug, G. H., Koutavas, A., Lund, S. (2004). Decline of surface temperature and salinity in the western tropical Pacific Ocean in the Holocene epoch. Nature, 431, 56–59.

Street-Perrott, F. A., Perrott, R. A. (1990). Abrupt climate fluctuations in the tropics: the influence of the Atlantic Ocean circulation. Nature, 343, 607–612.

Striewski, B., Cole, A. O., Flenley, J. R., Sutton, D. G. (1996). Date of colonisation of Northland (Vol. Part 1, Year 1): Massey University.

Striewski, B., Mayr, C., Flenley, J., Naumann, R., Turner, G., Lűcke, A. (2009). Multi-proxy evidence of late Holocene human-induced environmental changes at Lake Pupuke, Auckland (New Zealand). Quaternary International, 202, 69–93.

Stuiver, M., Braziunas, T. F. (1989). Atmospheric 14C and century-scale solar oscillations. [10.1038/338405a0]. Nature, 338, 405–408.

Stuiver, M., Grootes, P. M., Braziunas, T. F. (1995). The GISP2 18O record of the past 16,500 yrs and the role of the sun, ocean and volcanoes. Quaternary Research, 44, 341–354

Stuvier, M., Pollack, H. A. (1977). Discussion reporting C-14 data. Radiocarbon, 19, 355–363.

Suess, H. E. (1955). Radiocarbon Concentration in Modern Wood. Science, 122, 415-417.

Suggate, R. P. (1958). The geology of the Clarence Valley from Gore Stream to Bluff Hill. Transactions of the Royal Society of New Zealand, 85, 397–408.

Surovell, T. A., Finley, J. B., Smith, G. M., Brantingham, J., Kelly, R. (2009). Correcting temporal frequency distributions for taphonomic bias. Journal of Archaeological Science, 36, 1715–1724.

Sutton, D. G., Flenley, J. R., Xun, L., Todd, A., Butler, K., Summers, R., Chester, P. I. (2008). The timing of the human discovery and colonization of New Zealand. Quaternary International, 184, 109–121.

Syvitski, J. P. M., Kettner, A. (2011). Sediment flux and the Anthropocene. Philosophical Transactions of the Royal Society A: Mathematical, Physical and Engineering Sciences, 369, 957–975.

Syvitski, J. P. M., Vörösmarty, C. J., Kettner, A. J., Green, P. (2005). Impact of humans on the flux of terrestrial sediment to the Global coastal ocean. Science, 308, 376-380.

Tans, P. P., De Jong, A. F. M., Mook, W. G. (1979). Natural atmospheric 14C variation and the Suess effect. [10.1038/280826a0]. Nature, 280, 826-828.

Taylor, M. P., Macklin, M. G., Hudson-Edwards, K. (2000). River sedimentation and fluvial response to Holocene environmental change in the Yorkshire Ouse Basin, northern England. The Holocene, 10, 201–212.

Thompson, D. W. J., Wallace, J. M. (2000). Annular modes in the extratropical circulation. Part 1 month-month variability. Journal of Climate, 13, 1000–1016.

Thoms, M. C., Olley, J. M. (2004). The stratigraphy, mode of deposition and age of inset flood plains on the Barwon-Darling River, Australia. International Association of Hydrological Sciences Publication, 288, 316–325.

Thorndycraft, V. R., Benito, G. (2006a). The Holocene fluvial chronology of Spain: evidence from a newly compiled radiocarbon database. Quaternary Science Reviews, 25, 223–234.

Thorndycraft, V. R., Benito, G. (2006b). Late Holocene fluvial chronology of Spain: The role of climatic variability and human impact. Catena, 66, 34–41.

Tipping, R. (1994). Fluvial chronology and valley floor evolution of the upper bowmont valley, borders region, Scotland. Earth Surface Processes and Landforms, 19, 641–657.

Törnqvist, T. E. (1994). Middle and late Holocene avulsion history of the River Rhine (Rhine-Meuse delta, Netherlands). Geology, 22, 711–714.

Tornqvist, T. E., Hijma, M. P. (2012). Links between early Holocene ice-sheet decay, sea-level rise and abrupt climate change. Nature Geoscience, 5, 601–606.

Trenberth, K. E. (1997). The Definition of El Niño. Bulletin of the American Meteorological Society, 78, 2771–2777.

Trenberth, K. E., Branstator, G. W., Karoly, D., Kumar, A., Lau, N.-C., Ropelewski, C. (1998). Progress during TOGA in understanding and modeling global teleconnections associated with tropical sea surface temperatures. Journal of Geophysical Research, 103, 14291–14324.

Turner, J. N., Macklin, M. G., Jones, A. F., Lewis, H. (2010). New perspectives on Holocene flooding in Ireland using meta-analysis of fluvial radiocarbon dates. Catena, 82, 183–190.

Turney, C. S. M., Fifield, L. K., Hogg, A. G., Palmer, J. G., Hughen, K., Baillie, M. G. L., Galbraith, R., Ogden, J., Lorrey, A., Tims, S. G., Jones, R. T. (2010). The potential of New Zealand kauri (Agathis australis) for testing the synchronicity of abrupt

climate change during the Last Glacial Interval (60,000–11,700 years ago). Quaternary Science Reviews, 29, 3677–3682.

Turney, C. S. M., Kershaw, A. P., Lowe, J. J., van der Kaars, S., Johnstone, R., Rule, S., Moss, P., Radke, L., Tibby, J., McGlone, M. S., Wilmshurst, J., Vandergoes, M. J., Fitzsimons, S. J., Bryant, C., James, S., Branch, N. P., Cowley, J., Kalin, R. M., Ogle, N., Jacobsen, G., Fifield, L. K. (2006). Climatic variability in the southwest Pacific during the Last Termination (20–10 kyr BP). Quaternary Science Reviews, 25, 886–903.

Turney, C. S. M., McGlone, M. S., Wilmshurst, J. M. (2003). Asynchronous climate change between New Zealand and the Noth Atlantic during the last deglaciation. Geological Society of America, 31, 223–226.

Tyson, P. D. (1980). Temporal and spatial variation of rainfall anomalies in Africa south of latitude 22° during the period of meteorological record. Climatic Change, 2, 363–371.

Ummenhofer, C. C., England, M. H. (2007). Interannual extremes in New Zealand precipitation linked to modes of Southern Hemisphere climate variability. Journal of Climate, 20, 5418–5440.

Ummenhofer, C. C., Sen Gupta, A., England, M. H. (2009). Causes of late twentieth-century trends in New Zealand precipitation. Journal of Climate, 22, 3–19.

Van Dissen, R. J., Berryman, K. R. (1996). Surface rupture earthquakes over the last ~1000 years in the Wellington region, New Zealand, and implications for ground shaking hazard. Journal of Geophysical Research, 101, 5999–6019.

Van Dissen, R. J., Berryman, K. R., Pettinga, J. R., Hill, N. L. (1992). Paleoseismicity of the Wellington-Hutt Valley segment of the Wellington Fault, North Island, New Zealand. New Zealand Journal of Geology and Geophysics, 35, 165–176.

Van Dissen, R. J., Sutherland, D. G., Bowers, R. J., Redwine, J. L. (2006). Forest burial by large rock avalanche in Miller Stream, Seaward Kaikoura Range, New Zealand, c. 1700 years ago. New Zealand Journal of Geology and Geophysics, 49, 151–157.

Vandenberghe, J. (1995). Timescales, climate and river development. Quaternary Science Reviews, 14, 631–638.

Varma, V., Prange, M., Lamy, F., Merkel, U., Schulz, M. (2010). Solar-forced shifts of the Southern Hemisphere Westerlies during the late Holocene. Climate of the Past Discussions, 6, 369–384.

Vella, P., Kaewyana, W., Vuectich, C. G. (1988). Late Quaternary terraces and their cover beds, north-western Wairarapa, New Zealand, and provisional correlations with oxygen isotope stages. Journal of the Royal Society of New Zealand, 18, 309–324.

Vera, C., Silvestri, G., Liebmann, B., González, P. (2006). Climate change scenarios for seasonal precipitation in South America from IPCC-AR4 models. Geophysical Research Letters, 33, L13707.

Walker, M., Johnsen, S., Rasmussen, S. O., Popp, T., Steffensen, J.-P., Gibbard, P., Hoek, W., Lowe, J., Andrews, J., Björck, S., Cwynar, L. C., Hughen, K., Kershaw, P., Kromer, B., Litt, T., Lowe, D. J., Nakagawa, T., Newnham, R., Schwander, J. (2009). Formal definition and dating of the GSSP (Global Stratotype Section and Point) for the base of the Holocene using the Greenland NGRIP ice core, and selected auxiliary records. Journal of Quaternary Science, 24, 3–17.

Walker, M. J. C., Berkelhammer, M., Björck, S., Cwynar, L. C., Fisher, D. A., Long, A. J., Lowe, J. J., Newnham, R. M., Rasmussen, S. O., Weiss, H. (2012). Formal subdivision of the Holocene Series/Epoch: a Discussion Paper by a Working Group of INTIMATE (Integration of ice-core, marine and terrestrial records) and the Subcommission on Quaternary Stratigraphy (International Commission on Stratigraphy). Journal of Quaternary Science, 27, 649–659.

Walling, D. E. (2006). Human impact on land-ocean sediment transfer by the world's rivers. Geomorphology, 79, 192–216.

Wang, H. J., Fan, K. (2005). Central-north China precipitation as reconstructed from the Qing dynasty: Signal of the Antarctic Atmospheric Oscillation. Geophysical Research Letters, 32, L024562.

Wang, Y., Cheng, H., Edwards, R. L., He, Y., Kong, X., An, Z., Wu, J., Kelly, M. J., Dykoski, C. A., Li, X. (2005). The Holocene Asian Monsoon: links to solar changes and North Atlantic climate. Science, 308, 854–857.

Wanner, H., Solomina, O., Grosjean, M., Ritz, S. P., Jetel, M. (2011). Structure and origin of Holocene cold events. Quaternary Science Reviews, 30, 3109–3123.

Wardle, P. (1963). Evolution and distribution of the New Zealand flora as affected by Quaternary climates. New Zealand Journal of Botany, 1, 3–17.

Wardle, P. (1991). Vegetation of New Zealand. Cambridge: Cambridge University Press.

Webb, A. A., Erskine, W. D. (2003). Distribution, recruitment, and geomorphic significance of large woody debris in an alluvial forest stream: Tonghi Creek, southeastern Australia. Geomorphology, 51, 109–126.

Williams, P. W., Neil, H. L., Jian-Xin, Z. (2010). Age frequency distribution and revised stable isotope curves for New Zealand speleothems: palaeoclimatic implications. International Journal of Speleology, 39, 99–112.

Wilmshurst, J. M., Anderson, A. J., Higham, T. F. G., Worthy, T. H. (2008). Dating the late prehistoric dispersal of Polynesians to New Zealand using the commensal Pacific rat. PNAS, 105, 7676–7680.

Wilmshurst, J. M., Eden, D. N., Froggatt, P. C. (1999). Late Holocene forest disturbance in Gisborne, New Zealand : a comparison of terrestrial and marine pollen records. New Zealand Journal of Botany, 37, 523–540.

Wilson, K., Berryman, K., Cochran, U., Little, T. (2007). A Holocene incised valley infill sequence on a tectonically active coast: Pakarae River, New Zealand. Sedimentary Geology, 197, 333–354.

Winkler, S., Matthews, J. A. (2010). Holocene glacier chronologies: Are 'high-resolution' global and inter-hemispheric comparisons possible? The Holocene, 20, 1137–1147.

Wolman, M. G., Gerson, R. (1978). Relative scales of time and effectiveness of climate in watershed geomorphology. Earth Surface Processes, 3, 189–208.

Wolman, M. G., Miller, J. P. (1960). Magnitude and frequency of forces in geomorphic processes. Journal of Geology, 68, 54–74.

Woodward, J. C., Hamlin, R. H. B., Macklin, M. G., Hughes, P. D., Lewin, J. (2008). Glacial activity and catchment dynamics in northwest Greece: Long-term river behaviour and the slackwater sediment record for the last glacial to interglacial transition. Geomorphology, 101, 44–67.

Woodward, J. C., Lewin, J., Macklin, M. G. (1995). Glaciation, river behaviour and Palaeolithic settlement in upland northwest Greece. In J. Lewin, M. G. Macklin J. C. Woodward (Eds.), *Mediterranean Quaternary river environments* (pp. 115–129). Rotterdam: A. A. Balkema.

Woolfe, K. J., Purdon, R. G. (1996). Deposits of a rapidly eroding meandering river: Terrace cut and fill in the Taupo Volcanic Zone. New Zealand Journal of Geology and Geophysics, 39, 243–249.

Yuan, X. (2004). ENSO-related impacts on Antarctic sea ice: a synthesis of phenomenon and mechanisms. Antarctic Science, 16, 415–425.

Yuan, X., Martinson, D. G. (2001). The Antarctic dipole and its predictability. Geophysical Research Letters, 28, 3609–3612.

Zachariasen, J., Berryman, K. R., Langridge, R., Prentice, C., Rymer, M., Stirling, M., Villamor, P. (2006). Timing of late Holocene surface rupture of the Wairau Fault, Marlborough, New Zealand New Zealand Journal of Geology and Geophysics, 49, 159–174.

Zhang, Q., Xu, C.-y., Jiang, T., Wu, Y. (2007). Possible influence of ENSO on annual maximum streamflow of the Yangtze River, China. Journal of Hydrology, 333, 265–274.

Zhang, Y., Wallace, J. M., Battisti, D. S. (1997). ENSO-like interdecadal variability: 1900–93. Journal of Climate, 10, 1004–1020.

Zhou, S. Z., Chen, F. H., Pan, B. T., Cao, J. X., Li, J. J., Derbyshire, E. (1991). Environmental change during the Holocene in western China on a millennial timescale. Holocene, 1, 151–156.

Zielhofer, C., Faust, D. (2008). Mid- and Late Holocene fluvial chronology of Tunisia. Quaternary Science Reviews, 27, 580–588.

Zielinski, G. A. (2000). Use of paleo-records in determining variability within the volcanism-climate system. Quaternary Science Reviews, 19, 417–438.

Appendix A

Contents of the DVD

A DVD accompanies this thesis and is stored in a pocket at the rear. The DVD contains the following files:

A PDF copy of the thesis.

Meta-analysis data for Chapter 4 (file name: NZ_14C_metaanalysis_original.xlsx).

The updated New Zealand fluvial ^{14}C database with new Northland data and meta-analysis data for Chapters 6 and 7 (file name: NZ_14Cdatabase_metaanalysis_withnorthland.xls).

Grainsize data for Kaeo exposure K1 (file name: Grainsize_data_Kaeo.xlsx).

XRF data, optical images and radiographs for Kaeo core (folder name: XRF_data_Kaeo).

Appendix B

Optically stimulated luminescence dating

1. Introduction

Optically stimulated luminescence (OSL) dating is a technique used to date Quaternary sediments, by providing a measure of the time elapsed since mineral grains (quartz and feldspars) were exposed to sunlight (Huntly et al., 1985). The technique has been rapidly evolving in recent decades (e.g., Duller, 2008) and has been used to provide chronological control in a range of sedimentary environments (Lian and Roberts, 2006). In the fluvial setting the OSL technique offer a means by which the age of sediment deposition can be directly dated, thereby avoiding some of the issues associated with ^{14}C dating (i.e., reliance on the preservation of suitable organic material and sediment reworking). However, OSL dating of fluvial sediments can be problematic due to incomplete resetting of the luminescence signal during fluvial deposition (partial bleaching), resulting in age overestimations (Rittenour, 2008). The aim of this pilot study was to assess the use of OSL dating in fluvial depositional environments in Northland by targeting sections that had ^{14}C age control.

2. Method

Five samples from three sites in Northland (Takahue River, Mangakahia River and Wairua River; see Fig. 6.1 for locations) were OSL dated by the Victoria University of Wellington Luminescence Dating Laboratory using the Multiple Aliquot Additive Dose method (MAAD) on feldspar (see luminescence dating technical report No 3/12 attached).

3. Results

See luminescence dating technical report No 3/12 attached.

4. Discussion

Figure B.1 shows the Takahue site details, cross-section and locations of samples tak211 and tak111 dated using OSL. Samples were retrieved from a freshly exposed terrace riser. Radiocarbon dates from organic material in two cores (T3 and T2) suggest the terrace is of Holocene age. OSL ages obtained from the terrace sediments were much older than expected (with reported OSL ages of 57.3 ± 10.8 ka and 68.7 ± 6.4 ka). Figure B.2 shows the Nukutawhiti site details, cross-section and locations of samples nuk111 and nuk211 dated using OSL. At this site samples were obtained from a freshly exposed stream bank and organic material from core M2 suggests that the terrace is of Holocene age. OSL results from samples nuk111 and nuk 211 were also considerably older than expected (101 ± 12.4 ka and 72 ± 7.4 ka). It is likely that the overestimation in OSL ages at the Nukutawhiti and Takahue sites is the result of incomplete zeroing (partial bleaching) of the luminescence signal in the feldspar grains. In fluvial environments this can be caused by a number of factors that limit the amount of solar exposure. Incomplete bleaching prior to deposition can occur when sediment travels only short distances, when sunlight is restricted or when suspended sediment concentrations are high (Rittenour, 2008). Rapid erosion of unbleached sediment from older deposits during high-discharge events can also contribute to age overestimation (Rittenour, 2008). In addition to being older than expected the OSL ages from the Nukutawhiti site were reversed, adding support to the assertion that the fluvial sediments were not completely bleached prior to deposition.

Figure B.3 displays a cross-section for the Poroti site. At this site organic material at the base of core P1 returned a ^{14}C age of > 50,000 BP (representing the maximum limit of ^{14}C dating). The OSL date suggests the age of the deposit is 16.4 ± 3.1 ka, however there is no ^{14}C data to corroborate this. Based on the OSL results from the Nukutawhiti and Takahue sites there is little confidence that the Poroti sample OSL has not been similarly affected by partial bleaching.

5. Conclusion

This pilot study has found that the use of OSL dating of Northland floodplain sediments using the MAAD method on feldspar produces overestimated ages. This is most likely due to incomplete resetting of the luminescence signal in the mineral grains prior to deposition. On the basis of these results it can be concluded that the OSL technique (MAAD method on feldspar) is not suitable for dating Holocene fluvial deposits in Northland.

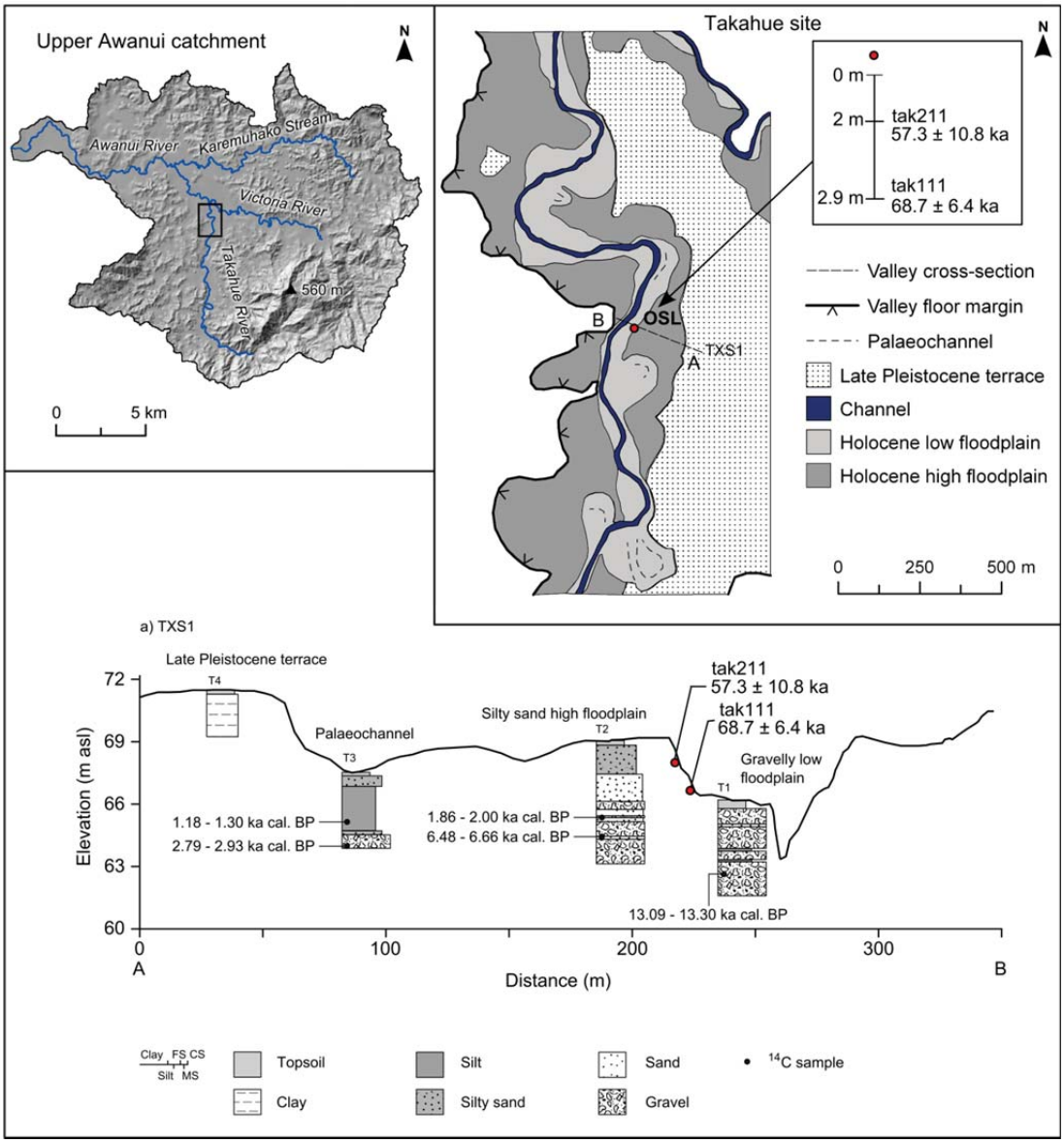

Fig. B.1. Catchment DEM, planform map and cross-section for the Takahue site (see Fig. 6.1 for location). Red circles show location of OSL samples.

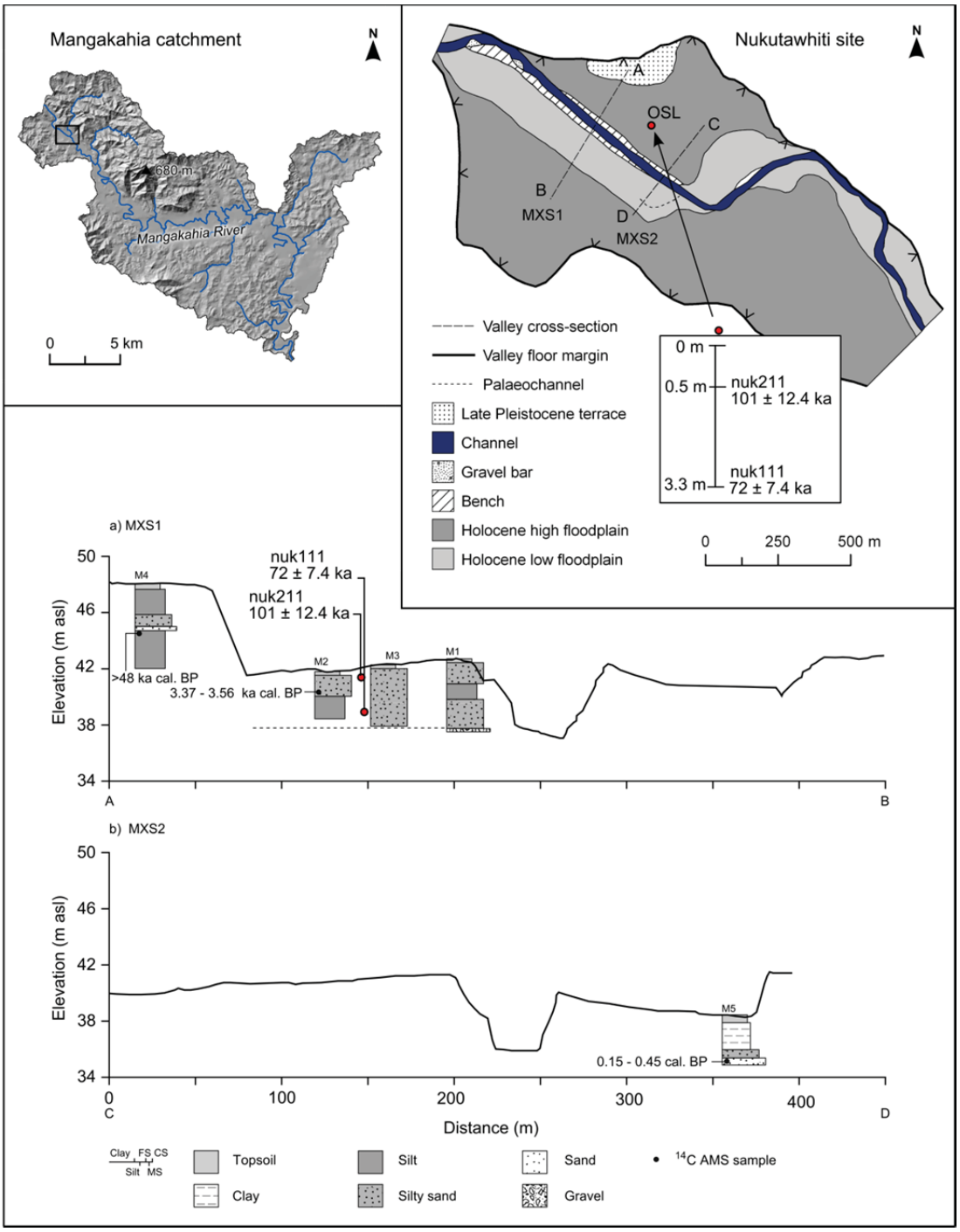

Fig. B.2. Catchment DEM, planform map and cross-section for the Nukutawhiti site (see Fig. 6.1 for location). Red circles show location of OSL samples.

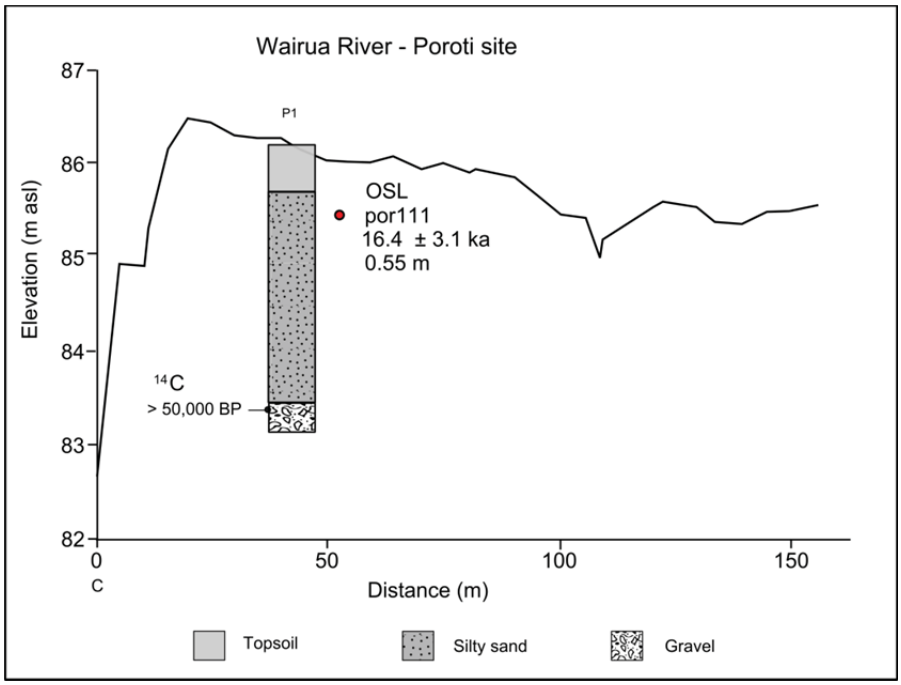

Fig. B.3. Cross-section for the Poroti site (see Fig. 6.1 for location). Red circle shows location of OSL sample.

References

Huntley, D. J., Godfrey-Smith, D. I., Thewalt, M. L. W. (1985). Optical dating of sediments. Nature, 313, 105–107.

Rittenour, T. M. (2008). Luminescence dating of fluvial deposits: application to geomorphic, palaeoseismic and archaeological research. Boreas, 37, 613–635

Duller, G. A. (2008). Single-grain optical dating of Quaternary sediments: why aliquot size matters in luminescence dating. Boreas, 37, 580–612.

Lian, O. B., Roberts R. G. (2006). Dating the Quaternary: progress in luminescence dating of sediments. Quaternary Science Reviews, 25, 2449–2468.

Report No. 3/12

Luminescence Dating Technical Report

Luminescence Dating Laboratory
School of Geography, Environment and Earth Sciences
Victoria University of Wellington
Wellington
New Zealand

Reported by: Ms. Ningsheng Wang
Date of Issue: 20-2-2012
Contact: Room 414
Cotton Building
Victoria University of Wellington
Ph: (04) 463 6127

1

CONTENTS

1. SUMMARY

Five samples (Field code: nuk111, nuk211, tak111, tak211 and por111) were submitted for luminescence dating by Dr. Nicola Litchfield, GNS Science. The laboratory codes of the samples are WLL960-WLL964.

Due to the sample being fine material, the fine grain (4-11µm) preparation technique was used. The paleodose (the equivalent dose) of all samples was evaluated using the Multiple Aliquot Additive Dose method (MAAD) based on measurements of blue luminescence from the fine grain feldspar produced during infrared stimulation. The dose rate was determined on the basis of gamma spectrometry measurements.

2. EXPERIMENTAL WORK

A) Sample Preparation

Samples had their outer surfaces removed. "Fresh" sample material, that had outer surfaces removed earlier (unexposed light sample material), was treated in 10% HCl. This was carried out overnight until all carbonate was removed by the reaction. Following this treatment the sample was further reacted overnight with 10% H_2O_2 in order to remove organic matter. The next step involved 200ml CBD* solution being added to the sample for 12 hours to remove iron oxide coatings. Note, after every chemical treatment procedure distilled water was used to wash the sample several times. After chemical treatment, calgon solution (1g sodium hexametaphosphate per litre distilled water) was added to make thick slurry. This slurry was placed into an ultrasonic bath and mechanically agitated for an hour. The sample was then placed into a 1L measuring cylinder, filled with a certain amount of distilled water to separate out the 4-11µm grains according to Stokes' Law.
The 4-11µm grains were then rinsed with ethanol and acetone and a suspension of these grains were then deposited evenly onto 70 aluminium disks (diameter 9.8mm).

This removed outer scraping was then dried in an oven, milled, weighed and sealed in air tight perspex containers, then stored for at least four weeks before the gamma

spectrometer analysis. The storage time minimizes the loss of the short lived noble gas ^{222} Rn and allows ^{226}Ra to reach equilibrium with its daughters ^{214} Pb and ^{214} Bi.

A plastic cube was then filled with remaining scrapings in preparation for water content measuring.

*CBD solution: 71g sodium citrate, 8.5 g sodium bicarbonate, and 2g sodium dithionate per litre of distilled water

B) Measurements

Luminescence age was determined by two factors: the equivalent dose (D_e) and the dose rate. It involves measurements of luminescence for determination of D_e and concentrations of ^{238}U, ^{232}Th, ^{40} K and water contents (used to determine of dose rate).

Equivalent dose: obtained from the lab equivalents to the paleodose absorbed by samples during the burial time in the natural environment since their last exposure to the light.
Dose rate: amount dose received by the sample each year.

B1. Determination of Equivalent Dose (D_e)

D_e for all of these samples were obtained by using the *Multiple Aliquot Additive Dose Method (MAAD)*.

The test dose obtained from an initial test measurement was used for the MAAD. As luminescence vary between disks, all disks for MAAD need to be normalised before β irradiation. 0.1 second infrared measurements were taken before irradiation of all aliquots. Six groups (30 disks divided by five) were β irradiated up to five times of the test dose. Beta irradiation were done on the Riso TL-DA-15 ^{90}Sr/Y β irradiator, calibrated against ^{60}Co gamma source, SFU, Vancouver, Canada with about 3% uncertainty. Three groups (three disks per group) were α irradiated up to three times of the test dose. The α irradiation was carried out on a ^{241} Am irradiator, supplied and calibrated by ELSEC Littlemore, UK. The next step was that these 39

disks together with nine non-irradiated disks (total of 48 disks) were stored for four weeks to relax the crystal lattice after irradiation.

After storage, the 48 disks were preheated for five minutes at 230°C, then were measured using a Riso TL-DA-15 reader with infrared diodes at 880nm used to deliver a stimulated beam (30mW/cm^2)at the room temperature for 100s. Blue luminescence centred about 410nm emission from feldspar was then detected by an EMI 9235QA photomultiplier fixed behind two filters consisting of a Schott BG-39 and Kopp 5-58.

Luminescence growth curve (β induced luminescence intensity versus added dose) was constructed by using the initial the 10 seconds of the shine down curves and subtracting the average of the last 20 seconds, along with the so called late light which was thought to be a mixture of background and hardly bleachable components. Extrapolation of this growth curve to the dose axis was obtained the equivalent dose De which was used as a paleodose. The shine plateau was checked to be flat after this manipulation.

Measurement of a-value

A similar plot for the alpha irradiated disks allows for an estimation of α efficiency, a-value (a-value is measured by comparing the luminescence induced by alpha irradiation with that induced by beta or gamma irradiation). The a-value was for dose rate calculation.

B2: Determination of Dose Rate

Dose rate consisted of two parts.
(i) Dose rate from sample's burial environment
(ii) Dose rate from cosmic rays.

(i) *Dose rate from burial environment*

Dose rate from sample's burial environment was determined by radionuclide contents of ^{238}U, ^{232}Th and ^{40}K, a-value and water content.

5

Determination of Contents of U, Th and K by Gamma spectrometry

Gamma rays produced from sample material was counted for a minimum time of 24 hours by a high resolution and broad energy gamma spectrometer. The spectra were then analysed using GENIE2000 software. The contents of U, Th and K were obtained by comparison with standard samples. The dose rate calculation was based on the activity concentration of the nuclides ^{40} K, ^{208}TL, ^{212}Pb, ^{228} Ac, ^{214} Bi, ^{214}Pb, ^{226} Ra, using dose rate conversion factors published by Adamiec and Aitken (1998).

Measurement of Water Contents

Water content was measured as weight of water divided by dry weight of the sample taking into account a 25% uncertainty.

(ii) *Dose rate from cosmic rays*

Dose rate from cosmic rays were determined by the depth of sample below the surface along with its longitude, latitude and altitude, convention formula and factors published by Prescott, J.R. & Hutton, J.T. (1994).

3. RESULTS

Table 1 Cosmic Dose Rates

Table 2 Water Contents, Radionuclide Contents

Table 3 a- Values, Equivalent Doses, Dose Rates and Luminescence Ages

Table 1: Cosmic Dose Rates

Laboratory Code	Depth Below the Surface(m)	Cosmic Dose Rate (Gy/ka)	Field Code
WLL960	3.3	0.1322±0.0066	nuk111
WLL961	0.5	0.1925±0.0096	nuk211
WLL962	2.9	0.1404±0.0070	tak111
WLL963	2.0	0.1581±0.0079	tak211
WLL964	0.55	0.1922±0.0096	por 111

Table 2: Water Contents, Radionuclide Contents

Laboratory Code	Water content (%)	U(ppm) from ^{234}Th	U(ppm) from ^{226}Ra, ^{214}Pb, ^{214} Bi	U(ppm) from ^{210}Pb	Th(ppm) From ^{208}Tl ^{212} Pb ^{228} Ac	K(%)	Field Code
WLL960	36.4	0.91±0.16	1.11±0.10	1.22±0.14	4.19±0.07	0.81±0.02	nuk111
WLL961	43.3	1.15±0.15	1.01±0.10	0.87±0.12	4.13±0.07	0.76±0.02	nuk211
WLL962	38.2	0.76±0.12	0.75±0.08	0.73±0.11	2.58±0.05	0.75±0.02	tak111
WLL963	37.2	0.82±0.14	0.81±0.09	0.83±0.11	3.01±0.06	0.76±0.02	tak211
WLL964	51.2	3.94±0.25	3.23±0.16	2.51±0.17	13.44±0.15	0.32±0.01	por 111

Table 3: a-Values, Equivalent Doses, Dose Rates and Luminescence Ages

Laboratory Code	a-value	D_e(Gy)	Dose Rate(Gy/ka)	**Luminescence Age(ka)**	Field Code
WLL960	0.06±0.02	95.90±5.87	1.33±0.11	**72.1±7.4**	nuk111
WLL961	0.06±0.02	127.22±11.12	1.26±0.11	**101.0±12.4**	nuk211
WLL962	0.06±0.02	73.02±13.05	1.06±0.05	**68.7±6.4**	tak111
WLL963	0.05±0.01	64.21±11.21	1.12±0.09	**57.3±10.8**	tak211
WLL964	0.09±0.01	37.91±6.89	2.32±0.10	**16.4±3.1**	por 111

4. REFERENCES

Adamiec, G. & Aitken, M. 1998: Dose- rate conversion factors: update. Ancient TL, Vol.16, No.2, 37-50

Murry, A.S. & Wintle, A.G. 2000: Luminescence dating of quartz using an improved single aliquot regenerative dose protocol. Radiation Measurements 32, 57-73.

Prescott, J.R. & Hutton, J.T. 1994: Cosmic ray contributions to dose rates for luminescence and ESR dating: Large depths and long-term time variations. Radiation Measurements. Vol.23,Nos.2/3, 497-500.

Appendix C

Bank exposure and percussion core lithological logs

Bank exposures and sediment cores (collected using a percussion coring system) were logged in the field according to sediment colour, grain size and texture. Significant facies boundaries were noted and organic material was collected for ^{14}C dating. Core details and data are displayed in the following core logs, which have been prepared using WinLoG v.4. A key for the core log lithological symbols is presented below.

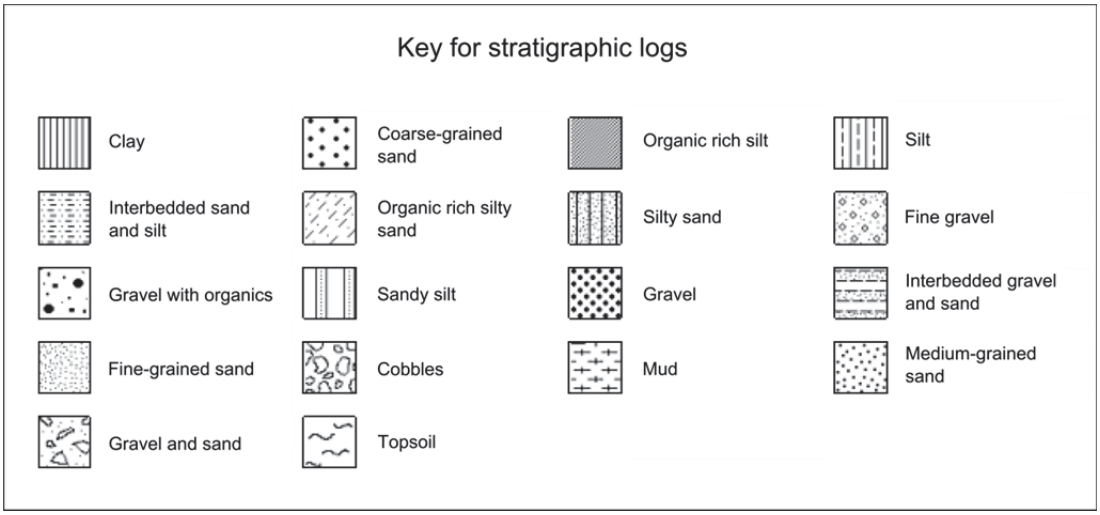

Project: Northland Flood History *Date:* 03.12.09

Core Location: Awanui palaeochannel Nth Kaitaia *Catchment:* Awanui River

Core Code: Awanui 1 (A1) *NZTM Coordinates:* 1622961E 6116015N

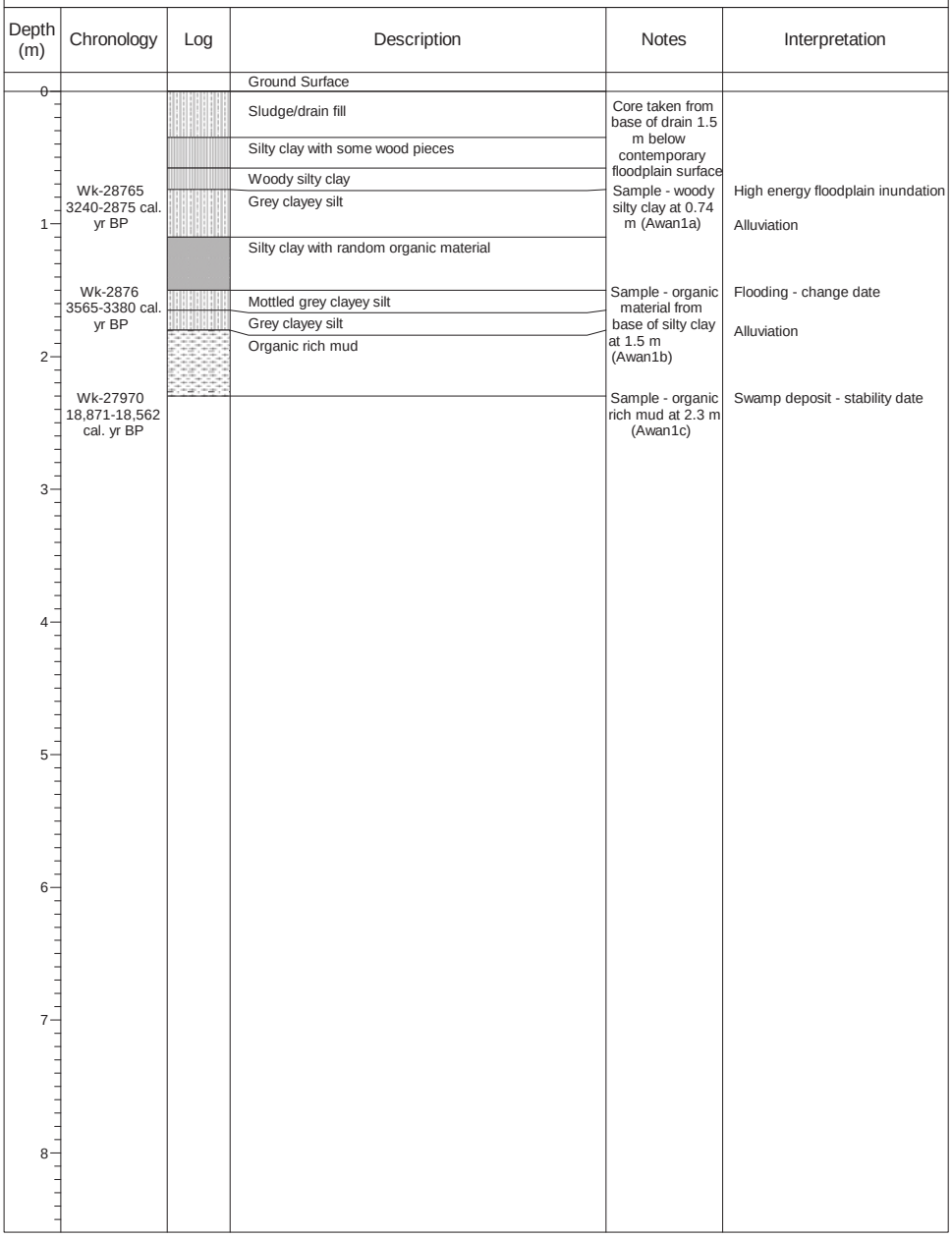

Project: Northland Flood History *Date:* 03.12.09

Exposure Location: Kaeo Green Lane *Catchment:* Kaeo River

Exposure Code: Kaeo 1 (K1) *NZTM Coordinates:* 1672045E 6114932N

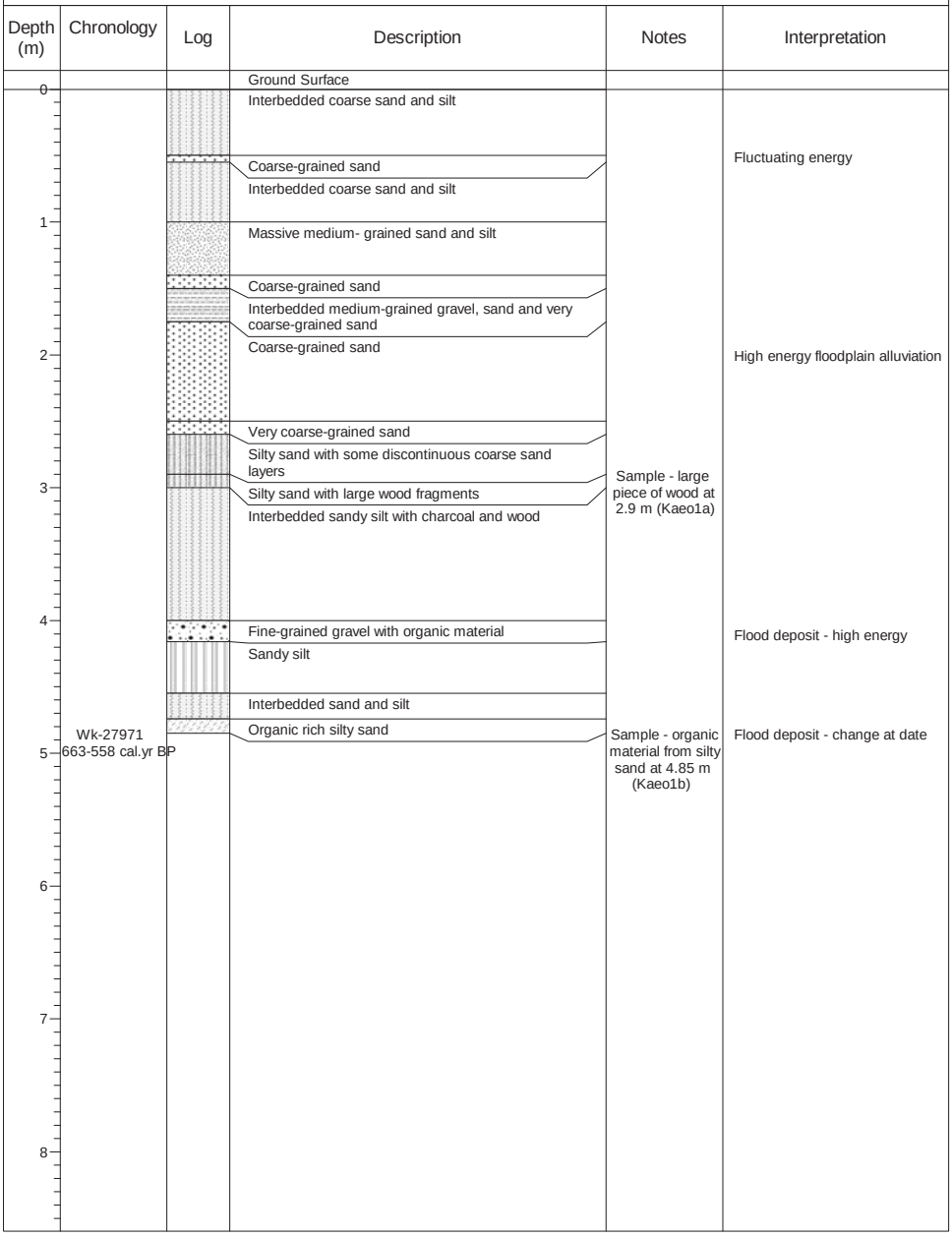

Project: Northland Flood History *Date:* 13.12.10

Core Location: Kaeo *Catchment:* Kaeo River

Core Code: Kaeo 4 (K4) *NZTM Coordinates:* 1671036E 6115214N

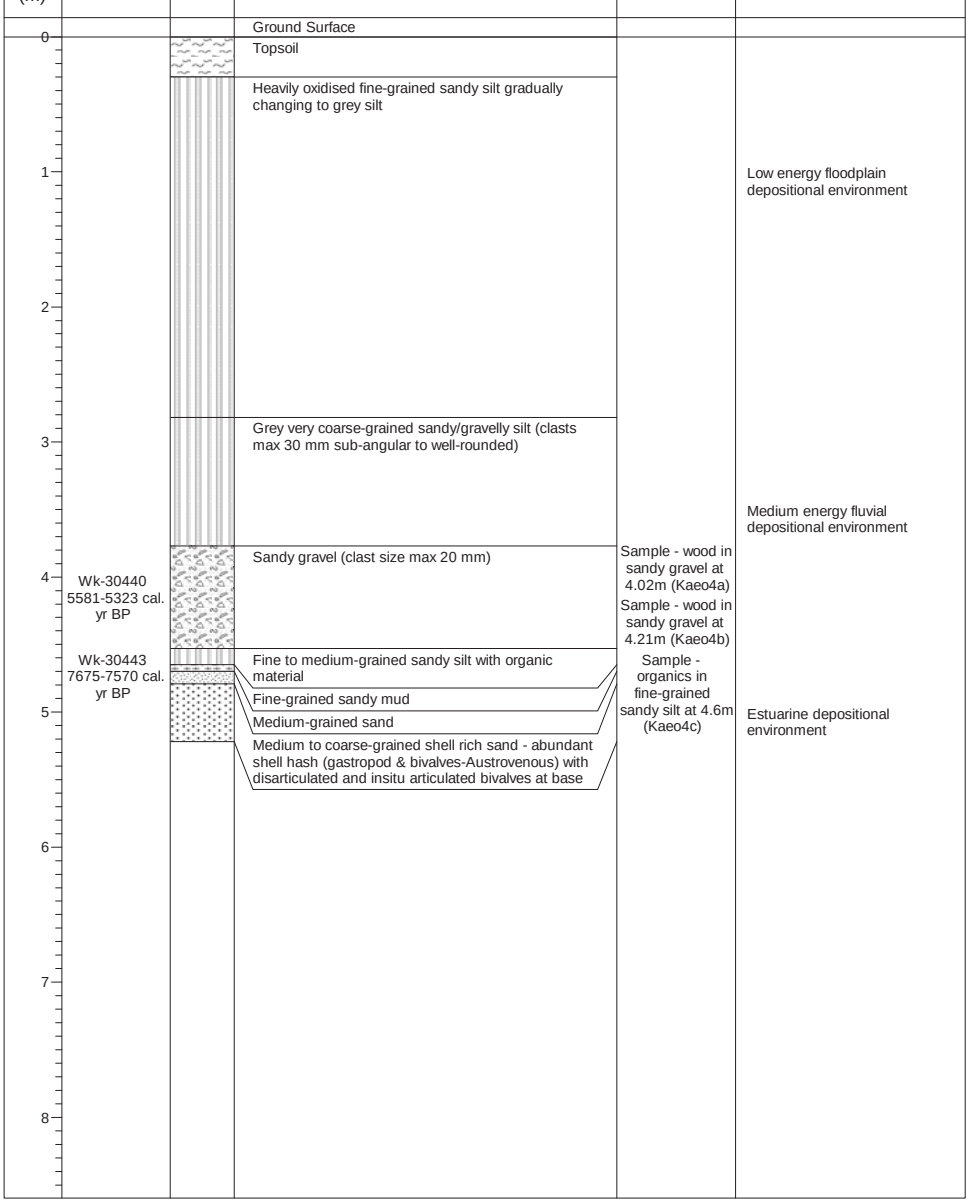

Project: Northland Flood History *Date:* 11.12.10

Core Location: Maitahi *Catchment:* Kaihu River

Core Code: Kaihu 2 (KH2) *NZTM Coordinates:* 1669199E 6032871N

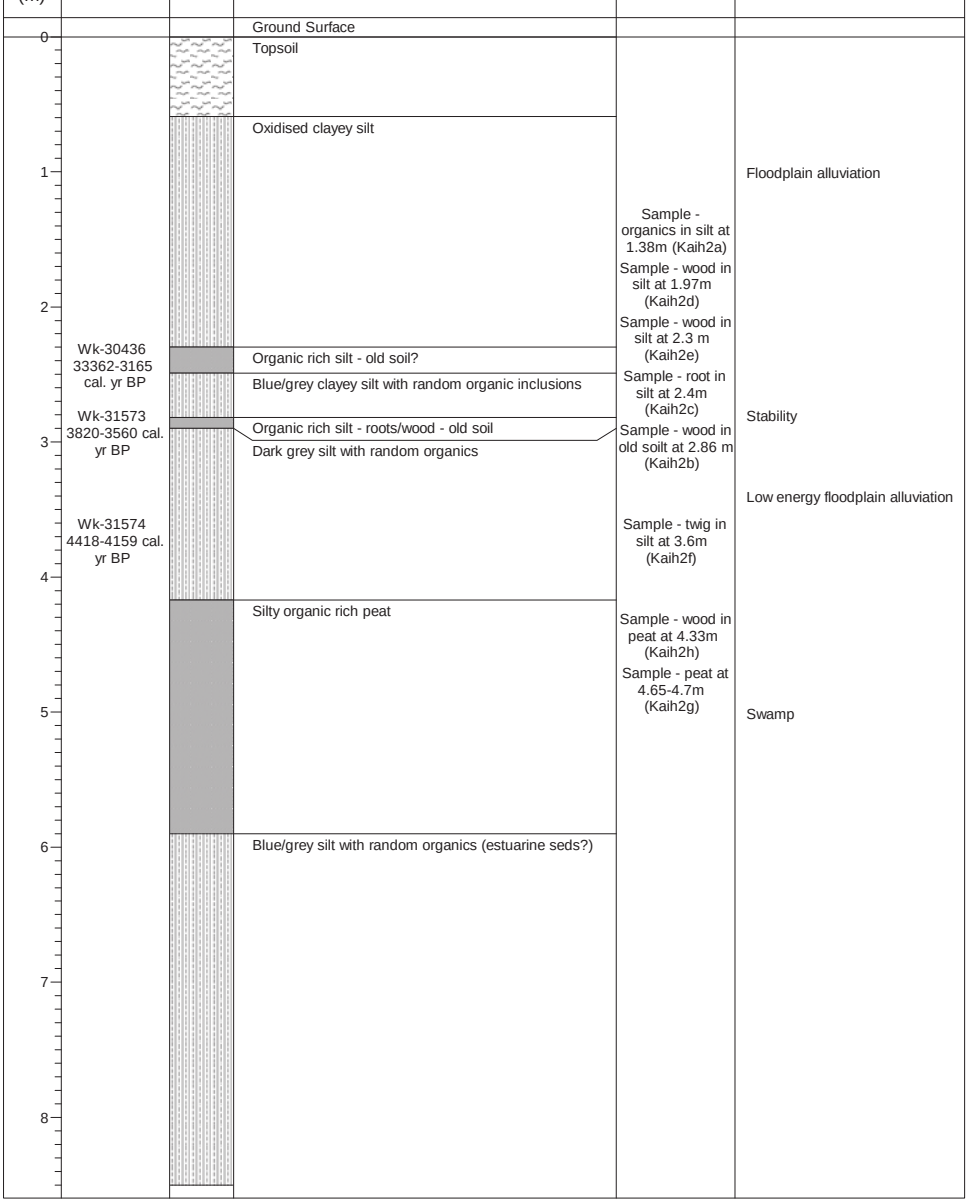

Project: Northland Flood History *Date:* 12.12.10

Core Location: Maitahi *Catchment:* Kaihu River

Core Code: Kaihu 4 (KH4) *NZTM Coordinates:* 1668919E 6032694N

Depth (m)	Chronology	Log	Description	Notes	Interpretation
			Ground Surface		
0			Topsoil		
			Heavily oxidised silt changing gradually to mottled silt then grey silt - hard/compacted		
1					
2					
3					
4					
5					
6					
7					
8					

Project: Northland Flood History *Date:* 01.12.09

Exposure Location: Mangakahia Titoki Bridge *Catchment:* Mangakahia River

Exposure Code: Titoki 1 (TI1) *NZTM Coordinates:* 1695130E 6044963N

Depth (m)	Chronology	Log	Description	Notes	Interpretation
			Ground Surface		
0			Interbedded sand/silt (4 sand layers visible)		Floodplain alluviation - variable energy
1					
2					
3					
4					
5					
6					
7	Wk-27967 788-669 cal. yr BP		Organic rich silt	Sample - orgain rich silt at 7.4 m (Mang1a)	Change date - flood deposit
8					

Project: Northland Flood History *Date:* 09.12.10

Core Location: Nukutawhiti *Catchment:* Mangakahia River

Core Code: Mangakahia 1 (M1) *NZTM Coordinates:* 167810E 605550N

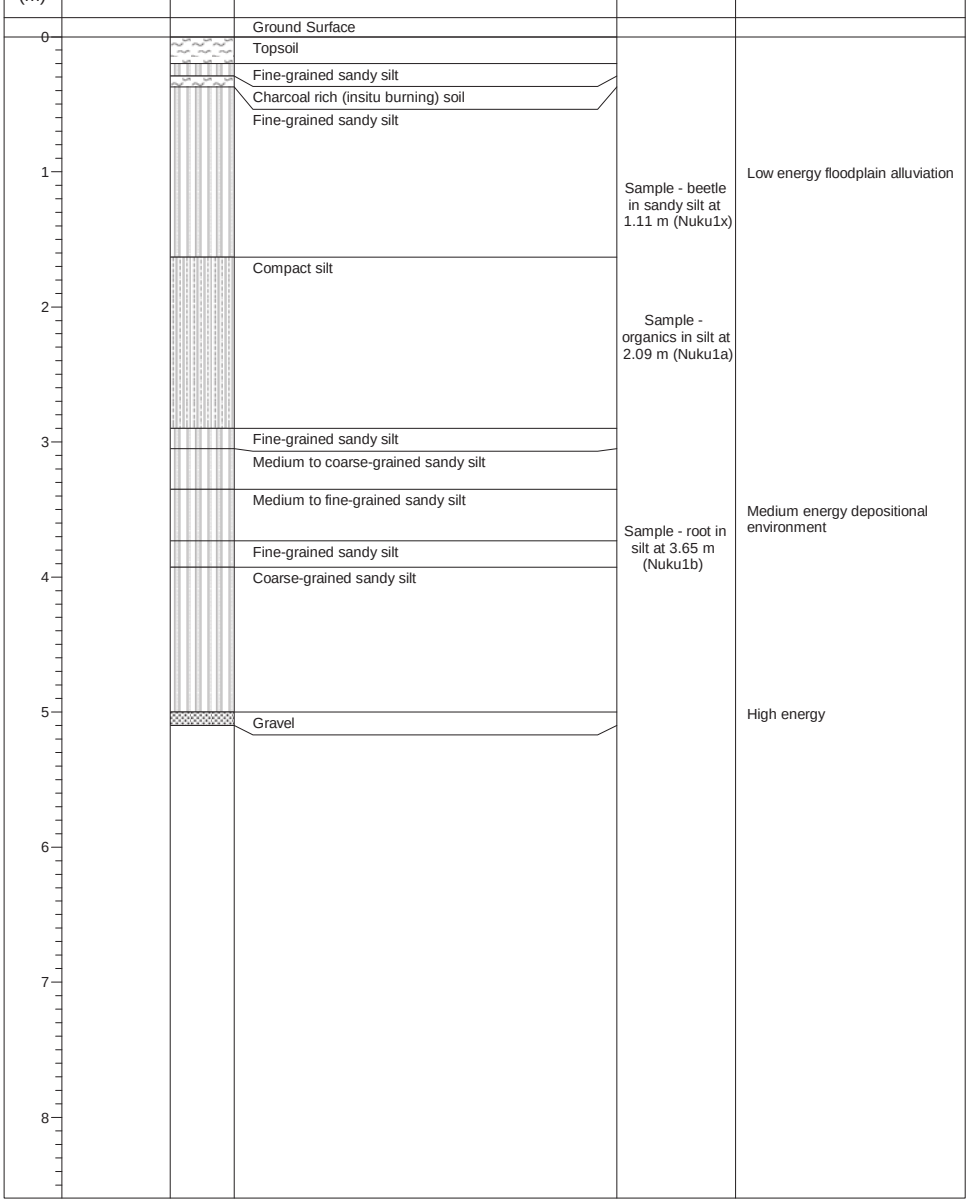

Project: Northland Flood History *Date:* 09.12.10

Core Location: Nukutawhiti *Catchment:* Mangakahia River

Core Code: Mangakahia 2 (M2) *NZTM Coordinates:* 1678156 E 6055489 N

Depth (m)	Chronology	Log	Description	Notes	Interpretation
			Ground Surface		
0	Wk-31576 3557-3379 cal. yr BP		Topsoil	Sample - organic material in fine-grained sandy silt at 1.47 m (Nuku2a) Sample - organic material in clayey silt at 2.23 m (Nuku2b) Sample - wood in clayey silt at 2.39 m (Nuku2c) Sample - wood in clayey silt at 2.45 m (Nuku2d)	Low energy depositional environment
1			Fine-grained sandy silt		
2			Grey clayey silt		
3					
4					
5					
6					
7					
8					

Project: Northland Flood History *Date:* 09.12.10

Core Location: Nukutawhiti *Catchment:* Mangakahia River

Core Code: Mangakahia 3 (M3) *NZTM Coordinates:* 167810E 605560N

Depth (m)	Chronology	Log	Description	Notes	Interpretation
			Ground Surface		
0			Topsoil		
			Fine-grained sandy silt		
1					Low energy depositional environment
2					
3					
4			Medium-grained sandy silt		
			Very fine-grained sandy silt		
5					
6					
7					
8					

Project: Northland Flood History *Date:* 10.12.10

Core Location: Nukutawhiti *Catchment:* Mangakahia River

Core Code: Mangakahia 4 (M4) *NZTM Coordinates:* 167815E 605560N

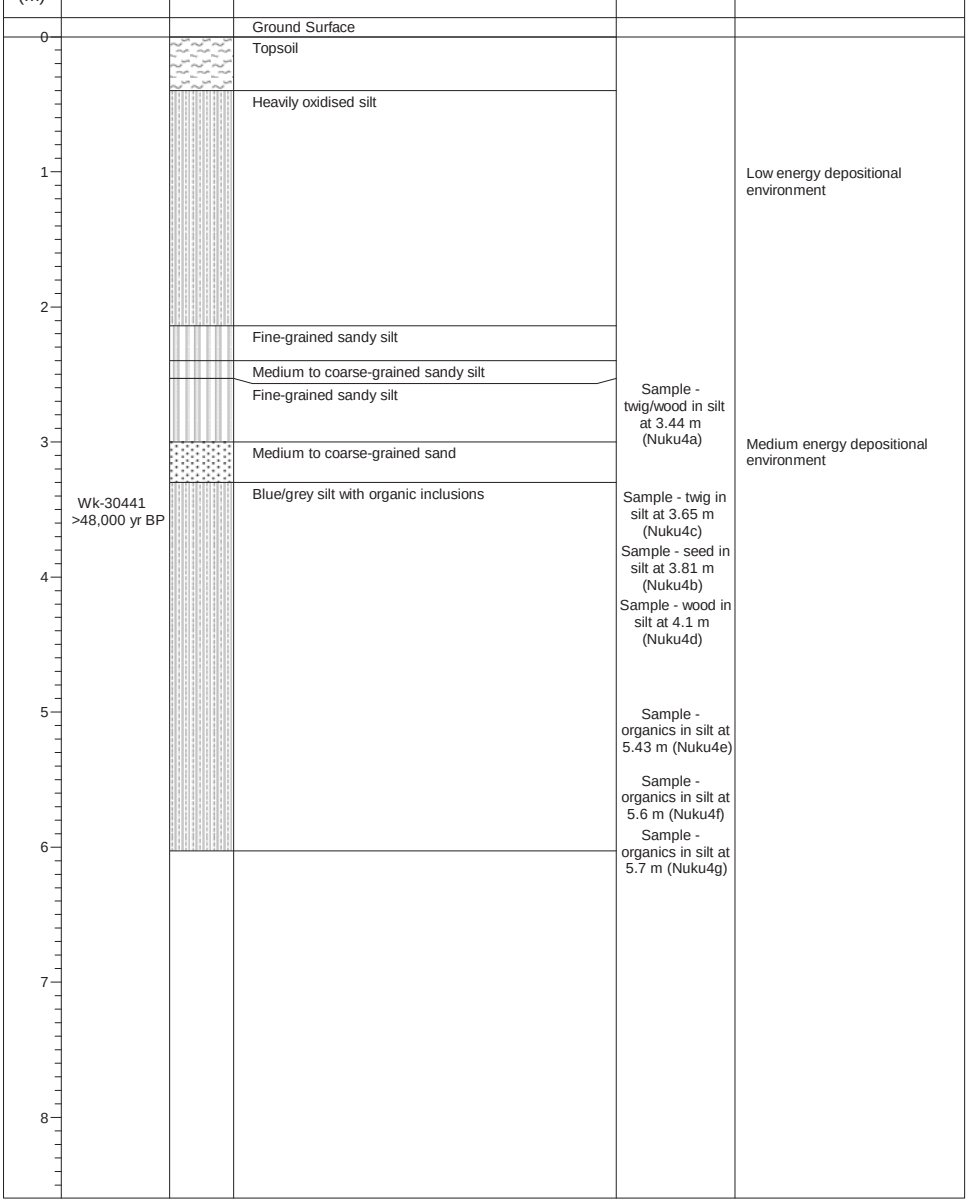

Project: Northland Flood History *Date:* 09.04.2010

Core Location: Mangakahia palaeochannel Nukutawhiti *Catchment:* Upper Mangakahia River

Core Code: Mangakahia 5 (M5) *NZTM Coordinates:* 1678250E 6055200N

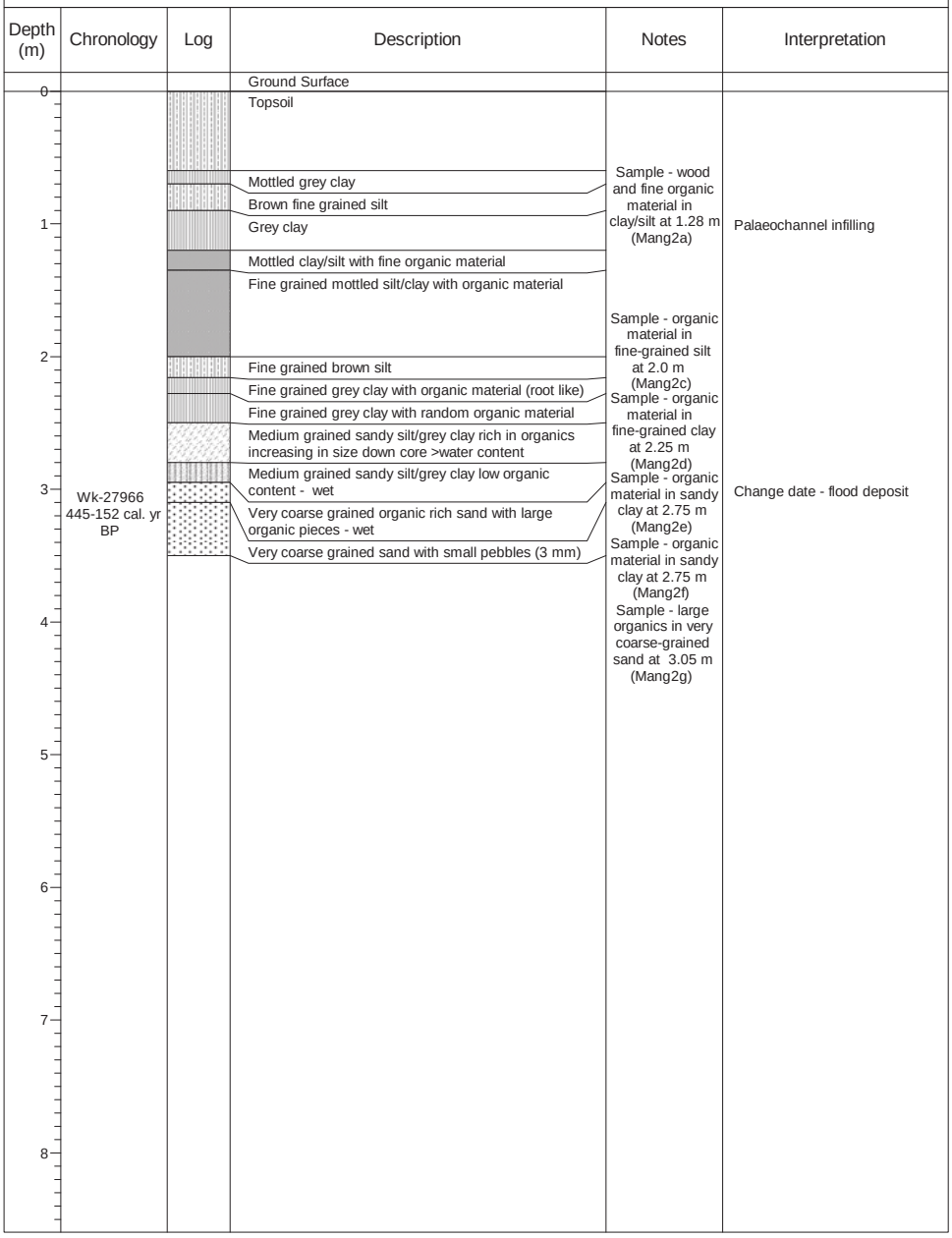

Project: Northland Flood History *Date:* 02.12.09

Exposure Location: Whakarapa Stream Panguru *Catchment:* Panguru

Exposure Code: Panguru 2 (P2) *NZTM Coordinates:* 1684991E 6084593N

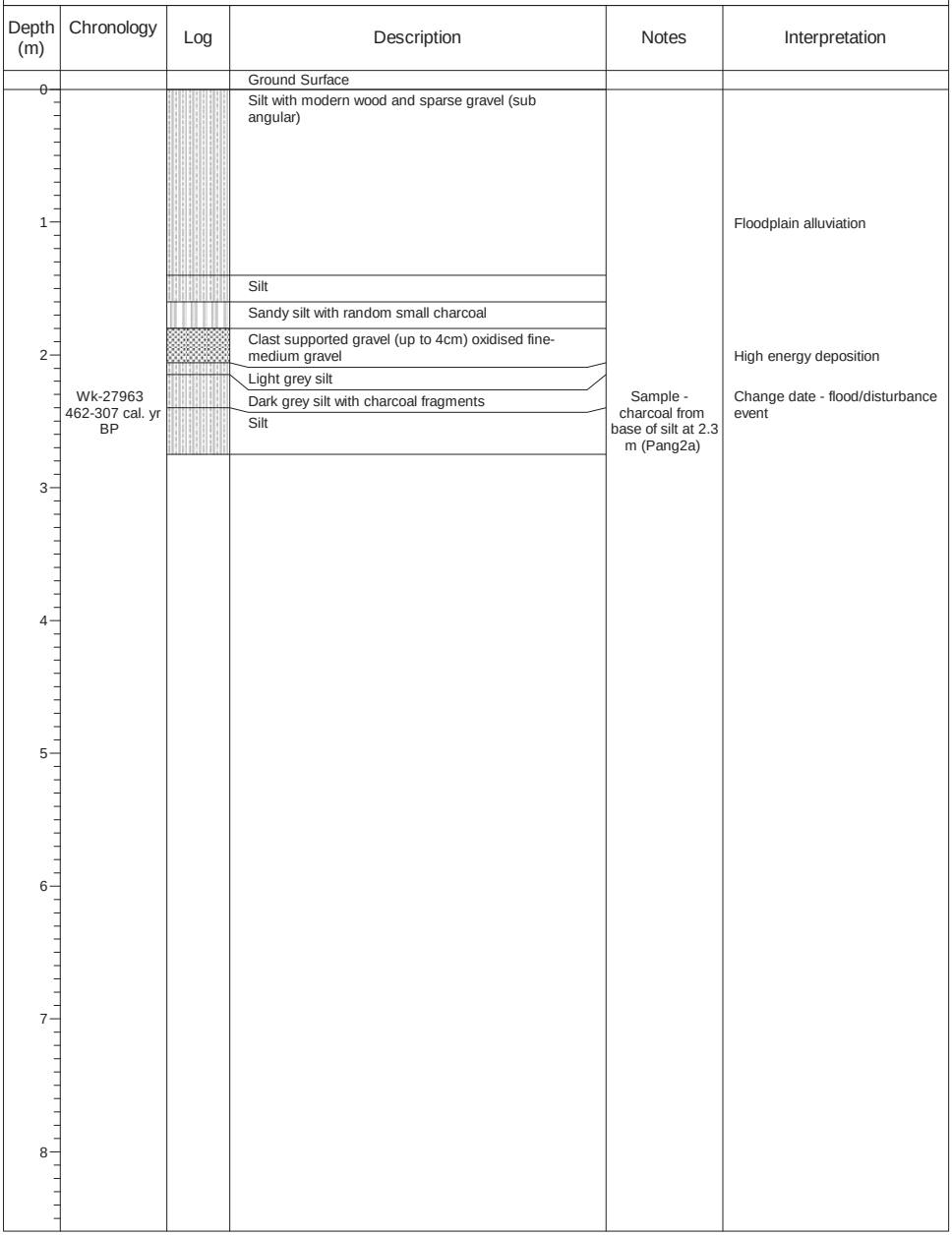

Project: Northland Flood History *Date:* 16.12.10

Core Location: Poroti palaeochannel *Catchment:* Wairua River

Core Code: Poroti 4 (P4) *NZTM Coordinates:* 1699114 E 6045407 N

Depth (m)	Chronology	Log	Description	Notes	Interpretation
0			Ground Surface		
			Topsoil		
			Very dark brown organic rich peaty silt with large roots		Stability
			Very dark brown clay with fine organic flecks		
1			Very dark greyish brown peaty clay with large organic material roots/wood (15 mm dia)		
			Dark brown clay with root inclusions		
			Pale brown silt with large roots (10 mm dia)		
	Wk-30763 10,108-9983 cal. yr BP		Fine-grained grey-green silt with organic inclusions	Sample - organic material in silt at 1.72 m (Poro4a)	
2			Grey-green clay with rare random organic material	Sample - wood in clay at 2.1 m (Poro4b - low confidence)	Activity - low energy
3					
4					
5					
6					
7					
8					

Project: Northland Flood History *Date:* 17.12.10

Core Location: Takahue Pamapuria *Catchment:* Takahue River

Core Code: Takahue 1 (T1) *NZTM Coordinates:* 1632004E 6110784N

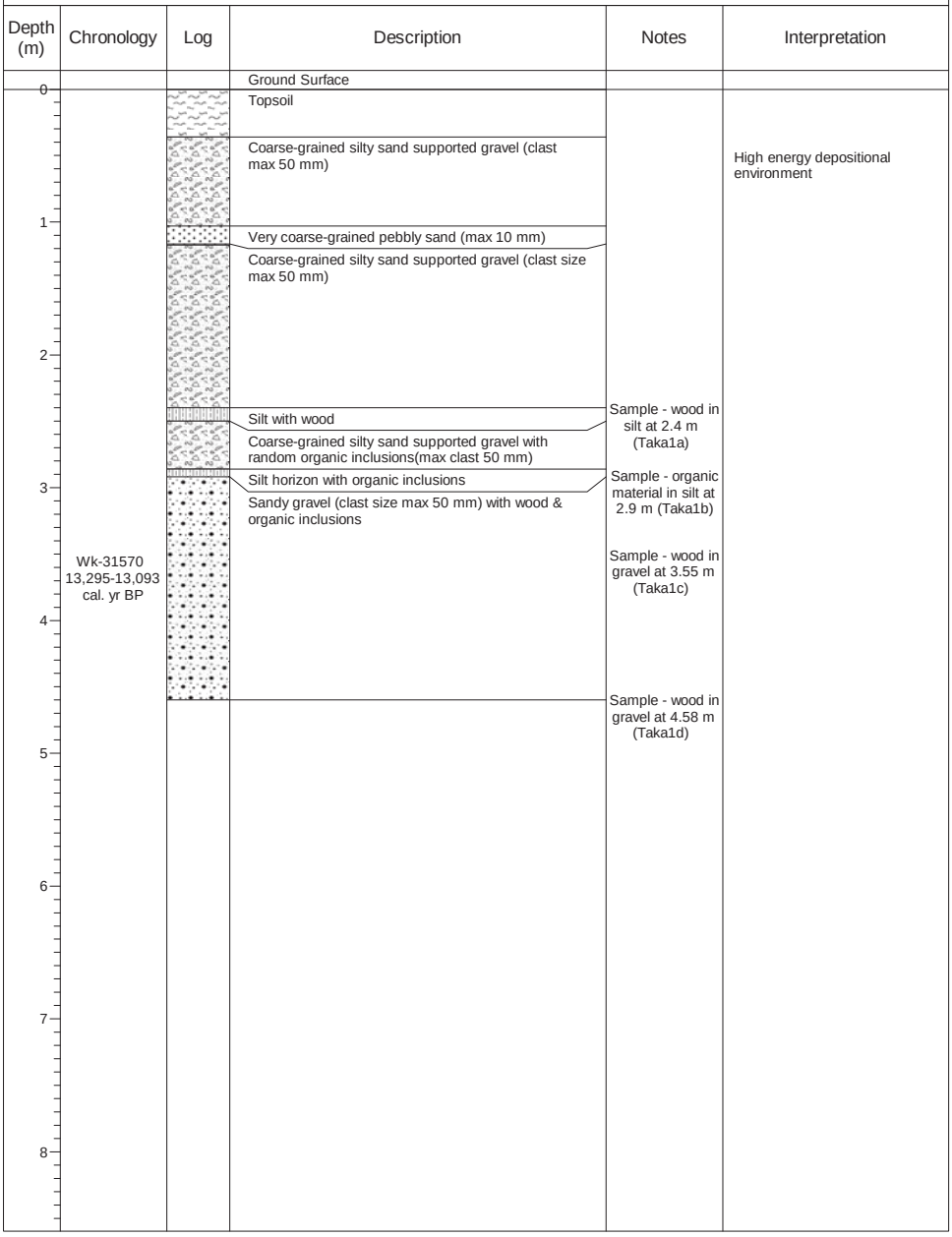

Project: Northland Flood History *Date:* 17.12.10

Core Location: Takahue Pamapuria *Catchment:* Takahue River

Core Code: Takahue 2 (T2) *NZTM Coordinates:* 1632067E 6110791N

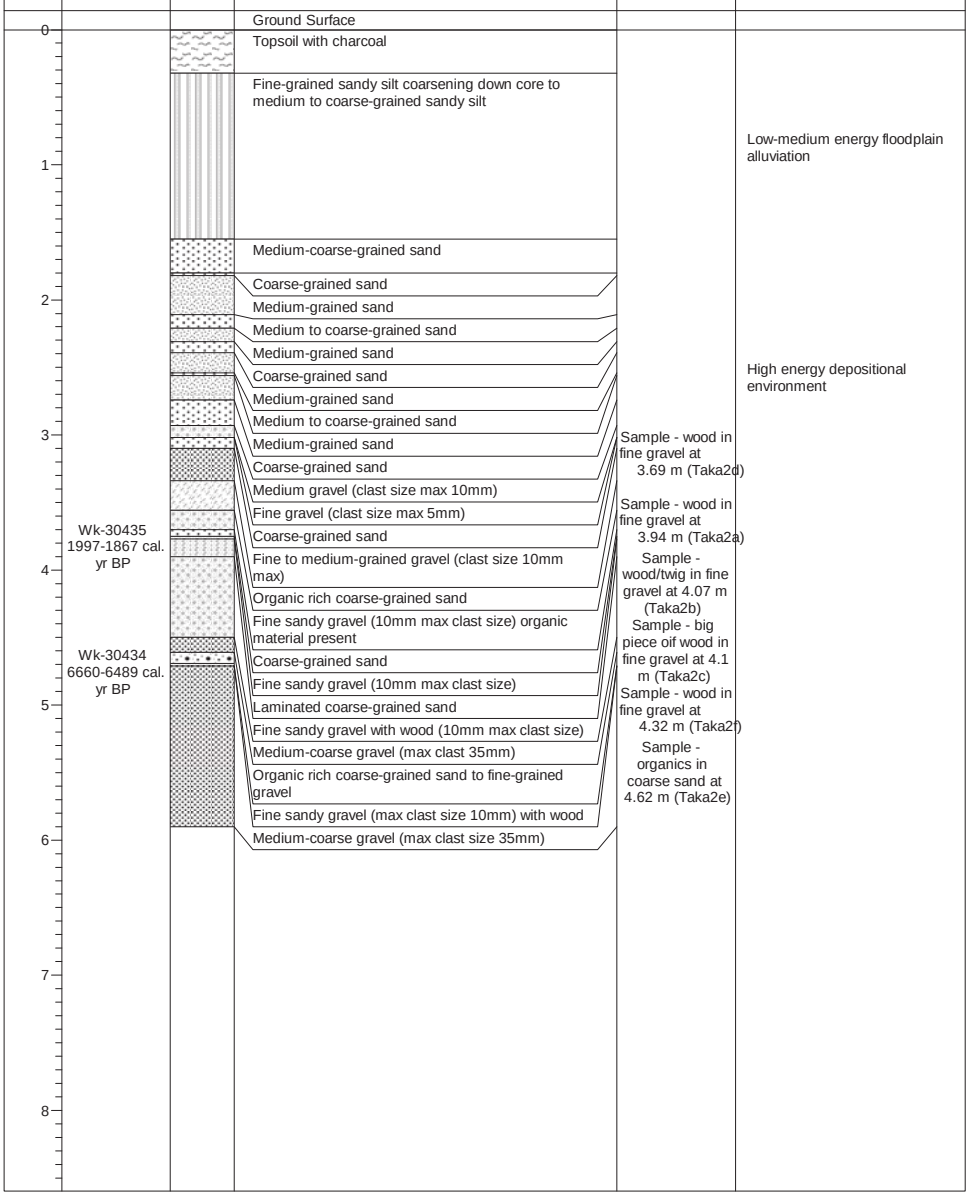

Project: Northland Food History *Date:* 08.12.10

Exposure Location: Takahue Pamapuria palaeochannel *Catchment:* Takahue River

Exposure Code: Takahue 3 (T3) *NZTM Coordinates:* 1632161E 6110762N

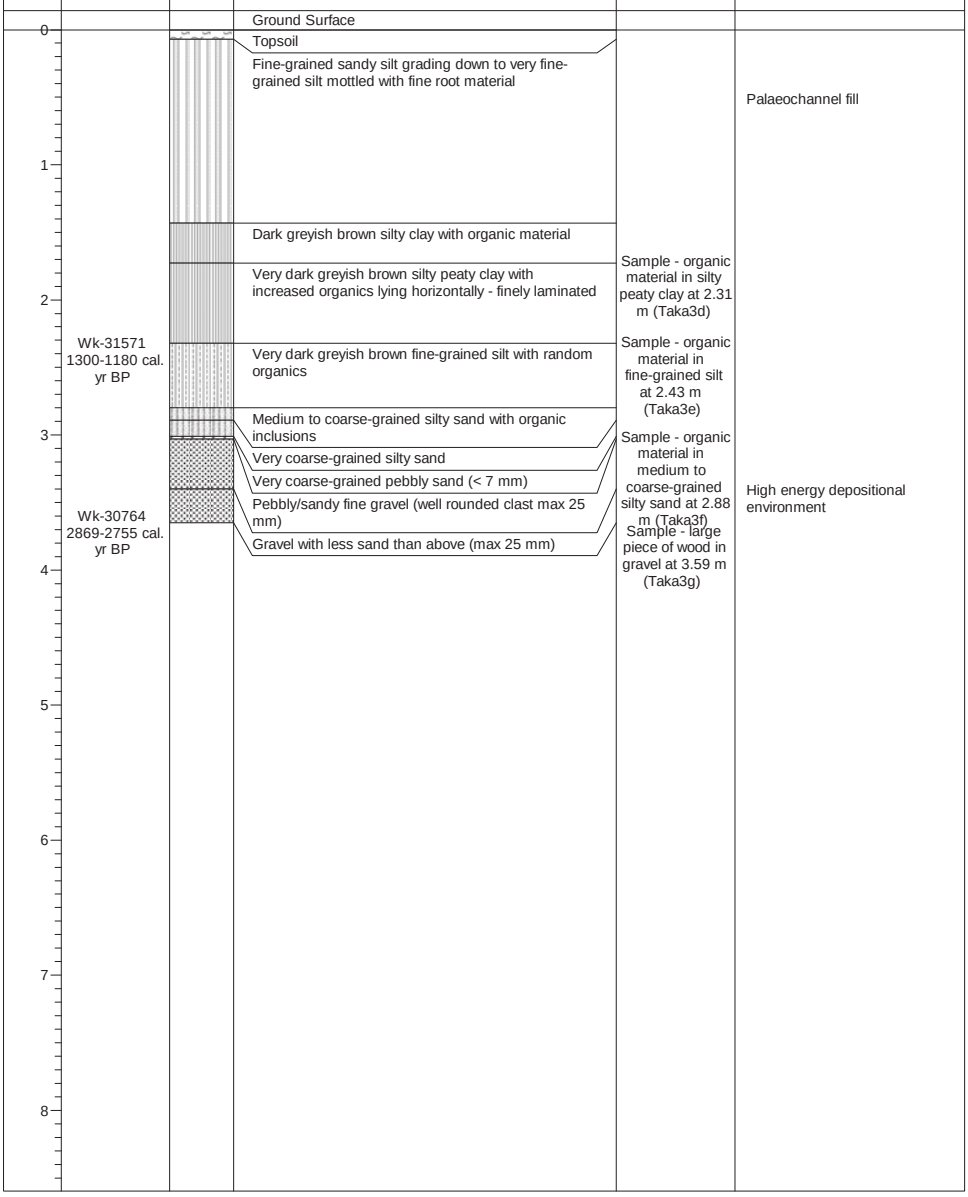

Project: Northland Flood History *Date:* 18.12.10

Core Location: Takahue Pamapuria *Catchment:* Takahue River

Core Code: Takahue 4 (T4) *NZTM Coordinates:* 1632220E 6110742N

Depth (m)	Chronology	Log	Description	Notes	Interpretation
0			Ground Surface		
			Topsoil		
			Oxidised silty clay (compact/hard)		High terrace surface
1					
2					
3					
4					
5					
6					
7					
8					

Project: Northland Flood History *Date:* 02.12.09

Exposure Location: Waihou River Panguru *Catchment:* Waihou River

Exposure Code: Waihou 3 (WA3) *NZTM Coordinates:* 1631925E 6082811N

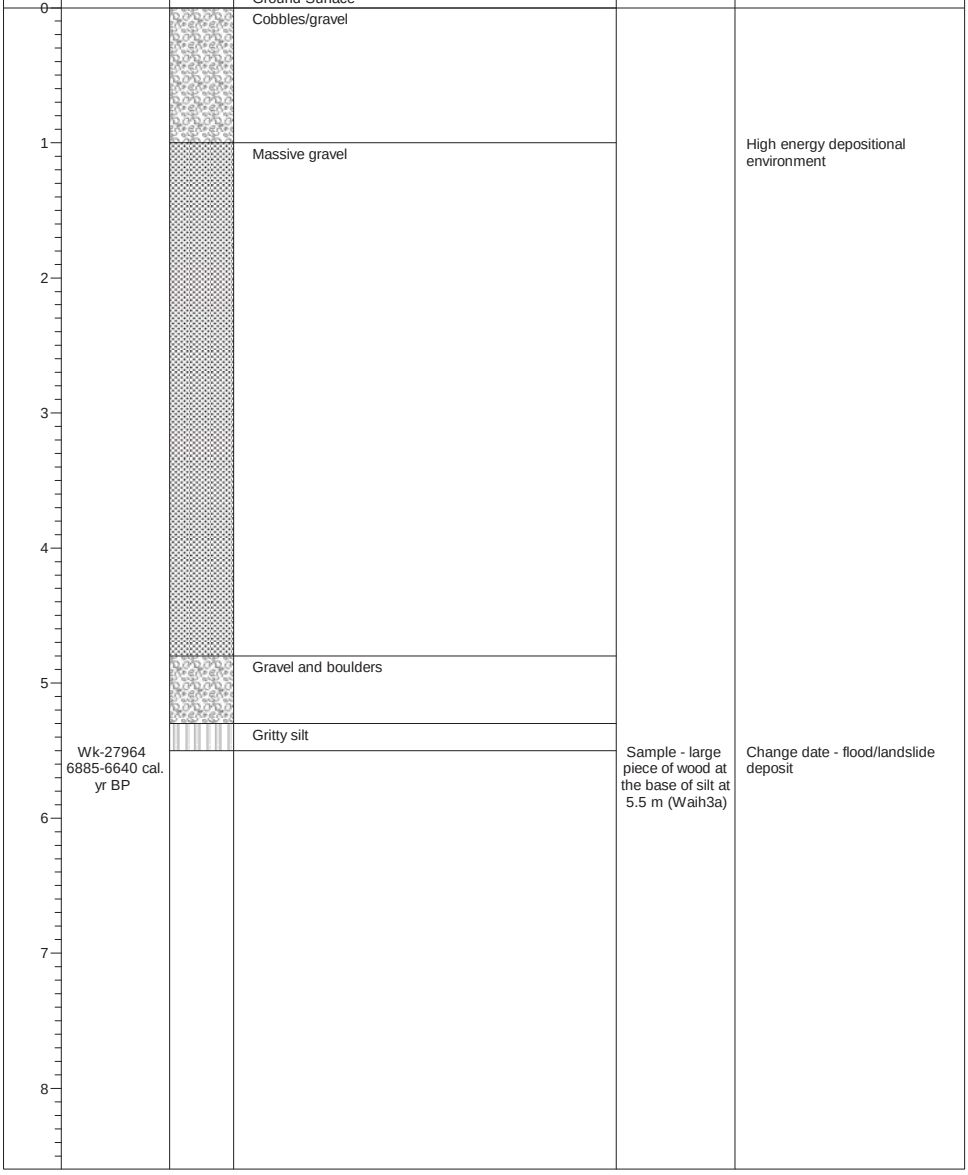

Project: Northland Flood History *Date:* 02.12.09

Exposure Location: Waimamaku Hooks & Hall Rd *Catchment:* Waimamaku River

Exposure Code: Waimamaku 1 (W1) *NZTM Coordinates:* 1641495E 6065132N

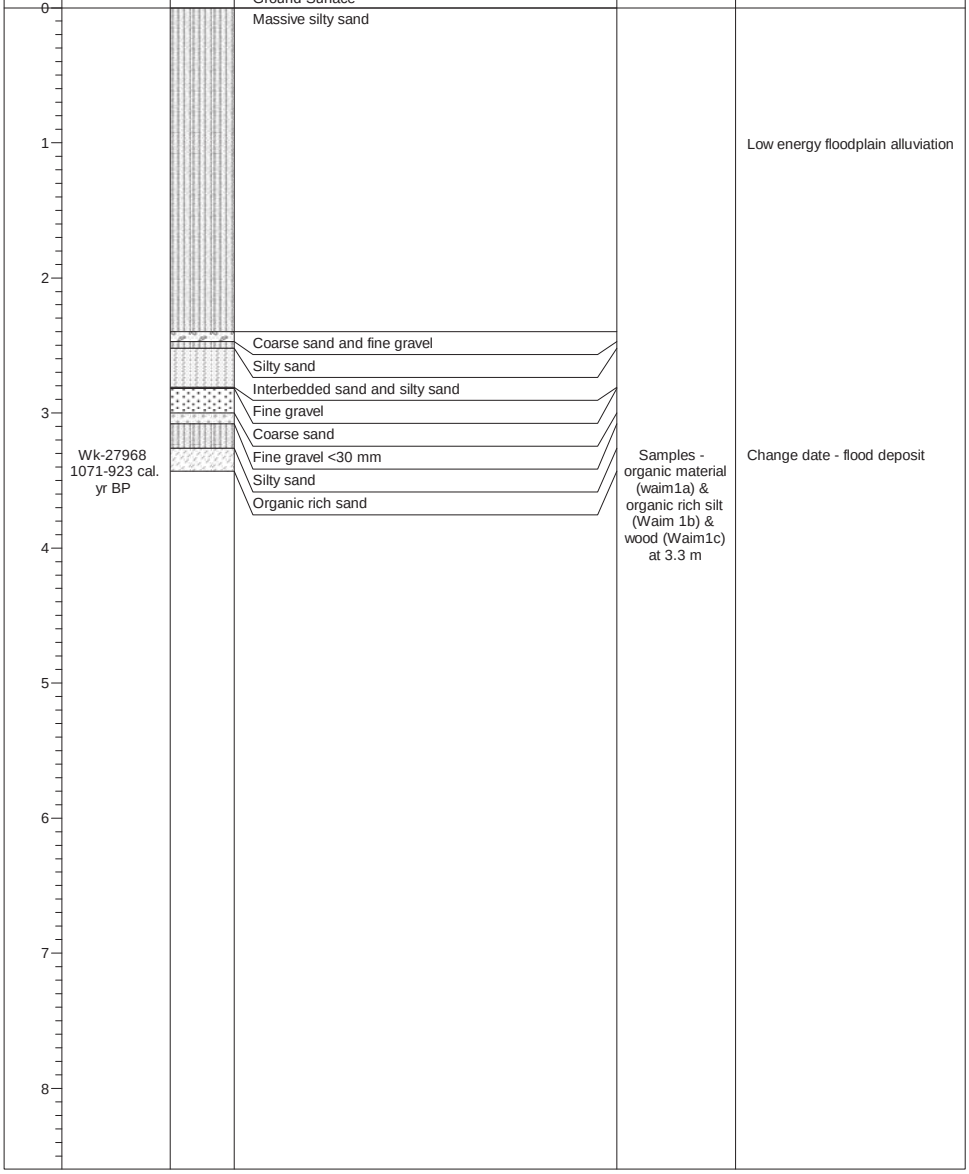

Project: Northland Flood History *Date:* 07.12.10

Core Location: Hooks and Hall Rd *Catchment:* Waimamaku River

Core Code: Waimamaku 3 (W3) *NZTM Coordinates:* 6065250E 1641900N

Depth (m)	Chronology	Log	Description	Notes	Interpretation
			Ground Surface		
0			Topsoil	Sample - roots near top of gravel at 1.7 m (Waim3a)	Floodplain alluviation
			Gritty silt		
1			Coarse sandy silt with manganese inclusions and oxidised rootlets		
2			Coarse sandy silt with gravel clasts (max 50 mm)		
3					
4					
5					
6					
7					
8					

Project: Northland Flood History *Date:* 07.12.10

Core Location: Waimamaku Hooks and Hall Rd *Catchment:* Waimamaku River

Core Code: Waimamaku 4 (W4) *NZTM Coordinates:* 1641795E 6065161N

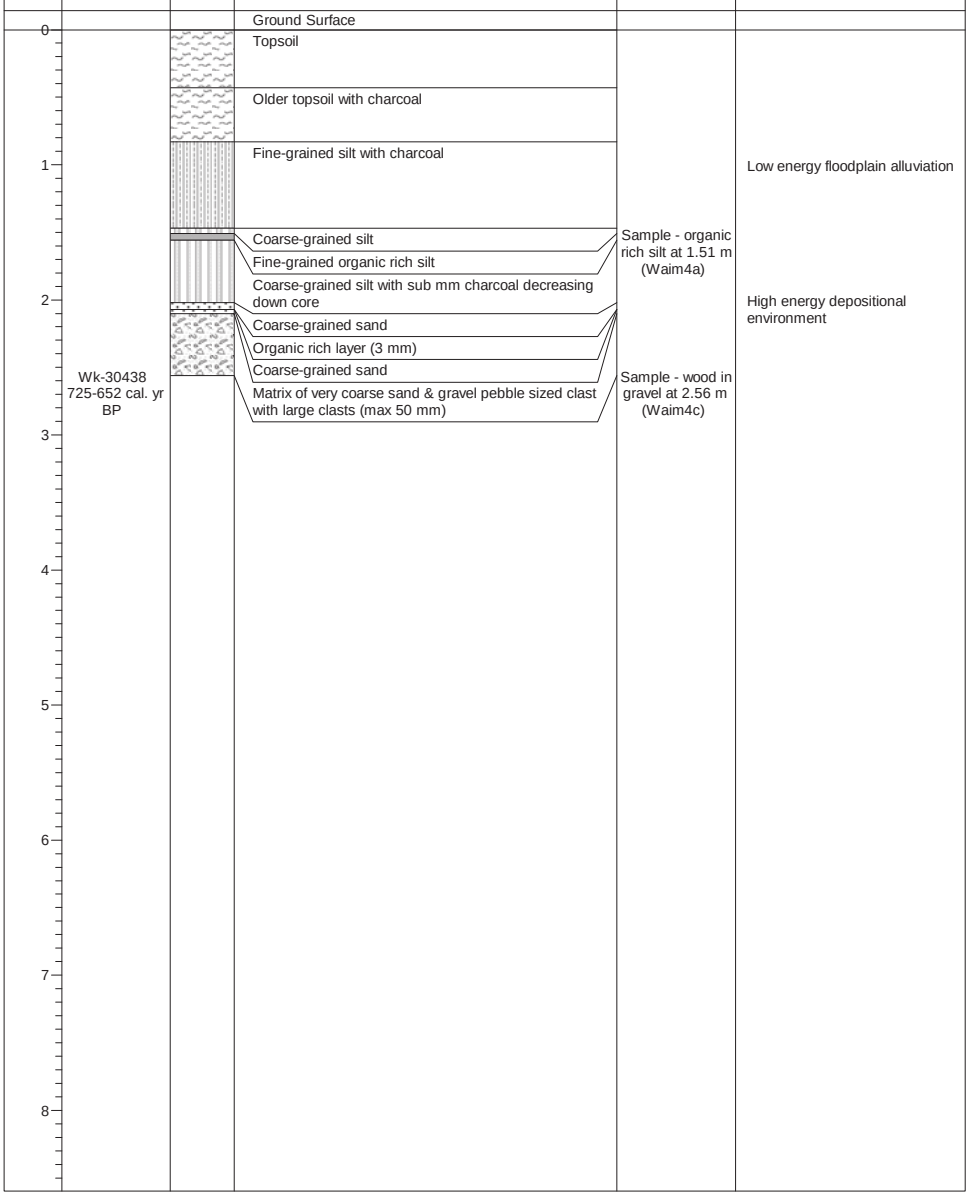

Project: Northland Flood History *Date:* 07.12.10

Core Location: Waimamaku Hooks and Hall Rd *Catchment:* Waimamaku River

Core Code: Waimamaku 5 (W5) *NZTM Coordinates:* 1641950E 6065300N

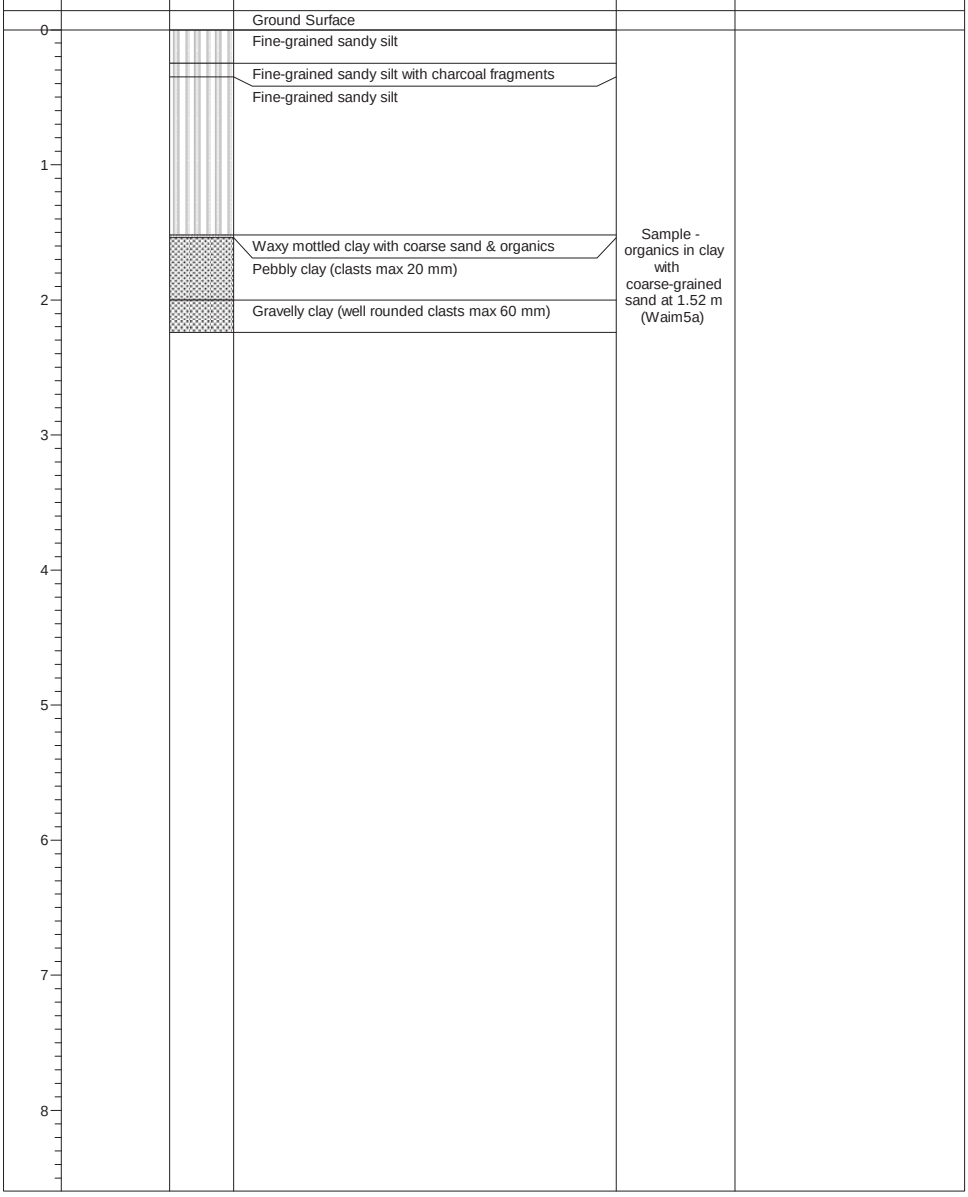

Project: Northland Flood History *Date:* 07.12.10

Core Location: Waimamaku Hooks & Hall Rd *Catchment:* Waimamaku River

Core Code: Waimamaku 6 (W6) *NZTM Coordinates:* 1641797 E 6065276 N

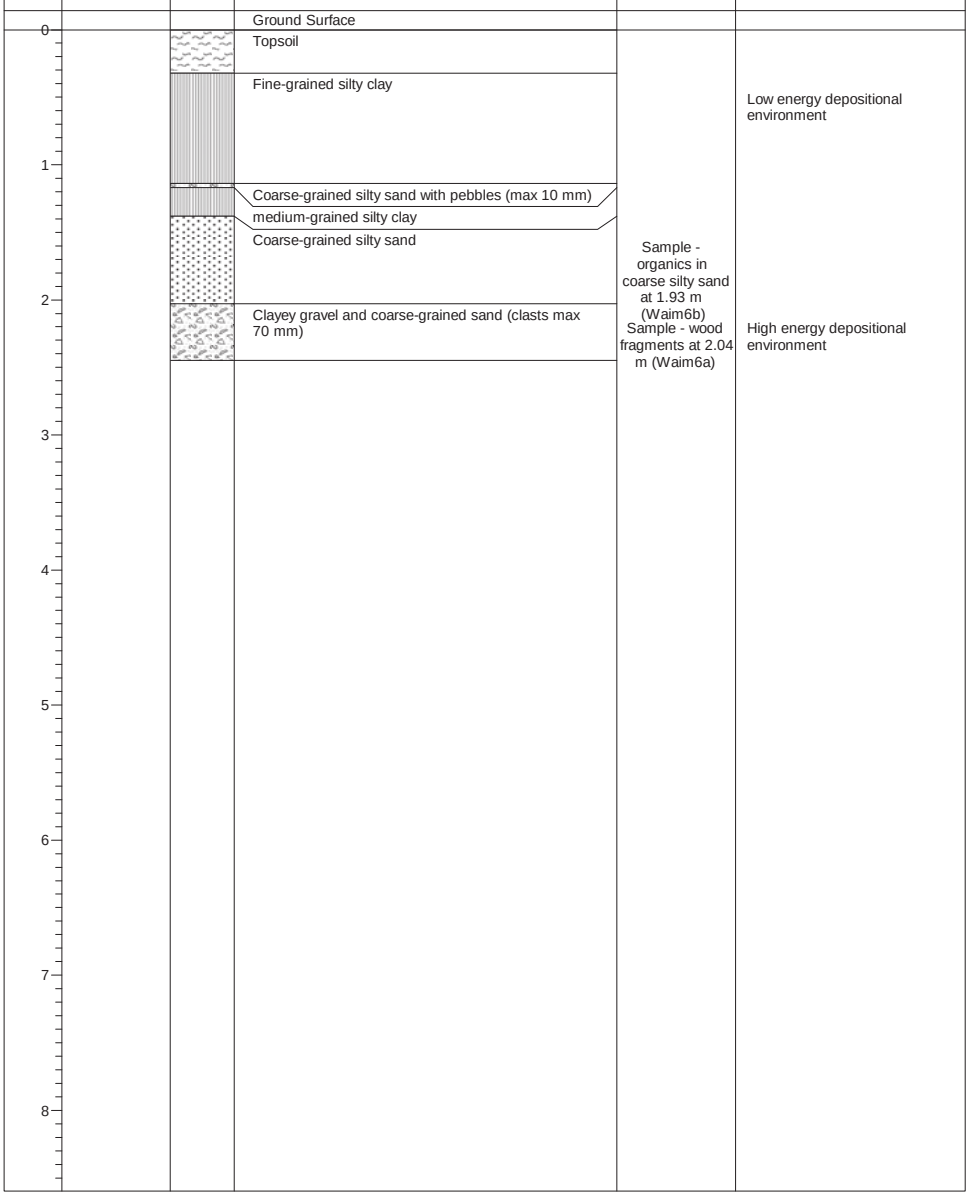

Project: Northland Flood History *Date:* 08.12.10

Core Location: Waimamaku Hooks and Hall Rd *Catchment:* Waimamaku River

Core Code: Waimamaku 8 (W8) *NZTM Coordinates:* 1641900E 6065300N

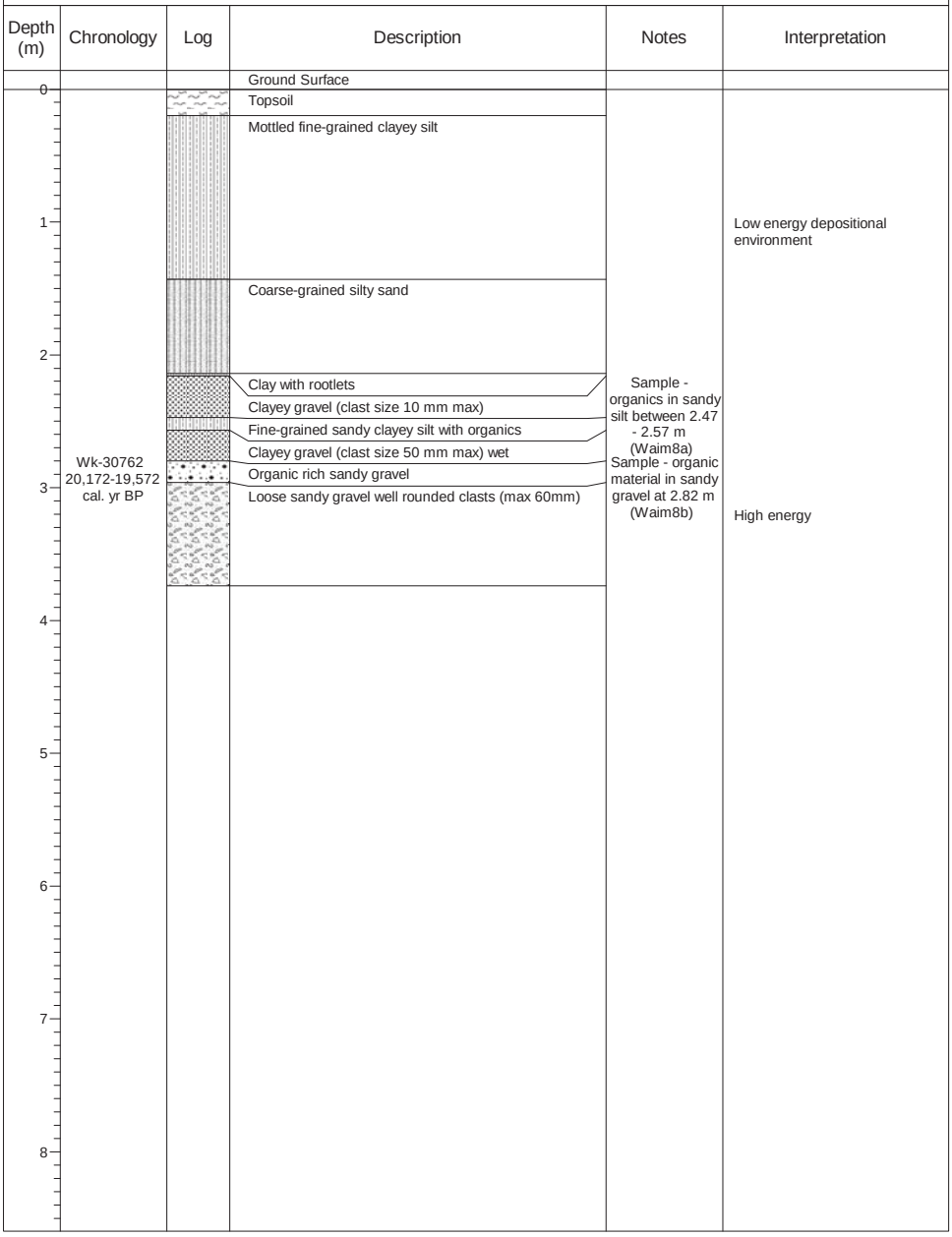

Project: Northland Flood History *Date:* 08.12.10

Core Location: Waimamaku Hooks and Hall Rd *Catchment:* Waimamaku River

Core Code: Waimamaku 9 (W9) *NZTM Coordinates:* 1641900 E 6065200 N

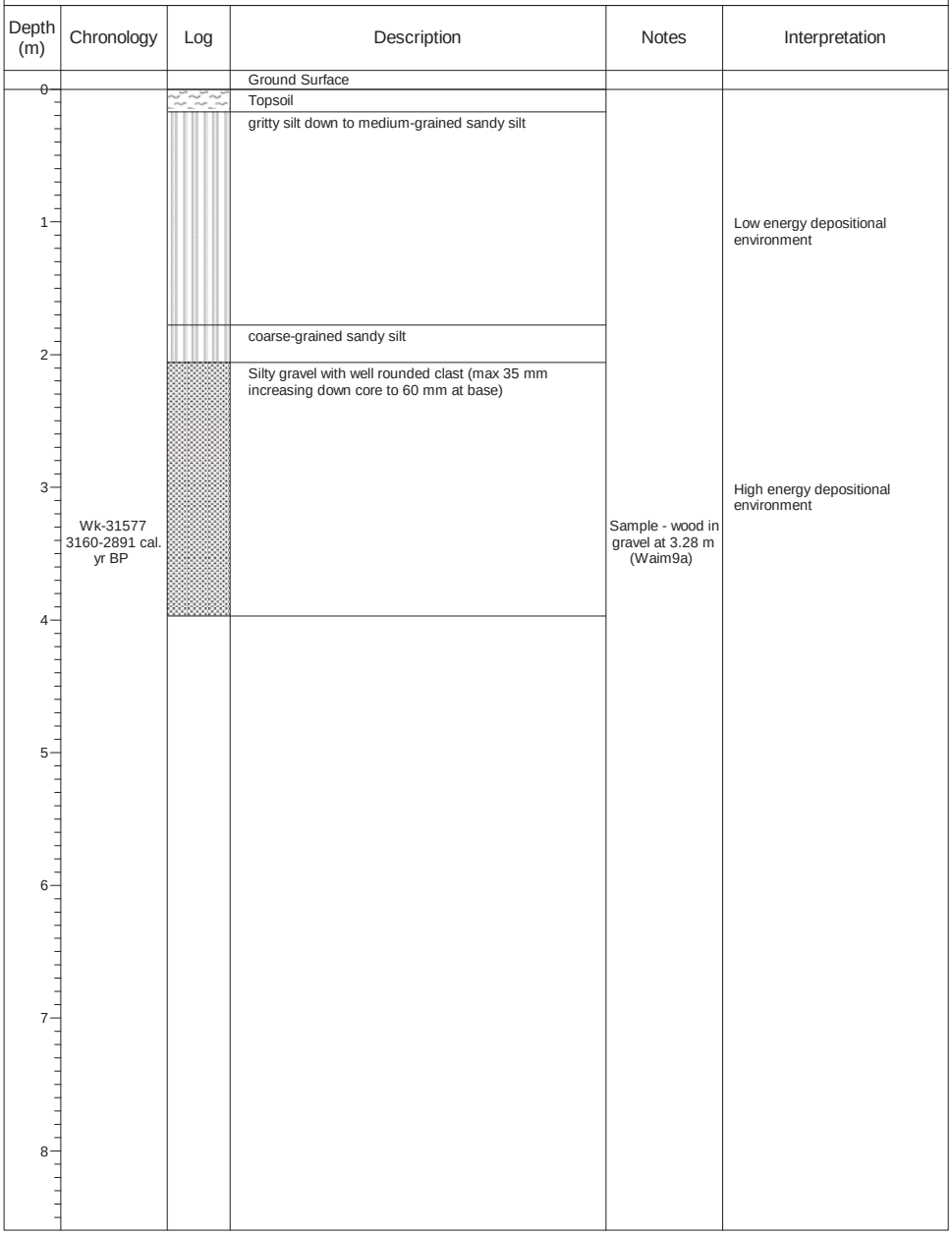

Appendix D

Radiocarbon results

Reports on radiocarbon age determinations undertaken by the University of Waikato Radiocarbon Dating Laboratory on organic samples collected from Northland floodplains and palaeochannels during this research.

The University of Waikato
Radiocarbon Dating Laboratory

Private Bag 3105
Hamilton,
New Zealand.
Fax +64 7 838 4192
Ph +64 7 838 4278
email c14@waikato.ac.nz
Head: Dr Alan Hogg

Report on Radiocarbon Age Determination for Wk- 27963

(AMS measurement)

Submitter	J Richardson
Submitter's Code	Pang 2a
Site & Location	Te Rapa Steam, Panuru, Northland, New Zealand
Sample Material	Charcoal
Physical Pretreatment	Sample cleaned.
Chemical Pretreatment	Sample washed in hot HCl, rinsed and treated with multiple hot NaOH washes. The NaOH insoluble fraction was treated with hot HCl, filtered, rinsed and dried.

$\delta^{13}C$	-27.3 ±	0.2 ‰
$D^{14}C$	-42.9 ±	3.0 ‰
$F^{14}C\%$	95.7 ±	0.3 %
Result	**353 ± 30 BP**	

Comments

22/7/10

- Result is *Conventional Age or Percent Modern Carbon (pMC)* following Stuiver and Polach, 1977, Radiocarbon 19, 355-363. This is based on the Libby half-life of 5568 yr with correction for isotopic fractionation applied. This age is normally quoted in publications and must include the appropriate error term and Wk number.
- Quoted errors are 1 standard deviation due to counting statistics multiplied by an experimentally determined Laboratory Error Multiplier.
- The isotopic fractionation, $\delta^{13}C$, is expressed as ‰ wrt PDB.
- $F^{14}C\%$ is also known as *Percent Modern Carbon (pMC)* .

The University of Waikato

Radiocarbon Dating Laboratory

Private Bag 3105
Hamilton,
New Zealand.
Fax +64 7 838 4192
Ph +64 7 838 4278
email c14@waikato.ac.nz
Head: Dr Alan Hogg

Report on Radiocarbon Age Determination for Wk- 27964

Submitter	J Richardson
Submitter's Code	Waih 3a
Site & Location	Waihou River, Panguru, Northland, New Zealand
Sample Material	Wood
Physical Pretreatment	Surfaces scraped clean. The wood was washed in ultrasonic bath, then ground.
Chemical Pretreatment	Sample was washed in hot 10% HCl, rinsed and treated with hot 1% NaOH. The NaOH insoluble fraction was treated with hot 10% HCl, filtered, rinsed and dried.

$\delta^{13}C$	-27.9 ±	0.2 ‰
$D^{14}C$	-524.8 ±	2.8 ‰
$F^{14}C\%$	47.5 ±	0.3 %
Result	**5977 ± 47 BP**	

Comments

22/7/10

- Result is *Conventional Age or Percent Modern Carbon (pMC)* following Stuiver and Polach, 1977, Radiocarbon 19, 355-363. This is based on the Libby half-life of 5568 yr with correction for isotopic fractionation applied. This age is normally quoted in publications and must include the appropriate error term and Wk number.
- Quoted errors are 1 standard deviation due to counting statistics multiplied by an experimentally determined Laboratory Error Multiplier.
- The isotopic fractionation, $\delta^{13}C$, is expressed as ‰ wrt PDB.
- $F^{14}C\%$ is also known :*Percent Modern Carbon (pMC)* .

The University of Waikato
Radiocarbon Dating Laboratory

Private Bag 3105
Hamilton,
New Zealand.
Fax +64 7 838 4192
Ph +64 7 838 4278
email c14@waikato.ac.nz
Head: Dr Alan Hogg

Report on Radiocarbon Age Determination for Wk- 27966

(AMS measurement)

Submitter	J Richardson
Submitter's Code	Mang 2g
Site & Location	Mangakahia River palaeochannel, Nukutawhiti, Northland, New Zealand
Sample Material	Wood - twig
Physical Pretreatment	Sample cleaned and ground.
Chemical Pretreatment	Sample washed in hot HCl, rinsed and treated with multiple hot NaOH washes. The NaOH insoluble fraction was treated with hot HCl, filtered, rinsed and dried.

$\delta^{13}C$	-27.4 ±	0.2 ‰
$D^{14}C$	-35.6 ±	4.2 ‰
$F^{14}C\%$	96.4 ±	0.4 %
Result	**291 ± 35 BP**	

Comments

22/7/10

- Result is *Conventional Age or Percent Modern Carbon (pMC)* following Stuiver and Polach, 1977, Radiocarbon 19, 355-363. This is based on the Libby half-life of 5568 yr with correction for isotopic fractionation applied. This age is normally quoted in publications and must include the appropriate error term and Wk number.
- Quoted errors are 1 standard deviation due to counting statistics multiplied by an experimentally determined Laboratory Error Multiplier.
- The isotopic fractionation, $\delta^{13}C$, is expressed as ‰ wrt PDB.
- $F^{14}C\%$ is also known as *Percent Modern Carbon (pMC)* .

The University of Waikato

Radiocarbon Dating Laboratory

Private Bag 3105
Hamilton,
New Zealand.
Fax +64 7 838 4192
Ph +64 7 838 4278
email c14@waikato.ac.nz
Head: Dr Alan Hogg

Report on Radiocarbon Age Determination for Wk- 27967

Submitter	J Richardson
Submitter's Code	Mang 1a
Site & Location	Mangakahiu River, Titoki Bridge, Northland, New Zealand
Sample Material	Silt
Physical Pretreatment	Visible contaminants removed.
Chemical Pretreatment	Washed in hot 10% HCl, rinsed and treated with hot 1% NaOH. The NaOH insoluble fraction was treated with hot 10% HCl, filtered, rinsed and dried.

$\delta^{13}C$	-29.7 ±	0.2 ‰
$D^{14}C$	-100.5 ±	4.4 ‰
$F^{14}C\%$	90.0 ±	0.4 %
Result	**850 ± 39 BP**	

Comments

22/7/10

- Result is *Conventional Age or Percent Modern Carbon (pMC)* following Stuiver and Polach, 1977, Radiocarbon 19, 355-363. This is based on the Libby half-life of 5568 yr with correction for isotopic fractionation applied. This age is normally quoted in publications and must include the appropriate error term and Wk number.
- Quoted errors are 1 standard deviation due to counting statistics multiplied by an experimentally determined Laboratory Error Multiplier.
- The isotopic fractionation, $\delta^{13}C$, is expressed as ‰ wrt PDB.
- $F^{14}C\%$ is also known as *Percent Modern Carbon (pMC)* .

The University of Waikato
Radiocarbon Dating Laboratory

Private Bag 3105
Hamilton,
New Zealand.
Fax +64 7 838 4192
Ph +64 7 838 4278
email c14@waikato.ac.nz
Head: Dr Alan Hogg

Report on Radiocarbon Age Determination for Wk- 27968

Submitter	J Richardson
Submitter's Code	Waim 1c
Site & Location	Waimamaku River, Hooks and Hall Road, Northland, New Zealand
Sample Material	Wood
Physical Pretreatment	Surfaces scraped clean. The wood was washed in ultrasonic bath, then ground.
Chemical Pretreatment	Sample was washed in hot 10% HCl, rinsed and treated with hot 1% NaOH. The NaOH insoluble fraction was treated with hot 10% HCl, filtered, rinsed and dried.

$\delta^{13}C$	-26.7 ±	0.2 ‰
$D^{14}C$	-132.1 ±	4.4 ‰
$F^{14}C\%$	86.8 ±	0.4 %
Result	**1138 ± 41 BP**	

Comments

22/7/10

- Result is *Conventional Age or Percent Modern Carbon (pMC)* following Stuiver and Polach, 1977, Radiocarbon 19, 355-363. This is based on the Libby half-life of 5568 yr with correction for isotopic fractionation applied. This age is normally quoted in publications and must include the appropriate error term and Wk number.
- Quoted errors are 1 standard deviation due to counting statistics multiplied by an experimentally determined Laboratory Error Multiplier.
- The isotopic fractionation, $\delta^{13}C$, is expressed as ‰ wrt PDB.
- $F^{14}C\%$ is also known as *Percent Modern Carbon (pMC)* .

The University of Waikato
Radiocarbon Dating Laboratory

Private Bag 3105
Hamilton,
New Zealand.
Fax +64 7 838 4192
Ph +64 7 838 4278
email c14@waikato.ac.nz
Head: Dr Alan Hogg

Report on Radiocarbon Age Determination for Wk- 27970

Submitter	J Richardson
Submitter's Code	Awan 1c
Site & Location	Awanui River palaeochannel, Nth Kaitaia, New Zealand
Sample Material	Organic rich mud
Physical Pretreatment	Visible contaminants removed.
Chemical Pretreatment	Washed in hot 10% HCl, rinsed and treated with hot 1% NaOH. The NaOH insoluble fraction was treated with hot 10% HCl, filtered, rinsed and dried.

$\delta^{13}C$	-29.6 ±	0.2 ‰
$D^{14}C$	-854.7 ±	1.5 ‰
$F^{14}C\%$	14.5 ±	0.2 %
Result	**15,495 ± 84 BP**	

Comments

22/7/10

- Result is *Conventional Age or Percent Modern Carbon (pMC)* following Stuiver and Polach, 1977, Radiocarbon 19, 355-363. This is based on the Libby half-life of 5568 yr with correction for isotopic fractionation applied. This age is normally quoted in publications and must include the appropriate error term and Wk number.
- Quoted errors are 1 standard deviation due to counting statistics multiplied by an experimentally determined Laboratory Error Multiplier.
- The isotopic fractionation, $\delta^{13}C$, is expressed as ‰ wrt PDB.
- $F^{14}C\%$ is also known :*Percent Modern Carbon (pMC)* .

The University of Waikato
Radiocarbon Dating Laboratory

Private Bag 3105
Hamilton,
New Zealand.
Fax +64 7 838 4192
Ph +64 7 838 4278
email c14@waikato.ac.nz
Head: Dr Alan Hogg

Report on Radiocarbon Age Determination for Wk- 27971

(AMS measurement)

Submitter	J Richardson
Submitter's Code	Kaeo 1b
Site & Location	Kaeo River, Green lane, Northland, New Zealand
Sample Material	Organic rich mud
Physical Pretreatment	Visible contaminants removed.
Chemical Pretreatment	Sample washed in hot HCl, rinsed and treated with multiple hot NaOH washes. The NaOH insoluble fraction was treated with hot HCl, filtered, rinsed and dried.

$\delta^{13}C$	-28.2 ±	0.2 ‰
$D^{14}C$	-82.4 ±	4.0 ‰
$F^{14}C\%$	91.8 ±	0.4 %
Result	**691 ± 35 BP**	

Comments

22/7/10

- Result is *Conventional Age or Percent Modern Carbon (pMC)* following Stuiver and Polach, 1977, Radiocarbon 19, 355-363. This is based on the Libby half-life of 5568 yr with correction for isotopic fractionation applied. This age is normally quoted in publications and must include the appropriate error term and Wk number.
- Quoted errors are 1 standard deviation due to counting statistics multiplied by an experimentally determined Laboratory Error Multiplier.
- The isotopic fractionation, $\delta^{13}C$, is expressed as ‰ wrt PDB.
- $F^{14}C\%$ is also known as *Percent Modern Carbon (pMC)* .

The University of Waikato

Radiocarbon Dating Laboratory

Private Bag 3105
Hamilton,
New Zealand.
Fax +64 7 838 4192
Ph +64 7 838 4278
email c14@waikato.ac.nz
Head: Dr Alan Hogg

Report on Radiocarbon Age Determination for Wk- 28764

(AMS measurement)

Submitter	J Richardson
Submitter's Code	Awan 1b
Site & Location	Awanui River paleochannel, Nh Kaitaia, Northland, New Zealand
Sample Material	Soil organics
Physical Pretreatment	Visible contaminants removed.
Chemical Pretreatment	Sample washed in hot HCl, rinsed and treated with multiple hot NaOH washes. The NaOH insoluble fraction was treated with hot HCl, filtered, rinsed and dried.

$\delta^{13}C$	-28.1 ±	0.2 ‰
$D^{14}C$	-336.8 ±	2.9 ‰
$F^{14}C\%$	66.3 ±	0.3 %
Result	**3299 ± 35 BP**	

Comments

AGHogg

27/10/10

- Result is *Conventional Age or Percent Modern Carbon (pMC)* following Stuiver and Polach, 1977, Radiocarbon 19, 355-363. This is based on the Libby half-life of 5568 yr with correction for isotopic fractionation applied. This age is normally quoted in publications and must include the appropriate error term and Wk number.
- Quoted errors are 1 standard deviation due to counting statistics multiplied by an experimentally determined Laboratory Error Multiplier.
- The isotopic fractionation, $\delta^{13}C$, is expressed as ‰ wrt PDB.
- $F^{14}C\%$ is also known as *Percent Modern Carbon (pMC)* .

The University of Waikato
Radiocarbon Dating Laboratory

Private Bag 3105
Hamilton,
New Zealand.
Fax +64 7 838 4192
Ph +64 7 838 4278
email c14@waikato.ac.nz
Head: Dr Alan Hogg

Report on Radiocarbon Age Determination for Wk- 28765

Submitter	J Richardson
Submitter's Code	Awan 1a
Site & Location	Awanui River paleochannel, Nh Kaitaia, Northland, New Zealand
Sample Material	Soil organics
Physical Pretreatment	Surfaces scraped clean. The wood was washed in ultrasonic bath, then ground.
Chemical Pretreatment	Sample was washed in hot 10% HCl, rinsed and treated with hot 1% NaOH. The NaOH insoluble fraction was treated with hot 10% HCl, filtered, rinsed and dried.

$\delta^{13}C$	28.7 ±	0.2 ‰
$D^{14}C$	-308.4 ±	4.7 ‰
$F^{14}C\%$	69.2 ±	0.5 %
Result	**2962 ± 55 BP**	

Comments

AGHogg
27/10/10

- Result is *Conventional Age or Percent Modern Carbon (pMC)* following Stuiver and Polach, 1977, Radiocarbon 19, 355-363. This is based on the Libby half-life of 5568 yr with correction for isotopic fractionation applied. This age is normally quoted in publications and must include the appropriate error term and Wk number.
- Quoted errors are 1 standard deviation due to counting statistics multiplied by an experimentally determined Laboratory Error Multiplier.
- The isotopic fractionation, $\delta^{13}C$, is expressed as ‰ wrt PDB.
- $F^{14}C\%$ is also known as *Percent Modern Carbon (pMC)* .

The University of Waikato
Radiocarbon Dating Laboratory

Private Bag 3105
Hamilton,
New Zealand.
Fax +64 7 838 4192
Ph +64 7 838 4278
email c14@waikato.ac.nz
Head: Dr Alan Hogg

Report on Radiocarbon Age Determination for Wk- 30434

(AMS measurement)

Submitter	J Richardson
Submitter's Code	Taka 2e
Site & Location	Takahue River, Pamapuria, New Zealand
Sample Material	Wood
Physical Pretreatment	Sample cleaned and ground.
Chemical Pretreatment	Sample washed in hot HCl, rinsed and treated with multiple hot NaOH washes. The NaOH insoluble fraction was treated with hot HCl, filtered, rinsed and dried.

$\delta^{13}C$	-26.6 ±	0.2 ‰
$D^{14}C$	-515.9 ±	1.4 ‰
$F^{14}C\%$	48.4 ±	0.1 %
Result	**5828 ± 25 BP**	

Comments

11/05/11

- Result is *Conventional Age or Percent Modern Carbon (pMC)* following Stuiver and Polach, 1977, Radiocarbon 19, 355-363. This is based on the Libby half-life of 5568 yr with correction for isotopic fractionation applied. This age is normally quoted in publications and must include the appropriate error term and Wk number.
- Quoted errors are 1 standard deviation due to counting statistics multiplied by an experimentally determined Laboratory Error Multiplier.
- The isotopic fractionation, $\delta^{13}C$, is expressed as ‰ wrt PDB.
- $F^{14}C\%$ is also known as *Percent Modern Carbon (pMC)* .

The University of Waikato
Radiocarbon Dating Laboratory

Private Bag 3105
Hamilton,
New Zealand.
Fax +64 7 838 4192
Ph +64 7 838 4278
email c14@waikato.ac.nz
Head: Dr Alan Hogg

Report on Radiocarbon Age Determination for Wk- 30435

(AMS measurement)

Submitter	J Richardson
Submitter's Code	Taka 2d
Site & Location	Takahue River, New Zealand
Sample Material	Wood
Physical Pretreatment	Sample cleaned and ground.
Chemical Pretreatment	Sample washed in hot HCl, rinsed and treated with multiple hot NaOH washes. The NaOH insoluble fraction was treated with hot HCl, filtered, rinsed and dried.

$\delta^{13}C$	-30.3 ±	0.2 ‰
$D^{14}C$	-223.6 ±	2.2 ‰
$F^{14}C\%$	77.6 ±	0.2 %
Result	**2033 ± 25 BP**	

Comments

11/05/11

- Result is *Conventional Age or Percent Modern Carbon (pMC)* following Stuiver and Polach, 1977, Radiocarbon 19, 355-363. This is based on the Libby half-life of 5568 yr with correction for isotopic fractionation applied. This age is normally quoted in publications and must include the appropriate error term and Wk number.
- Quoted errors are 1 standard deviation due to counting statistics multiplied by an experimentally determined Laboratory Error Multiplier.
- The isotopic fractionation, $\delta^{13}C$, is expressed as ‰ wrt PDB.
- $F^{14}C\%$ is also known as *Percent Modern Carbon (pMC)* .

The University of Waikato
Radiocarbon Dating Laboratory

Private Bag 3105
Hamilton,
New Zealand.
Fax +64 7 838 4192
Ph +64 7 838 4278
email c14@waikato.ac.nz
Head: Dr Alan Hogg

Report on Radiocarbon Age Determination for Wk- 30436

(AMS measurement)

Submitter	J Richardson
Submitter's Code	Kaih 2e
Site & Location	Maitahi, Kaihu River, New Zealand
Sample Material	Wood
Physical Pretreatment	Sample cleaned and ground.
Chemical Pretreatment	Sample washed in hot HCl, rinsed and treated with multiple hot NaOH washes. The NaOH insoluble fraction was treated with hot HCl, filtered, rinsed and dried.

$\delta^{13}C$	-26.5 ±	0.2 ‰
$D^{14}C$	-320.9 ±	2.1 ‰
$F^{14}C\%$	67.9 ±	0.2 %
Result	**3109 ± 25 BP**	

Comments

11/05/11

- Result is *Conventional Age or Percent Modern Carbon (pMC)* following Stuiver and Polach, 1977, Radiocarbon 19, 355-363. This is based on the Libby half-life of 5568 yr with correction for isotopic fractionation applied. This age is normally quoted in publications and must include the appropriate error term and Wk number.
- Quoted errors are 1 standard deviation due to counting statistics multiplied by an experimentally determined Laboratory Error Multiplier.
- The isotopic fractionation, $\delta^{13}C$, is expressed as ‰ wrt PDB.
- $F^{14}C\%$ is also known as *Percent Modern Carbon (pMC)* .

The University of Waikato
Radiocarbon Dating Laboratory

Private Bag 3105
Hamilton,
New Zealand.
Fax +64 7 838 4192
Ph +64 7 838 4278
email c14@waikato.ac.nz
Head: Dr Alan Hogg

Report on Radiocarbon Age Determination for Wk- 30437

(AMS measurement)

Submitter	J Richardson
Submitter's Code	Poro 1c
Site & Location	Poroti, New Zealand
Sample Material	Wood
Physical Pretreatment	Sample cleaned and ground.
Chemical Pretreatment	Sample washed in hot HCl, rinsed and treated with multiple hot NaOH washes. The NaOH insoluble fraction was treated with hot HCl, filtered, rinsed and dried.

$\delta^{13}C$	-29.3 ±	0.2 ‰
$D^{14}C$	-1000.0 ±	0.1 ‰
$F^{14}C\%$	0.0 ±	0.0 %
Result	**>50,000 BP**	

Comments

11/05/11

- Result is *Conventional Age or Percent Modern Carbon (pMC)* following Stuiver and Polach, 1977, Radiocarbon 19, 355-363. This is based on the Libby half-life of 5568 yr with correction for isotopic fractionation applied. This age is normally quoted in publications and must include the appropriate error term and Wk number.
- Quoted errors are 1 standard deviation due to counting statistics multiplied by an experimentally determined Laboratory Error Multiplier.
- The isotopic fractionation, $\delta^{13}C$, is expressed as ‰ wrt PDB.
- $F^{14}C\%$ is also known as *Percent Modern Carbon (pMC)* .

The University of Waikato

Radiocarbon Dating Laboratory

Private Bag 3105
Hamilton,
New Zealand.
Fax +64 7 838 4192
Ph +64 7 838 4278
email c14@waikato.ac.nz
Head: Dr Alan Hogg

Report on Radiocarbon Age Determination for Wk- 30438

(AMS measurement)

Submitter	J Richardson
Submitter's Code	Waim 4c
Site & Location	Waimamaku River, Hooks and Hall Road, New Zealand
Sample Material	Wood
Physical Pretreatment	Sample cleaned and ground.
Chemical Pretreatment	Sample washed in hot HCl, rinsed and treated with multiple hot NaOH washes. The NaOH insoluble fraction was treated with hot HCl, filtered, rinsed and dried.

$\delta^{13}C$	-27.0 ±	0.2 ‰
$D^{14}C$	-92.5 ±	2.7 ‰
$F^{14}C\%$	90.8 ±	0.3 %
Result	**780 ± 25 BP**	

Comments

11/05/11

- Result is *Conventional Age or Percent Modern Carbon (pMC)* following Stuiver and Polach, 1977, Radiocarbon 19, 355-363. This is based on the Libby half-life of 5568 yr with correction for isotopic fractionation applied. This age is normally quoted in publications and must include the appropriate error term and Wk number.
- Quoted errors are 1 standard deviation due to counting statistics multiplied by an experimentally determined Laboratory Error Multiplier.
- The isotopic fractionation, $\delta^{13}C$, is expressed as ‰ wrt PDB.
- $F^{14}C\%$ is also known as *Percent Modern Carbon (pMC)* .

The University of Waikato
Radiocarbon Dating Laboratory

Private Bag 3105
Hamilton,
New Zealand.
Fax +64 7 838 4192
Ph +64 7 838 4278
email c14@waikato.ac.nz
Head: Dr Alan Hogg

Report on Radiocarbon Age Determination for Wk- 30440

(AMS measurement)

Submitter	J Richardson
Submitter's Code	Kaeo 4a
Site & Location	Kaeo River, Kaeo, New Zealand
Sample Material	Wood
Physical Pretreatment	Sample cleaned and ground.
Chemical Pretreatment	Sample washed in hot HCl, rinsed and treated with multiple hot NaOH washes. The NaOH insoluble fraction was treated with hot HCl, filtered, rinsed and dried.

$\delta^{13}C$	-23.7 ±	0.2 ‰
$D^{14}C$	-447.7 ±	1.6 ‰
$F^{14}C\%$	55.2 ±	0.2 %
Result	**4769 ± 25 BP**	

Comments

11/05/11

- Result is *Conventional Age or Percent Modern Carbon (pMC)* following Stuiver and Polach, 1977, Radiocarbon 19, 355-363. This is based on the Libby half-life of 5568 yr with correction for isotopic fractionation applied. This age is normally quoted in publications and must include the appropriate error term and Wk number.
- Quoted errors are 1 standard deviation due to counting statistics multiplied by an experimentally determined Laboratory Error Multiplier.
- The isotopic fractionation, $\delta^{13}C$, is expressed as ‰ wrt PDB.
- $F^{14}C\%$ is also known as *Percent Modern Carbon (pMC)* .

The University of Waikato

Radiocarbon Dating Laboratory

Private Bag 3105
Hamilton,
New Zealand.
Fax +64 7 838 4192
Ph +64 7 838 4278
email c14@waikato.ac.nz
Head: Dr Alan Hogg

Report on Radiocarbon Age Determination for Wk- 30441

(AMS measurement)

Submitter	J Richardson
Submitter's Code	Nuku 4a
Site & Location	Upper Mangakahia River, Nukutawhiti, New Zealand
Sample Material	Wood
Physical Pretreatment	Sample cleaned and ground.
Chemical Pretreatment	Sample washed in hot HCl, rinsed and treated with multiple hot NaOH washes. The NaOH insoluble fraction was treated with hot HCl, filtered, rinsed and dried.

$\delta^{13}C$	-29.2 ±	0.2 ‰
$D^{14}C$	-998.4 ±	0.6 ‰
$F^{14}C\%$	0.2 ±	0.1 %
Result	**>48000 BP**	

Comments

11/05/11

- Result is *Conventional Age or Percent Modern Carbon (pMC)* following Stuiver and Polach, 1977, Radiocarbon 19, 355-363. This is based on the Libby half-life of 5568 yr with correction for isotopic fractionation applied. This age is normally quoted in publications and must include the appropriate error term and Wk number.
- Quoted errors are 1 standard deviation due to counting statistics multiplied by an experimentally determined Laboratory Error Multiplier.
- The isotopic fractionation, $\delta^{13}C$, is expressed as ‰ wrt PDB.
- $F^{14}C\%$ is also known as *Percent Modern Carbon (pMC)* .

The University of Waikato
Radiocarbon Dating Laboratory

Private Bag 3105
Hamilton,
New Zealand.
Fax +64 7 838 4192
Ph +64 7 838 4278
email c14@waikato.ac.nz
Head: Dr Alan Hogg

Report on Radiocarbon Age Determination for Wk- 30443

(AMS measurement)

Submitter	J Richardson
Submitter's Code	Kaeo 4c
Site & Location	Kaeo River, Kaeo, New Zealand
Sample Material	Soil, organics
Physical Pretreatment	Visible contaminants removed.
Chemical Pretreatment	Sample washed in hot HCl, rinsed and treated with multiple hot NaOH washes. The NaOH insoluble fraction was treated with hot HCl, filtered, rinsed and dried.

$\delta^{13}C$	-28.0 ±	0.2 ‰
$D^{14}C$	-572.1 ±	1.4 ‰
$F^{14}C\%$	42.8 ±	0.1 %
Result	**6820 ± 26 BP**	

Comments

11/05/11

- Result is *Conventional Age or Percent Modern Carbon (pMC)* following Stuiver and Polach, 1977, Radiocarbon 19, 355-363. This is based on the Libby half-life of 5568 yr with correction for isotopic fractionation applied. This age is normally quoted in publications and must include the appropriate error term and Wk number.
- Quoted errors are 1 standard deviation due to counting statistics multiplied by an experimentally determined Laboratory Error Multiplier.
- The isotopic fractionation, $\delta^{13}C$, is expressed as ‰ wrt PDB.
- $F^{14}C\%$ is also known as *Percent Modern Carbon (pMC)* .

The University of Waikato

Radiocarbon Dating Laboratory

Private Bag 3105
Hamilton,
New Zealand.
Fax +64 7 838 4192
Ph +64 7 838 4278
email c14@waikato.ac.nz
Head: Dr Alan Hogg

Report on Radiocarbon Age Determination for Wk- 30762

(AMS measurement)

Submitter	J Richardson
Submitter's Code	Waim8b
Site & Location	Hooks and Hall Rd., Waimamaku, New Zealand
Sample Material	River silts
Physical Pretreatment	Visible contaminants removed.
Chemical Pretreatment	Sample washed in hot HCl, rinsed and treated with multiple hot NaOH washes. The NaOH insoluble fraction was treated with hot HCl, filtered, rinsed and dried.

$\delta^{13}C$	-20.6 ± 0.2 ‰
$D^{14}C$	-875.4 ± 0.8 ‰
$F^{14}C\%$	12.5 ± 0.1 %
Result	**16,730 ± 52 BP**

Comments

20/06/11

- Result is *Conventional Age or Percent Modern Carbon (pMC)* following Stuiver and Polach, 1977, Radiocarbon 19, 355-363. This is based on the Libby half-life of 5568 yr with correction for isotopic fractionation applied. This age is normally quoted in publications and must include the appropriate error term and Wk number.
- Quoted errors are 1 standard deviation due to counting statistics multiplied by an experimentally determined Laboratory Error Multiplier.
- The isotopic fractionation, $\delta^{13}C$, is expressed as ‰ wrt PDB.
- $F^{14}C\%$ is also known as *Percent Modern Carbon (pMC)* .

The University of Waikato
Radiocarbon Dating Laboratory

Private Bag 3105
Hamilton,
New Zealand.
Fax +64 7 838 4192
Ph +64 7 838 4278
email c14@waikato.ac.nz
Head: Dr Alan Hogg

Report on Radiocarbon Age Determination for Wk- 30763

(AMS measurement)

Submitter	J Richardson
Submitter's Code	Poro 4a
Site & Location	Poroti, Northland, New Zealand
Sample Material	River silts
Physical Pretreatment	Visible contaminants removed.
Chemical Pretreatment	Sample washed in hot HCl, rinsed and treated with multiple hot NaOH washes. The NaOH insoluble fraction was treated with hot HCl, filtered, rinsed and dried.

$\delta^{13}C$	-26.0 ±	0.2 ‰
$D^{14}C$	-713.6 ±	1.1 ‰
$F^{14}C\%$	28.6 ±	0.1 %
Result	**10,045 ± 31 BP**	

Comments

20/06/11

- Result is *Conventional Age or Percent Modern Carbon (pMC)* following Stuiver and Polach, 1977, Radiocarbon 19, 355-363. This is based on the Libby half-life of 5568 yr with correction for isotopic fractionation applied. This age is normally quoted in publications and must include the appropriate error term and Wk number.
- Quoted errors are 1 standard deviation due to counting statistics multiplied by an experimentally determined Laboratory Error Multiplier.
- The isotopic fractionation, $\delta^{13}C$, is expressed as ‰ wrt PDB.
- $F^{14}C\%$ is also known as *Percent Modern Carbon (pMC)* .

The University of Waikato

Radiocarbon Dating Laboratory

Private Bag 3105
Hamilton,
New Zealand.
Fax +64 7 838 4192
Ph +64 7 838 4278
email c14@waikato.ac.nz
Head: Dr Alan Hogg

Report on Radiocarbon Age Determination for Wk- 30764

(AMS measurement)

Submitter	J Richardson
Submitter's Code	Taka 3g
Site & Location	Takahue R., Pamapuria, Northland, New Zealand
Sample Material	Wood
Physical Pretreatment	Sample cleaned and ground.
Chemical Pretreatment	Sample washed in hot HCl, rinsed and treated with multiple hot NaOH washes. The NaOH insoluble fraction was treated with hot HCl, filtered, rinsed and dried.

$\delta^{13}C$	-27.3 ±	0.2 ‰
$D^{14}C$	-291.7 ±	2.2 ‰
$F^{14}C\%$	70.8 ±	0.2 %
Result	**2770 ± 25 BP**	

Comments

20/06/11

- Result is *Conventional Age or Percent Modern Carbon (pMC)* following Stuiver and Polach, 1977, Radiocarbon 19, 355-363. This is based on the Libby half-life of 5568 yr with correction for isotopic fractionation applied. This age is normally quoted in publications and must include the appropriate error term and Wk number.
- Quoted errors are 1 standard deviation due to counting statistics multiplied by an experimentally determined Laboratory Error Multiplier.
- The isotopic fractionation, $\delta^{13}C$, is expressed as ‰ wrt PDB.
- $F^{14}C\%$ is also known as *Percent Modern Carbon (pMC)* .

The University of Waikato
Radiocarbon Dating Laboratory

Private Bag 3105
Hamilton,
New Zealand.
Fax +64 7 838 4192
Ph +64 7 838 4278
email c14@waikato.ac.nz
Head: Dr Alan Hogg

Report on Radiocarbon Age Determination for Wk- 31570

(AMS measurement)

Submitter	J Richardson
Submitter's Code	Taka 1c
Site & Location	Takahue, Northland, New Zealand
Sample Material	Wood in organic-rich fluvial silts
Physical Pretreatment	Sample cleaned and ground.
Chemical Pretreatment	Sample washed in hot HCl, rinsed and treated with multiple hot NaOH washes. The NaOH insoluble fraction was treated with hot HCl, filtered, rinsed and dried.

$\delta^{13}C$	-28.7 ±	0.2 ‰
$D^{14}C$	-754.5 ±	1.4 ‰
$F^{14}C\%$	24.6 ±	0.1 %
Result	**11,282 ± 45 BP**	

Comments

30/08/11

- Result is *Conventional Age or Percent Modern Carbon (pMC)* following Stuiver and Polach, 1977, Radiocarbon 19, 355-363. This is based on the Libby half-life of 5568 yr with correction for isotopic fractionation applied. This age is normally quoted in publications and must include the appropriate error term and Wk number.
- Quoted errors are 1 standard deviation due to counting statistics multiplied by an experimentally determined Laboratory Error Multiplier.
- The isotopic fractionation, $\delta^{13}C$, is expressed as ‰ wrt PDB.
- $F^{14}C\%$ is also known as *Percent Modern Carbon (pMC)* .

The University of Waikato
Radiocarbon Dating Laboratory

Private Bag 3105
Hamilton,
New Zealand.
Fax +64 7 838 4192
Ph +64 7 838 4278
email c14@waikato.ac.nz
Head: Dr Alan Hogg

Report on Radiocarbon Age Determination for Wk- 31571

(AMS measurement)

Submitter	J Richardson
Submitter's Code	Taka 3d
Site & Location	Takahue River, Northland, New Zealand
Sample Material	Organic-rich fluvial silts
Physical Pretreatment	Visible contaminants removed.
Chemical Pretreatment	Washed in hot 10% HCl, rinsed and treated with hot 1% NaOH. The NaOH insoluble fraction was treated with hot 10% HCl, filtered, rinsed and dried.

$\delta^{13}C$	-29.1 ±	0.2 ‰
$D^{14}C$	-157.9 ±	2.6 ‰
$F^{14}C\%$	84.2 ±	0.3 %
Result	**1381 ± 25 BP**	

Comments

30/08/11

- Result is *Conventional Age or Percent Modern Carbon (pMC)* following Stuiver and Polach, 1977, Radiocarbon 19, 355-363. This is based on the Libby half-life of 5568 yr with correction for isotopic fractionation applied. This age is normally quoted in publications and must include the appropriate error term and Wk number.
- Quoted errors are 1 standard deviation due to counting statistics multiplied by an experimentally determined Laboratory Error Multiplier.
- The isotopic fractionation, $\delta^{13}C$, is expressed as ‰ wrt PDB.
- $F^{14}C\%$ is also known as *Percent Modern Carbon (pMC)* .

The University of Waikato
Radiocarbon Dating Laboratory

Private Bag 3105
Hamilton,
New Zealand.
Fax +64 7 838 4192
Ph +64 7 838 4278
email c14@waikato.ac.nz
Head: Dr Alan Hogg

Report on Radiocarbon Age Determination for Wk- 31573

(AMS measurement)

Submitter	J Richardson
Submitter's Code	Kaih 2b
Site & Location	Kaihu River, Northland, New Zealand
Sample Material	Wood in organic-rich fluvial silts
Physical Pretreatment	Sample cleaned and ground.
Chemical Pretreatment	Sample washed in hot HCl, rinsed and treated with multiple hot NaOH washes. The NaOH insoluble fraction was treated with hot HCl, filtered, rinsed and dried.

$\delta^{13}C$	-27.5 ±	0.2 ‰
$D^{14}C$	-349.7 ±	2.3 ‰
$F^{14}C\%$	65.0 ±	0.2 %
Result	**3457 ± 28 BP**	

Comments

30/08/11

- Result is *Conventional Age or Percent Modern Carbon (pMC)* following Stuiver and Polach, 1977, Radiocarbon 19, 355-363. This is based on the Libby half-life of 5568 yr with correction for isotopic fractionation applied. This age is normally quoted in publications and must include the appropriate error term and Wk number.
- Quoted errors are 1 standard deviation due to counting statistics multiplied by an experimentally determined Laboratory Error Multiplier.
- The isotopic fractionation, $\delta^{13}C$, is expressed as ‰ wrt PDB.
- $F^{14}C\%$ is also known as *Percent Modern Carbon (pMC)* .

The University of Waikato
Radiocarbon Dating Laboratory

Private Bag 3105
Hamilton,
New Zealand.
Fax +64 7 838 4192
Ph +64 7 838 4278
email c14@waikato.ac.nz
Head: Dr Alan Hogg

Report on Radiocarbon Age Determination for Wk- 31574

(AMS measurement)

Submitter	J Richardson
Submitter's Code	Kaih 2f
Site & Location	Kaihu River, Northland, New Zealand
Sample Material	Wood in organic-rich fluvial silts
Physical Pretreatment	Sample cleaned and ground.
Chemical Pretreatment	Sample washed in hot HCl, rinsed and treated with multiple hot NaOH washes. The NaOH insoluble fraction was treated with hot HCl, filtered, rinsed and dried.

$\delta^{13}C$	-27.0 ±	0.2 ‰
$D^{14}C$	-387.1 ±	2.2 ‰
$F^{14}C\%$	61.3 ±	0.2 %
Result	**3933 ± 28 BP**	

Comments

30/08/11

- Result is *Conventional Age or Percent Modern Carbon (pMC)* following Stuiver and Polach, 1977, Radiocarbon 19, 355-363. This is based on the Libby half-life of 5568 yr with correction for isotopic fractionation applied. This age is normally quoted in publications and must include the appropriate error term and Wk number.
- Quoted errors are 1 standard deviation due to counting statistics multiplied by an experimentally determined Laboratory Error Multiplier.
- The isotopic fractionation, $\delta^{13}C$, is expressed as ‰ wrt PDB.
- $F^{14}C\%$ is also known as *Percent Modern Carbon (pMC)* .

The University of Waikato
Radiocarbon Dating Laboratory

Private Bag 3105
Hamilton,
New Zealand.
Fax +64 7 838 4192
Ph +64 7 838 4278
email c14@waikato.ac.nz
Head: Dr Alan Hogg

Report on Radiocarbon Age Determination for Wk- 31576

(AMS measurement)

Submitter	J Richardson
Submitter's Code	Nuku 2a
Site & Location	Nukutawhiti River, Northland, New Zealand
Sample Material	Organic-rich fluvial silts
Physical Pretreatment	Visible contaminants removed.
Chemical Pretreatment	Sample washed in hot HCl, rinsed and treated with multiple hot NaOH washes. The NaOH insoluble fraction was treated with hot HCl, filtered, rinsed and dried.

$\delta^{13}C$	-27.5 ±	0.2 ‰
$D^{14}C$	-335.8 ±	2.4 ‰
$F^{14}C\%$	66.4 ±	0.2 %
Result	**3287 ± 30 BP**	

Comments

30/08/11

- Result is *Conventional Age or Percent Modern Carbon (pMC)* following Stuiver and Polach, 1977, Radiocarbon 19, 355-363. This is based on the Libby half-life of 5568 yr with correction for isotopic fractionation applied. This age is normally quoted in publications and must include the appropriate error term and Wk number.
- Quoted errors are 1 standard deviation due to counting statistics multiplied by an experimentally determined Laboratory Error Multiplier.
- The isotopic fractionation, $\delta^{13}C$, is expressed as ‰ wrt PDB.
- $F^{14}C\%$ is also known as *Percent Modern Carbon (pMC)* .

The University of Waikato

Radiocarbon Dating Laboratory

Private Bag 3105
Hamilton,
New Zealand.
Fax +64 7 838 4192
Ph +64 7 838 4278
email c14@waikato.ac.nz
Head: Dr Alan Hogg

Report on Radiocarbon Age Determination for Wk- 31577

(AMS measurement)

Submitter	J Richardson
Submitter's Code	Waim 9a
Site & Location	Waimamaku River, Northland, New Zealand
Sample Material	Wood in organic-rich fluvial silts
Physical Pretreatment	Sample cleaned and ground.
Chemical Pretreatment	Sample washed in hot HCl, rinsed and treated with multiple hot NaOH washes. The NaOH insoluble fraction was treated with hot HCl, filtered, rinsed and dried.

$\delta^{13}C$	-25.8 ±	0.2 ‰
$D^{14}C$	-307.1 ±	2.4 ‰
$F^{14}C\%$	69.3 ±	0.2 %
Result	**2947 ± 27 BP**	

Comments

30/08/11

- Result is *Conventional Age or Percent Modern Carbon (pMC)* following Stuiver and Polach, 1977, Radiocarbon 19, 355-363. This is based on the Libby half-life of 5568 yr with correction for isotopic fractionation applied. This age is normally quoted in publications and must include the appropriate error term and Wk number.
- Quoted errors are 1 standard deviation due to counting statistics multiplied by an experimentally determined Laboratory Error Multiplier.
- The isotopic fractionation, $\delta^{13}C$, is expressed as ‰ wrt PDB.
- $F^{14}C\%$ is also known as *Percent Modern Carbon (pMC)* .

Appendix E

X-ray fluorescence and X-ray diffraction results

High resolution multi-element X-ray fluorescence (XRF) analysis of Kaeo floodplain sediments was undertaken using an ITRAX X-ray core scanner (IEGS, Aberystwyth University, UK) with a 3 kW molybdenum target tube operating at 30 kV and 30 mA. Four sections of a floodplain core (K4) were scanned at a resolution of 500 μm with a count time of 10 seconds/increment and 28 elements were measured.

The refractive index was required for particle size analysis of Kaeo floodplain sediment and was determined through XRD analysis. XRF spectra were obtained using a GBC EMMA X-ray diffractometer (INR, Massey University) operating at 35 kV and 20 mA using monochromatic Co Ka radiation.

Kaeo 4 (K4) core log and XRF plots for Al, Si, P, S, Cl, Ar, K, Ca and Ti (30 kV 30 mA, step size: 500 microns, count-time: 10 seconds/increment).

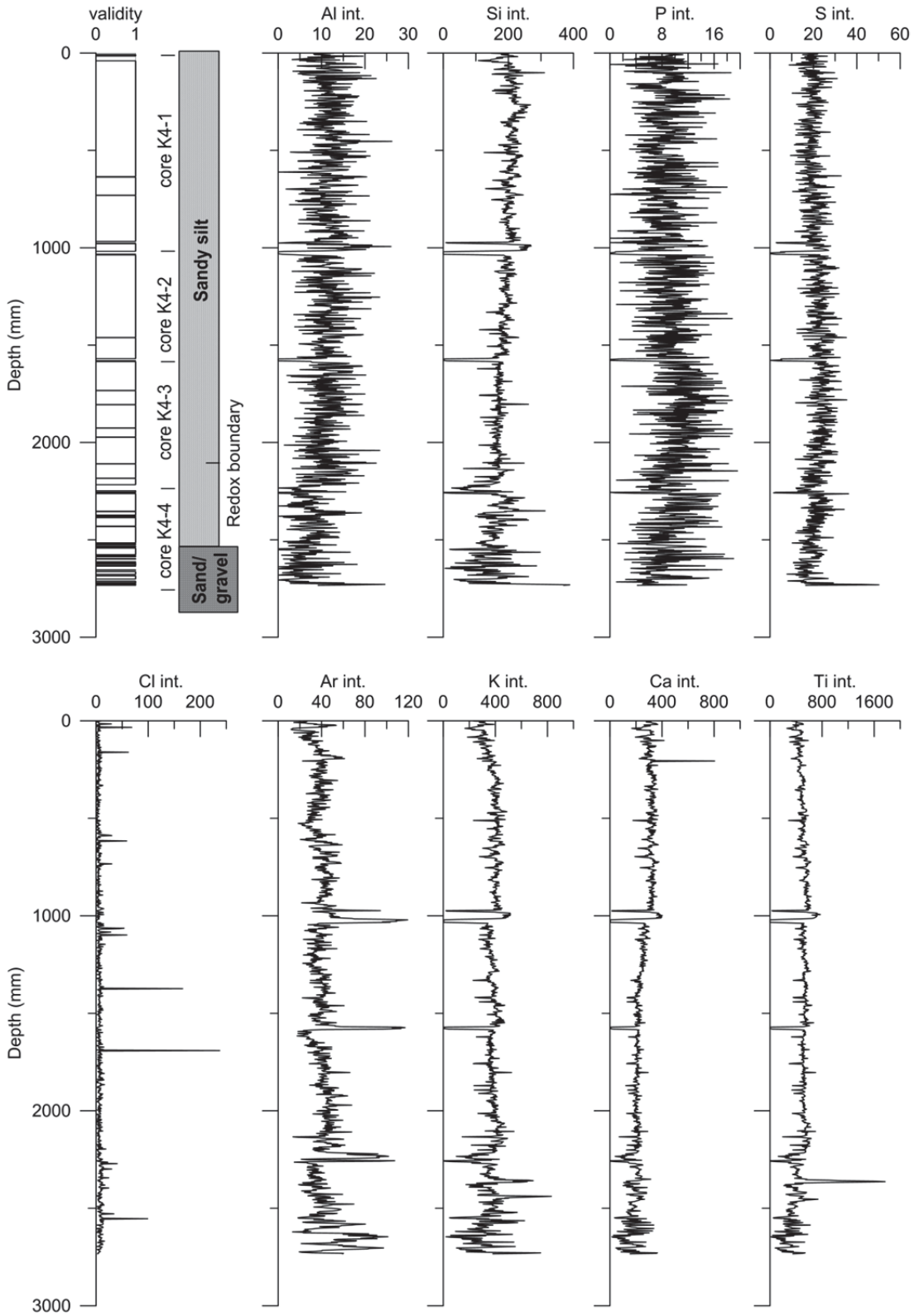

Kaeo 4 (K4) core log and XRF plots for V, Cr, Mn, Fe, Ni, cu, Zn, Ga and Se (30 kV 30 mA, step size: 500 microns, count-time: 10 seconds/increment).

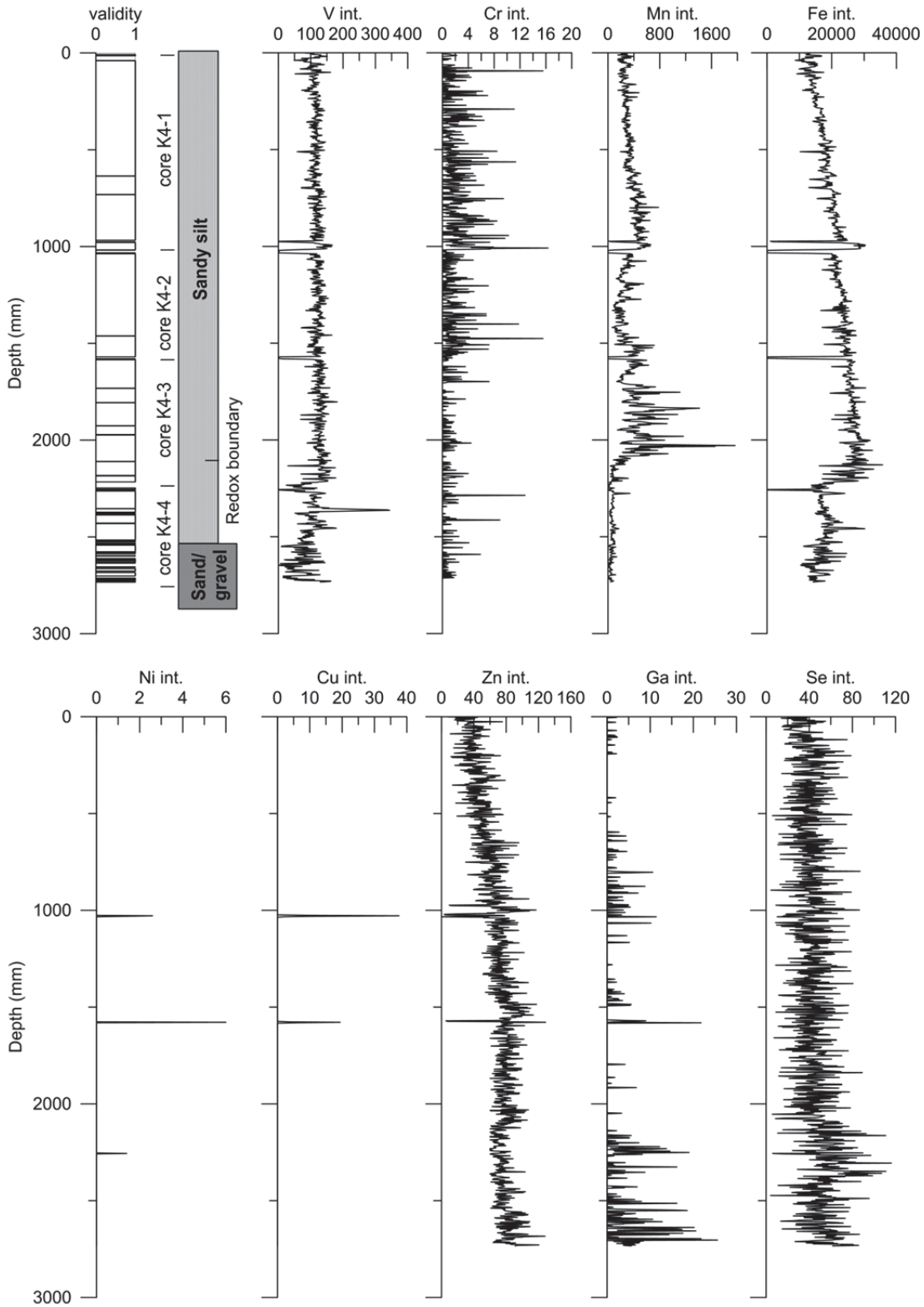

Kaeo 4 (K4) core log and XRF plots for Br, Rb, Sr, Y, Ba, Ce, Ta, W and Pb (30 kV 30 mA, step size: 500 microns, count-time: 10 seconds/increment).

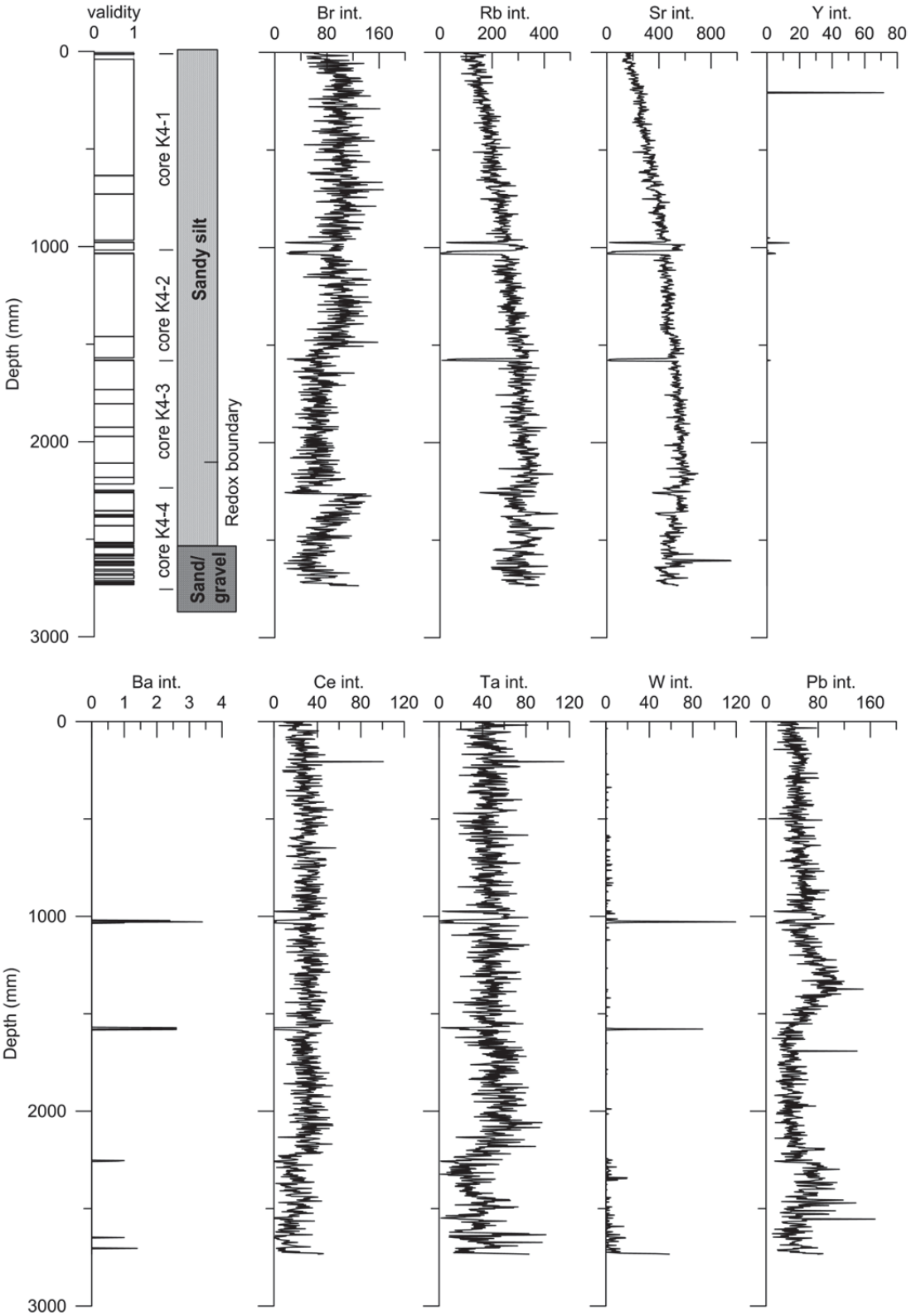

Optical images of Kaeo floodplain core K4.

Core section: Kaeo 4-1

1030 mm ← **heavily oxidised fine-grained sandy silt** **0 mm**

Core section: Kaeo 4-2

1580 mm ← **1031mm**

Core: Kaeo 4-3

2255 mm | **redox boundary 2000 mm** **1581 mm**

Core: Kaeo 4-4

2735 mm **sand/gravel** | **2500 mm** **2256 mm**

XRD spectra for Kaeo river floodplain sediment obtained using a GBC EMMA X-ray diffractometer operating at 35 kV and 20 mA using monochromatic Co Ka radiation. Scans parameters were 2^{o} 2θ/min scan rate at steps of 0.1^{o} 2θ

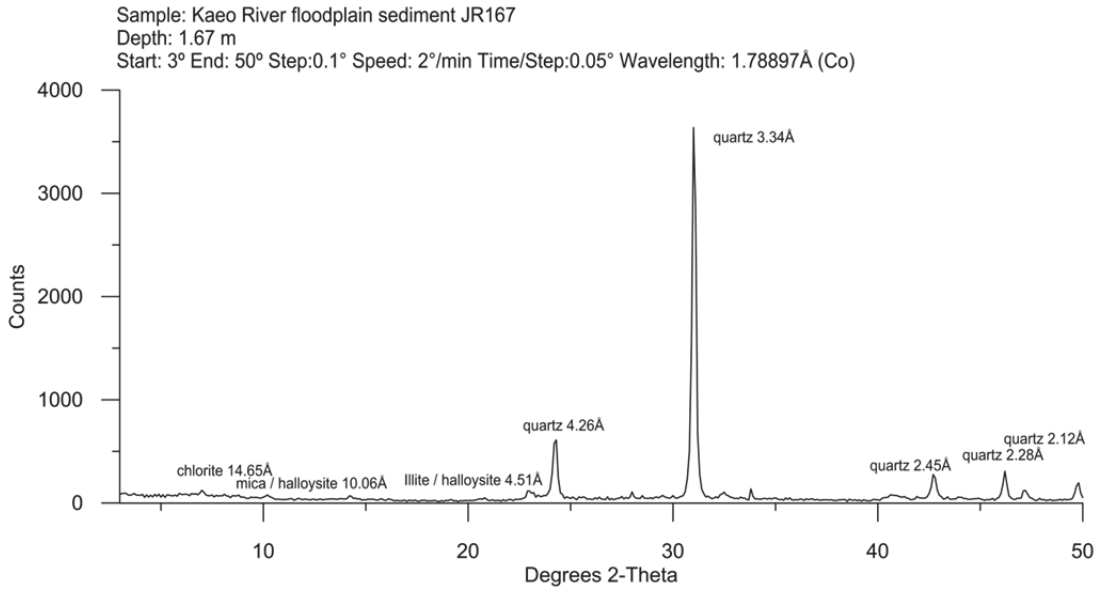

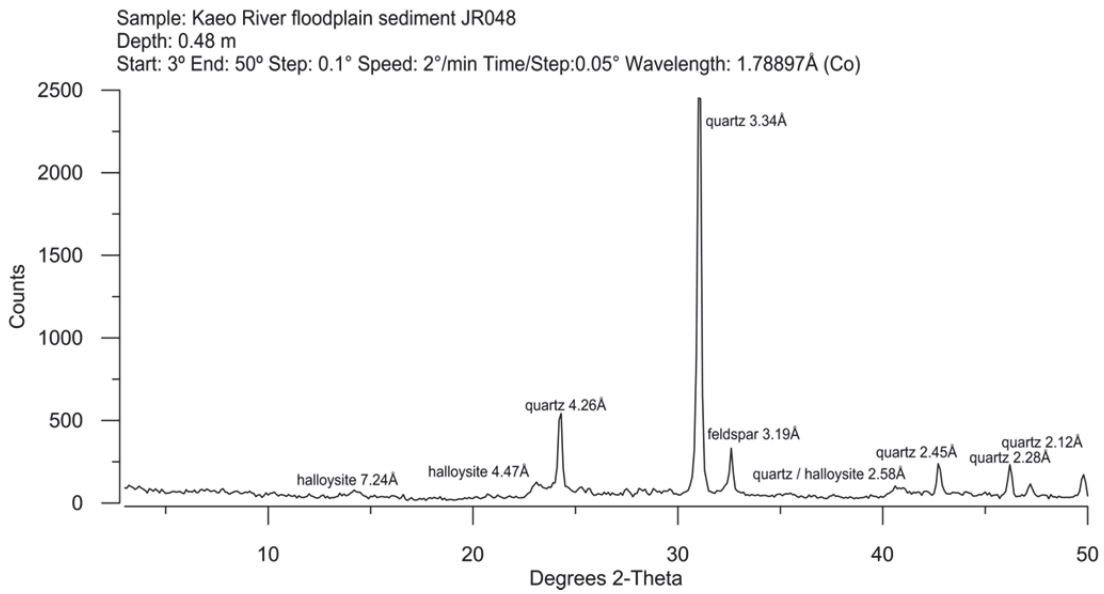

Appendix F

Statements of contribution to doctoral thesis containing publications

DRC 16

MASSEY UNIVERSITY
GRADUATE RESEARCH SCHOOL

STATEMENT OF CONTRIBUTION TO DOCTORAL THESIS CONTAINING PUBLICATIONS

(To appear at the end of each thesis chapter/section/appendix submitted as an article/paper or collected as an appendix at the end of the thesis)

We, the candidate and the candidate's Principal Supervisor, certify that all co-authors have consented to their work being included in the thesis and they have accepted the candidate's contribution as indicated below in the *Statement of Originality*.

Name of Candidate: Jane Richardson

Name/Title of Principal Supervisor: Dr Ian Fuller

Name of Published Research Output and full reference:

J.M. Richardson, I.C. Fuller, M.G. Macklin, A.F Jones, K.A. Holt, N.J. Litchfield, M. Bebbington (In review). Holocene river behaviour in New Zealand: response to regional centennial–scale climate forcing, Quaternary Science Reviews.

In which Chapter is the Published Work: Chapter 4

Please indicate either:

- The percentage of the Published Work that was contributed by the candidate:

  and / or

- Describe the contribution that the candidate has made to the Published Work:

  Jane Richardson was the principal author in the preparation of the manuscript. Co–authors provided advice and contributed to the final editing of the manuscript. Dr Mark Bebbington performed the statistical analysis presented in the paper. Dr Anna Jones advised on the analysis of the New Zealand fluvial radiocarbon database. Use of the New Zealand fluvial radiocarbon database is referenced as Macklin et al. (2012a).

Candidate's Signature — Date: 03/01/2013

Principal Supervisor's signature — Date: 3/1/13

GRS Version 3– 16 September 2011

DRC 16

MASSEY UNIVERSITY
GRADUATE RESEARCH SCHOOL

STATEMENT OF CONTRIBUTION TO DOCTORAL THESIS CONTAINING PUBLICATIONS

(To appear at the end of each thesis chapter/section/appendix submitted as an article/paper or collected as an appendix at the end of the thesis)

We, the candidate and the candidate's Principal Supervisor, certify that all co-authors have consented to their work being included in the thesis and they have accepted the candidate's contribution as indicated below in the *Statement of Originality*.

Name of Candidate: Jane Richardson

Name/Title of Principal Supervisor: Dr Ian Fuller

Name of Published Research Output and full reference:

J.M. Richardson, I.C. Fuller, K.A. Holt, N.J. Litchfield, M.G. Macklin (In review). The role of valley floor confinement as a control on Holocene floodplain development: an example from Northland, New Zealand, Geomorphology.

In which Chapter is the Published Work: Chapter 5

Please indicate either:

- The percentage of the Published Work that was contributed by the candidate:

  and / or

- Describe the contribution that the candidate has made to the Published Work:

  Jane Richardson carried out all the fieldwork in Northland between November 2009 and October 2011, and was assisted at different times by co–authors. Jane Richardson was the principal author in the preparation of manuscript. Co–authors provided advice and contributed to the final editing of the manuscript.

Candidate's Signature — 03/01/2013 Date

Principal Supervisor's signature — 3/1/13 Date

GRS Version 3– 16 September 2011

DRC 16

MASSEY UNIVERSITY
GRADUATE RESEARCH SCHOOL

STATEMENT OF CONTRIBUTION TO DOCTORAL THESIS CONTAINING PUBLICATIONS

(To appear at the end of each thesis chapter/section/appendix submitted as an article/paper or collected as an appendix at the end of the thesis)

We, the candidate and the candidate's Principal Supervisor, certify that all co-authors have consented to their work being included in the thesis and they have accepted the candidate's contribution as indicated below in the *Statement of Originality*.

Name of Candidate: Jane Richardson

Name/Title of Principal Supervisor: Dr Ian Fuller

Name of Published Research Output and full reference:

J.M. Richardson, I.C. Fuller, K.A. Holt, N.J. Litchfield, M.G. Macklin (In review). Fluvial records of Holocene climate variability and evidence of a 3500–2800 cal. yr BP cold event from northern New Zealand, The Holocene.

In which Chapter is the Published Work: Chapter 7

Please indicate either:

- The percentage of the Published Work that was contributed by the candidate:

  and / or

- Describe the contribution that the candidate has made to the Published Work:

  Jane Richardson carried out all the fieldwork in Northland between November 2009 and October 2011, and was assisted at different times by co–authors. Jane Richardson was the principal author in the preparation of manuscript. Co–authors provided advice and contributed to the final editing of the manuscript.

Candidate's Signature

03/01/2013
Date

Principal Supervisor's signature

3/1/13
Date

GRS Version 3– 16 September 2011

DRC 16

MASSEY UNIVERSITY
GRADUATE RESEARCH SCHOOL

STATEMENT OF CONTRIBUTION TO DOCTORAL THESIS CONTAINING PUBLICATIONS

(To appear at the end of each thesis chapter/section/appendix submitted as an article/paper or collected as an appendix at the end of the thesis)

We, the candidate and the candidate's Principal Supervisor, certify that all co-authors have consented to their work being included in the thesis and they have accepted the candidate's contribution as indicated below in the *Statement of Originality*.

Name of Candidate: Jane Richardson

Name/Title of Principal Supervisor: Dr Ian Fuller

Name of Published Research Output and full reference:

J.M. Richardson, I.C. Fuller, K.A. Holt, N.J. Litchfield, M.G. Macklin (In review). Post–settlement fluvial response in Northland, New Zealand, Catena.

In which Chapter is the Published Work: Chapter 8

Please indicate either:

- The percentage of the Published Work that was contributed by the candidate:

  and / or

- Describe the contribution that the candidate has made to the Published Work:

  Jane Richardson carried out all the fieldwork in Northland between November 2009 and October 2011, and was assisted at different times by co–authors. Jane Richardson was the principal author in the preparation of manuscript. Co–authors provided advice and contributed to the final editing of the manuscript.

Candidate's Signature — 03/01/2013 Date

Principal Supervisor's signature — 3/1/13 Date

GRS Version 3– 16 September 2011